Wissenschaftszentrum Weihenstephan für Ernährung, Landnutzung und Umwelt
Fachgebiet Biodiversität der Pflanzen, Prof. Dr. Hanno Schäfer
Technische Universität München

Patterns and processes of fungal community ecology

Franz-Sebastian Krah

Vollständiger Abdruck der von der Fakultät Wissenschaftszentrum Weihenstephan für Ernährung, Landnutzung und Umwelt der Technischen Universität München zur Erlangung des akademischen Grades eines

Doktors der Naturwissenschaften (Dr.rer.nat.)

genehmigten Dissertation.

Vorsitzender:

      Prof. Dr. Aurelien Tellier

Prüfende der Dissertation:

    1. Prof. Dr. Hanno Schäfer

    2. Prof. Dr. Jörg Müller,
       Julius-Maximilians-Universität Würzburg

    3. Prof. Dr. Johan Philipp Benz

Die Dissertation wurde am 14.01.2019 bei der Technischen Universität München eingereicht und durch die Fakultät Wissenschaftszentrum Weihenstephan für Ernährung, Landnutzung und Umwelt am 18.04.2019 angenommen.

Funding

Acknowledgements

Summary

Community ecology is the study of the patterns of species distributions and the processes underlying these patterns. Community ecologists increasingly concur that niche selection, dispersal and ecological drift jointly influence the assembly of natural communities. Although patterns of many organism groups have been extensively studied, the processes that influence the assembly of fungal communities are not well understood. Communities of saprotrophic mushroom-forming fungi provide important ecosystem services such as decomposition, and thus play important roles in global carbon and nutrient cycling. This thesis thus aims at understanding basic mechanisms of fungal community ecology. To understand assembly processes two fundamental approaches are important. First, species underlie natural selection, favoring traits that make them better adapted to the environment. An understanding of the distribution of traits along the fungal tree of life thus yields first clues to which environmental factors may act as ecological niche selection. Further, the response of traits along environmental gradients allows to identify the influence of niche selection of traits. Although phylogeny- and trait-based studies yield a direct link between the environment and species features – natural selection – many variables are correlated under natural conditions prohibiting the interpretation of independent effects. Therefore, the second approach utilizes experiments to disentangle environmental quantities and to understand the relative importance of environmental variables on fungal diversity.

After a general introduction, the second chapter thus examines the evolution of saprotrophic fungal host specificity to increase our understanding of the importance of the host as a filter for fungal communities. The third chapter then uses a morphological trait of mushrooms – the reproductive organ of many fungi –, to ask whether mushroom color effects fungal prevalence across Europe. To disentangle potentially confounding variables, the consecutive two chapters use a dead-wood experiment, where the host (identity and size) and the environment (stand microclimate and local dead wood) were independently manipulated. In detail, the fourth chapter explicitly tests for the independent effects of the host and the environment using fruit body inventories. Using a subset of this dead-wood experiment, the fifth chapter tests whether organism size pre-

Summary

dicts assembly processes, expanding the taxon sampling to bacteria, fungi and beetles. This thesis revealed high specialization of white rot fungi towards angiosperm tree species and primarily generalism in brown rot fungi (Chapter 2). Further, host identity was found to be an important driver for the assembly of wood-inhabiting fungi (Chapter 4) and even more important than microclimate. Fungal communities on an angiosperm tree were further more similar than the community composition on a conifer tree species, suggesting that wood-inhabiting fungi are selected by the host identity, thus that different fungal species are adapted to decompose specific substrates. Further, this thesis showed that the occurrence of fungi could be explained by morphological and life-history traits. In detail, saprotrophic species with dark-colored mushrooms were more prevalent in cold environments than light-colored species (Chapter 3), suggesting the theory of thermal melanism for multicellular fungi. Further, using a combined approach (trait-based and experiment-based), organism size predicted differences in the niche selection to ecological drift ratio (Chapter 5), suggesting that assembly processes differ between macro- and microorganisms.

Based on two approaches to study potential mechanisms of fungal assembly, this thesis could increase our understanding of how evolutionary constraints together with species traits structures fungal assemblages. Fungal adaptations towards the host tree species as well as morphological traits and life-history traits influence the assembly of saprotrophic fungal communities. Further, besides niche selection, demographic differences due to community sizes may play an important role in structuring fungal assemblages by regulating the influence of stochasticity.

To further increase our understanding of assembly processes on fungal community ecology, future directions are outlined. In particular the integration of fungal occurrences together with signals of the phylogeny, traits and the environment within a single methodological framework promise further insights into the relative importance of different assembly processes on fungal communities.

Zusammenfassung

Die Ökologie der Artengemeinschaften befasst sich mit Mustern der Vorkommen von Artengemeinschaften und den Prozessen der Artgemeinschaftsbildung. Ökologische Studien zeigen, dass Nischenselektion, Verbreitung und ökologische Drift gemeinsam Artgemeinschaftsbildungsprozesse beeinflussen. Obwohl viele Muster der Artgemeinschaftsbildung bereits intensiv untersucht wurden, sind Prozesse der Artgemeinschaftsbildung von holzbewohnenden Pilzen bisher noch wenig verstanden. Holzbewohnende pilzliche Artengemeinschaften leisten wichtige Ökosystemprozesse, wie den Abbau pflanzlicher Biomasse und spielen deshalb eine wichtige Rolle im globalen Nährstoff- und Kohlenstoffkreislauf. Die vorliegende Doktorarbeit zielt daher darauf ab, zentrale Mechanismen und Prozesse der Artgemeinschaftsbildung von Pilzen zu verstehen.

Um Prozesse der Artgemeinschaftsbildung zu studieren, können zwei grundsätzliche Wege verfolgt werden. Zum einen unterliegen Arten der natürlichen Selektion (Evolution), die diejenigen Eigenschaften fördert, die eine bessere Anpassung an die Umwelt gewährleisten. Ein Verständnis der Evolution von Eigenschaften und deren Verteilung im Artenstammbaum kann erste Einsichten darüber ermöglichen, welche Umweltfaktoren zu deren Selektion beigetragen haben. Zudem kann die Prävalenz von Arteigenschaften entlang eines Umweltgradienten Aufschlüsse darüber geben, welche Nischen selektierend wirken und dadurch Artgemeinschaften beeinflussen. Obwohl Studien der Evolution und Eigenschaften im Umweltgradienten ein direktes Verständnis zwischen der Umwelt und Artgemeinschaften erlauben – natürliche Selektion – birgt dieser Ansatz auch Schwierigkeiten. Werden Daten im Feld unter natürlichen Bedingungen erhoben, sind meist viele der gemessenen Umweltvariablen korreliert und dadurch ist es nicht möglich deren unabhängige Effekte zu schätzen. Daher ist es nötig diese Variablen in Experimenten unabhängig zu verändern, um deren relative und unabhängige Effekte testen zu können.

Nach einer Einleitung widmet sich das zweite Kapitel der Evolution der Wirtsspezifizität holzbewohnende Pilze um die Relevanz der Wirtspflanze als Nische für Pilzgemeinschaften besser zu verstehen. Das dritte Kapitel beschäftigt sich dann mit der Frage ob die Hutfarbe als Eigenschaft von Pilzfruchtkörpern – dem reproduktiven Or-

Zusammenfassung

gan von Pilzen – die Prävalenz von Pilzartgemeinschaften in Europa beeinflusst. In den folgenden zwei Kapiteln werden dann verschiedene Umweltvariablen anhand eines Totholzexperiments unabhängig voneinander verändert. Hier liegt ein besonderer Fokus darauf, die unabhängigen Effekte des Wirts (Wirtsbaumart und -größe) und Umwelt (Bestandesmikroklima und lokales Totholz) zu testen.

Das vierte Kapitel testet explizit die unabhängigen Effekte des Wirts und der Umwelt auf holzbewohnende Pilzgemeinschaften basierend auf Fruchtkörperinventuren. Das fünfte Kapitel untersucht dann, ob die Organismengröße Artgemeinschaftsbildungsprozesse vorhersagen kann, indem zusätzlich zu Pilzen auch Bakterien- und Käfergemeinschaften des Totholzes untersucht werden. Diese Arbeit zeigte eine hohe Spezialisierung der Weißfäulepilze auf angiospermen Baumarten und einen hohen Anteil an Generalisten bei Braunfäulepilzen (Kapitel 2). Die Wirtsbaumart erwies sich ebenfalls als wichtiger Treiber für die Gemeinschaft von holzbewohnenden Pilzen (Kapitel 4) und überwog den Effekt des Bestandesmikroklimas. Zudem waren die Pilzgemeinschaften auf einer angiospermen Baumart ähnlicher als die auf einer gymnospermen Baumart, was darauf hindeutet, dass holzbewohnende Pilze durch Anpassung an Wirtsbaumarten durch die Umwelt selektiert werden. In der vorliegenden Arbeit konnte zudem gezeigt werden, dass die Prävalenz von Pilzen durch morphologische Eigenschaften beeinflusst wird. Holz- und Laubbewohnende Arten mit dunkel-farbigen Pilzhüten sind häufiger in kalten Umgebungen als helle Arten (Kapitel 3). Dieses Ergebnis ist konsistent mit der Theorie des thermischen Melanismus. Diese besagt, dass dunkle Organismen Vorteile in kalten Habitaten haben, da sie durch die dunkle Oberfläche schneller aufwärmen als helle Organismen. Darüber hinaus konnte die Organismengröße Unterschiede in den Prozessen der Artgemeinschaftsbildung (Nischenselektion und ökologische Drift) vorhersagen (Kapitel 5). Dies deutet darauf hin, dass sich die Prozesse der Artgemeinschaftsbildung zwischen Makro- und Mikroorganismen unterscheiden.

Basierend auf zwei grundlegenden Ansätzen zur Untersuchung von Artgemeinschaftsbildungsprozesse, konnte diese Arbeit zu einem besseren Verständnis beitragen, wie evolutionäre Anpassung und verschiedene Umweltvariablen Pilzartgemeinschaften strukturiert. Die Anpassung von Pilzarten an Wirtsbaumarten sowie morphologische Merkmale beeinflussen die Artgemeinschaftsbildung von Pilzgemeinschaften. Neben der Nischenselektion können demografische Unterschiede wie z.B. die Größe der Organismen eine wichtige Rolle bei der Strukturierung von Pilzartgemeinschaften spielen.

Zusammenfassung

xii

Contents

3   Effects of temperature on pigmentation of mushrooms across Europe   55

Contents

List of Figures

List of Tables

List of Tables

List of Tables

1 Introduction

1.1 Community ecology

1.1.1 A brief historical overview

Community ecology is the study of 1) the pattern in the richness, abundance, and composition of species and 2) the processes underlying these patterns [Vellend, 2010]. Historically, biology/ecology started as purely descriptive, mainly focusing on the formal classification of species. In the 18th and early 19th century the description of patterns was seen as the main goal of biology. Linnaeus named/diagnosed more than 13000 species [Stearn, 1959, Müller-Wille, 2006] based on morphology and became the father of modern taxonomy by applying a binary classification system based on a genus name and a species epithet. Alexander von Humboldt quantified the natural world wherever he could, and also formally described species, however together with further information, e.g., the collection locality and so developed a first classification of distinct plant communities along an altitudinal gradient ('Naturgemälde') [von Humboldt, 1807]. Darwin later provided the theoretical background to understand why species occurred in some locations and not in others. The theory of evolution by natural selection states that species change over time and become more adapted to their environment or go extinct [Darwin, 1859]. However, only in the early 20th century, scientists such as Henry Gleason and Frederic Clements asked why specific communities of species occurred together and why some habitats support more species than others [Clements, 1916, Gleason, 1922]. Whereas Clements had the opinion that communities are holistic entities (superorganism-theory), Gleason had a more individuum-based view of communities. Although these theories inspired much research, they did, however, not provide a mechanistic understanding of the underlying assembly processes. The niche-theory provided such a framework, first formulated by Charles Elton [1927], but usually attributed to George Evelyn Hutchinson [Hutchinson, 1957]. The niche theory states that only adapted species persist in a niche, whereas maladapted species are excluded from this niche (see below). Another influential theory was the 'competitive exclusion principle' stating that two species, which are 'too similar' cannot co-exist due to competition for the same resource [Gause, 1964]. A

student of Hutchinson, MacArthur, provided mathematical and further theoretical foundation [MacArthur and Levins, 1967] to niche-theory but also to other processes such as dispersal. Another milestone in community ecology was the neutral theory, which was first seen as opposed to niche theory. The neutral theory assumes that species share the same traits and emphasized the importance of stochasticity [Hubbell, 2001] such as ecological drift, introduced e.g., by demographic properties. One study, however, found that assembly processes change along environmental gradients and thus proposed the continuum hypothesis [Gravel et al., 2006]. The continuum hypothesis states that different assembly processes (e.g. niche vs. neutral) are different ends of a continuous gradient, rather than opposing.

In the following decades, the field of community ecology expanded with increasing numbers of survey- and experimental studies, which were describing pattern of species communities. However, while many studies still describe patterns, the focus within community ecology has shifted towards the study of underlying processes rather than patterns [Beck et al., 2012, Keith et al., 2012]. The integration of experiments and phylogenetic, and trait information into community ecology, together with computationally intensive methods (e.g., null models or Approximate Bayesian Computation) provides new opportunities to understand processes of community assembly [McGill et al., 2006]. Parallel to the advancement of community ecology, population genetics developed rapidly and served as blue print for later developments in theoretical community ecology.

1.1.2 Towards assembly processes

Some scientists refer to community ecology as 'a mess' [Lawton, 1999], which does not allow for general rules, whereas most theoretical ecologists agree that general rules can be discovered, if the theoretical background is sufficient [MacArthur and Levins, 1967, Simberloff, 2004]. The advances in population genetics are seen as a model for community ecology, because population genetics have a strong theoretical foundation which led to general and predictable rules [Vellend, 2010]. Population genetics are based on four fundamental processes: selection, drift, mutation, and gene flow (also called the 'Modern Evolutionary Synthesis', [Huxley, 1942]). Although a comparable theoretical basis is still missing for community ecology, recently a conceptual synthesis was developed with population genetics as model [Vellend, 2010]. Vellend reduced the mechanisms leading to local assemblages to four fundamental processes [Vellend, 2010], inspired by the Modern Evolutionary Synthesis in population genetics: speciation, selection, dispersal and ecological drift (Figure 1.1). Previous attempts to a conceptual synthesis [Leibold et al., 2004] were less intuitive as they lacked parallelism to population genetic theory.

Speciation is the evolutionary process that generates new species in a community. Selection refers to the biotic (e.g., competition) and abiotic (e.g., temperature) sorting of species and is thus mainly based on niche-theory. Dispersal was further separated in dispersal limitation and homogenizing dispersal. Dispersal limitation can be the result of niche selection for dispersal relevant traits (e.g., propagule size) or stochastic (e.g., a random change in population or community size). Homogenizing dispersal refers to a process of very high dispersal rates ('mass effects'), which ultimately leads to more similar communities than expected and can thus overwhelm niche selection [Leibold and Chase, 2017]. Ecological drift was initially introduced by neutral theory, which argues that random change in demographic properties (e.g., birth/death or colonization rate) of populations or communities has effects on the community assembly. It has been argued that all proposed theories can be reduced to one of these four fundamental processes [Vellend, 2010]. For example, the mass effects theory can be reduced to homogenizing dispersal; the competitive-exclusion principle and niche theory to selection; neutral theory to dispersal and ecological drift [Stegen et al., 2012]. Concerning the processes that can result in diverging local communities, selection was referred to as deterministic processes, whereas ecological drift and dispersal limitation were referred to as stochastic processes. Much of the earlier debate was centered around the question whether deterministic (thus niche-based) processes vs. stochasticity (neutral processes) determine community assembly [Zhou and Ning, 2017]. However, as studies accumulated both deterministic and neutral processes were found to act together in shaping community assembly, also known as the 'continuum hypotheses' [Gilbert and Lechowicz, 2004, Gravel et al., 2006]. This hypothesis states that community assembly is driven by the joint effects of deterministic and stochastic (thus niche and neutral processes) and that different biological systems differ in the relative contribution of those processes. Further, the relative influence of deterministic and stochastic processes were found to depend on the spatial scale of the study [Nemergut et al., 2013, Barberán et al., 2014, Leibold and Chase, 2017]. Conceptually, local communities are more affected by biotic and abiotic niche selection, low or absent dispersal limitation and a high degree of stochasticity in dispersal and demographic properties [Barberán et al., 2014, Leibold and Chase, 2017]. Whereas regional and global community assembly is more affected by historic (phylogenetic) effects, abiotic niche selection and dispersal limitation and stochasticity become less influential [Barberán et al., 2014, Leibold and Chase, 2017].

Species traits

Ecological Drift

Niche selection

Global community

Regional community

Speciation/
Adaptation

Local community

Dispersal

Observed community
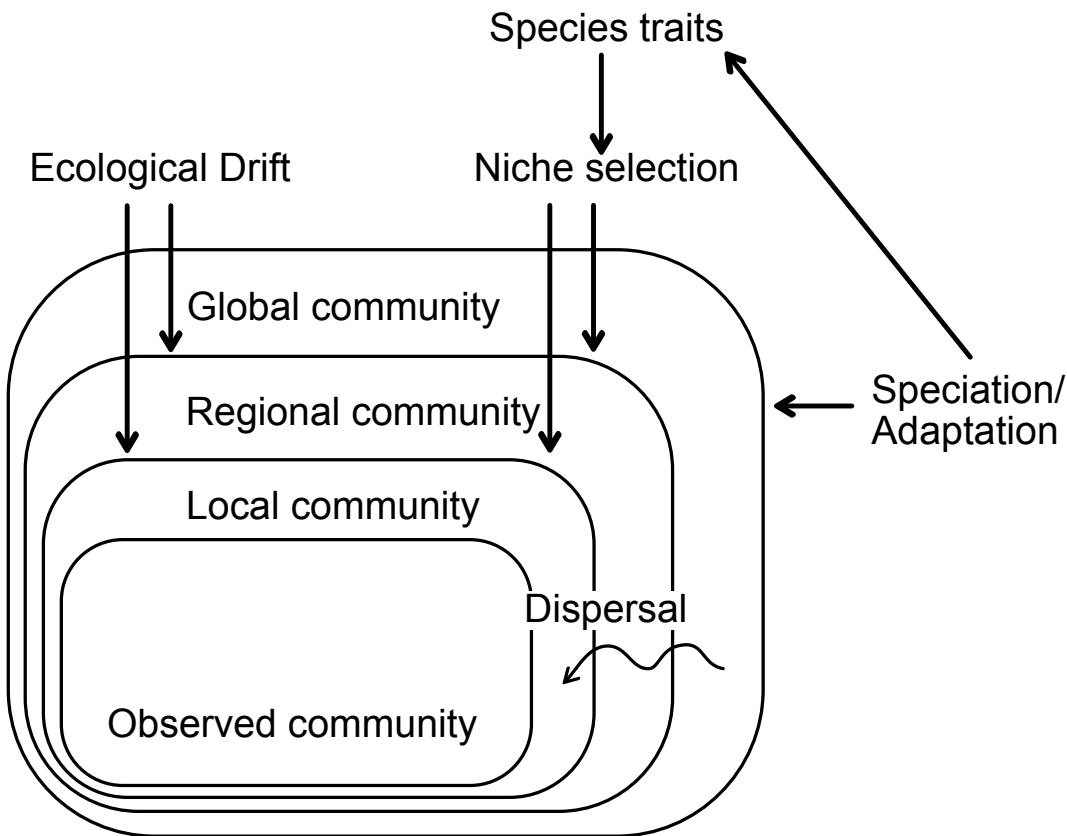
Figure 1.1: Conceptual synthesis showing four basic assembly processes across spatial scales. Graphical concept adapted from [Vellend, 2010] and [Ovaskainen et al., 2017].

1.2 Fungal ecology

1.2.1 Importance of fungi in the terrestrial ecosystem

Fungi are extremely species-rich and perform important ecosystem functions [Van Der Heijden et al., 2008, Hibbett et al., 2014, Larsen et al., 2017]. However, we still lack a basic understanding of the processes underlying fungal community assembly and have also only preliminary knowledge of the evolutionary history of many groups compared with the animal and plant kingdoms [Hinchliff et al., 2015]. Fungi are a very species rich group with a global estimate of 2.2 to 160 million species [Hawksworth and Luecking, 2017, Larsen et al., 2017] and currently approximately 140,000 described species (http://www.catalogueoflife.org/annual-checklist/2018/). Fungi further display a huge diversity of nutritional modes and lifestyles, e.g., parasitic, mutualistic and saprotrophic [Nagy et al., 2017].

Fungi are a kingdom, taxonomically positioned in the Ophistokonta together with the

animal kingdom [Schalchian-Tabrizi et al., 2008]. Fungi are composed of eight divisions, and mushroom-forming fungi are situated paraphyletic within the 'true fungi' (hereafter fungi) formally, the subkingdom Dikarya [Hibbett et al., 2007]. Dikarya consist of two large clades (phyla), Ascomycota and Basidiomycota which differ in the spore-bearing structure, the ascus and the basidium, which gives the clades the names. Within both phyla mushroom-forming fungi can be found in various lineages [Nagy et al., 2017], however, the most commonly known ('typical') fruit body forms can be found in Agaricomycetes, with a stem and cap. Mushroom-forming fungi have the advantage of being easily detected by their mushroom, which have enough features for species identification. Thus, mushroom-forming fungi are of great importance to estimate quantities of community ecology for observed communities, e.g., species richness. Further, the mushroom is the reproductive organ, where sexual spores are produced and released for dispersal, and thus are important structures necessary to the complete the fungal life-cycle [Webster and Weber, 2007].

The majority of mushroom-forming fungi can be classified into either mycorrhizal or saprotrophic [Tedersoo et al., 2010, 2014]. Mycorrhizal fungi are an important component of the diversity of soil microorganismal communities in most terrestrial ecosystems and have tremendous effects on nutrient cycling and plant productivity [Van Der Heijden et al., 2008, Clemmensen et al., 2013, Averill et al., 2014]. Mycorrhizal fungi provide water and nutrients to their plant hosts and also enhance pathogen resistance. In exchange, mycorrhizal fungi retrieve carbon from the plants [Smith and Read, 2010]. Within forest ecosystems the most common and most species-rich mycorrhizal type is the ectomycorrhiza, which forms symbiosis with roots of woody plants without invading the host cells [Smith and Read, 2010]. Saprotrophic fungi decay dead organic matter and release carbon and nutrients, which is crucial in carbon and nutrient cycling [Floudas et al., 2012]. Saprotroph fungi can be classified as either leaf-litter decayer or dead-wood decayer and display a high morphological diversity and host variability (Figure 1.2). Whereas Ascomycota are major agents of litter decay along with litter-decomposing Agaricomycetes, dead-wood is primarily decomposed through Agaricomycetes. This thesis focuses on wood-decay fungi. Most wood-decay fungi can be classified as either white or brown rot decay mode [Riley et al., 2014]. White rot fungi degrade both cellulose and lignin [Blanchette, 1991], reflected by high copy numbers of genes encoding lignin-degrading class II peroxidases and enzymes acting on crystalline cellulose (cellobiohydrolases and lytic polysaccharide monooxygenases [LPMOs]) [Riley et al., 2014]. Brown rot fungi attack cellulose but do not significantly degrade lignin [Worrall et al., 1997], reflected

by loss of many genes encoding class II peroxidases and diverse carbohydrate-active enzymes [Floudas et al., 2012, Riley et al., 2014, Nagy et al., 2015].
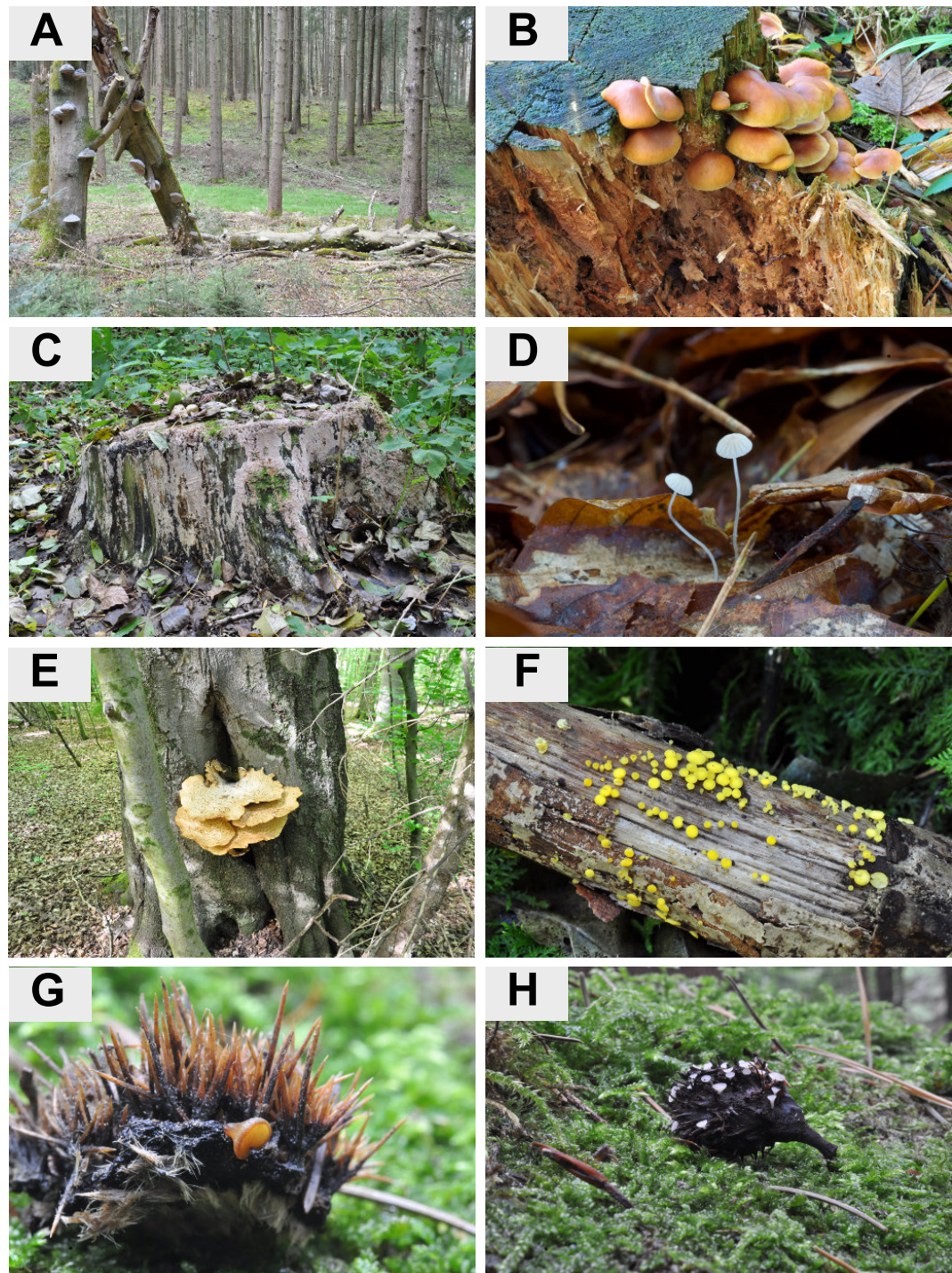
Figure 1.2: Examples for saprotrophic fungi of different fruit body types and on various substrates. A) Bracket fungus, *Fomes fomentarius* on beech (*Fagus sylvatica*) dead wood. B) Pileate mushroom of *Gymnopilus penetrans* on conifer stump. C) Corticoid *Peniophora spec.* on angiosperm stump. D) Pileate mushroom of *Mycena capillaris* on beech leaf. E) *Polyporus squamosus* on beech tree. F) Apothecia of *Bisporella citrina* on conifer branch. G) Apothecia of *Lanzia echinophila* on pericarp of *Castanea sativa*. H) Apothecia of *Phaeohelotium fagineum* on pericarp of *Fagus sylvatica*. Photographs by Franz-S. Krah.

1.2.2 Pattern of fungal community ecology

The patterns of community ecology differ with the spatial scale of the study. On global spatial scales saprotroph fungi were shown to be mainly driven by climate, such as mean annual precipitation [Tedersoo et al., 2014]. Saprotrophs were further affected by spatial predictors [Tedersoo et al., 2014], which indicates dispersal limitation on large spatial scales or unmeasured variables [Lindström and Langenheder, 2012]. On local scales, wood-inhabiting fungi are affected by leaf litter quality (litter saprotrophs, [Hättenschwiler et al., 2011]), host tree identity [Baber et al., 2016, Kahl et al., 2017], microclimate, size of dead wood, amount of dead wood [Heilmann-Clausen and Christensen, 2004, Bässler et al., 2010] and local dead wood [Rolstad et al., 2004, Olsson et al., 2011]. The importance of the amount of dead wood further becomes clear considering threats of modern forestry. Under modern forestry, saprotrophic fungi are threatened because of declining dead-wood amount [Grove, 2002, Bässler et al., 2010]. The decline of dead-wood amount ranges between 90% and 99.5% of that in natural old growth forests [Heilmann-Clausen and Vesterholt, 2008]. Further, fragmentation of dead-wood habitats (forests) threatens wood-inhabiting fungi on local and regional scales [Heilmann-Clausen and Vesterholt, 2008]. Fungi with specialized host requirements were shown to be affected much more from fragmentation at various spatial scales than generalist species [Nordén et al., 2013]. Besides landscape fragmentation, also change in the composition of dead-wood can negatively affect wood-inhabiting diversity. Forest management increases the amount of coniferous wood and reduces the prevalence of large diameters of dead wood [Heilmann-Clausen and Vesterholt, 2008]. A gradient of increasing management intensity has been shown to result in a decrease of functional diversity among saprotrophic fungi [Bässler et al., 2014a].

1.3 Research gap and approaches

Studies on assembly processes of saprotrophic fungi are extremely rare. However, one study found decreasing functional diversity (measured as phylogenetic diversity and based on traits) with increasing management intensity, suggesting changing assembly processes along a land-use gradient [Bässler et al., 2014a]. Further, fungal spores were found to have limited dispersal range [Galante et al., 2011, Norros et al., 2014] and especially rare fungi may be dispersal limited as total propagule numbers are low [Norros et al., 2012], although saprotrophic fungi in general do not seem to be dispersal limited at the landscape scale [Komonen and Müller, 2018]. A recent study tested whether traits

could predict saprotrophic fungal assembly processes and found strong niche selection [Abrego et al., 2017]. Our knowledge about fungal assembly processes is thus restricted to only a few studies, which have mainly been operating at the local to landscape spatial scale.

To study the ecology of species and their interactions, researchers have mainly used methods to produce descriptive statistics, such as alpha diversity measures (e.g., species richness) or beta diversity measures (e.g., community dissimilarity) or other descriptive measures such as SADs or distance decay analysis [Vellend, 2010]. However, all have the disadvantage of being based on anonymous or taxonomic identity. The presence/absence or abundance of a species might however, result from various assembly processes [Leibold and Chase, 2017].

Two fundamental approaches may be followed in understanding assembly processes. First, species share a common evolutionary history. Natural selection favored species traits, which were more adapted to the environment. A central issue with focusing on the taxonomic identity alone, is that species are treated as statistically independent. However, from an evolutionary point of view, this assumptions is wrong and can lead to spurious interpretations [Felsenstein, 1985]. Species share a common evolutionary history, and thus it is often assumed that more closely related species share more similar traits (if traits are phylogenetically conserved), which will ultimately allow them to exist in similar habitats (niche conservatism, [Losos, 2008]).

Thus, a first approach is to ask for the environmental forces which have selected for the traits we observe today in extant species. A fundamental understanding of the evolutionary history of species and the environmental selection that leads to species differences allows to understand and hypothesize distributions of species in the environment. A consequent next step is then to test how traits affect the prevalence of species along environmental gradients, which allows to identify the influence of niche selection by the environment based on species traits. In other words, if the environment selects for the occurrence of a species in a given environment, one might expect to find traits associated with habitats in that environment. The difference in the distribution of traits between habitats could then serve as a measure of niche selection. Thus, instead of comparing species distributions, an alternative and more informative approach is, for example, to focus on the trait distribution of species. The integration of phylogenies into community ecological analysis has become crucial for understanding historical effects underlying community assembly [Webb et al., 2002, Stegen et al., 2012].

This phylogenetic approach has the advantage of a rich evolutionary theory and thus

a mechanistic understanding of how natural selection acts to shape species traits in response to the environment. On the other hand, environmental variables that explain trait distributions are often highly correlated with other environmental variables and thus independent interpretations of their effects are not possible.

Therefore, a second approach is the use of experiments to independently manipulate otherwise confounded environmental gradients. A classical issue in community ecology is the species-area relationship, which states that larger areas harbor a higher diversity of species (pattern). At least two opposing theories explain this observed pattern. The species-energy hypothesis predicts higher resource availability with increasing area [Stokland et al., 2012, Wright, 1983]; the habitat-heterogeneity hypothesis predicts higher habitat diversity with increasing area [MacArthur and MacArthur, 1961]. Experiments have the advantage to disentangle both resource availability and resource heterogeneity and thus address their independent effects. However, such experiments often operate at small ecological scales and a subset of potentially relevant variables, often permitting generalization of results.

1.4 Thesis outline and objectives

The goal of this thesis was to improve the understanding of basic processes of the community assembly of mushroom-forming fungi. Following the two approaches outlined in the previous section, I was first interested in the evolution of saprotrophic fungal host specificity to increase our understanding of the general importance of the host as a filter for fungal evolution and potential selection of traits associated with wood decay. Further following a phylogeny- and trait-based approach, I was then interested whether a morphological trait of mushrooms – their color – explains fungal habitat prevalence across Europe. Following the second approach, I then used a dead-wood experiment to disentangle independent effects of the host and environmental factors on the diversity of saprotrophic wood-inhabiting fungi. In a first analysis, the relative effects on classical quantities of community ecology were of importance to be able to compare results to previous, inconsistent, studies. A second analysis based on the experiment compared the influence of different assembly processes on fungal communities in comparison to other wood-inhabiting taxa. The aim was to test if differences in assembly processes could be explained by the trait organism size by also integrating phylogenetic information. Based on these results, I provide a deeper mechanistic understanding of the processes underlying saprotrophic wood-inhabiting fungal assembly based on two fundamental ap-

proaches, and thus lay the ground for new hypotheses and future directions.

The specific objectives of this thesis were (Figure 1.3):

1. To test whether different saprotrophic functional groups (decay modes) differ in their host specificity, to increase the mechanistic understanding of the host as a driver of niche selection of the diversity of saprotrophic wood-inhabiting fungi

2. To test whether color explains the prevalence of fungi along a large spatial environmental gradient, to generate a mechanistic understanding on how morphological traits of the reproductive organ of fungi (mushroom) affect the assembly of fungal communities

3. To identify the independent drivers of the diversity of saprotrophic wood-inhabiting fungi in a dead-wood experiment. In particular, the relative and independent effects of the host vs. the environment on diversity of saprotrophic wood-inhabiting fungi

4. To test whether organism size predicts assembly processes of three wood-inhabiting taxa (bacteria, fungi and beetles) to generate a mechanistic understanding of underlying assembly processes of various saproxylic organism groups
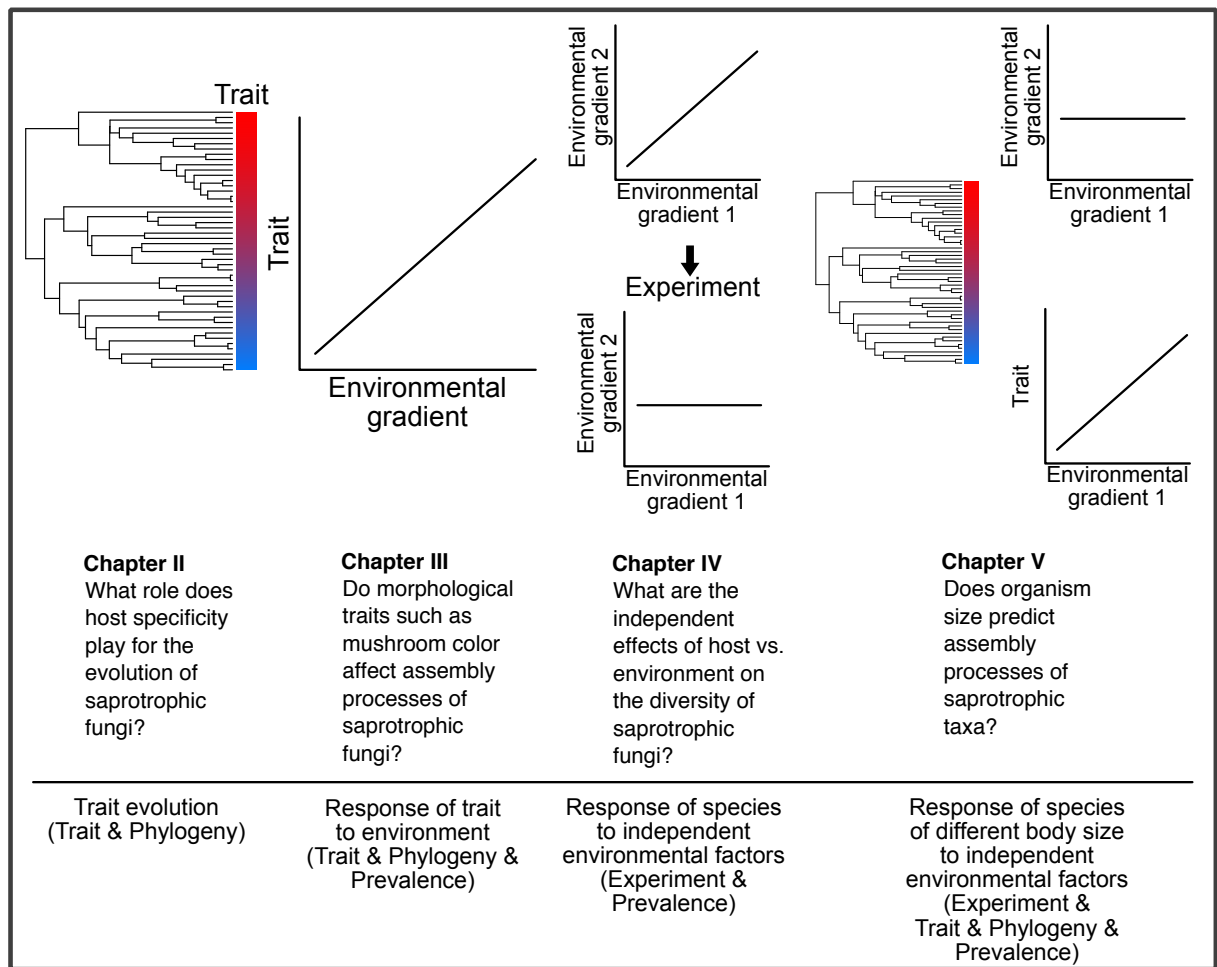
Figure 1.3: Conceptual overview of PhD thesis.

The chapters 2, 4 and 6 are published:

- Franz-Sebastian Krah, Sebastian Seibold, Roland Brandl, Petr Baldrian, Jörg Müller, and Claus Bässler. Independent effects of host and environment on the diversity of wood-inhabiting fungi. *Journal of Ecology*, 106(4):1428–1442, 2018b; Impact factor: 5.17 (2017); https://besjournals.onlinelibrary.wiley.com/doi/10.1111/1365-2745.12939

- Franz-Sebastian Krah, Claus Bässler, Christoph Heibl, John Soghigian, Hanno Schaefer, and David S Hibbett. Evolutionary dynamics of host specialization in wood-decay fungi. *BMC Evolutionary Biology*, 18(1):119–132, 2018a; Impact

factor: 3.03 (2017); `https://bmcevolbiol.biomedcentral.com/articles/10.1186/s12862-018-1229-7`

- Franz-Sebastian Krah, Scott T. Bates, and Andrew N. Miller. rmycoportal - an r package to interface with the mycology collections portal. *Biodiversity Data Journal*, 7:e31511, 2019; Impact factor: 1.26 (2017); `https://bdj.pensoft.net/article/31511/`

1.5 Authors contributions

Chapter 2

FSK designed the study, carried out the sequence assembly and statistical analyses and wrote the manuscript. Further, **FSK** wrote the code for the R package "rusda".
Part of the data was generated within the Masters thesis of Franz-S. Krah, but data and statistical analyses used changed significantly between the masters thesis and the PhD thesis.

DSH designed the study and drafted the manuscript; CB and HS drafted earlier versions of the manuscript. JS helped with statistical method selection and drafted the manuscript. CH carried out sequence assembly. All authors read and commented on the final version of the manuscript. This research was supported by United States National Science Foundation awards IOS-1456777 to DSH.

Chapter 3

FSK had the original idea, designed the study, sampled color data, planned and performed statstical analyses, interpreted the results and wrote the manuscript. **FSK** further conducted temperature experiment and prepared environmental grid data for analysis.

CB had the original idea, designed the study, planned analyses, interpreted the results and wrote the manuscript; UB, HS, LB, CA, ACG, EH, JHC, JM, IK-G, TWK, JD, RH, JN and HK commented on drafts and helped to refine and focus the writing and interpretation; HK, JHK, PMK, IK-G, TWK, BSI, SE, ACG, KH; JN, and FR contributed fungal distribution data; AH contributed sampling of color data; RK conducted temperature experiment; CH helped construct the phylogeny; RF advised on phylogenetic data analyses; CA, and PP prepared environmental grid data for analysis.

Fungal distribution data was provided by the Climate change effects on the fungal ecosystem component (ClimFun) project funded by the Research Council of Norway. For details see [Andrew et al., 2017].

Chapter 4

FSK analysed and interpreted the data and wrote the manuscript. **FSK** conducted field work (fungal identification on dead wood logs).

CB, JM, PB and RB designed the concept of the study; CB contributed analysis, interpretation and drafting the manuscript. RB contributed to data analysis; SS contributed to data collection and interpretation of the data. All authors critically revised the manuscript.

The dead wood experiment within the BioHolz project was funded by the Bundesministerium für Bildung und Forschung (Grant/Award Number: 01LC1323A). The fungal inventories were mainly performed by taxonomic specialists.

Chapter 5

FSK designed the concept of the study, analyzed the data, interpreted results and wrote the manuscript.

CB, JM, PB invented the study design. CB designed the concept of the study and contributed interpretation and drafting the manuscript. SS contributed to data collection. PB conducted sequencing. PJ helped with early, JH with late drafts of the manuscript.

The dead wood experiment within the BioHolz project was funded by the Bundesministerium für Bildung und Forschung (Grant/Award Number: 01LC1323A). Sequencing of environmental samples (meta-barcoding) was done by PB. PB was supported by the research concept of the Czech Science Foundation (grant number 17-20110S).

Chapter 6

FSK had the initial idea of the R package, wrote the R code and the first draft of the manuscript.

SB and AM revised the manuscript.

List of co-authors

Name		Abbreviation
Carrie	Andrew	CA
Petr	Baldrian	PB
Claus	Bässler	CB
Scott	Bates	SB
Lynne	Boddy	LB
Roland	Brandl	RB
Ulf	Büntgen	UB
Jeffrey	Dietz	JD
Simon	Egli	SE
Robert	Freckleton	RF
Alan C.	Gange	ACG
Jonas	Hagge	JH
Rune	Halvorsen	RH
Einar	Heegard	EH
Christoph	Heibl	CH
Antje	Heideroth	AH
Jacob	Heilmann-Clausen	JHC
David S.	Hibbett	DSH
Klaus	Høiland	KH
Pu	Jia	PJ
Ritwika	Kar	RK
Håvard	Kauserud	HK
Paul M.	Kirk	PMK
Irmgard	Krisai-Greilhuber	IK-G
Thomas W.	Kuyper	TWK
Andrew	Miller	AM
Jörg	Müller	JM
Jenni	Norden	JN
Phillip	Papastefanou	PP
Hanno	Schäfer	HS
Sebastian	Seibold	SS
Beatrice	Senn-Irlet	BSI
John	Soghigian	JS

1 Introduction

2 Evolutionary dynamics of host specialization in wood-decay fungi

Abstract

The majority of wood decomposing fungi are mushroom-forming Agaricomycetes, which exhibit two main modes of plant cell wall decomposition: white rot, in which all plant cell wall components are degraded, including lignin, and brown rot, in which lignin is modified but not appreciably removed. Previous studies suggested that brown rot fungi tend to be specialists of gymnosperm hosts and that brown rot promotes gymnosperm specialization. However, these hypotheses were based on analyses of limited datasets of Agaricomycetes. Overcoming this limitation, we used a phylogeny with 1157 species integrating available sequences, assembled decay mode characters from the literature, and coded host specialization using the newly developed R package, *rusda*.

We found that most brown rot fungi are generalists or gymnosperm specialists, whereas most white rot fungi are angiosperm specialists. A six-state model of the evolution of host specialization revealed high transition rates between generalism and specialization in both decay modes. However, while white rot lineages switched most frequently to angiosperm specialists, brown rot lineages switched most frequently to generalism. A time-calibrated phylogeny revealed that Agaricomycetes is older than the flowering plants but many of the large clades originated after the diversification of the angiosperms in the Cretaceous. Our results challenge the current view that brown rot fungi are primarily gymnosperm specialists and reveal intensive white rot specialization to angiosperm hosts. We thus suggest that brown rot associated convergent loss of lignocellulose degrading enzymes was correlated with host generalism, rather than gymnosperm specialism. A likelihood model of host specialization evolution together with a time-calibrated phylogeny further suggests that the rise of the angiosperms opened a new mega-niche for wood-decay fungi, which was exploited particularly well by white rot lineages.

2.1 Introduction

About 2000 billion tons of carbon is present in terrestrial ecosystems [McCarl et al., 2007], of which 550 billion tons are fixed in vegetation [Siegenthaler and Sarmiento, 1993]. In forest ecosystems, most plant biomass is stored in the form of dead wood [Horwath, 2007]. Woody plant cell walls consist mainly of the lignocellulose complex which is composed of the polymeric polysaccharides cellulose, hemicellulose and lignin heteropolymers [Lundell et al., 2010, Welker et al., 2015]. Cellulose is a macropolymer consisting of linear chains of glucose subunits that can take on a recalcitrant crystalline form [Medie et al., 2012]. Hemicelluloses are matrix polysaccharides consisting of various heteropolymers, e.g., of xylans and glucomannans [Sjöström, 1981]. Lignin is a complex aromatic polymer that is resistant to hydrolytic degradation [Bugg et al., 2011]. The amount of cellulose in woody plants is 40–50% of the wood dry weight and for hemicelluloses and lignin 15–30% each. The plant biomass further consists of macromolecules such as lipids, waxes, proteins and phenolic compounds [Horwath, 2007]. The most efficient agents of the decay of the lignocellulose complex are saprotrophic fungi, which therefore play pivotal roles in the cycling of carbon [Heimann and Reichstein, 2008] and nutrients [Harley, 1971] in the forest ecosystem. Wood is produced by angiosperms and gymnosperms, which together comprise more than 60,000 species [Beech et al., 2017]. Angiosperms regularly have lower amounts of lignin than gymnosperms, whereas angiosperms regularly have higher amounts of cellulose than gymnosperms [Cornwell et al., 2009, Thakur and Thakur, 2014]. Further, angiosperms often have lower amounts of non-structural secondary compounds (plant extractives) than gymnosperms [Pichersky and Gang, 2000, Pallardy, 2008, Cornwell et al., 2009, Thakur and Thakur, 2014], with some exceptions, e.g., species of the genera *Quercus*, *Fagus* or *Malus* [Wagenführ and Scheiber, 2007].

The main agents of wood decay are members of the class Agaricomycetes (Basidiomycota). Agaricomycetes contains about 21,000 species with a worldwide distribution, including many lifestyles, e.g. mycorrhizal symbionts, pathogens, and saprotrophs. Most saprotrophic fungi within the Agaricomycetes are dead wood decaying fungi. Dead wood decay modes can be classified as either white or brown rot. Brown rot fungi attack cellulose but do not significantly degrade lignin [Worrall et al., 1997], resulting in a brownish residue that breaks into cubical fragments, whereas white rot fungi degrade both cellulose and lignin [Blanchette, 1991], leaving a bleached fibrous residue (Figure 2.1). Hemicellulose can be degraded by both brown and white rot fungi [Lundell et al., 2014]. Whereas dead wood is mainly decayed by Agaricomycetes, in plant litter decay, Ascomycota play

a significant role along with litter-decomposing Agaricomycetes [Schneider et al., 2012, Lundell et al., 2014]. Other decay modes are also present, such as 'soft rot' in some Ascomycota and 'grey rot' in some Basidiomycota such as *Schizophyllum commune* [Riley et al., 2014]. Although many ectomycorrhizal fungi are partially saprotrophic, their decay abilities are considered marginal compared to wood decay fungi [Maijala et al., 1991, Rineau et al., 2013].
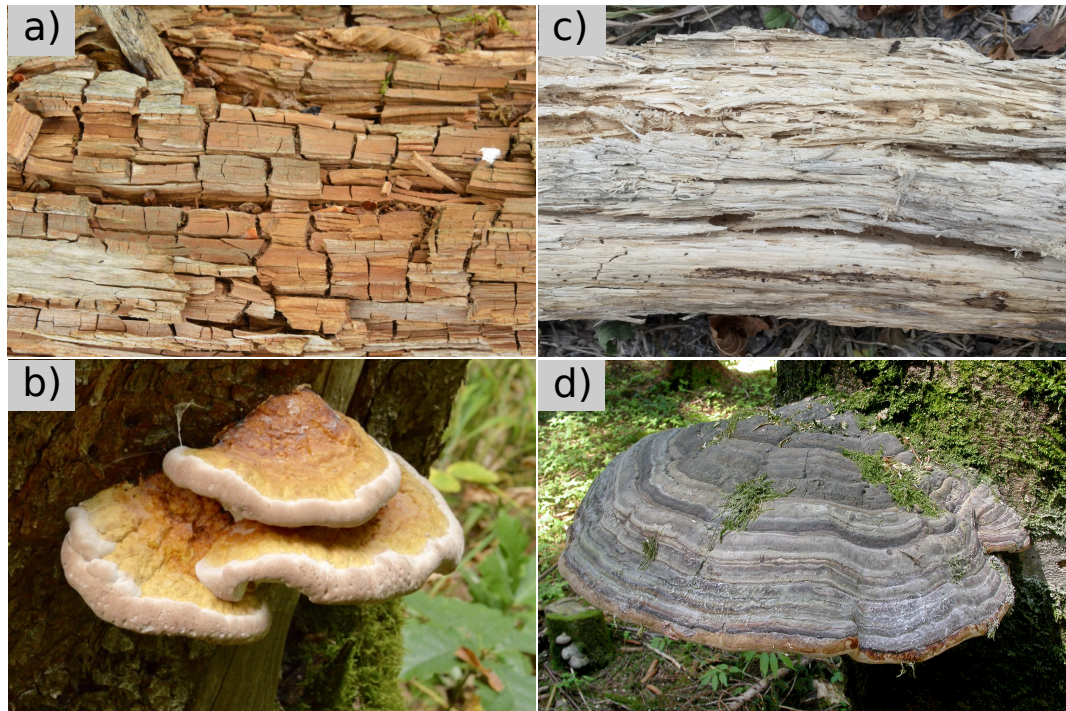
Figure 2.1: Brown and white rot residues and fungal fruit bodies. a) Brown rot residue, b) brown rot fungus, *Fomitopsis pinicola* (Polyporales, Fomitopsidaceae), c) white rot residue, d) white rot fungus, *Fomes fomentarius* (Polyporales, Polyporaceae). Photographs by Franz-S. Krah (a,b,c) and Heinrich Holzer (d).

The enzymatic basis of the differences between white rot and brown rot has been studied extensively in comparative genomic analyses [Floudas et al., 2012, Riley et al., 2014, Nagy et al., 2014, Kohler et al., 2015]. White rot fungi are distinguished by high copy numbers of genes encoding different carbohydrate-active enzymes (CAZymes) which are classified based on the CAZy database [Lombard et al., 2014]. In general, CAZymes, which act on crystalline cellulose are more abundant in white rot genomes compared with brown rot [Floudas et al., 2012]. Glycoside hydrolase (GH) families (e.g., GH6 and GH7, including cellobiohydrolases) are more abundant in white rot compared with brown rot fungi [Floudas et al., 2012]. Further, lytic polysaccharide monooxygenases (LPMOs)

from the AA9 family are more abundant in white than brown rot fungi [Floudas et al., 2012]. Apart from Agaricomycetes, LPMOs can be found in Ascomycetes and Mucoromycotina [Floudas et al., 2012, Riley et al., 2014]. Finally, lignin-degrading class II peroxidases (AA2) and other heme-containing peroxidases are more common in white rot, and reduced or absent in brown rot fungi [Kohler et al., 2015] (for mechanisms of action see [Hofrichter et al., 2010]). The most recent common ancestor of Agaricomycetes was a white rot species (based on an inferred expansions of AA2 and other lignocellulolytic enzymes) with at least four independent origins of brown rot, correlated with parallel losses of genes encoding diverse CAZys, and the complete loss of ligninolytic class II peroxidases (AA2) [Floudas et al., 2012], making reversals to white rot unlikely. This white rot ancestor likely lived roughly 290 (+/- ca. 70) million years ago (MYA) [Floudas et al., 2012]. Analyses of a sample of 62 genomes [Nagy et al., 2014] suggested that expansions of cellobiohydrolases (GH6, GH7), LPMOs (AA9), and other plant cell wall degrading enzymes occurred early in the evolution of Agaricomycetes, prior to the expansion of class II peroxidases (AA2).

Gilbertson [Burdsall et al., 2012] investigated ecological differences between white and brown rot decay modes, noting that brown rot fungi preferentially occur on gymnosperm hosts [Gilbertson, 1980]. Gilbertson thus suggested a correlated evolution of brown rot decay mode and gymnosperm specialization. One study tested Gilbertson's hypothesis using phylogenetic comparative methods [Hibbett and Donoghue, 2001]. Their results suggested that the evolution of brown rot was correlated with the evolution of exclusive decay of gymnosperm hosts. However, this inference was made from a dataset with limited taxonomic sampling, with only a total of 130 species [Hibbett and Donoghue, 2001].

To assess the evolution of decay modes and patterns of host specialization among wood decay fungi in Agaricomycetes, we utilized a time-calibrated mega-phylogeny approach and drew on the extensive Fungus-Host Distribution Database built by the United States Department of Agriculture (USDA) [Farr et al., 2017]. We then used this mega-phylogeny and host associations, which encompassed 1157 species from 14 orders, to test two hypotheses: (1) brown rot fungi occur primarily on gymnosperm hosts; and (2) brown rot fungi switched more frequently towards gymnosperm hosts than white rot lineages. We further use this large-scale dataset to investigate white rot specialization pattern and mechanisms, a topic currently neglected due to a focus on specialization pattern of brown rot fungi.

2.2 Material and Methods

2.2.1 Trait data and character matrix

To test our hypotheses, we gathered data on decay mode and host associations for Agaricomycetes. For decay mode, we used the 'decay.type' as published in [Tedersoo et al., 2014], which is available on the genus level, and we also conducted a literature search for additional genera. This study investigated lifestyle-dependent global fungal diversity and therefore coded the trophic status (six states, e.g., biotroph), the lifestyle (17 states, e.g., ectomycorrhizal) and decay type (four states, e.g. white rot, brown rot) for more than 10000 genera [Tedersoo et al., 2014]. We used only species with either white or brown rot in our analysis and excluded other lifestyles (e.g., mycorrhizal). This gave us the decay mode of particular species in the genera. We then extrapolated this decay mode to the remaining species of a genus (with one exception, see below). Our justification is that decay mode has often been a focus of taxonomists and thus was widely used to distinguish genera such as *Antrodia* and *Antrodiella* [Kim et al., 2003], *Lentinus* and *Neolentinus-Heliocybe* [Molina et al., 1992], and *Daedalea* and *Daedaleopsis* [Rathod, 2011]. We found only three genera where more than one decay mode has been reported: *Clitocybula* [Wesenberg et al., 2002, Barrasa et al., 2006], *Hyphoderma* [Gilbertson et al., 1974], and *Mucronella* [Gilbertson et al., 1974, Petersen, 1980]. *Clitocybula* and *Mucronella* were deleted from the dataset because no host data were available. For *Hyphoderma* we used only the two species where decay mode references were found. To estimate how this strategy might affect our interpretations, we re-sampled a single species per genus from our final dataset (hereafter 'one-genus-subset') and repeated the analyses described below 100 times.

To gather data on host associations, we used the R package 'rusda', written for this study, as an interface to the USDA Fungus-Host Distribution Database (FHDD) [Farr et al., 2017]. The FHDD contains fungus-host combinations, but does not provide information on the occurrence frequencies on a particular host (other than the number of published records on each host). The 'rusda' package makes it possible to retrieve ('query') host data for fungal species, and vice versa. For a detailed description, basic usage and evaluation of the R package 'rusda', see Supplementary Text 1 (p. 91).

To retrieve host associations from the FHDD we used the function associations, which takes an input of species names and provides an output list of fungus-host combinations. As input we used the NCBI taxonomy for fungi and re-classified the order level where necessary (Table 2.1). We then produced a dataset of plant phyla by matching host genera to the Spermatophyta taxonomy downloaded from NCBI taxonomy using the R

package 'megaptera'. Thus, we retrieved the phylum information 'Acrogymnosperma' and 'Magnoliophyta' for each host species. We refer to 'Magnoliophyta' as angiosperm (A) and 'Acrogymnosperma' as gymnosperm (G) and stored the number of gymnosperm and angiosperm associations for each fungus species in a table. Species which did not belong to either Acrogymnosperma or Magnoliophyta were deleted from the dataset. We further deleted all non-woody plants based on the woodiness dataset which classified more than 35000 plants into woody and non-woody [FitzJohn et al., 2014]. Thus, the final host dataset included only woody plants from Acrogymnosperma or Magnoliophyta; seedless vascular plants, bryophytes, algae, and non-plant hosts were excluded. The FHDD covers mainly temperate North America and Europe [Farr et al., 2017].

The host association data were used to calculate the number of angiosperm and gymnosperm host species for each fungus species. We defined the 'gymnosperm association' by dividing the number of gymnosperm host tree species (NG) by the sum of the number of angiosperm (NA) and gymnosperm host tree species: gymnosperm associations [%] = NG/(NG + NA). Thus, a gymnosperm association of 100% means that a fungus is reported exclusively on gymnosperm hosts in the Fungus-Host database, whereas 0% means only angiosperm hosts are reported. We classified host preferences into three states: (1) generalism, (2) angiosperm specialization, or (3) gymnosperm specialization. Based on the distribution of gymnosperm association [%] (Figure 2.7C), we defined specialization based on the gymnosperm association [%] with a threshold of $\geqslant 90\%$ for gymnosperm specialization and a threshold of $\leqslant 10\%$ for angiosperm specialization (hereafter '90-10 specialization'). Previous studies used exclusivity as a measure of host association [Hibbett and Donoghue, 2001], but missing or incorrect data for a single fungus observation may then lead to wrong classification of a species. Nonetheless, we also inferred our final model (see Statistics and models of host specialization, p. 78) using the exclusivity coding (hereafter '100-0 exclusivity'). However, in the exclusivity coding, generalists and non-exclusive specialists are coded in one state ('generalists') and thus results might be hard to interpret.

2.2.2 Mega-phylogeny approach

To test dynamics of host switching, we used phylogenetic comparative methods (PCMs). For this purpose, we applied a mega-phylogeny approach using the R package 'megaptera' V. 1.0-25, a pipeline for large-scale automated sequence-retrieval and alignment [Heibl, 11-15.11.2014] (version available on https://github.com/heibl/megaptera). The mega-phylogeny approach aims at maximising taxon sampling integrating previous knowledge (e.g. taxonomic information, backbone trees) into the tree inference [Smith et al., 2009].

For our mega-phylogeny approach, we used a backbone guide tree based on phylogenomic analyses [Floudas et al., 2012, Nagy et al., 2014, Kohler et al., 2015] to provide information for deep splits (order level), as resolving such ancient divergences can be difficult due to sequence saturation [Smith et al., 2009]. Further, mega-phylogeny approaches often lead to a high number of gaps or missing data, often more than 90% [Smith et al., 2009]. To reduce the bias of missing data, we computed a reliability measure for each column of the alignment, which is then supplied to the tree inference program. In this way, uncertain regions in the alignment are down-weighted in the phylogeny inference step.

First, we used the R package 'megaptera' to download all sequences for the species with decay mode and host association information from GenBank [Benson et al., 2012] (queried February 2017). We selected seven DNA regions: 18S, 28S and 5.8S rRNA (nuclear ribosomal RNA genes), genes encoding RNA polymerase b (rpb1, rpb2), translation elongation factor 1 (tef1), and ATP synthetase (atp6). We chose the rRNA regions to obtain high species numbers and the other regions for resolution of deeper nodes [Binder et al., 2013]. Only sequences of samples identified to species level were accepted.

We used single sequences where only one sequence for a particular species and DNA region was available. If multiple sequences were available, all sequences of the same DNA region and organism (putative conspecific sequences) were aligned and a majority rule consensus sequence was calculated. In the next step, all sequences were compared to three to six Agaricomycotina reference sequences for each DNA region as a quality check (Table 2.2).

Table 2.1: Re-classification of taxonomic orders based on [Binder et al., 2005, Hibbett et al., 2014, Larsson, 2007]

NCBI Taxonomy	Order	Genus
Polyporales	Agaricales	*Grifola*
Atheliales	Agaricales	*Plicaturopsis*
Polyporales	Agaricales	*Xerotus*
Polyporales	Amylocorticiales	*Anomoloma*
Polyporales	Amylocorticiales	*Anomoporia*
Russulales	Atheliales	*Cristinia*
Amylocorticiales	Atheliales	*Irpicodon*
Atheliales	Corticiales	*Athelopsis*
Hymenochaetales	Corticiales	*Basidioradulum*
Polyporales	Corticiales	*Byssomerulius*
Polyporales	Corticiales	*Candelabrochaete*
Polyporales	Corticiales	*Crustoderma*
Agaricales	Corticiales	*Cylindrobasidium*
Russulales	Corticiales	*Dendrophora*
Polyporales	Corticiales	*Dentocorticium*
Polyporales	Corticiales	*Hyphoderma*
Hymenochaetales	Corticiales	*Hyphodontia*
Atheliales	Corticiales	*Hypochniciellum*
Polyporales	Corticiales	*Hypochnicium*
Russulales	Corticiales	*Laurilia*
Polyporales	Corticiales	*Phlebia*
Polyporales	Corticiales	*Pulcherricium*
Agaricales	Corticiales	*Radulomyces*
Polyporales	Corticiales	*Rhizochaete*
Hymenochaetales	Corticiales	*Schizopora*
Polyporales	Corticiales	*Scopuloides*
Cantharellales	Corticiales	*Sistotrema*
Hymenochaetales	Corticiales	*Tubulicrinis*
Polyporales	Gloeophyllales	*Neolentinus*
Russulales	Gomphales	*Ramaricium*
Polyporales	Hymenochaetales	*Phaeolus*
Polyporales	Hymenochaetales	*Resinicium*
Amylocorticiales	Polyporales	*Ceraceomyces*
Corticiales	Russulales	*Galzinia*
Agaricales	Russulales	*Granulobasidium*
Polyporales	Russulales	*Lopharia*

Table 2.2: Table of reference species and association numbers from NCBI

Subdivision	Species	5.8S rRNA	28S rRNA	18S rRNA	rpb1	rpb2	tef1	atp6
Agaricomycotina	*Clavaria zollingeri*			AY657008				
Agaricomycotina	*Coprinus comatus*	AF438568	AY635772	AY665772	AY857983	AY780934	AY881026	DQ131603
Agaricomycotina	*Climacodon sepentrionalis*			AY705964				
Agaricomycotina	*Ramaria rubella*			AY707095				
Agaricomycotina	*Calocera cornea*			AY771610				
Agaricomycotina	*Rhizoctonia solani*			Genome				

We used the R package 'megaptera' to calculate the identity (proportion of nucleotides identical) and coverage (proportion of nucleotide positions in common) with the reference. Based on the coverage and identity values, thresholds can be adjusted aiming to maximize both quality and number of taxa. The default values are 0.75 for identity and 0.5 for coverage. Based on visual inspection of the alignments, we chose identity thresholds between 0.5 and 0.75 and coverage thresholds between 0.25 and 0.5 for the seven gene regions. All sequences outside these limits were discarded.

We aligned the remaining sequences for each gene region separately, using GUIDANCE2 [Penn et al., 2010, Sela et al., 2015] with the multiple sequence alignment program MAFFT [Katoh and Standley, 2013]. GUIDANCE2 computes a reliability score for each column based on alternative alignments produced by bootstrap guide trees and four co-optimal alignments based on each bootstrap alignment, created by the heads or tails algorithm [Landan and Graur, 2008]. We passed the resulting column score as character weights to the phylogeny inference program RAxML (flag -a; see additional details on phylogenetic inference below) rather than filtering the alignment using the column score, which is not recommended [Tan et al., 2015]. We used IQ-TREE version 1.5.3 with specification '-TESTMERGEONLY' [Nguyen et al., 2015, Chernomor et al., 2016] to select a partition scheme among the gene regions. IQ-TREE found six blocks as the best partitioning scheme (merging the 5.8S rRNA and 28S rRNA into one partition; Table 2.3). The final alignment had 37466 sites and the proportion of gaps was 92.07% with 16814 distinct alignment patterns.

Table 2.3: Best partition scheme found by IQ-Tree.

DNA	58s & 28s rRNA	1-7098, 7099-14016
DNA	18s rRNA	14017-18413
DNA	rpb1	18414-25159
DNA	rpb2	25160-29754
DNA	atp6	29755-33001
DNA	tef1	33002-37466

We produced a comprehensive backbone guide tree by first assembling an order-level 'genomic' based backbone tree (Figure 2.2A) from the literature [Floudas et al., 2012, Nagy et al., 2014, Kohler et al., 2015] and then attaching all species on the order-level tips of the genomic backbone tree (Figure 2.2 B). We performed maximum likelihood estimation, using the concatenated supermatrix of the seven DNA regions, with RAxML [Stamatakis et al., 2008] on the CIPRES Science Gateway v.3.3 (RAxML -HPC2 on XSEDE 8.1.11) [Miller et al., 2011] under the GTRGAMMA model with partitioning as

Table 2.4: Tip state frequencies of white and brown rot specialization based on different thresholds of host association [%]. Exclusivity: 100% = gymnosperm specialist, 0% = angiosperm specialist. 90-10 specialization: > 90% = gymnosperm specialist, < 10% = angiosperm specialist. A = Angiosperm; G = Gymnosperm; Gen = Generalist; W = White rot; B = Brown rot.

Specialisation threshold	A-B	A-W	G-B	G-W	Gen-B	Gen-W
90-10 Specialization	35	530	36	169	55	332
100-0 Exclusivity	31	428	26	145	69	458

described above, the GUIDANCE2 column score (flag –a) and the comprehensive backbone tree (flag –g). We subsequently conducted 1000 approximate Shimodaira–Hasegawa likelihood ratio tests (SH-aLRT branch support). SH-aLRT which are fast, accurate and robust even for larger phylogenies [Anisimova et al., 2011].

We estimated divergence times of the resulting phylogeny using penalized likelihood as implemented in the R function chronos from the R package 'ape' [Paradis et al., 2008]. We used two calibration points, a Late Cretaceous mushroom fossil *Archaeomarasmius legetti* [Hibbett et al., 1997], which bears a strong resemblance to extant Agaricales (particularly Marasmiaceae), and a Middle Eocene ectomycorrhizal fossil, which has been interpreted as a representative of Boletales [LePage et al., 1997]. We followed the strategy of a previously published study and used the ectomycorrhizal fossil to calibrate Boletales with a stem age of 40-60 MYA [Kohler et al., 2015] and *A. legetti* to date Agaricales with a stem age range of 70-110 MYA. We also tried the approach of [Floudas et al., 2012] and used 50 and 90-94 MYA as age priors, which yielded almost identical divergence time estimates (results not shown).

We applied chronos with three different models of substitution rate variation among branches: 'relaxed', 'correlated' and 'strict' and compared the model fits using ΦIC [Paradis, 2013]. The 'correlated' model had lowest ΦIC values and thus was used for further analysis. We are aware that penalized likelihood does not make use of the sequence data and does not incorporate phylogenetic uncertainty. However, algorithms that perform joint inferences of the tree and divergence times currently do not implement an option for character weights, e.g. BEAST [Drummond and Bouckaert, 2015] or character weights and guide tree, e.g. ExaBayes [Aberer et al., 2014].

To account for phylogenetic uncertainty at nodes with low support values, we produced alternative trees based on the maximum likelihood phylogeny (Figure 2.3). We created hard polytomies on nodes with SH-like support values < 80 based on the non-ultrametric ML tree (Appendix Figure A.1).

We then used the function multi2di from the R package 'ape' [Paradis et al., 2008] and resolved the polytomies randomly and used chronos (as described above) to estimate divergence times. We repeated this 100 times and summarized the dated trees using TreeAnnotator [Drummond et al., 2012] to calculate a maximum clade credibility tree (MCCT) with the node option 'Common ancestor heights' (because the nodes did not share the same ancestors since polytomies were created at random). We displayed confidence intervals of the divergence time estimates as HPD (highest posterior density) for the brown rot clades and the root. Furthermore, we use the 100 ultrametric trees as input for the transition rates estimation to measure robustness of the results against phylogenetic uncertainty.
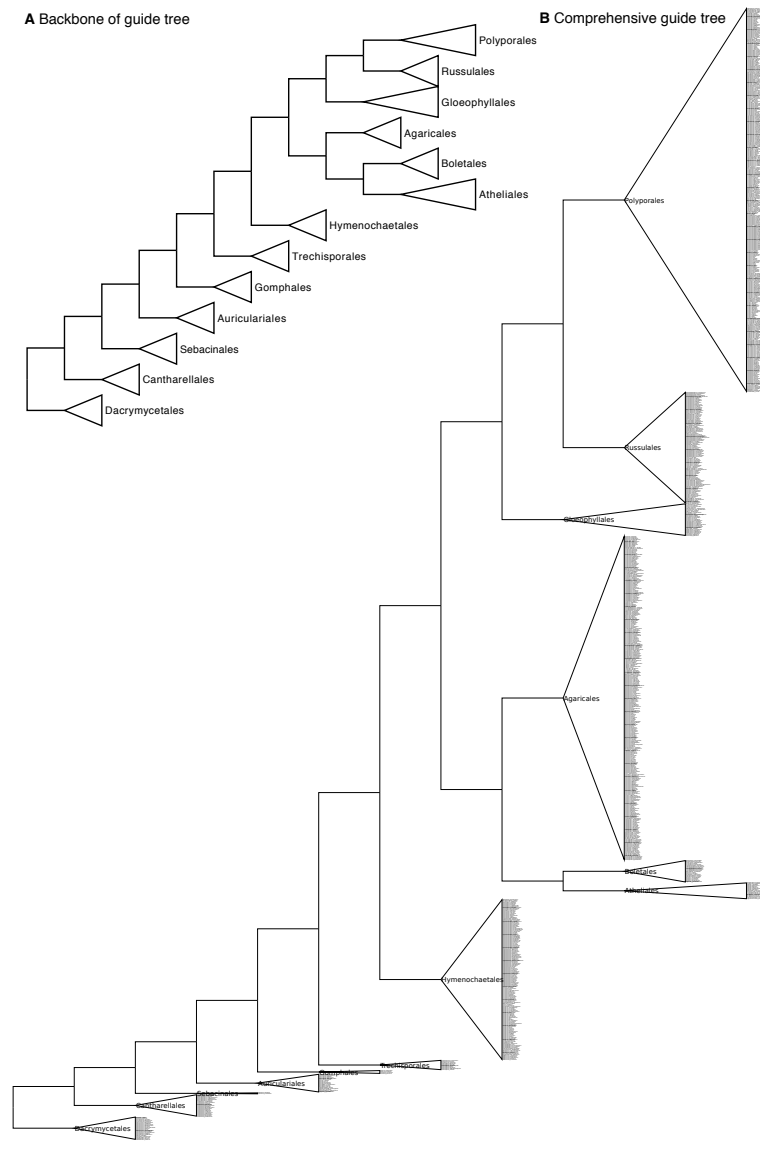
Figure 2.2: Genomic phylogenetic tree compiled from [Floudas et al., 2012, Kohler et al., 2015, Nagy et al., 2015] used as the backbone for the comprehensive guide tree for the RAxML tree inference. Dacrymycetales served as outgroup. A) Backbone of the guide tree. B) Comprehensive guide tree, which is the backbone guide tree with species attached based on their systematic order classification with zero branch lengths.
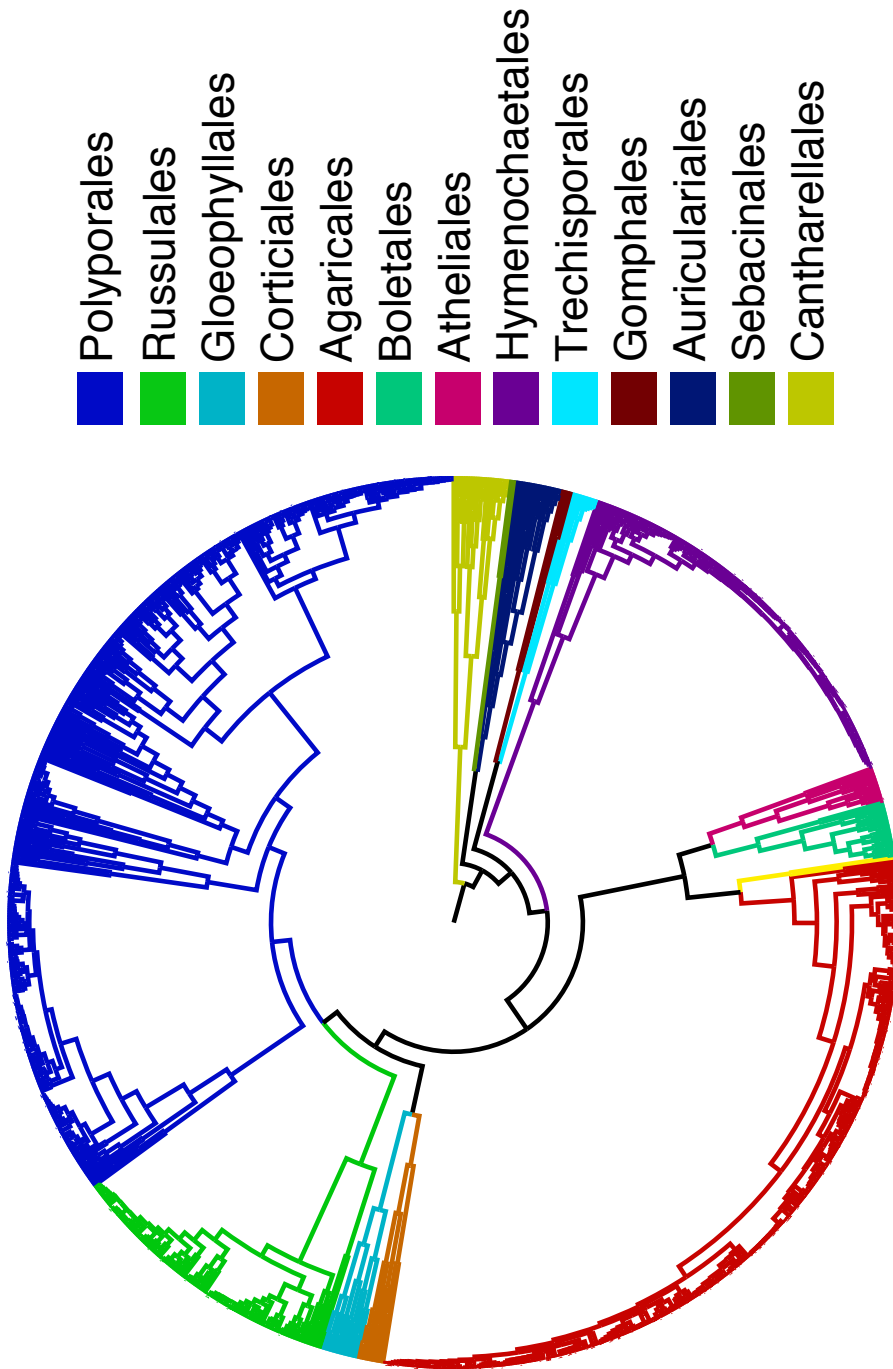
Figure 2.3: Maximum Likelihood phylogeny of the Agaricomycetes with color coding for 14 orders. The largest orders in terms of tips are Polyporales, Agaricales, Hymenochaetales and Russulales.

2.2.3 Statistics and models of host specialization

We first tested preferences of host species among extant fungi of the two decay modes using a phylogenetic linear model in the R package 'phylolm' [Ho and Ané, 2014]. We tested whether the number of host species (host range) differed between decay modes as a binary predictor variable. As an evolutionary model for the residual variance-covariance matrix we used the lambda model [Pagel, 1999]. The number of host tree species was $\log_{10}$-transformed.

We modeled dynamics and pattern of host specialization evolution in white and brown rot lineages using multistate likelihood-based models. We used the function rayDISC from the R package 'corHMM' [Beaulieu et al., 2014], which implements a multi-state version of a continuous-time Markov model, where the Markov process is characterized by a Q-matrix. The Q matrix specifies the transition rates between the character states and hence the model of discrete character evolution. All models were based on our six-state character coding and the transition rate matrix was a 6x6 matrix: (1) white rot/angiosperm specialist, (2) brown rot/angiosperm specialist, (3) white rot/-gymnosperm specialist, (4) brown rot/ gymnosperm specialist, (5) white rot/generalist, and (6) brown rot/generalist.

The first model allows for all transitions to occur in single steps, e.g. an angiosperm specialist can switch directly to a gymnosperm specialist without first passing through a generalist state. Further, in this model transitions between white rot and brown rot are allowed in both directions. All models allow white rot to brown rot transitions. We call this the 'Uncorrelated' model, because switches between the states are not conditioned on previous states. This model may not be biologically realistic. Transitions from an angiosperm specialist to a gymnosperm specialist may require a transition first through a generalist, before passing to a gymnosperm specialist, and thus could require two 'steps'. Thus, we coded further models implementing correlated (dependent) character evolution. In the second model, we prohibited transitions leading directly from one specialist to another by setting the direct transition parameters to zero. We call this the 'Correlated hosts' model. Both the 'Uncorrelated' and the 'Correlated hosts' model allow for brown rot to white rot reversals. However, brown rot evolution is correlated with complete losses of genes encoding ligninolytic class II peroxidases (AA2) and reductions in other decay enzymes, making reversals to white rot unlikely [Floudas et al., 2012]. Accordingly, we constructed a third model where we further disallowed transitions from brown rot states to white rot states. We call this the 'Correlated hosts - norev' model.

For the coding of the Q matrices, see Figure 2.4.

$$Q_{uncor} = \begin{array}{c} \\ A-W \\ A-B \\ G-W \\ G-B \\ Gen-W \\ Gen-B \end{array} \begin{array}{cccccc} A-W & A-B & G-W & G-B & Gen-W & Gen-B \\ - & 6 & 11 & 16 & 21 & 26 \\ 1 & - & 12 & 17 & 22 & 27 \\ 2 & 7 & - & 18 & 23 & 28 \\ 3 & 8 & 13 & - & 24 & 29 \\ 4 & 9 & 14 & 19 & - & 30 \\ 5 & 10 & 15 & 20 & 25 & - \end{array}$$

$$Q_{cor} = \begin{array}{c} \\ A-W \\ A-B \\ G-W \\ G-B \\ Gen-W \\ Gen-B \end{array} \begin{array}{cccccc} A-W & A-B & G-W & G-B & Gen-W & Gen-B \\ - & 3 & - & - & 9 & - \\ 1 & - & - & - & - & 12 \\ - & - & - & 7 & 10 & - \\ - & - & 5 & - & - & 13 \\ 2 & - & 6 & - & - & 14 \\ - & 4 & - & 8 & 11 & - \end{array}$$

$$Q_{cor\_norev} = \begin{array}{c} \\ A-W \\ A-B \\ G-W \\ G-B \\ Gen-W \\ Gen-B \end{array} \begin{array}{cccccc} A-W & A-B & G-W & G-B & Gen-W & Gen-B \\ - & - & - & - & 7 & - \\ 1 & - & - & - & - & 10 \\ - & - & - & - & 8 & - \\ - & - & 4 & - & - & 11 \\ 2 & - & 5 & - & - & - \\ - & 3 & - & 6 & 9 & - \end{array}$$

Figure 2.4: Transition rates between the states in 6x6 Q-matrices with six states: (1) white rot/angiosperm specialist, (2) brown rot/angiosperm specialist, (3) white rot/gymnosperm specialist, (4) brown rot/ gymnosperm specialist, (5) white rot/generalist, and (6) brown rot/generalist. The first model displays is the 'Uncorrelated' model (Q_{uncor}) with 30 parameters (rates). The second model is the 'Correlated hosts' model (Q_{cor}), which forces host shifts to pass through intermediate states (e.g., A-W to Gen-W to G-W, instead of A-W to G-W). The third model displays is the 'Correlated hosts' model, which additionally does not allow reversals from white rot brown rot ($Qcor_{norev}$). Numbers are indices of the rates.

We fitted the three models with equal rates (ER) and all rates different (ARD) and compared the fit of the models by Akaike's information criterion (AIC) [Akaike, 1974] from the log-likelihoods. For model selection we applied a simple root state with equal weights among the six character states (root.p = NULL). Brown rot has been shown to evolve repeatedly from white rot ancestors [Nagy et al., 2013, 2015], so we applied an additional root state treatment which only allows white rot as root state. Thus, after model selection we ran the final (best) model using an additional root state coding,

which assumed zero probability for brown rot and equal probabilities for each of the three white rot states, and compared the models.

Another framework to estimate pattern of host evolution is the coding as three independent binary states: white rot - brown rot; angiosperm - no angiosperm; gymnosperm - no gymnosperm (e.g. using the function corDISC, from the R package 'corHMM'). However, this model requires unobserved states (no angiosperm and no gymnosperm host). Such unobserved states may yield high rates as a methodological artifact [Beaulieu and Donoghue, 2013]. Thus, we decided to use the multi-state implementation in the function rayDISC.

2.2.4 Phylogenetic signal

We computed phylogenetic signal in decay mode, gymnosperm association, and the six-state character coding (as defined above). For the decay mode (binary state) we used the phylogenetic D statistic, which is calculated as the sum of sister-clade differences based on reconstructed values on all nodes of the tree [Fritz and Purvis, 2010]. The observed D is then compared against (1) a random expectation (random shuffling of trait values along the tips), and (2) a trait simulated according to a Brownian motion model of character evolution along the tree, after the values were converted to a binary according to a threshold. For the computation we used the function phylo.d in the R package 'caper' [Orme, 2013] with 1000 permutations. For the gymnosperm association we calculated two measures of phylogenetic signal: Pagel's lambda [Pagel, 1999] using the function phylosig from the R package 'phytools' [Revell et al., 2012], and phylogenetic correlograms using the function phyloCorrelogram from the R package 'phylosingal' [Keck et al., 2016]. Lambda measures the phylogenetic dependence of a trait under the assumption of a pure Brownian motion model of evolution. Lambda is a transformation (weight) of the variance-covariance matrix, if other factors than the phylogenetic history had an effect on the trait. If lambda equals 1 the model fits a Brownian motion model of evolution. Phylogenetic correlograms measure phylogenetic signal in dependence of the phylogenetic distance (that is distance in branch lengths). For a single trait, phylogenetic signal is measured as the autocorrelation (Moran's I) based on a sequence of phylogenetic weights matrices differing in their mean (phylogenetic distance if method = 'lag-norm'). We conducted 100 bootstraps for 100 points to generate a confidence interval. If the confidence interval falls below or above 0 the signal becomes significant. We rescaled the phylogeny to a tree height of 1 for this analysis.

For the six state character coding we calculated the phylogenetic signal following the method described in [Bush et al., 2016] (function phylo.signal.disc, the script is available

at: https://github.com/juliema/publications/blob/master/BrueeliaMS/Maddison.Slatkin.R).
A parsimony score of the discrete trait along the tree is compared to a randomized par-
simony score inferred by randomizing tip states. If the parsimony score falls outside the
random distribution, this indicates a higher conservation than under a random expecta-
tion.

2.3 Results

Our core dataset consisted of 1157 fungal species, including 126 brown rot and 1031
white rot species. Based on the 90-10 specialization coding, we found 205 gymnosperms
specialists, 565 angiosperm specialists and 387 generalists (for tip state frequencies, see
Table 2.4). Our time-calibrated phylogeny contains five brown rot clades (Figure 2.5,
all clades had SH-like support values above 90, Figure A.1), including two in Poly-
porales, one in Gloeophyllales, one in Agaricales and one in Boletales. Clade 1, the
Auriporia-Crustoderma clade, within the Polyporales includes Laetiporaceae, Sparas-
sidaceae, Dacryobolaceae pro parte (*Dacryobolus karstenii*), *Crustoderma* and *Pycno-
porellus*. Clade 2, the *Antrodia-Fomitopsis* clade, within the Polyporales includes Fomi-
topsidaceae, Dacrybolaceae pro parte (*Spongiporus*, *Oligoporus*, *Postia* pro parte) and
Fibroporia gossypinum. Clade 3, the *Gloeophyllum-Neolentinus* clade, falls within the
Gloeophyllales. Clade 4, the *Fistulina* clade, falls within the Agaricales (*Fistulina pallida*
and *F. antarctica*). Clade 5, the *Serpula-Hygrophoropsis* clade, falls within the Bole-
tales (Figure 2.5). The tree and alignment have been deposited in the Dryad repository
(doi:10.5061/dryad.4mc3s).

Figure 2.5: Agaricomycetes species-level dated tree of wood-decay fungi. The species-
level chronogram is based on the maximum clade credibility tree (MCCT)
topology, dated with two fossils indicated by red points. Clades: (1)
Auriporia-Crustoderma (Polyporales), (2) *Antrodia-Fomitopsis* (Polyporales), (3)
Gloeophyllum-Neolentinus (Gloeophyllales), (4) *Fistulina* (Agaricales), (5) *Serpula-
Hygrophoropsis* (Boletales). Blue bars on the brown rot crown nodes indicate
confidence intervals (HPD) from 100 alternative trees. For a detailed maximum
likelihood phylogeny with SH support values and tip labels, see Figure 4.3 and
supplementary data. Figure next page.
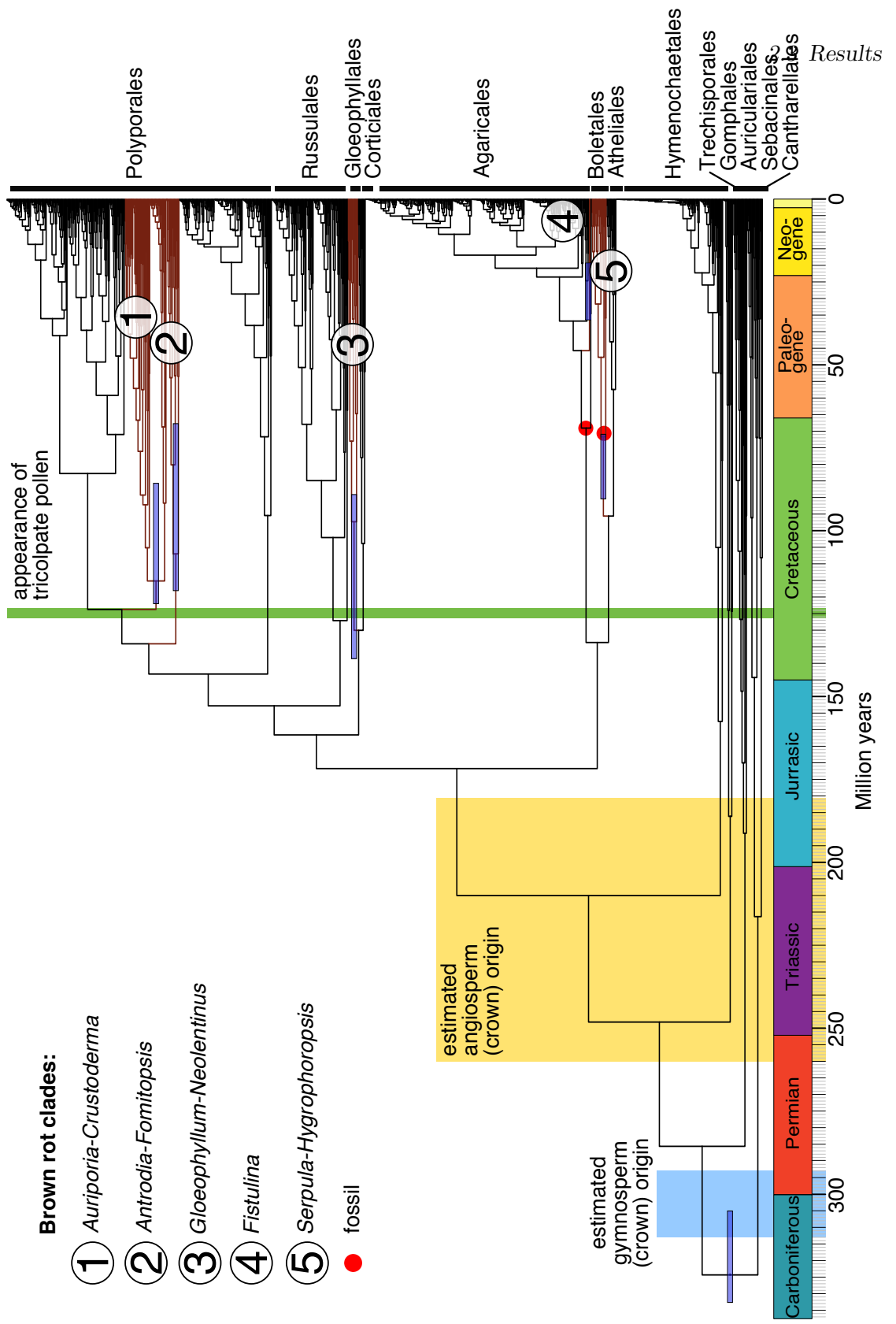
2.3.1 Phylogenetic signal

For decay mode, we found a phylogenetic D value of -0.38, which had a high probability resulting from a Brownian motion phylogenetic structure (P=0.998) and a corresponding low probability resulting from a random phylogenetic structure (P=0.00, Figure 2.6A). We found a lambda value of 0.73 for gymnosperm association and an increasing phylogenetic signal towards the tips (Figure 2.6B, red and blue lines indicates significance). For the six-state character coding, we found that the observed parsimony score was significantly smaller than under a random expectation (Figure 2.6C).
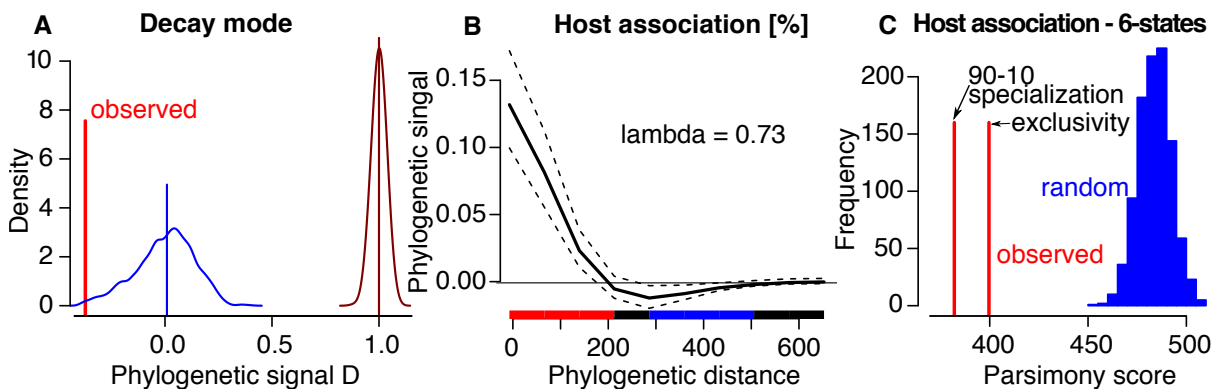
Figure 2.6: Phylogenetic signal for decay mode, and two measures of gymnosperm association. A) Phylogenetic signal D for decay mode (binary variable). A value smaller than 0 indicates strong conservatism. B) Pagel's lambda and phylogenetic correlogram for gymnosperm association. A lambda value of 0.73 indicates non-random trait evolution which is not as conserved as Brownian motion. The phylogenetic signal increased towards the tips. Displayed is the mean phylogenetic signal with a 95% confidence interval resulting from 100 bootstraps. C) Phylogenetic signal C for the six-state coding. The observed value outside of the random expectation distribution indicates conservatism.

2.3.2 Host preferences among decay fungi

We assessed host preferences among extant decay fungi based on the average number of host tree species. White and brown rot fungi did not significantly differ in their average number of host tree species (phylogenetic regression, Figure 2.7A, B, statistics Table 2.5), although visible trends suggested that white rot species have a larger average host range on angiosperms (Figure 2.7A), while brown rot species have a larger average host range on gymnosperms (Figure 2.7B). The histogram of the gymnosperm association showed a bimodal distribution with two peaks towards the ends of the distribution, representing extremes of angiosperm vs. gymnosperm specialization (Figure 2.7C). Thus, among

the specialized decay fungi most occur exclusively on either angiosperm or gymnosperm hosts (Figure 2.7C). Based on the gymnosperm association we found that 51% of white rot species are specialized to angiosperm hosts, whereas 27% of brown rot fungi are specialized on angiosperms (Figure 2.7D). Among brown rot fungi, however, we found a higher proportion of generalists and gymnosperm specialists than in white rot fungi (Figure 2.7D).

Of the five brown rot clades (Figure 2.5), two consisted of mainly generalist species (Polyporales clades: *Auriporia-Crustoderma* and *Antrodia-Fomitopsis*). Two clades consist of mainly gymnosperm specialists (Gloeophyllales: *Gloeophyllum-Neolentinus*; Boletales: *Serpula-Hygrophoropsis*). One clade consists of mainly angiosperm specialists (Agaricales: *Fistulina*) (Figure 2.7E). The two Polyporales clades, *Auriporia-Crustoderma* and *Antrodia-Fomitopsis*, however, also display a considerable amount of angiosperm specialists, exceeding gymnosperm specialists (Figure 2.7E).

Table 2.5: Phylogenetic and normal linear regression on the number of angio- and gymnosperm hosts between white and brown rot species. Note that the number of fungal species was $\log_{10}$-transformed. Significant effects were highlighted in bold. We present only results, which were based on the lambda model as a model of covariance among species. We compared all available models in the function phylolm from the R package 'phytools'. The lambda model was the best model based on AIC scores (not shown).

		Phylogenetic linear model				**Linear model**	
		t value	p value	lambda	t value 100 trees	t value	p value
Angio-sperm	Intercept	2.93	0.003	0.36	3.73 (3.70 - 3.76)	12.74	0.000
	Decay mode WR vs. BR	1.23	0.221		1.32 (1.30 - 1.35)	1.84	0.066
Gymno-sperm	Intercept	2.81	0.005	0.62	3.88 (3.84 - 3.93)	17.85	0.000
	Decay mode WR vs. BR	-1.60	0.111		-1.66 (-1.71 - -1.62)	-7.86	0.000

Twelve of the 14 orders in our dataset contained white rot lineages (Figure 2.7F). Three of these had less than five species (Amylocorticiales, Gomphales, Sebacinales) and thus we did not interpret host associations for them. White rot species within six orders were primarily angiosperm specialists (Agaricales, Auriculariales, Corticiales, Hymenochaetales, Polyporales, Russulales) (Figure 2.7F). White rot species within three orders were primarily generalists (Atheliales, Cantharellales, Trechisporales) (Figure 2.7F).
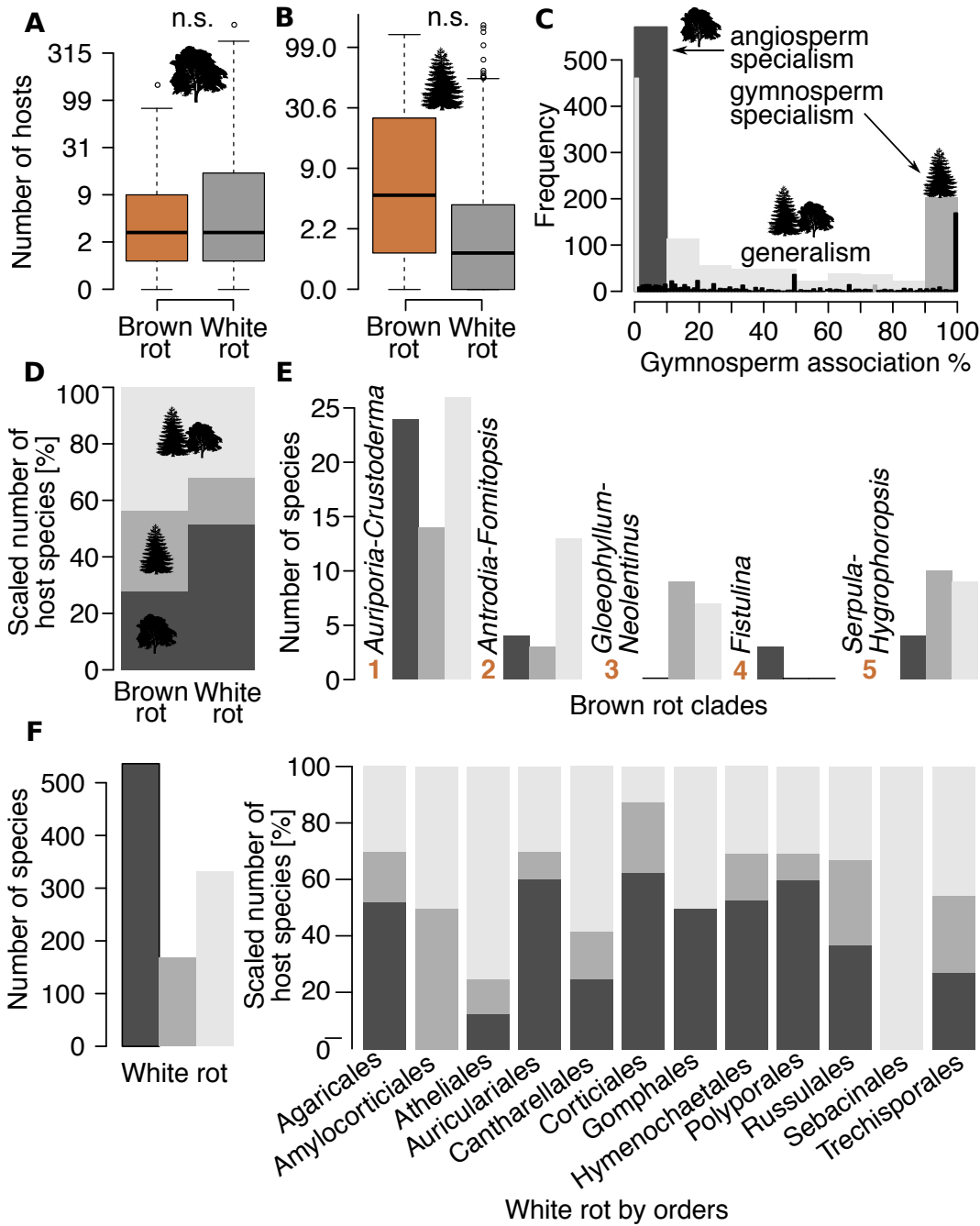
Figure 2.7: Distribution of gymnosperm association among wood-decay fungi and five major brown rot lineages within Agaricomycetes. A) Number of angiosperm host tree species for white and brown rot species. B) Number of gymnosperm host tree species for white and brown rot species. Note the log scale of the y-axis and that the values were back-transformed. Significances were inferred using phylogenetic regression (Table 2.5). C) Bimodal distribution of gymnosperm association of wood-decay fungi. The six-state character coding was based on the gymnosperm association. A gymnosperm association above 90% was classified as gymnosperm specialist, below 10% as angiosperm specialist and others as generalists ('90-10 specialization', for details see Trait data and character matrix). D) Scaled number of host tree species grouped by the 90-10 specialization coding. E) Number of species for the five observed brown rot clades (Figure 2.5). F) Number of species for white rot fungi and scaled number of host tree species grouped by the 90-10 specialization coding. Note that Amylocorticiales, Gomphales and Sebacinales had less than five host data points. Angiosperm tree image by Michele M. Tobias under creative commons (http://phylopic.org, https://creativecommons.org/licenses/by-nc-nd/3.0/).

2.3.3 Dynamics of Host Switches

Based on the models of discrete trait evolution describing host switching dynamics among white and brown rot fungi, we found the 'Correlated hosts – norev' model, with all rates different, as the best model (model 3.2, Table 2.6). This model assumed host paths via a generalist state and prohibited reversal from brown rot to white rot, which is consistent with our expectation that swtiches between angiosperm and gymnosperm specialization cannot occur in a single step, and that losses of AA2s and other lignocellulolytic enzymes makes reversals from brown rot to white rot unlikely. The version of this model that specified the root state with equal weights for white rot states and zero probability for brown rot states (model 3.3) performed better than the model which assumed equal weights among all six states. We display transition rates based on model 3.3 (Figure 2.8). We found disparity in rates of transitions between generalism and angiosperm specialization between the decay modes. While white rot lineages display high transition rates from generalism to angiosperm specialization, brown rot lineages display higher rates from gymnosperm specialization to generalism (Figure 2.8). White rot lineages further show higher rates of transitions towards angiosperm specialization than the reverse, whereas brown rot lineages show the opposite, with higher rates from angiosperm specialization to generalism than the reverse. White and brown rot lineages both switch more frequently from gymnosperm specialization to generalism than the reverse (Figure 2.8). The transition rate estimates were consistent across 100 alternative trees (Figure 2.8A, B). The 100 one-genus-subsets yielded consistent relative rates, but rates of white rot states were higher (especially rates from generalists to gymnosperm specialists, Figure 2.8A, C). Concerning the rates of transitions from white to brown rot estimated based on the ML phylogeny, the alternative trees and one-genus-subsets did not yield a clear picture. The rate estimates based on the ML phylogeny showed one transition rate from white to brown rot angiosperm specialists (Figure 2.8). The 100 alternative trees further displayed equally high rates from white to brown rot generalists (Figure 2.9A, B).
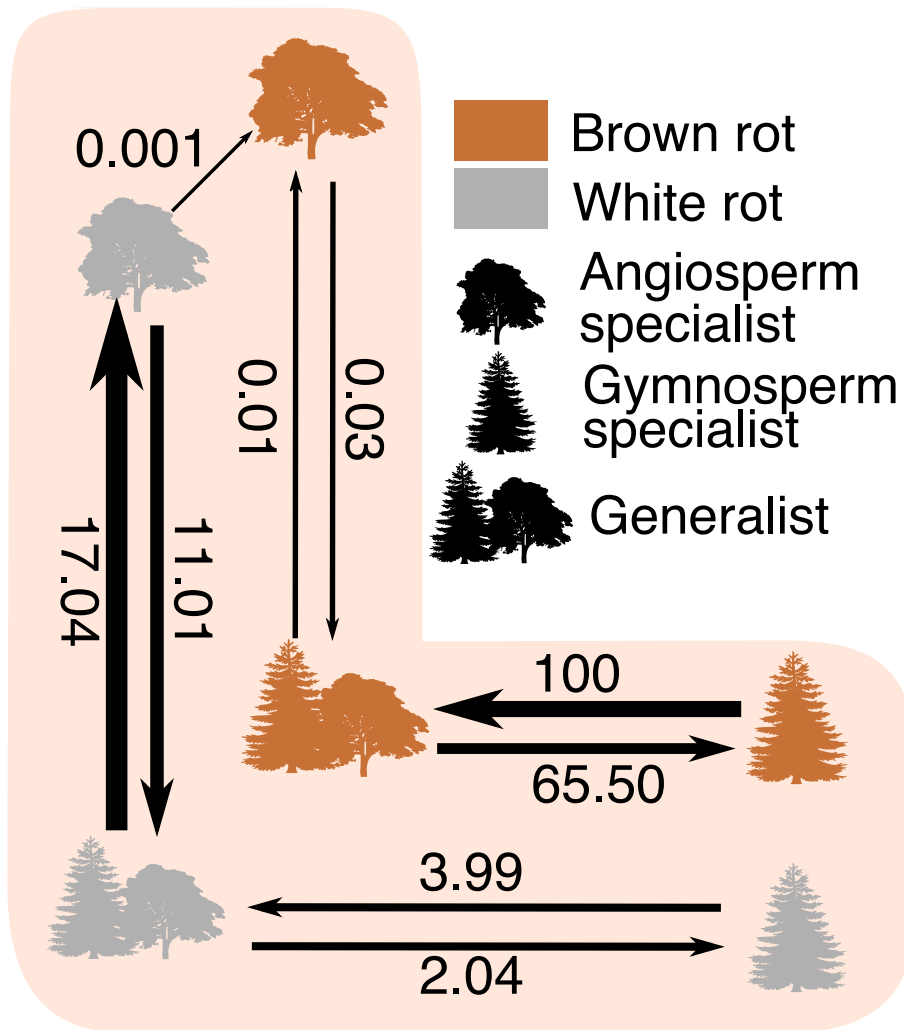
Figure 2.8: Dynamics of host specialization evolution in wood-decay fungi within Agaricomycetes based on a multi-state likelihood model. Transition rates based on the best model ('Correlated hosts – norev', Table 4.1) and the maximum likelihood phylogeny among six character states: white or brown rot generalist; white or brown rot angiosperm specialist and white or brown rot gymnosperm specialist. The six-state character coding was based on the gymnosperm association. A gymnosperm association above 90% was classified as gymnosperm specialist, below 10% as angiosperm specialist and others as generalists ('90-10 specialization', for details see Trait data and character matrix). Numbers above and below arrows denote transition rates and the arrow width reflects the rate size. For rate estimates based on alternative trees and the one-genus-subsets see Figure 2.9. Angiosperm tree image by Michele M. Tobias under creative commons (http://phylopic.org, https://creativecommons.org/licenses/by-nc-nd/3.0/).
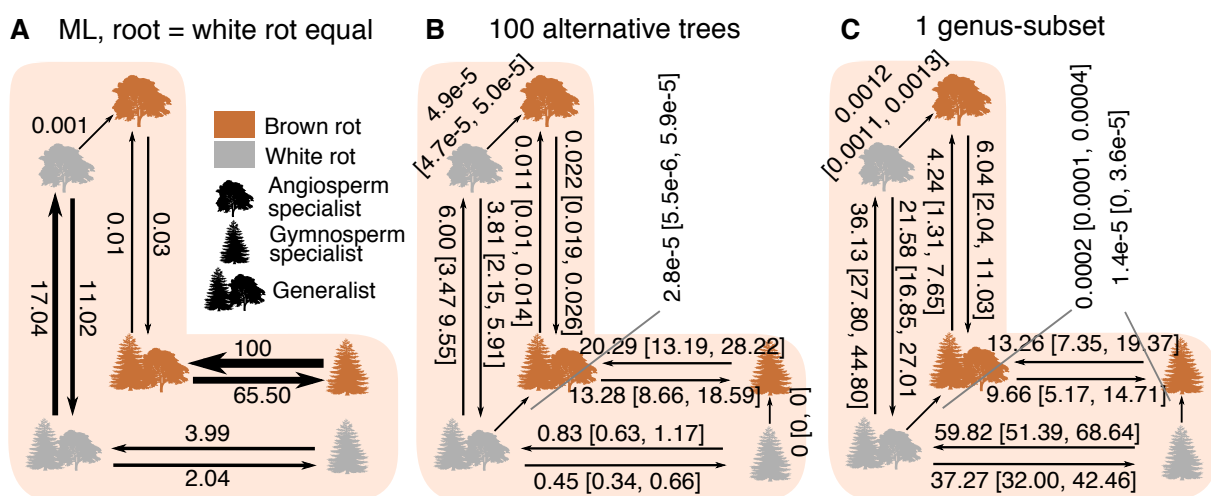
Figure 2.9: Transition rates among six character states based on a maximum likelihood (ML) phylogeny, 100 alternative trees and the one-genus-subset (100 times bootstrapped). Transition rates based on the 90-10 (%) specialization thresholds with root state set to equal probabilities among the white rot states and zero probability for brown rot states (Table 4.1). Numbers above and below arrows denote transition rates and the arrow width reflects the rate size. A) Same as Figure 4.8B) Transition rates based on 100 alternative trees with the bootstrapped 95% confidence interval (function smean.cl.boot from the R package 'Hmisc', [Harrell Jr and others, 2017]). Rates are consistent with the ML rates (A) in terms of relative size. 100 trees were produced by creating hard polytomies on nodes below a SH support threshold of 80. The polytomies were then resolved 100 times and divergence time (function chronos) was estimated (for details see method section). C) We extended species decay mode information to the genus, where further data was missing. Thus we bootstrapped the full dataset and phylogeny to a single species per genus and estimated transition rates. Although relative rates (especially between rates and their reversal rates) remain consistent, white rot transition rates are much higher in total. This might be explained by the extreme imbalance of the number of genera (brown rot: 40 genera, white rot: 232 genera) together with a very small phylogeny (Ntip = 272).

Within the 100 alternative trees, brown rot clades were not collapsed since SH-like support values were > 90. Transition rates from white to brown rot gymnosperm specialists were either estimated as zero or very low (Figures 2.8, 2.9).

2.4 Discussion

Brown rot fungi as a whole comprise a larger proportion of gymnosperm specialists than white rot (Figure 2.7D), which is consistent with Gilbertson's observations [Gilbertson, 1980]. Nevertheless, most brown rot fungi are generalists and only two of five brown

Table 2.6: The fit of three alternative models of host evolution among decay fungi of Agaricomycetes. The best model (shown in bold), based on Akaike weights (w), was the model 3.3, which allowed only intermediate host transitions ('Correlated hosts'), no brown rot to white rot reversals ('norev') and a root prior with equal probabilities among white rot fungi and zero probability for brown rot states ('white rot equal'). For model selection based on the exclusivity coding, see Table 2.7.

Model	-Ln L	AIC	Δ AIC	w
Uncorrelated, ER	-1870.83	3743.65	1355.72	0.00
Uncorrelated, ARD	-1180.64	2421.27	33.34	0.00
Correlated hosts, ER	-1774.09	3550.19	1162.25	0.00
Correlated hosts, ARD	-1183.56	2395.12	7.19	0.02
Correlated hosts – norev, ER	-1941.71	3885.41	1497.48	0.00
Correlated hosts – norev, ARD, root = equal	-1183.66	2389.32	1.39	0.33
Correlated hosts – norev, ARD, root = white rot equal	**-1182.97**	**2387.93**	**0.00**	**0.65**

rot clades display mainly gymnosperm specialists (clades *Gloeophyllum-Neolentinus* and *Serpula-Hygrophoropsis*, Figure 2.7D, E). Brown rot lineages show a higher rate of switches to gymnosperm specialization than white rot fungi, but brown rot display the highest rate towards generalism. Brown rot further displayed dynamic transitions between generalism and specialization (Figure 2.8). White rot fungi are highly specialized on angiosperm hosts (Figures 2.7, 2.8).

Gilbertson suggested that "85% of brown-rot polypores occur primarily on conifers", which was the basis for later hypotheses about brown rot evolution in general [Gilbertson, 1980]. Our analysis could not confirm that brown rot Polyporales occur primarily on gymnosperm hosts (Figure 2.7E). We found two brown rot clades within Polyporales, of which the *Auriporia-Crustoderma* clade consists of mainly generalists and angiosperm specialists and the *Antrodia-Fomitopsis* clade of mainly generalists (Figure 2.7E). Thus, neither of the two brown rot clades within the Polyporales were mainly specialized on gymnosperms (Figure 2.7E). Our dataset allowed us to extend and evaluate Gilbertson's statement for a broad range of brown rot lineages of different clades and orders. According to our analysis, only two of five brown rot clades consist of mainly gymnosperm specialists, the *Gloeophyllum-Neolentinus* (Gloeophyllales) and the *Serpula-Hygrophoropsis* (Boletales) clades (Figure 2.7E). Further, the majority of brown rot fungi are generalists (Figure 2.7D). Therefore, the hypothesis that brown rot fungi occur primarily on gymnosperms is not generally supported.

Based on our 90-10 specialization coding and a multi-state likelihood model of host evolution, we found that white rot fungi switched frequently between generalism and

Table 2.7: The fit of three alternative models of host association evolution in white and brown rot lineages of Agaricomycetes based on the **exclusivity** coding (100-0). The best model (shown in bold), based on Akaike weights (w), allowed only intermediate host transitions (paths), no brown rot to white rot reversals (no BR reversals) and assumed equal probabilities for the root state among the six tip states.

Model	-Ln L	AIC	Δ AIC	w
Uncorrelated, ER	−1870,83	3743,65	1354,33	0,000
Uncorrelated, ARD	−1180,64	2421,27	31,95	0,000
Correlated hosts, ER	−1774,09	3550,19	1160,86	0,000
Correlated hosts, ARD	−1183,56	2395,12	5,80	0,046
Correlated hosts – norev, ER	−1941,71	3885,41	1496,09	0,000
Correlated hosts - norev, ARD, root = equal	−1183,66	2389,32	0,00	0,830
Correlated hosts - norev, ARD, root = white rot	−1185,56	2393,12	3,79	0,124

angiosperm specialism with a higher rate towards angiosperm specialism (Figure 2.8). Within brown rot lineages, this pattern shifted towards frequent switches between generalism and gymnosperm specialization (Figure 2.8). This suggests that brown rot evolution promoted frequent shifts to gymnosperm specialization. However, the reversal rate from gymnosperm specialism to generalism is higher, suggesting that specializations towards conifer hosts are not restrictive (Figure 2.8). Based on a much smaller dataset, one study inferred a correlation between brown rot and exclusive decay of conifer hosts and suggested that brown rot promotes gymnosperm specialization [Hibbett and Donoghue, 2001]. However, within brown rot, transition rates between gymnosperm specialization and generalism are high in both directions, with a trend toward generalism, suggesting that specializations towards conifer hosts are not stable (Figure 2.8). Our findings are robust against topological and branch lengths variation (Figure 2.9A, B). Further, our results are robust against different assumptions concerning reversals from white to brown rot. Transition rate estimates of the model allowing reversals and the one disallowing reversals were nearly identical (data not shown, however, AIC difference only 7.19 which is often considered as not substantially different [Burnham and Anderson, 2002]).
Further, we estimated the likelihood model of host specialization evolution based on the exclusivity coding and found that the transition rate towards gymnosperm exclusivity was higher for brown rot compared with white rot lineages (Figure 2.9). This finding is consistent with the 90-10 specialization coding (Figure 2.8). Within the exclusivity model we found overall higher rates from host exclusivity to generalism (Figures 2.8, 2.10).
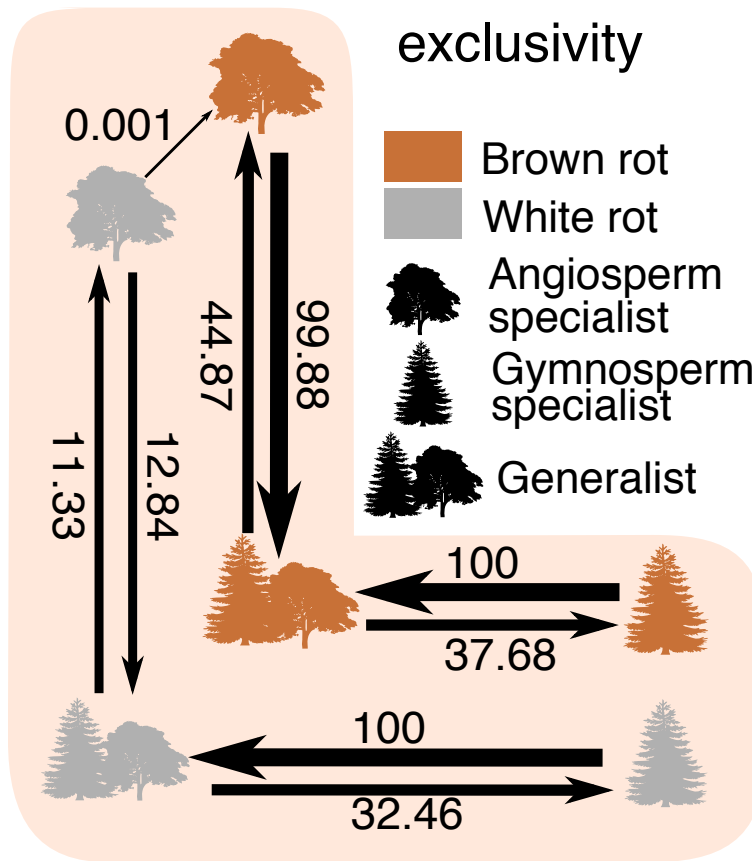
Figure 2.10: Dynamics of host specialization in wood decay fungi within the Agaricomycetes based on the 100-0 exclusivity coding. Transition rates were further based on the (best) model 3.3 (Table 4.1) and the maximum likelihood phylogeny. We used a multi-state model of host specialization evolution with six character states: white or brown rot generalist; white or brown rot angiosperm specialist and white or brown rot gymnosperm specialist. Rates towards generalism are likely overestimations because 'generalism' in this model incorporates generalists as well as specialists. Numbers above and below arrows denote transition rates and the arrow width reflects the rate size.

However, the stringency of this coding scheme may overestimate the number of generalist taxa, as species found at extremely high rates on a single host species (e.g. >90%, but less than 100%) are still coded as generalists. Thus, rates towards 'generalists' are probably overestimated in this coding scheme. Therefore, interpretations from the exclusivity model should be made with caution. For a more detailed picture, further analysis should thus include three states of host association, separating generalism, non-exclusive specialization and exclusivity and treat non-exclusive specialization as an intermediate state.

Based on our time-calibrated mega-phylogeny approach, we found that most lineages within Agaricomycetes radiated after the origins of gymnosperms and angiosperms (Figure 2.5). Our estimates for branching times are highly consistent with chronograms of previous studies with more limited species sampling, but more genomic information. One study found a mean age of 290 million years [Floudas et al., 2012] for the crown node of Agaricomycetes, which is consistent with our estimate of 282 million years (Figure 2.11). Using an uncorrelated relaxed molecular clock analysis to date a comprehensive plant tree of life, a study found mean crown origins of 301 million years for gymnosperms and 217 million years for angiosperms, respectively [Smith et al., 2010].
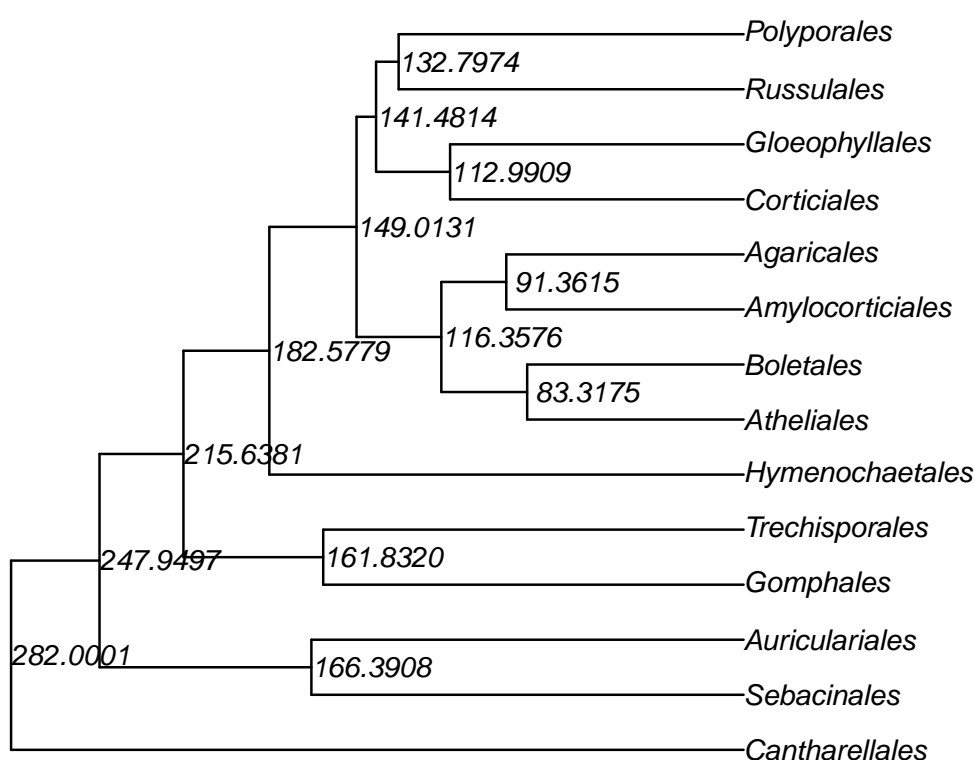
Figure 2.11: Branching times for backbone of time-dated Agaricomycetes phylogeny. Branching times are based on the maximum likelihood phylogeny. Here the full phylogeny was reduced to order level to display backbone crown age estimates. The root was dated with an age of 282 million years, which fits well to previous estimates for the Agaricomycetes [Floudas et al., 2012, Kohler et al., 2015].

Many of the large clades within Agaricomycetes originated before, but diversified after the angiosperm and gymnosperm origins (Figure 2.5). The estimated timing of origin of the fungal and plant groups is consistent with our inference that transitions from

white rot to brown rot occurred among angiosperm specialists (Figure 2.9) or possibly generalists (Figure 2.9). Relative transition rates in white rot fungi suggest a pattern of transition away from gymnosperm specialization and towards generalism, followed by relatively higher rates of angiosperm specialization (Figure 2.8). This pattern away from gymnosperm specialization and towards angiosperm specialization among white rot is consistent with the relatively high percentage of white rot angiosperm specialists we observed (Figure 2.7). Thus, it is plausible that the radiation of angiosperms created new niches for wood decayers and promoted diversification of white rot fungi.

In conclusion, our models of host evolution suggest that angiosperms may have served as a new mega-niche, which was exploited particularly well by white rot fungi leading to high specialization rates. Brown rot lineages switched more frequently towards generalism, suggesting that brown rot fungi were limited in exploiting angiosperm resources. Whether this limitation on the part of brown rot in exploiting angiosperm resources is directly related to the loss in copy number of decay-related genes [Kohler et al., 2015] seems plausible, but remains to be tested by future studies. Moreover, host shifts may be identifiable at the enzymatic level, if expression patterns for genes coding for key decay enzymes differ between clades with different host specializations. Such studies represent exciting future possibilities in this system, and may elucidate the underlying molecular mechanisms controlling decay mode shifts.

2.5 Supplementary Information

2.5.1 rusda: an R interface to the United States Department of Agriculture's Fungus-Host Distribution Database

2.5.1.1 Introduction

The United States Department of Agriculture (USDA) has made great effort to compile global fungus-host combinations data. The USDA thus created the Fungus-Host-Distribution Database (FHDD) to store this data and enable public access. However, data from this database is not easily available, requiring users to download species information by hand. This procedure is very time consuming. If large amounts of data are downloaded, error might occur while compilation of many single files. The risk of such error increases with the number of taxa required, which increased in recent years. Comparative analysis often require hundreds or even thousands of species [Smith and Donoghue, 2008, Smith et al., 2009, Zanne et al., 2013]. A fast and open access to these data may provide basic research on the ecology and evolution of fungus-host associations.

To this end, the first author (Franz-S. Krah) developed an R package allowing rapid and automated access to a large global database of fungus-host combinations by the FHDD. This database involves more than 300.000 unique fungus-host combinations [Farr et al., 2017]. However, the web interface of the database makes data analysis difficult, limiting the use of this database. The aim of the R package 'rusda' is to make the data contained in the FHDD readily accessible from R, an open source statistical programming environment.

2.5.1.2 Core package function

Here, the core functions of the 'rusda' package will be presented. The R package 'rusda' is available on GitHub via the rOpenSci collective. rOpenSci is a research community committed to make scientific data retrieval open and reproducible using shared data and reusable software. The package can be downloaded using the following code:

```
# Install R package 'rusda'
install.packages("devtools")
devtools::install_github("ropensci/rusda")
library("rusda")
```

2.5.1.3 Querying the database

The USDA Fungus-Host Distribution Database (FHDD) contains data on host (plants)-fungus combinations. Further it contains a Nomenclature and a Literature database, which are also accessible via 'rusda'. Within the FHDD only published literature was used as data basis. Besides the FHDD there is the Specimens Database (SD) which refers to deposited specimens in the U.S. National Fungus Collections (BPI). The core function of 'rusda' is the function associations. Using associations queries can be made to find all plant associations of a known fungus (spec_type = "fungus") or to find all fungal associations of a known plant host (spec_type = "plant"). When querying the FHDD, the user can input species or genus names or any higher taxon.

```
# The following example code queries fungus−host
# associations for the fungal species: Magnaporthe oryzae

magna.hosts <− associations(x = "Magnaporthe oryzae",
                            spec_type = "fungus", database = "FH")


# The following example code queries fungus−host
# associations for all species within the plant family: Cucurbitaceae
curc.fungi <− associations(x = "Cucurbitaceae",
                           spec_type = "plant", database = "FH")
```

The argument "database" specifies whether the FHDD or the SD or both should be queried. Further arguments allow clean steps, verbosity of the function or if synonyms of the input should be incorporated in the search. The default is with a cleaning step, which eliminates non-Linnean species names from the results list. Further, by default synonyms are queried to increase query success. The resulting structure of the "curc.fungi" object is a list of three objects. The first lists synonyms of the input names. The second is a data table with the input species and the queried combinations and the country of the record. The third is a data table with the input species and the study identifier number (ID). The IDs can be directly used as input to the function "getStudy" to obtain the full citation.

2.5.1.4 Exploration of the Fungus-Host Distribution Database (FHDD)

The website of the FHDD website does not yield detailed information about the taxonomic distribution of the data stored in the database. To assess the general usability of the FHDD database, and therefore the R package 'rusda', we used two species input datasets. We therefore downloaded two taxonomies for all species of Dikarya and Sper-

matophyta from the NCBI taxonomy (function stepA from the R package 'megaptera' [Heibl, 2014]). The resulting taxonomies exhibit Linnean species names only, which were used as input for the function associations of 'rusda'. The length of the input species sets were 29,591 for Dikarya and 105,350 for Spermatophyta. The function associations queries the related fungal (for plant input) or plant (for fungus input) associations for each species from the datasets. Note that the function associations also accepts names of higher taxa as input, however we the plant and fungus input names were too long to download within single sessions. Thus, we downloaded associations in batches of 1000 species.

We used both databases and considered results for synonyms of the input species and queried fungus-host associations for the two input species sets. We found data for 11,146 Dikarya (37.6 % of input) and 17,345 for Spermatophyta (16.5 % of input). A total of 268,752 (90 % of website information) combinations were found for Dikarya in the FHD. The discrepancy of 10 % can be explained by the cleaning step of our algorithm. It deletes records that are no valid species or genera names (e.g., 'wood, submerged') since usually the user is only interested in taxonomic data. Another reason is that we did not query for non-fungal lineages like Oomycetes (e.g. *Phytophthora*), which are also present (as pathogens) in the database. We found 87,232 unique combinations for the Spermatophyta input set, which could not be evaluated due to lacking information on the website [Farr et al., 2017]. We then matched the retrieved hosts and fungi against the plant and fungus taxonomies to compute the number if species with host or fungus information respectively. Therefore, we compared the number of species with information based on the FHDD compared with the total species number for a given order in the NCBI taxonomy. The results are summarized in the Figure 2.12. We hope that this figure is a useful tool for scientists interested in host associations.

Here we want to point out that of the 13 investigated orders (bold) in this study, six orders had more or ca. 50% of species with host information. Among those are the orders with most representation in our dataset: Polyporales, Agaricales, Hymenochaetales. The other groups had below 50% of species with host information (Figure 2.12). On the plant side we found the two orders with the majority of woody plants in the temperate zone, Fagales and Pinales, have a very good representation in the database. All plant species within the NCBI taxonomy (with valid Genus and species names) have at least 1 host association information. However, there are other mainly-woody orders, that are not very well represented: e.g. Ericales. This overview shows the need for further recordings and assembly of fungus-host associations in the FHDD (Figure 2.12).
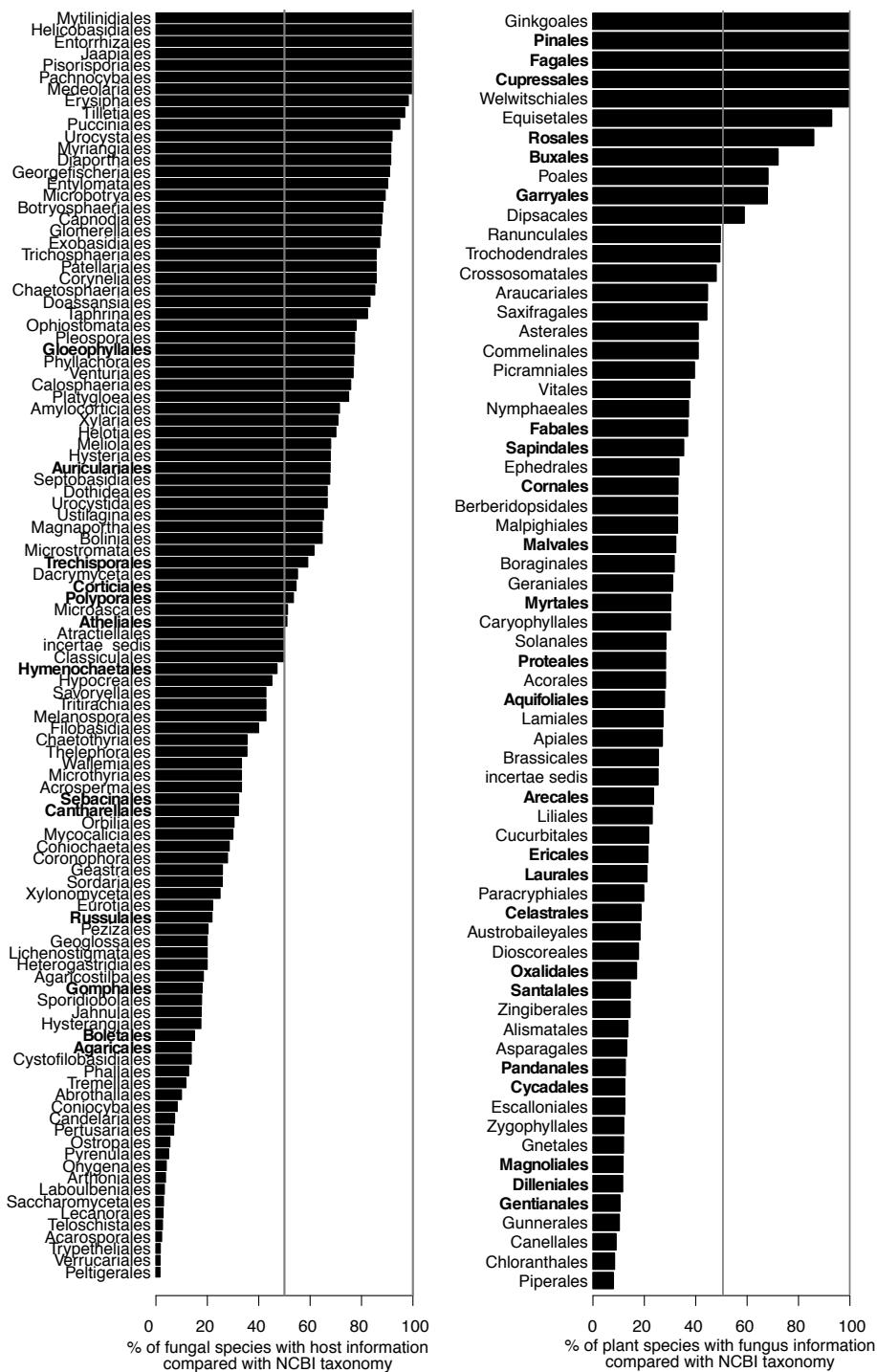
Figure 2.12: Overview of query results using R package 'rusda' based on the Fungus-Host Distribution Database (FHDD) using 29,591 Dikarya and 105,350 Spermatophyta species as input. A) Number of fungal species with plant (host) information (one or more records). B) Number of plant species with fungal information. Fungal orders used in this study in bold. Woody plant orders in bold, based on [FitzJohn et al., 2014].

3 Effects of temperature on pigmentation of mushrooms across Europe

Abstract

Many ectotherm animals show a prevalence of dark-colored species in cold environments, known as thermal melanism. The function of dark colors in the fungal kingdom, however, is poorly understood. Here, we tested whether the lightness of mushrooms is related to climate using a dataset of 3.2 million observations in 3,054 species from across Europe. We show that saprotrophic assemblages are significantly darker in cold climates and seasons, supporting a general theory of thermal melanism. Despite being significantly darker on average than free-living saprotrophs, the color of mutualistic ectomycorrhizal mushrooms was, however, only weakly related to temperature. We thus propose generalizing the thermal melanism hypothesis to fungi, but suggest that selection on pigmentation may depend on species' life history. Because fungi play an important role in terrestrial carbon and nutrient cycles, understanding the link between color and environmental temperature will be critical in assessing the response of fungi to global warming.

3.1 Introduction

In cold environments, ectothermic animals more commonly have dark-colored than light-colored bodies [Kalmus, 1941, Bogert, 1949, Willmer and Unwin, 1981, Kingsolver, 1995, Trullas et al., 2007] ('Bogert's rule' [Bogert, 1949]). This theory of 'thermal melanism' [Trullas et al., 2007] has often been studied in the animal kingdom [Kalmus, 1941, Bogert, 1949, Rapoport, 1969, Zeuss et al., 2014, Bishop et al., 2016, Pinkert et al., 2017, Pinkert and Zeuss, 2018, Heidrich et al., 2017], however, much less is known about the function of colors within the ectothermic fungal kingdom [Caro, 2017, Cuthill et al., 2017]. A recent study found dark-pigmented unicellular yeasts in colder environments of a macroclimatic gradient [Cordero et al., 2018]. Mushrooms are the multicellular reproductive organs of many fungi [Nagy et al., 2017], with extraordinary diversity in their pigmentation [Gill

and Steglich, 1987, Velíšek and Cejpek, 2011], however the causes and consequences of their coloration are still unknown. Mushrooms are anatomically characterized by fruit bodies composed of a pileus (cap) and stipe (stalk). The biological role of fruit bodies is sexual reproduction, and spores formed in the fruit bodies disperse and develop into mycelia that exploit resources and mate to form new reproductive individuals [Nagy et al., 2017]. Dark pigments (e.g., melanin) of fungal mycelia have been shown to allow colonization of cold Arctic and Antarctic environments [Savile, 1972, Robinson, 2001]. However, the pigmentation of mushrooms may also be an important trait of fungi in cold environments, because mushrooms are above-ground reproductive organs and thus more exposed to colder temperatures than the mycelium in the substrate (Figure 3.3). Thus, we test whether the lightness of mushroom assemblages is correlated with the thermal environment across Europe.

Temperature varies both spatially, across macroclimatic gradients, and temporally over seasons (Figure 3.2) and thus we considered its spatiotemporal variability. We used a Europe-wide dataset of 3,054 mushroom-forming fungal species (Table 3.1) of four orders within the systematic class Agaricomycetes (Basidiomycota), which covers nine countries and the past 40 years [Andrew et al., 2017] at a monthly resolution. We measured mushroom color on representative digital images of each species by decomposing color into three independent measures: hue, saturation, and lightness (HSL color space, Figure 3.1).

Table 3.1: Data overview. The total number of species in the European fungal dataset; the number of mushroom-forming species (mushroom = fruit body with cap and stipe) with color data; and the number of mushroom-forming species with color and sequence data. Percent values refer to the 'Mushroom-forming species' dataset. HSL is hue, saturation, and lightness. ECM = Ectomycorrhizal; SAP = Saprotroph; Other = parasitic, endophytic, unknown.

	Full dataset	Mushroom-forming species	Mushroom-forming species & HSL data	DNA sequences available
ECM	1,989	1,770	1,401 (79%)	1,010 (57%)
SAP	3,481	2,289	1,653 (72%)	1,046 (46%)
Other	261	-	-	-
Total	5,831	4,059	3,054 (75%)	2,056 (51%)

This method precisely differentiates the lightness values of the fungal species based on 29,490 color samples. Scaled from 0–100, lightness followed a Gaussian distribution around a mean of 58 (range: 18.0–97.8, Figure 3.3). We further generated a mega-phylogeny consisting of 2,056 mushroom-forming species using publicly available DNA
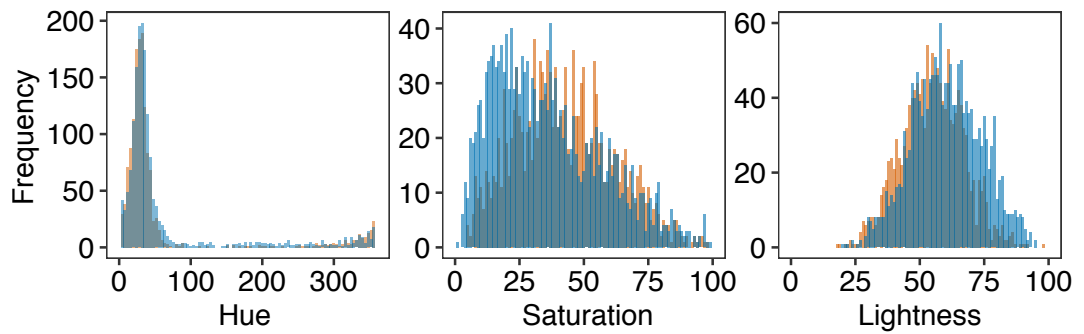
Figure 3.1: Histograms of mushroom hue, saturation and lightness for ectomycorrhizal and saprotrophic species (3,054 species). Both ectomycorrhizal fungi (orange) and saprotrophs (blue) show a hue peak in the interval 1–80 degree, which comprises the colors red, orange, and yellow (note that this includes brown colors). Ectomycorrhizal fungi have on average darker fruit bodies than saprotrophic fungi (Figure 3.7A, Table 3.5). Note that overlapping areas are displayed in darker blue.

sequence data (Figure A.2).
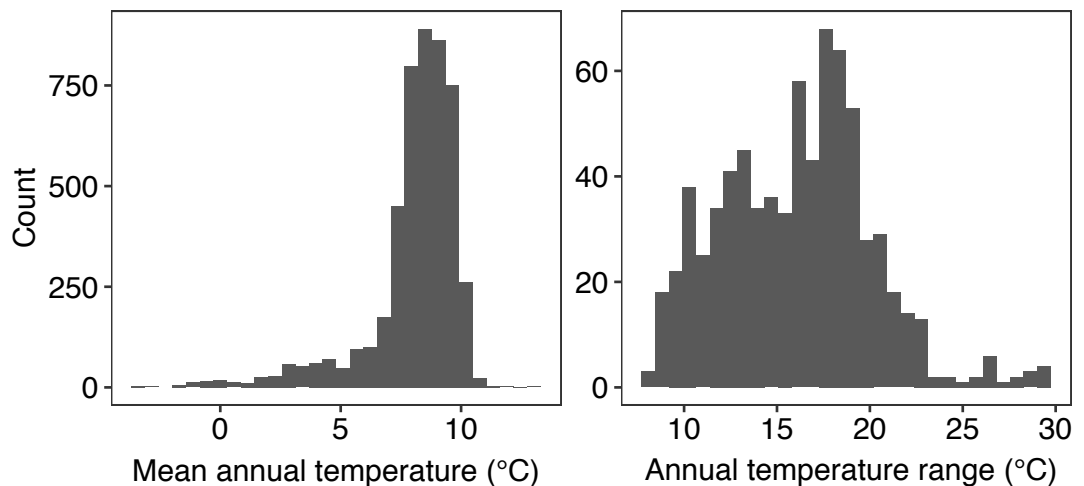
Figure 3.2: Histograms of temperature of the grids in the European dataset. Displayed are mean annual temperature values and the annual temperature ranges (maximum - minimum monthly temperature) of each grid cell used in this study.

Two predominant nutritional modes of carbon acquisition are present in mushroom-forming fungi: the free-living saprotrophs and mutualistic ectomycorrhizal fungi (ECM) [Kohler et al., 2015]. Fungi from both nutritional groups perform important ecosystem processes. As symbionts with many tree species, ECM fungi receive carbon from their host plants and in return increase mineral nutrition, water uptake, and resistance against

pathogens of their host trees [Smith and Read, 2010, Tedersoo et al., 2010]; thus ECM fungi shape the structure and productivity of many forest ecosystems. Saprotrophs decay dead organic matter and release nutrients, which is crucial in carbon and nutrient cycling [Floudas et al., 2012]. Saprotrophs and ECM fungi differ in their fruiting phenology [Büntgen et al., 2013, Boddy et al., 2014] and life history traits [Bässler et al., 2014b, Calhim et al., 2018, Halbwachs et al., 2015] as well as environmental responses [Tedersoo et al., 2014]. Previous studies have shown that ECM fungi invest more than free-living saprotrophs [Bässler et al., 2014b, Alday et al., 2017] in reproductive traits (e.g., larger fruit bodies). Based on the lightness of each species, we have calculated the average assemblage-based color lightness (hereafter 'mushroom color lightness') separately for saprotroph and ECM fungi at a European grid resolution of 50 km x 50 km for each month. We tested whether: (1) the lightness of mushrooms differs between free-living saprotrophic and mutualistic ectomycorrhizal species; and (2) whether mushroom color lightness increases in climates and seasons with higher temperatures.

3.2 Material and Methods

3.2.1 European fungal species distribution dataset and local dataset

This study utilized data from a component of the ClimFun meta-database, a source of unified, multi-source data that originated from many independent data repositories of fungal fruiting records across Europe [Andrew et al., 2017]. We used data from eight of nine countries with substantial numbers of records across the time span of 1970–2010. The composition of fungal assemblages was summarized within 50 km x 50 km grid cells, utilizing the UTM coordinate system (zone 32). Further analyses were based on the resulting community matrix, consisting of 5,725 species and 743 grid cells. Details of the local scale dataset can be found in [Büntgen et al., 2013] and a short description in the caption of Figure 3.5. We coded the main genus-level nutritional mode based on literature [Rinaldi et al., 2008, Tedersoo et al., 2010]. The nutritional modes were equally distributed across the latitudinal gradient of the dataset (Figure 3.4).

3.2.2 Environmental data

Our study aimed to test the hypothesis that the mushroom color lightness increases with temperature. Apart from temperature, we also considered other environmental variables that potentially impact the average color lightness of fungal assemblages. Among these variables, we expected that precipitation, UV radiation, and relative forest cover (as a
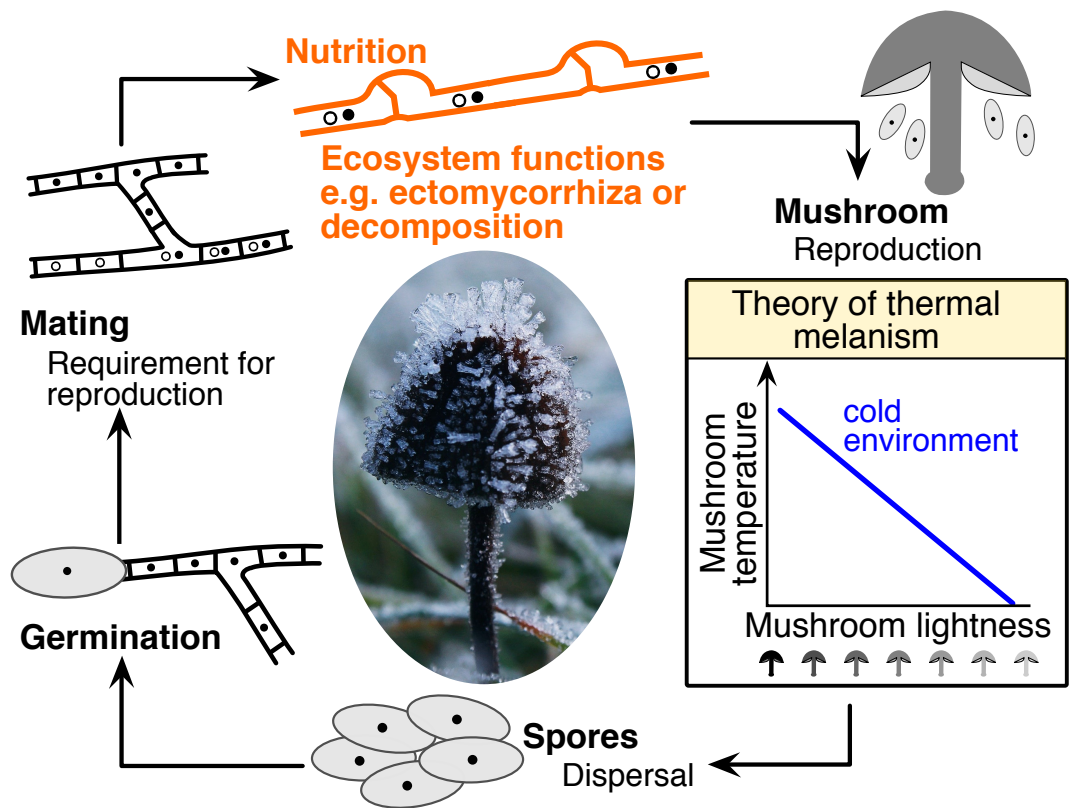
Figure 3.3: The theory of 'thermal melanism' for multicellular mushroom-forming fungi. The hypothesis predicts that dark-colored mushrooms heat up more rapidly than light-colored mushrooms and therefore have advantages in cold environments, such as increased reproductive success.

proxy for darker forests compared to sunnier grasslands and therefore a proxy for microclimate conditions reflecting e.g., local variation in temperature) may be particularly important [Tedersoo et al., 2014].

3.2.3 Grid data preparation

We used citizen-science, herbarium and museum data, which are of great potential for biogeographical and ecological studies despite their potentially biases [Andrew et al., 2017]. We downloaded temperature, precipitation, and altitude data from the WorldClim database version 1.4 (http://www.worldclim.org/current) (representative of 1960–1990 bioclimatic variables) [Hijmans et al., 2005], UV index data (UV radiation) from the NASA website [Newman and McKenzie, 2011], and satellite-based data on relative forest cover from the Forest MAP 2000 dataset [Pekkarinen et al., 2009]. All available
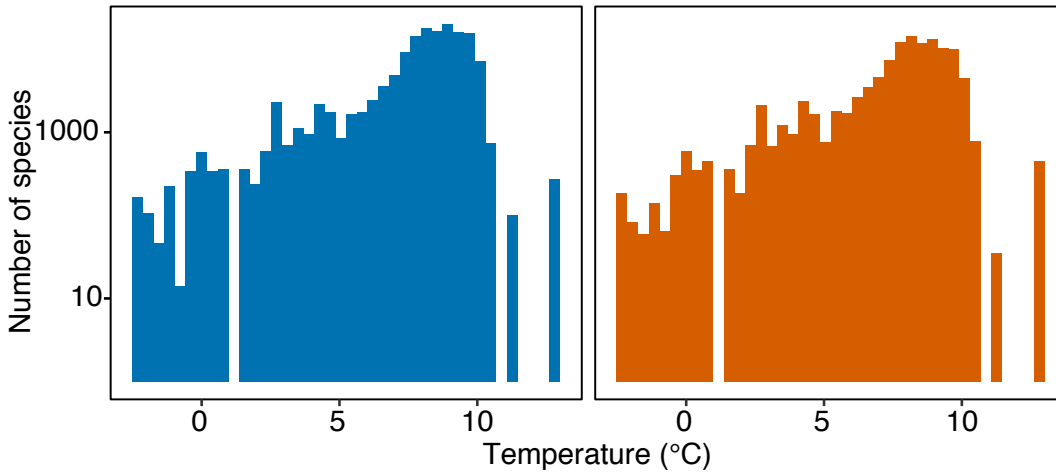
Figure 3.4: Density histogram of the number of species for saprotrophic (blue) and ecto-mycorrhizal (ECM) fungi (orange) along the temperature gradient. Note $\log_{10}$-transformation of the y-axis.

environmental variables were gridded at the 50 km x 50 km level. We calculated the grid cell means only within cells containing fungal records. Temperature, precipitation and altitude were extracted at 5 km resolution from WorldClim. For temperature, we used the average annual mean value for the period 1960–1990, along with mean monthly temperature (1960-1990) calculated from mean monthly minimum and maximum temperatures.

Mean annual temperature values reflect the variability of temperature conditions on a European scale. Surface temperature may be the most relevant value, because fruit bodies grow close to the surface, however the surface temperature is highly correlated with air temperature (temperature used in the analysis) at broad scales [Gunton et al., 2015]. For precipitation, we used the average annual sum for the same period. For the UV index, we downloaded all available grid data for each month of 2010 and calculated the mean UV index across the 12 months for each grid. As far as we know, no reliable long-term UV radiation data are available at the scale of our study. However, variability of UV radiation for a given locality across years is less pronounced than the variability across localities, indicated by straight and parallel isolines [Newman and McKenzie, 2011]. Solar radiation models show that UV radiation underwent a net change in UV-B radiation of ca. 3% in the time period 1970–2010 [Williamson et al., 2014]. Furthermore, these changes through time were spatially consistent across the latitudinal range of our study [Newman and McKenzie, 2011]. Thus, we consider the values of 2010 to be a robust proxy for UV radiation for the temporal scale of our study. For the relative forest

Table 3.2: Statistics of the effect of seasonality on mushroom color lightness using generalized
additive models (GAMs) based on a standardized local scale data set (La Chaneaz).
Effects (F-values) of mushroom color lightness in response to month are given for
saprotrophic and ectomycorrhizal fungi. Effects are presented as F-values and sig-
nificant effects are emboldened. The assemblage calculation was based on an abun-
dance community matrix of mushroom-forming fungi (194 ectomycorrhizal and 121
saprotrophic species). Results based on standardized effect sizes based on three null
models are shown. ECM = Ectomycorrhizal; SAP = Saprotroph

		Mushroom color lightness (non-linear)		Null model Standardized effect sizes					
				Ind. swap		Richness		Frequency	
		F	p value	F	p value	F	p value	F	p value
SAP	Month	3.24	0.021	2.94	0.033	2.84	0.037	3.31	0.018
	Adj. R^2	0.05	0.07	0.07	0.07				
ECM	Month	6.75	0.010	6.56	<0.001	6.66	0.011	3.76	0.011
	Adj. R^2	0.03	0.11	0.03	0.06				

cover per grid cell, each 50 km x 50 km plot covers 4x106 pixels of satellite imagery.
We obtained the relative forest cover per grid cell as the ratio of forest pixels to non-
forest pixels (e.g., grasslands). Note that some grid cells were partly covered by clouds,
hampering an exact estimation of forest cover. However, considering clouds to be forest
or ignoring clouds resulted in comparable estimates of forest cover (data not shown).
For the correlation among co-variables, Table 3.6 (all pairwise correlation coefficients
r<0.41).

Table 3.3: Pairwise correlation coefficients (r) among environmental variables. Prec. = Pre-
cipitation; RFC = Relative forest cover.

	Temp.	Log_{10} Prec.	UV index	RFC	Log_{10} Months
Temperature	-	-0.34	-0.21	-0.20	0.01
Log_{10} Prec.	-0.34	-	0.40	-0.09	0.03
UV index	-0.21	0.40	-	0.33	-0.09
Log_{10} RFC	-0.20	–0.09	0.33	-	-0.05

To address and reduce potential biases associated with observational data, we (i) re-
duced the dataset to mushroom-forming fungi, which are mainly found in the four orders
of the systematic class Agaricomycetes (Basidiomycota): Agaricales, Boletales, Russu-
lales, and Cantharellales. This standardized the dataset to a unique fruit body type,
characterized by soft-fleshed, above-ground stems and caps. This conspicuous mush-
room type attracts most mycologists. (ii) Because the number of records of a species

in a grid cell might reflect collection effort rather than true abundance, we only used the occurrence of each species in each grid cell. The long sampling period, comprising four decades, ensures that these data can be reliably interpreted as estimates of the presence/absence of the species. (iii) To account for possible spatial biases in collection activity, we only included grid cells with a minimum of 25 species occurrences for each nutritional mode in the analyses (resulting in 549 and 522 out of the 743 grid cells for saprotroph and ECM fungi respectively, reducing the dataset mostly in the very north of Norway). Despite this thorough data preparation, spatial biases in collection activity may still bias data interpretation. Thus, we applied null models to account for (1) uneven richness among grids (null model 'richness'), (2) uneven sampling probability of species (null model 'frequency'), and (3) both factors simultaneously (null model 'independent swap'). For a detailed description of the null model approaches, see Statistical Analysis. Note that our response of interest is a mean assemblage trait, calculated based on the lightness values of the species in an assemblage. If temperature acts as an environmental filter, the mean color value should reflect temperature conditions on a grid even though sampling effort differs among grids.

To address a possible shift in color lightness with climate change, we divided our 40-year dataset into two time intervals: 1970–1990 and 1991–2010. The time between the two time intervals is the approximate border of accelerated climate warming [Mann et al., 2004]. As temperature data, we used the E-OBS dataset from the EU-FP6 project EN-SEMBLES (http://ensembles-eu.metoffice.com) and the data provided in the ECA&D project (http://www.ecad.eu) [Haylock et al., 2008]. We gridded the temperature on our 50 km x 50 km grids by selecting the nearest-neighbor temperature value (from the 1/4 degree temperature data) within a maximum range of 15 km. For the analyses, we considered only grids with at least 25 species for each nutritional mode in each of the time periods. We reduced the datasets of the two time-intervals to a subset of common grids, resulting in 356 grid cells. The average temperature difference between the second and first time-interval was 0.7°C and was normally distributed with a range of 0.26 to 1.34°C. We then calculated the difference in temperature and the difference in mushroom color lightness between the second and first time-interval [Zeuss et al., 2014].

3.2.4 Color sampling

We recorded three independent variables for the cap color of each species, based on the cylindrical-coordinate representations of points in an HSL color model: hue (e.g., red, blue), saturation (amount/intensity of hue), and lightness (e.g., ranging from light red to dark red). For more details on the color model, see [van den Broek and van Rikxoort,

2004]. Such human vision models have been shown to reliably detect variation in color in the visible range [Bergeron and Fuller, 2018]. We used the independent component 'lightness' (L) as the basis to calculate the average assemblage lightness ('mushroom color lightness') based on the community matrix. We then used the mushroom color lightness as the response variable in our general additive models.

We searched relevant websites (general mushroom websites, e.g., mycokey.com, mykoweb.com, 123pilze.de, mushroomobserver.org, mushroomexpert.com, grzyby.pl, pilze-basel.ch, mycodb.fr, mycoleron.fr, mykologie.net, discoverlife.org, tintling.com, hlasek.com, fungipedia.org, Wikipedia, mykologie.net, mycoportal.org; and specialized taxon websites, e.g., mycena.no, cortinarius.org, amanitaceae.org, entoloma.de, inocybe.org, boletales.com) for representative images employing the following quality criteria: (i) experts (among authors) chose images with the best color representation of the mushrooms; (ii) at least half of the cap was visible; (iii) overexposed (flashy) or strongly shaded areas in images were not sampled; and (iv) cap areas with reflections by water drops, earthy dirt, or sticky leaves on the cap were not sampled. For species represented by adequate images, we sampled HEX values using the program pipette (Stefan Trost Media, http://www.sttmedia.com/). For all mushroom-forming species from the dataset, we sampled HEX values of nine areas on each mushroom cap, situated on a cross (center, edge, and between center and edge). For species with variable colors, we sampled at least two images. Each of the nine HEX values was then converted into three values (H, S, and L) using the website: http://rgb.to. Thus, each mushroom cap yielded at least nine values for hue, nine for saturation, and nine for lightness. We then calculated the means of H, S, and L separately for each species and used these mean values to characterize species color traits in further analyses. The mean hue for each species was calculated using a circular model (R package 'circular'). Visually, the species lightness sampling corresponded well with the opinions of experts (among co-authors) on mushroom colors (Figure 3.6). The main pigments of mushrooms are melanins, a diverse group of black to brown polymers, and the more colored, low molecular substances such as quinones, arylpyruvic acid derivatives, styrylpyrones and russupteridins [Gill and Steglich, 1987].

3.2.5 Mega-phylogeny approach

To test for phylogenetic constraints on mushroom lightness, and to carry out phylogenetic linear regressions (see Statistical Analysis), we applied a mega-phylogeny approach. The mega-phylogeny approach maximizes species sampling by integrating prior knowledge (e.g., guide tree) into the tree inference [Smith et al., 2009]. For our mega-phylogeny approach we followed the protocol described in Chapter 2. In short, we used five gene

regions (28S and 5.8S rRNA, rpb1, rpb2, tef1), with gene partitioning, that resulted from a partition scheme software [Chernomor et al., 2016], a comprehensive back bone guide tree based from phylogenomic analysis and a column reliability score. We further conducted 1,000 approximate Shimodaira–Hasegawa likelihood ratio tests to assess branching support (SH-aLRT branch support). The final phylogeny consisted of 1,010 ectomycorrhizal and 1,046 saprotrophic fungal species (see Appendix Figure A.2).

We estimated divergence times of the resulting phylogeny using penalized likelihood as implemented in the R function chronos. Although we did not interpret timing of events based on our phylogeny, we time-dated our phylogeny using two calibration points. The branching time estimates fall within the estimates of previous studies. To estimate the effect of phylogenetic uncertainty on our interpretations, we repeated phylogenetic analyses with a set of 100 alternative trees. These trees were derived by creating polytomies on nodes with an SH-aLRT branch support value below 80 based on the non-ultrametric ML tree. These multifurcations were then resolved randomly using the function multi2di from the R package 'ape' [Paradis et al., 2008]. We then estimated divergence times for each tree following the same calibration protocol as above using chronos. For more details see Chapter 2.

3.2.6 Phylogenetic signal

We calculated the phylogenetic signal in color lightness and the environmental variables using four indices: Pagel's lambda, Blomberg's K, Moran's I, and Abouheif's Cmean using the function phyloSignal (R package 'phylosignal' [Keck et al., 2016], with 99 randomizations) and phylosig from R package 'phytools' [Revell, 2012]. For a detailed description and simulation-based tests of all four indices, see [Münkemüller et al., 2012].

3.2.7 Statistical analyses

Based on the monthly grid-by-species community matrix and the species color lightness values, we calculated an average color lightness of assemblages ('mushroom color lightness'), where assemblages are defined as the total species composition found within a grid cell. We fitted generalized additive models (GAM) using the function gam from the R package 'mgcv' [Wood, 2010]. To test for the effect of temperature (mean annual and month) on mushroom color lightness, we fitted seven model structures: six models based on the European dataset (3,054 species) and one on the local-scale dataset (312 species). All models were applied separately for ECM and saprotrophic fungi: (1) a model with mushroom color lightness as the response and macroclimatic temperature

and month as predictors, along with species number ($\log_{10}$-transformed) and geographical latitude and longitude as covariates; (2) a model as in (1) but with standardized effect sizes as responses, calculated from three different null models (see below); (3) a model as in (1) but with the additional relevant environmental variables as predictors, namely mean annual precipitation ($\log_{10}$-transformed), UV index, and relative forest cover ($\log_{10}$-transformed) (refer to Environmental Data); and (4) a model as in (3) but with standardized effect sizes as responses, calculated from three different null models. For the local-scale data set, we applied a model with mushroom color lightness as response and the month as predictor variable. We also fitted model (1) using monthly mean temperature as an additional covariate and found highly consistent effects (results not shown). Within all GAMs we considered spatial location as a covariate ('s(longitude, latitude) ') as well as the grid cell as a random effect ('s(grid, bs = 're')').

Species are statistically non-independent as they share a common evolutionary history [Felsenstein, 1985]. Therefore, we fitted two additional models on the species level, considering those species with phylogenic data (2,056 species): (5) a model with species lightness as the response and species temperature means as the predictor with an interaction term for the species' nutritional mode. Restricting this analysis to those species that occurred on >10 grid cells, in order to obtain a robust mean value, resulted in 1,629 species (we also used 5 and 15 species as thresholds and obtained consistent results). Finally, we fitted a model (6) with species lightness as the response and nutritional mode (ectomycorrhizal versus saprotrophic) as a binary predictor variable. We repeated these models using 100 alternative phylogenetic trees to assess the effect of phylogenetic uncertainty. All 100 trees showed consistent results (Figures S 3.1, 3.5).

Three different null models were used to compute standardized effect sizes (SES): 'richness' (randomizes community data matrix within grids; maintains sample species richness), 'frequency' (randomizes the community data matrix within species; maintains species occurrence frequency), and 'independent swap' (randomizes community data matrix with the independent swap algorithm [Gotelli, 2000], maintaining species occurrence frequency and grid species richness) available in the function randomizeMatrix. We randomized the community matrix 1,000 times (and 1,000 swaps each) and computed the expected color lightness mean for each grid cell and the expected standard deviation. The standardized effect size (SES) was computed by subtracting the expected mean from the observed mean, and dividing by the standard deviation (SD, calculated from 1,000 values of the randomization). Note that in the null model approach, mean differences across groups (e.g., nutritional modes) become less pronounced if applied for groups separately. For models 5 and 6, we used phylogenetic regressions using the func-

tion phylolm from the R package 'phylolm' [Ho and Ané, 2014]. We fitted all models using four models of trait evolution: Brownian motion (BM), Ornstein-Uhlenbeck (OU) with random root, Pagel's lambda, and Early Burst (EB). We then compared models using Akaike's information criterion (AIC).

3.3 Results

3.3.1 Color lightness of mushrooms of ectomycorrhizal and saprotrophic species

To test our first hypothesis, we applied a cross-species phylogenetic regression using 2,056 species based on the European wide data set. We found that the mushrooms of ECM species are significantly darker than those of saprotrophs (Figure 3.7A, Table 3.5). Further, based on a linear mixed effect model we found that the average assemblage-based color lightness of ECMs was significantly darker than of saprotrophs (Table 3.4), a pattern consistent across all months of the year (Figure 3.7B).

Table 3.4: Linear mixed effects model for differences in assemblage mushroom color lightness between saprotroph and ectomycorrhizal fungi. A random effect of grid cell was incorporated due to repeated sampling of the nutritional modes within grid cells.

	t value	p value
Intercept	822.04	<0.001
Saprotroph vs. Ectomycorrhizal	126.39	<0.001

Table 3.5: Phylogenetic linear regression test of differences in species color lightness between saprotroph and ectomycorrhizal fungi. Phylogenetic linear regressions based on different models of trait evolution showed that saprotrophic fungi are significantly lighter in color than ectomycorrhizal (ECM) fungi. This was consistent across 100 alternative trees with variation in branch lengths and topology. BM, Brownian motion; OU, Ornstein-Uhlenbeck; Lambda, Pagel's lambda; and EB, Early Burst. We fitted the Lambda model with 100 alternative trees. Effects are presented as z-values (estimates divided by the respective standard error), and effect sizes above 1.96 or below -1.96 are highlighted in bold. Superscripts indicate rank of model selection based on AIC scores.

Model	Intercept	Saprotrophs vs. ECM
BM[3]	0.07	0.71
OU randomRoot[2]	116.74	9.02
Lambda[1]	4.73	3.28
EB[4]	0.07	0.71
Lambda 100 trees	7.15 (7.06–7.24)	3.01 (3.00–3.03)

3.3.2 Color lightness of mushrooms and the thermal environment

To test our second hypothesis, we used generalized additive models (GAMs) simultaneously using temperature and seasonality (months) and considering species numbers and spatial coordinates of grids as co-variates. First, we found that the model of mushroom color lightness of saprotrophic assemblages showed a higher explained variance (R^2=0.54) than the ECM model (R^2=0.25, Table 3.8). The mushroom color lightness of saprotrophs was significantly positive and almost linearly correlated with temperature (F value=12.92, Table 5.1, Figure 3.8A), meaning that assemblages in cold environments were characterized by a greater proportion of species with dark mushrooms (see also the mapped latitudinal gradient, Figure 3.8). In contrast, ECM color lightness showed a significant non-linear relationship with temperature, with an increase above 5°C (F value=5.26, Table 3.8, Figure 3.8B). Parametric (linear) fits within the ECM models nonetheless yielded consistent positive relationships between mushroom color lightness and temperature (Table 3.8).

Further, across Europe, saprotroph assemblages were significantly darker in the colder seasons of the year (spring, fall and winter), whereas ECM assemblages showed the opposite pattern (F value=94.80, Table 3.8, Figure 3.8). Note that species richness of saprotrophs and ECM fungi was equally distributed across Europe (Figure 3.4). In addition to the large-scale European analysis, we used a standardized local-scale and long-term data set from Switzerland [Büntgen et al., 2013] (32 years of weekly mushroom counts), to test seasonality effects on color lightness, independent of the latitudinal gradient present in the European dataset. Both presence/absence and abundance-weighted measures of the saprotroph assemblages consistently showed decreased mushroom color lightness in colder months of the year and a more pronounced effect for the abundance-weighted analysis (Supplementary Table 3.2 and Figure 3.5). Again, the ECM mushroom color lightness model showed lower explained variance by season compared to saprotrophs (Figure 3.5).

Together, these results showed that: (i) saprotroph assemblages exhibit darker mushroom color lightness in colder temperatures both spatially and temporally at a continental-scale; (ii) saprotrophic assemblages have higher numbers of dark-colored individuals in colder months in the local-scale dataset; and (iii) ECM assemblages had overall low explained variance and even more light-colored assemblages towards the end of the growing season.
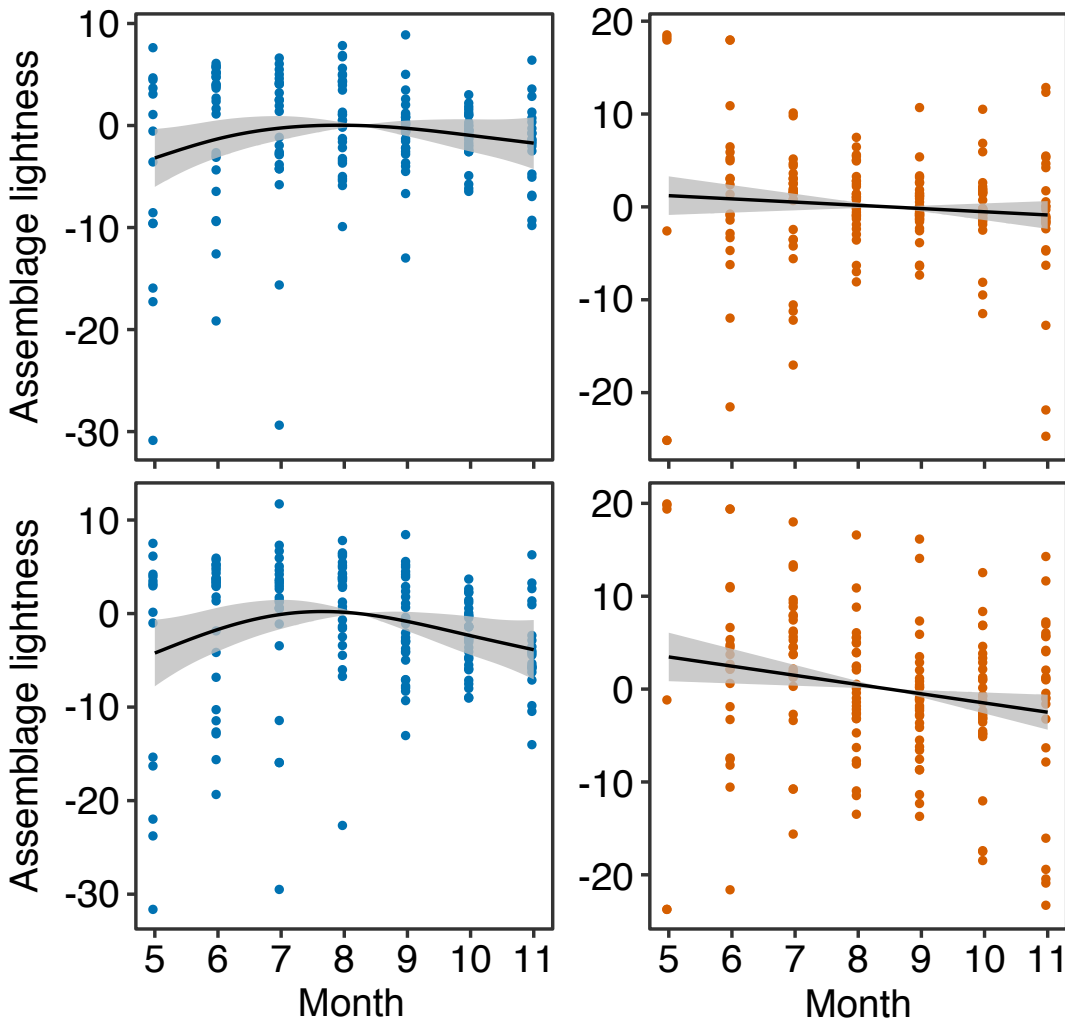
Figure 3.5: Partial effects of seasonality on mushroom color lightness for a local standardized dataset. Effect of months on the mushroom color lightness of saprotrophs (left, blue) and ectomycorrhizal fungi (right, orange). The data set is based on weekly mushroom counts (total 115.417 fruit bodies) between 1975 – 2006. Five plots of 300 m^2 were set up in the fungus reserve 'La Chanéaz' in western Switzerland in a temperate forest on area of 75 ha (for details see [Büntgen et al., 2013]). The dataset is standardized as it does not include an altitude gradient. We summed weekly records of all plots to obtain monthly values for each year and removed species which were found in less than three months across all years. Mushroom color lightness was calculated based on (A) presence/absence data (saprotroph: F-value=1.65, p=0.146; ectomycorrhizal: F-value=1.30, p=0.255), and (B) abundance data (saprotroph: F-value=3.24, p=0.021; ectomycorrhizal: F-value=6.75, p=0.01, Table 3.2). Slopes are estimates from generalized additive models (GAMs) with standard deviations.
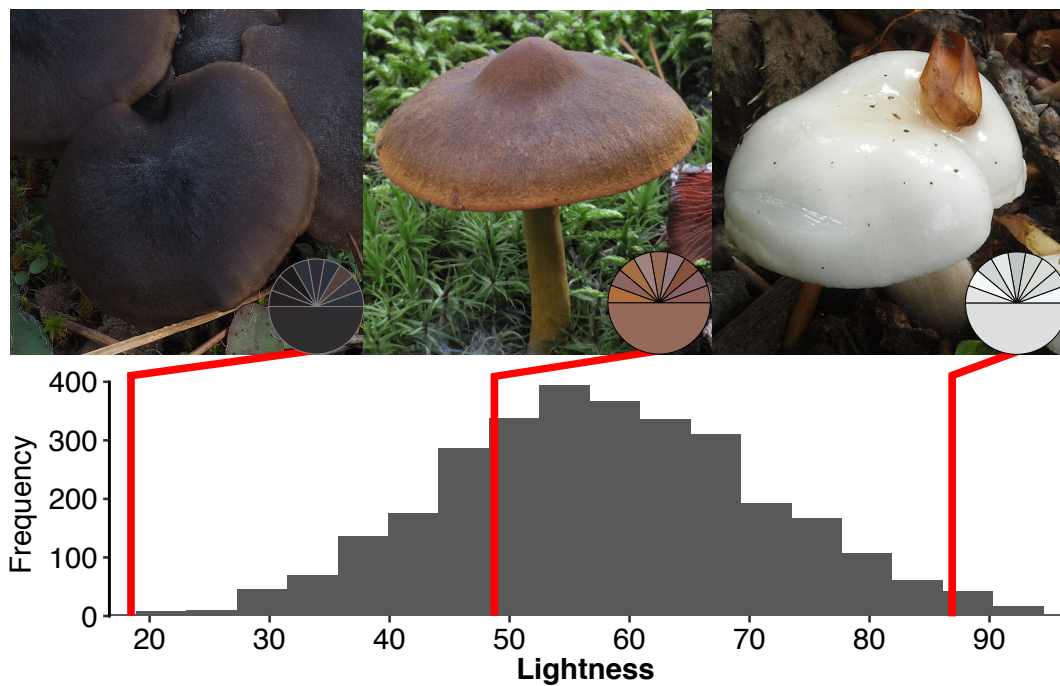
Figure 3.6: Histogram of mushroom lightness and examples of dark-, medium light- and light-colored mushroom-forming fungi. Histogram of color lightness of 3,054 mushroom-forming species. Three exemplar species are shown with their respective color lightness (upper half of the pie chart represents each of the 9 single cap measurements; lower half of the pie chart the respective mean). Species from left to right: *Entoloma sericeum*, *Cortinarius semisanguineus*, *Hygrophorus eburneus*. Photographs by Peter Karasch and Franz-S. Krah
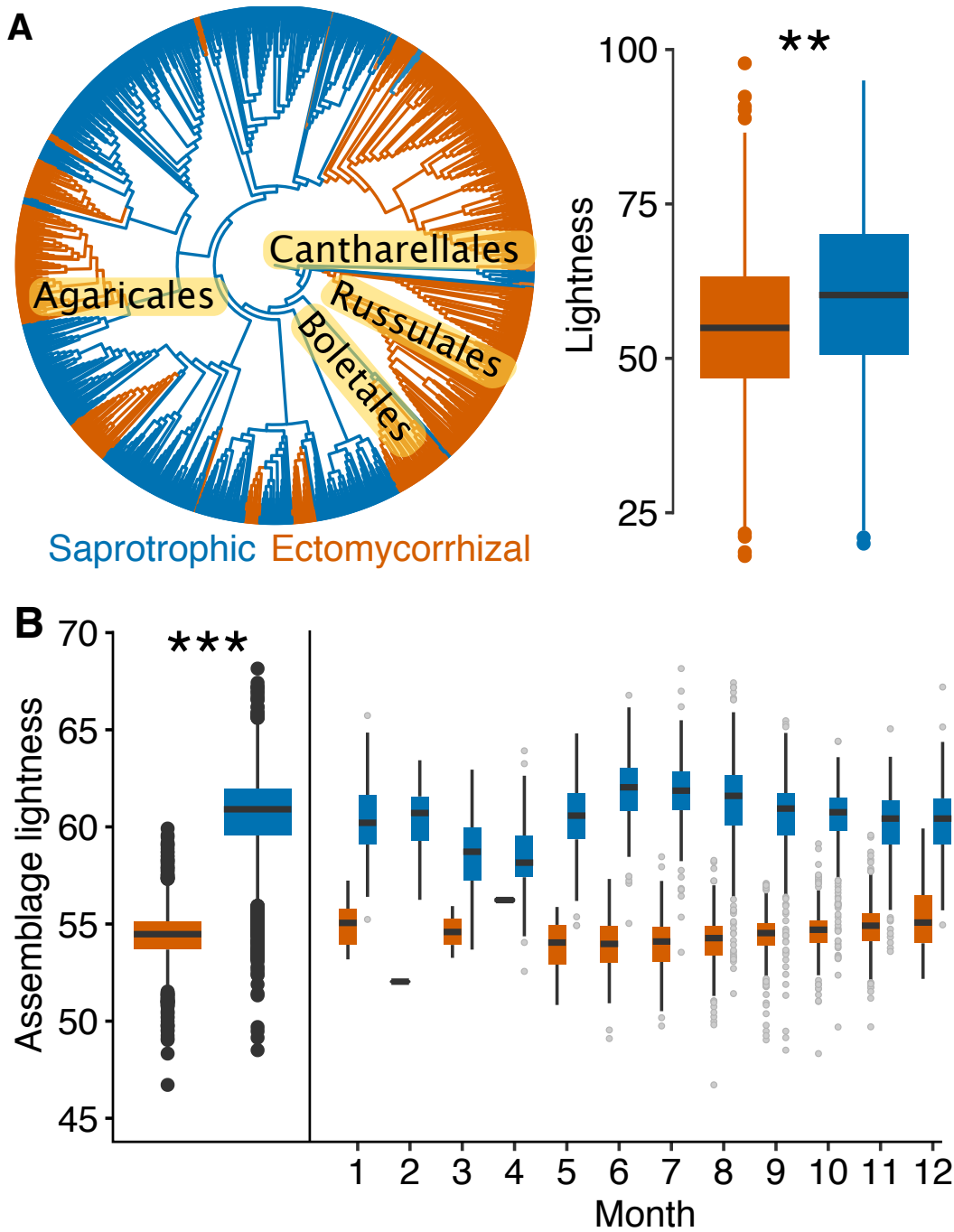
Figure 3.7: Differences in mushrooms color lightness between ectomycorrhizal and saprotrophic fungi. A) Phylogenetic distribution of saprotrophic (blue) and ectomycorrhizal fungi (orange). Boxplot shows the lightness of the two nutritional modes of fungi (ectomycorrhizal and saprotrophic fungi) and the test results based on phylogenetic linear regression (model Lambda; z = 3.28; p < 0.01; Supplementary Table 3.5). Boxplots denote the median (horizontal line) and interquartile range (colored box); whiskers show three times the interquartile range; points indicating values outside this range. B) Difference of the assemblage-based average mushroom color lightness between saprotrophic and ectomycorrhizal fungi (for linear mixed effects model, Table 3.4) and subdivided for each month of the year.
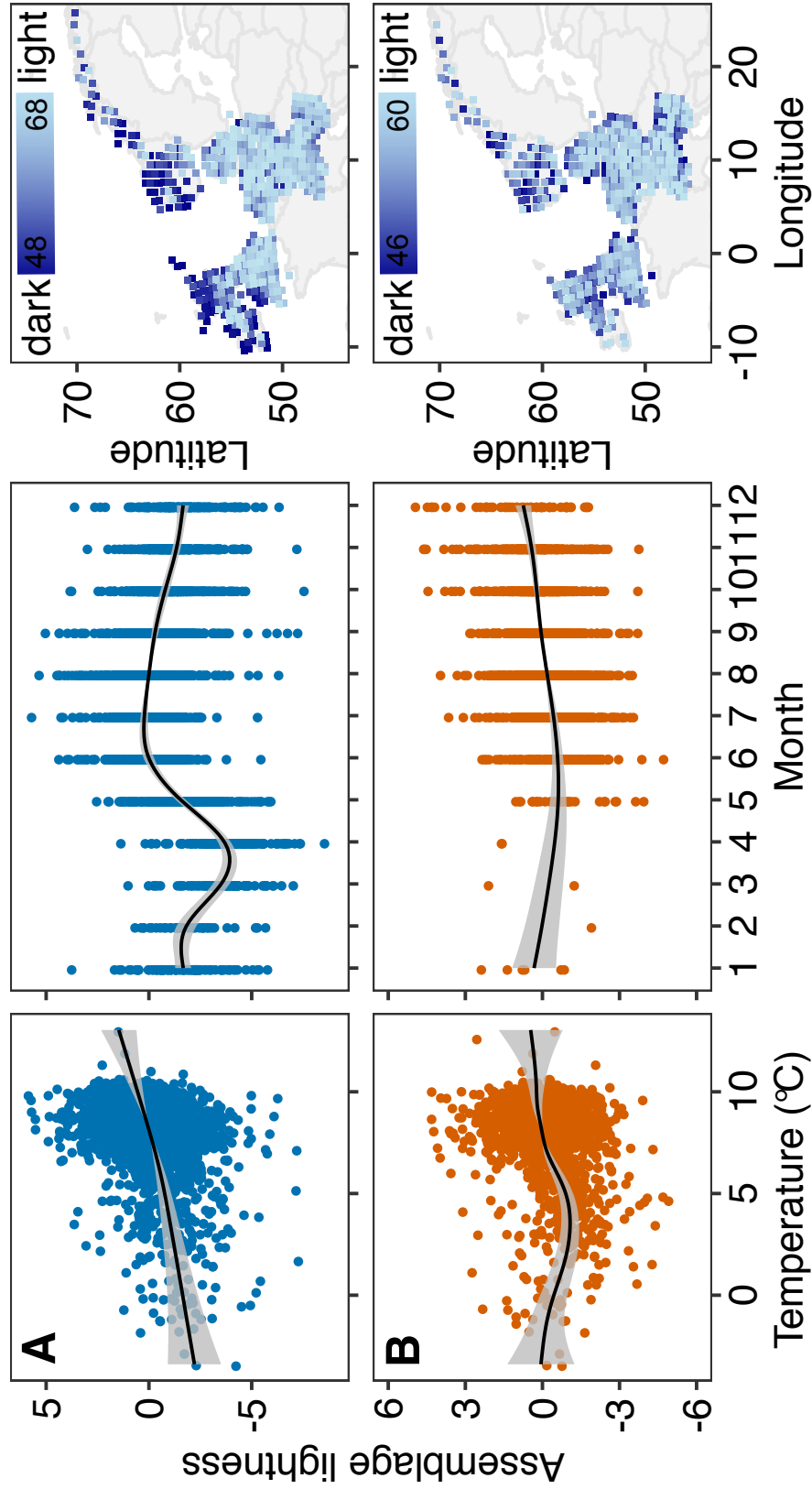
Figure 3.8: Partial effects of temperature and seasonality on mushroom color lightness of 3,054 fungi. Included here are four orders (Agaricales, Russulales, Boletales, and Cantharellales) of the systematic class Agaricomycetes (Basidiomycota). Partial effects of temperature and month on the mushroom color lightness of (A) saprotrophs (blue) and (B) ectomycorrhizal fungi (orange). Maps show mushroom color lightness across Europe. Slopes are estimates from generalized additive models (GAMs) with standard deviations (Table 3.8 for GAM statistics).

3.3.3 Effects of climate change on mushroom color lightness

Temperature increased 1°C on average in Europe across the last century [Pretzsch et al., 2014]. We thus expected saprotroph color lightness to increase accordingly. ECM fungi in contrast might either show no response or, if they experience thermal constraints in warm conditions due to overheating, a stronger effect than saprotrophic fungi. At the temporal scale of our study (1970-2010), the average warming of 0.7°C did not yet significantly affect mushroom color lightness for saprotrophic, nor ECM assemblages (Figure 3.13, linear model: saprotrophic fungi, R^2=–0.003, t=0.234, p=0.815; ECM fungi, adj. R^2=–0.002, t=0.496. P=0.621).

3.3.4 Phylogenetic signal of color lightness

Because species' shared evolutionary history can constrain traits, and species are not statistically independent in tests of how the environment affects the color lightness trait [Felsenstein, 1985], we applied a phylogenetic regression [Grafen, 1989]. We modeled species lightness as a function of the grid-based mean temperature of each species within our dataset. We tested various models of trait evolution and 100 alternative trees to account for phylogenetic uncertainty, as well as an additional model with a random effect on the genus, to reduce the effective number of degrees of freedom. Across all evolutionary models, we found consistent significant positive effects of temperature on species color lightness of saprotrophs, but not all evolutionary models revealed significant effects for ECM species (Tables 3.7, 3.3). Consistently, we found a low phylogenetic signal for lightness (Figure 3.10), and only a slight but significant increase of the phylogenetic signal could be observed towards the tips of the phylogeny (ca. 25 million years). We further (exemplary) explored phylogenetic signal in color in the widespread and species-rich genus *Entoloma*, which revealed lightness shifts on very small taxonomic scales, and a positive color lightness response with macroclimatic and seasonal temperature conditions (Figure 3.9).

3.3.5 Alternative hypotheses and null model analyses

Finally, we tested the robustness of our findings by extending analyses to potential alternative explanations of the observed results. We, therefore, tested whether temperature is confounded with other abiotic variables, including mean annual precipitation, UV index, and relative forest cover (as a proxy for microclimate conditions, i.e., darker forests compared to lighter open habitats). We found that these potential drivers were only weakly correlated with temperature (r<0.41, Table 3.6). General additive models including all

Table 3.6: Phylogenetic regression of the effect of temperature of fungal nutritional modes on species lightness based on various evolutionary models. Temperature was averaged for each species occurring at least on 10 grid cells (741 ectomycorrhizal and 797 saprotrophic species). BM, Brownian motion; OU, Ornstein-Uhlenbeck; Lambda, Pagel's lambda; and EB, Early Burst. We fitted the Lambda model based on 100 alternative trees. Effects are presented as t-values (estimates divided by the respective standard error), and significant effects are emboldened. Superscripts indicate rank of model selection based on AIC scores. ECM = Ectomycorrhizal; SAP = Saprotroph.

	Intercept		SAP		ECM	
	t value	p value	t value	p value	t value	p value
BM[3]	0.10	0.920	5.59	<0.001	12.50	<0.001
OUrandomRoot[2]	20.95	<0.001	4.59	<0.001	2.14	0.032
Lambda[1]	7.22	<0.001	3.17	0.002	1.69	0.091
EB[4]	0.10	0.920	5.59	<0.001	12.50	<0.001
Lambda 100 trees	7.58 (6.53-8.89)	<0.001	2.95 (2.77-3.11)	0.002 (0.002-0.006)	1.69 (1.61-1.84)	0.106 (0.065-0.160)

variables revealed that the model of mushroom color lightness of saprotrophic fungi explained more variance than the ECM model (Table 3.9). All models showed the largest effects for temperature and seasonality driving mushroom color lightness (Table 3.9). We then applied three null models to test whether uneven species richness or species frequency might bias interpretations. The 'richness' model accounts for uneven species richness among grids, the 'frequency' model for uneven sampling probability of species and the 'independentswap' for both factors simultaneously [Gotelli, 2000]. All three null models showed consistent effects with the observed average assemblage-based color lightness as response variable (Figure 3.11, Table 3.9).

Table 3.7: Analysis of variance (ANOVA) test of differences in species lightness between saprotroph and ectomycorrhizal fungi and the effect of temperature. Phylogenetic regressions might provide incorrect degrees of freedom if clades share the same trait owing to common descent. According to Grafen (Grafen 1989), each radiation (e.g., radiation of ectomycorrhizal fungal clade) should be treated as an independent data point with one degree of freedom ('radiation principle'). Thus, we also used a model that included 'genus' clades as a random effect in the function aov from the R package 'stats' ('+ Error(genus)') to test for lightness differences between nutritional modes. We used the "genus" because we found increased phylogenetic mainly within genera (Figure 3.10). The analysis of variance thus estimates a cross-genus and a within-genus effect of nutritional mode. The cross-genus effect applies one degree of freedom for each genus instance (e.g., 150 instead of 150+1386) and thus for each 'radiation' of ectomycorrhizal fungi. Based on this model, we found a significant difference of species lightness between the nutritional modes. Significant F values are in bold; Sq, sum of squares; Df, degrees of freedom.

		Sum Sq	Mean Sq	F value	P value	Df
Cross-genus	Saprotrophs vs. Ectomycorrhizal	13919	13919	31.24	<0.001	1
	Residuals	66836	446			150
Within-genus	Saprotrophs vs. Ectomycorrhizal					
	Residuals	193152	139.4			1386
Cross-genus	Nutr. mode: Temp.	15571	7786	17.8	<0.001	2
	Residuals	65184	437			149
Within-genus	Nutr. mode: Temp.	377	188.3	1.352	0.259	2
	Residuals	192776	139.3			1384
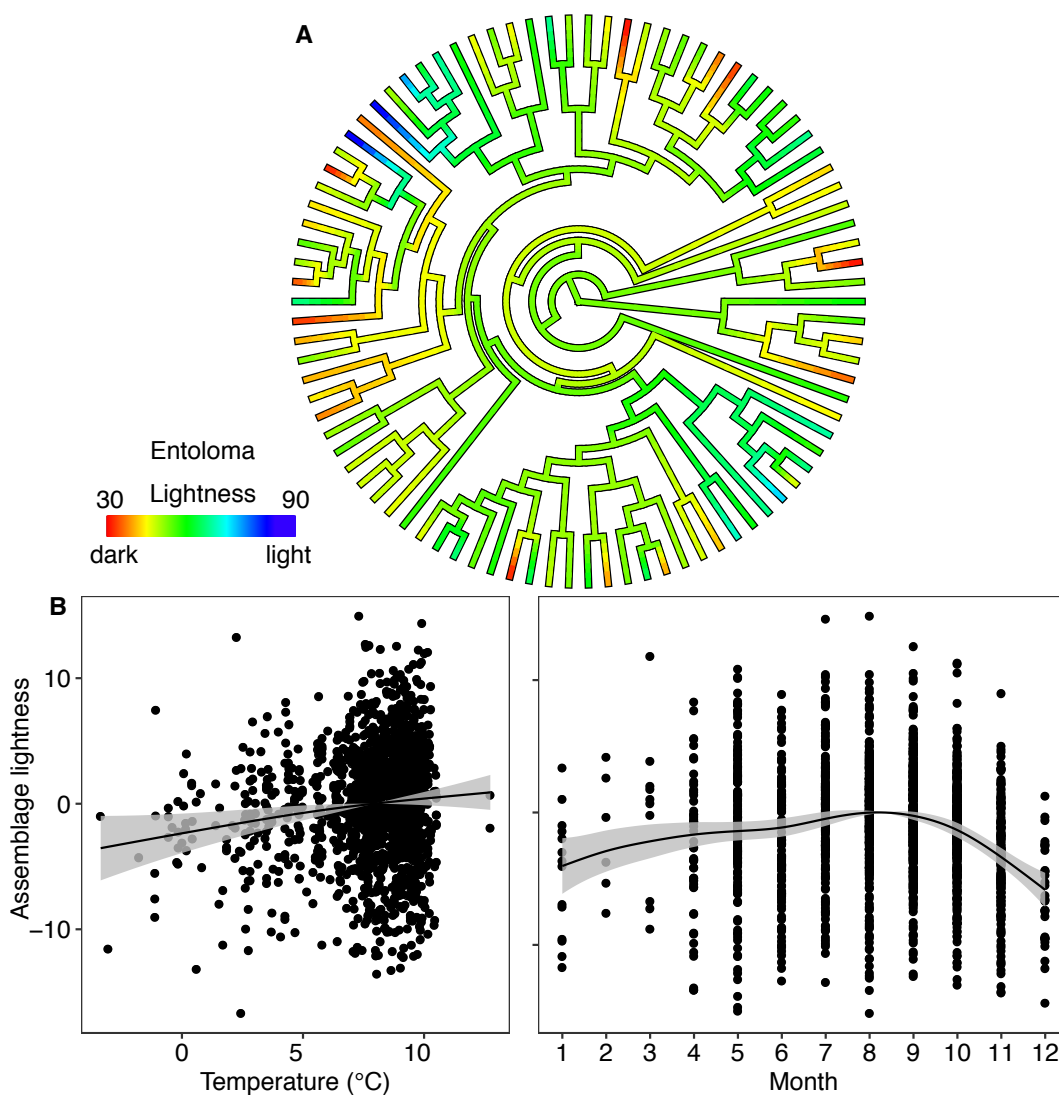
Figure 3.9: Partial effects of temperature and seasonality on the widespread and species rich genus *Entoloma*. A) Ancestral state estimation (function contMap, R package 'phytools') of the continuous lightness trait showing single-species or small clade divergences resulting in low phylogenetic signal (Figure 3.10). B) Partial effects of temperature (F-value=5.67, p<0.05) and month (F-value=18.00, p<0.001) on mushroom color lightness within the genus *Entoloma*, based on a generalized additive model (R^2=0.21). Model is based on 491 grids and 90 species. We additionally considered space (geographical latitude and longitude) as a covariate (F-value=11.64, p<0.001).
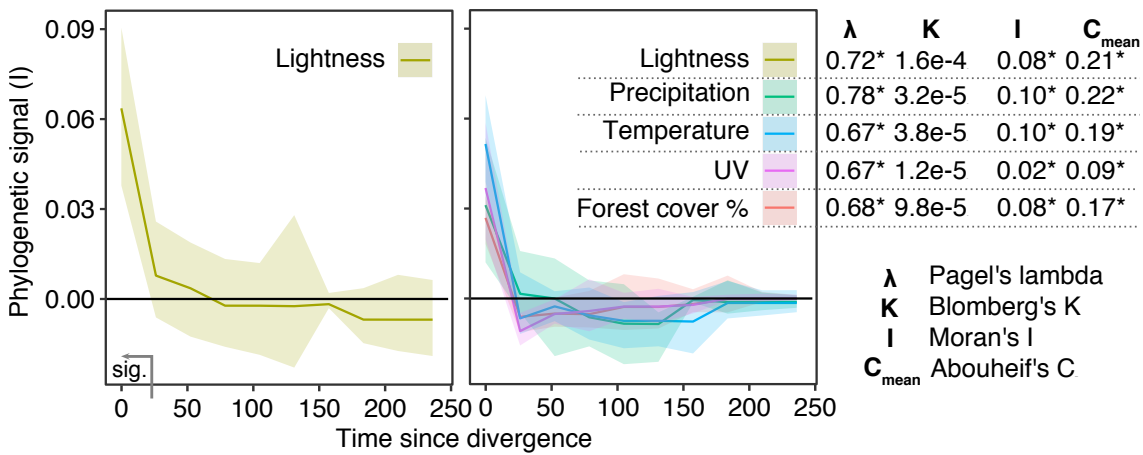
Figure 3.10: Phylogenetic signal of species mushroom lightness and environmental variables. The phylogenetic signal was calculated as four different measures (right side), and displayed based on Moran's I (phylogenetic correlogram). Confidence interval (CI) based on 99 bootstraps. Significant phylogenetic signal was detectable only on very short phylogenetic distances, i.e., between closely related taxa (CI above null line). The measures of phylogenetic signal show a low signal except for Pagel's lambda, which displayed medium-high values. Based on simulations, one study showed that Moran's I and Abouheif's Cmean of 0.1 and 0.2 each, indicate a strength of Brownian motion of approximately 0.3 (on a scale from 0 to 1) [Münkemüller et al., 2012].
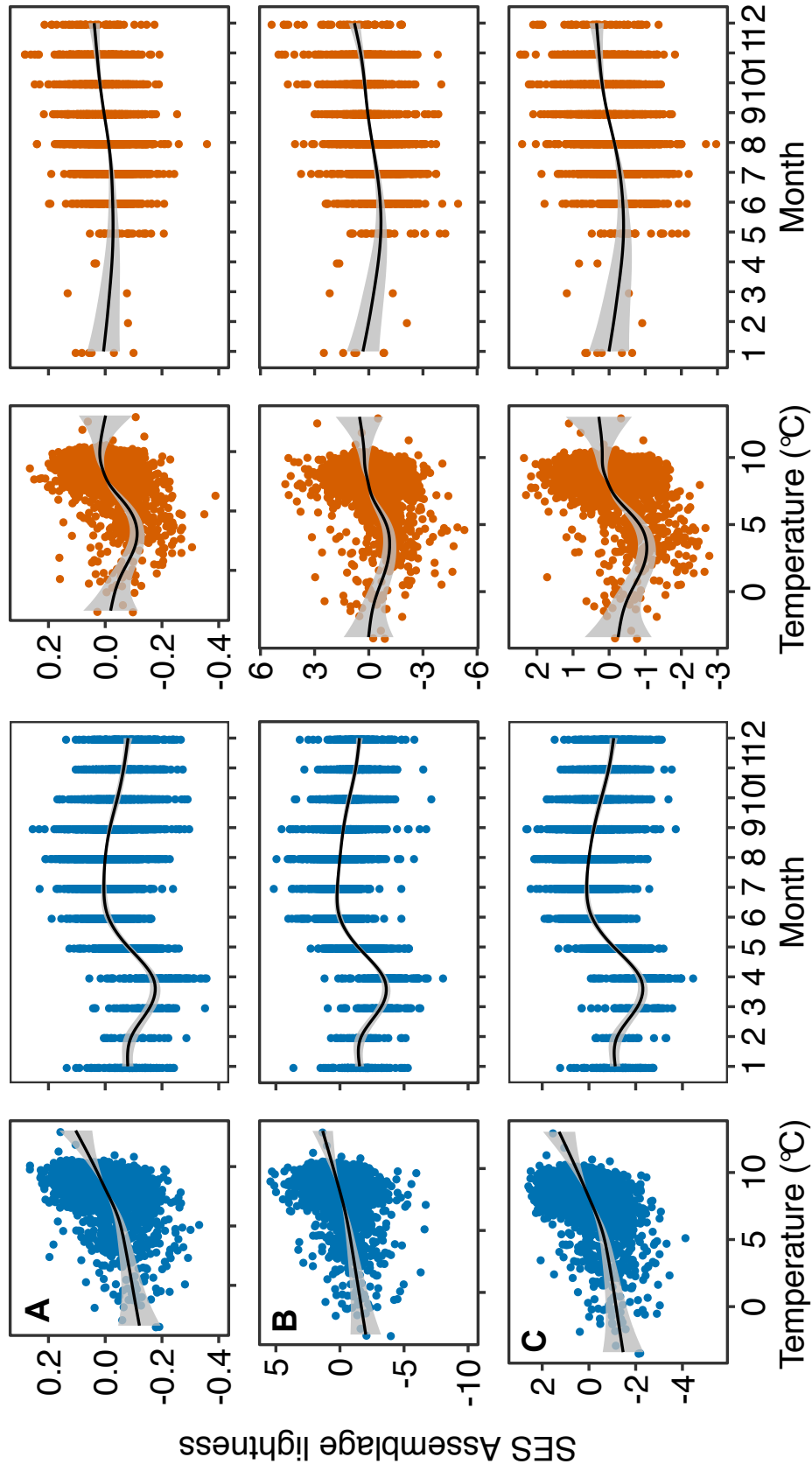
Figure 3.11: Partial effect of temperature and seasonality on standardized effect sizes (SES) of mushroom color lightness. Standardized effect sizes were calculated based on 1,000 randomizations of the community matrix (3,054 species) using the three null models: A) 'frequency', B) 'richness', and C) 'independent swap'. Saprotroph responses are shown in the two columns on the left (blue); ectomycorrhizal responses in the two columns on the right (orange). For statistics see Table 3.8.

3.3.6 Experimental heating of mushrooms with different color

Finally, we experimentally tested if mushrooms with a dark-colored cap heat up more rapidly than light-colored mushrooms using two cultured variants of *Agaricus bisporus* (Figure 3.12). Artificial solar radiation resulted in an increased warming of the dark-colored vs. light-colored mushroom caps. This difference became stronger over time. Using 12 replicates per color, we found that increased warming led to a significant average difference of 1.2°C after 5 minutes of artificial solar radiation (Figure 3.12)

Figure 3.12: Experimental effect of artificial solar radiation on mushroom cap temperature. We used two cultured breeding variants (brown=dark and white=light) of *Agaricus bisporus* [Genders, 1982] to test how mushroom cap lightness affects their temperature dynamics. All mushroom individuals were of similar size and fresh weight. We first cooled mushroom caps to ca. 12°C in a refrigerator and measured the initial cap temperature. We then placed caps beneath a solar lamp, which we positioned at a distance to create ca. 30°C on the cap surface. We measured the cap temperature at regular intervals over time using an infrared thermometer (removing the caps from the solar lamp for measurement). We alternated the order of measurement of dark and light caps. A) Using this experimental design, we first tested the temporal effect on mushroom cap temperature using 3 dark and 3 white caps of A. bisporus individuals. We found that dark mushrooms were warmer than light mushrooms and that this difference increased over time. Error bars denote the upper and lower range. B) For a more robust statistical test of the warming deficit of light caps, we then measured 12 dark and 12 light caps before and after solar lamp exposure and found significantly warmer mushroom caps of the dark variety after 5 minutes (difference between means: 1.21°C). Note finally that this result is consistent with studies demonstrating that dark-pigmented insects and yeasts heated up faster and reached higher temperatures than lighter individuals following irradiation [Kalmus, 1941, Willmer and Unwin, 1981]. Boxplots denote the median (horizontal line) and interquartile range (colored box); whiskers show three times the interquartile range. Figure on next page.

A n = 3

B n = 12

Time 0 min. | Time 5 min.

Dark | Light | Dark | Light

n.s. | ***
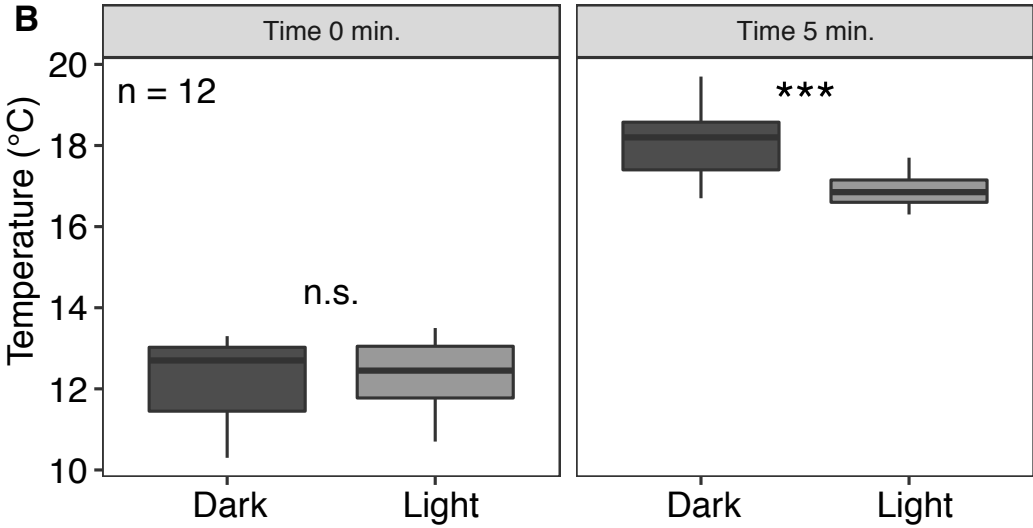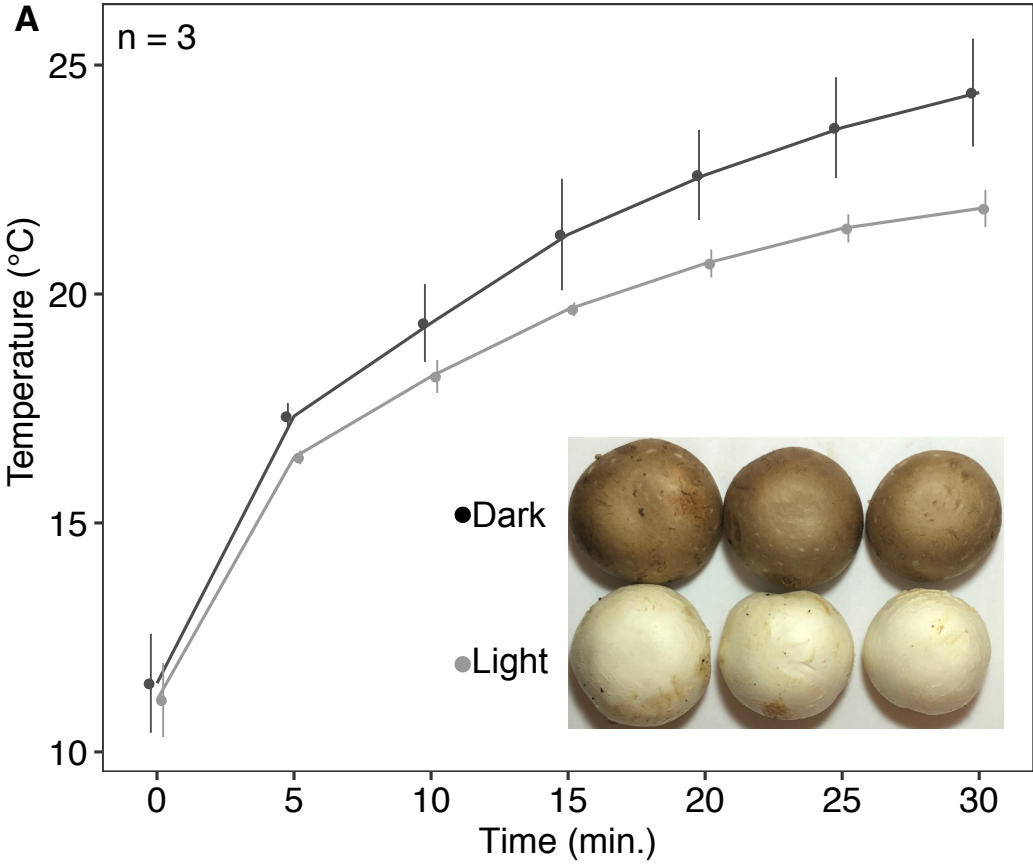
Table 3.8: Statistics of the effect of temperature and seasonality of fungal nutritional modes on the mushroom color lightness using generalized additive models (GAMs). We present effects (F-values) of the mushroom color lightness in response to mean annual temperature and month, using species number and space (latitude and longitude) as co-variates. Species numbers were $\log_{10}$-transformed. Effects are presented as F-values and significant effects are emboldened. The assemblage calculation was based on a presence/absence community matrix of mushroom-forming fungi (1,401 ectomycorrhizal; 1,653 saprotrophic species). Further, results based on standardized effect sizes based on three null models are shown.

| | | Mushroom color lightness | | | | | Standardized Effect Size - Null models | | | | |
| | | Temp. non-linear | | Temp. linear | | Independent swap | | Richness | | Frequency | |
		F	p value	F	p value	F	p value	F	p value	F	p value
SAP	Temperature	12.92	<0.001	7.29	<0.001	15.97	<0.001	12.75	<0.001	17.29	<0.001
	Month	94.80	<0.001	87.36	<0.001	70.34	<0.001	95.49	<0.001	96.10	<0.001
	Species number	7.85	<0.001	7.54	<0.001	1.08	0.383	7.95	<0.001	3.98	0.002
	Space	25.96	<0.001	37.07	<0.001	26.68	<0.001	25.36	<0.001	26.66	<0.001
	Adj. R^2	0.54	0.54	0.51	0.54	0.56					
ECM	Temperature	5.26	<0.001	5.23	<0.001	16.83	<0.001	9.70	<0.001	15.69	<0.001
	Month	94.63	<0.001	24.54	<0.001	22.52	<0.001	28.14	<0.001	29.53	<0.001
	Species number	7.83	<0.001	7.93	0.005	3.74	0.011	2.32	0.128	4.36	0.008
	Space	26.19	<0.001	4.93	<0.001	3.36	<0.001	4.02	<0.001	3.90	<0.001
	Adj. R^2	0.25	0.25	0.30	0.25	0.30					

Table 3.9: Statistics of effects of temperature and co-variables on mushroom color lightness using generalized additive models (GAM). We present effects (F-values) of the mushroom color lightness in response to mean annual temperature, month, mean annual precipitation, UV index, relative forest cover, species number and space (latitude and longitude). Precipitation, species numbers and relative forest cover were $\log_{10}$-transformed. Effects are presented as F-values and significant effects are emboldened. RFC = Relative forest cover. ECM = Ectomycorrhizal; SAP = Saprotroph

| | | Mushroom color lightness (non-linear) | | Null models - Standardized effect sizes | | | | | |
| | | | | Independent swap | | Richness | | Frequency | |
		F	p value	F	p value	F	p value	F	p value
SAP	Temperature	10.56	<0.001	8.10	<0.001	10.52	<0.001	11.64	<0.001
	Month	67.30	<0.001	45.11	<0.001	67.77	<0.001	61.05	<0.001
	Precipitation	6.14	<0.001	4.66	<0.001	5.54	<0.001	5.84	<0.001
	RFC	1.26	0.260	1.15	0.283	1.24	0.264	0.54	0.461
	UV index	0.35	0.751	0.73	0.392	0.38	0.731	0.03	0.867
	Species number	3.63	0.010	0.61	0.436	3.68	0.009	2.80	0.021
	Space	5.69	<0.001	6.23	<0.001	5.58	<0.001	6.41	<0.001
	Adj. R^2	0.48		0.45		0.48		0.50	
ECM	Temperature	6.81	<0.001	10.72	<0.001	7.09	<0.001	10.34	<0.001
	Month	20.25	<0.001	14.00	<0.001	20.37	<0.001	20.46	<0.001
	Precipitation	1.58	0.209	0.38	0.537	1.53	0.216	0.06	0.803
	RFC	0.34	0.562	0.28	0.594	0.34	0.562	0.14	0.707
	UV index	2.66	0.018	3.32	0.022	2.95	0.015	2.34	0.031
	Species number	6.17	0.013	3.40	0.026	5.82	0.016	0.93	0.402
	Space	2.69	<0.001	2.42	0.004	2.70	<0.001	2.66	0.001
	Adj. R^2	0.28		0.32		0.28		0.32	

3.4 Discussion

Using a large-scale European data set, we demonstrated that dark saprotrophic mushroom assemblages are more prevalent in colder areas and seasons of the year. Our results together with previous findings [Cordero et al., 2018] support the view that the theory of thermal melanism is evident across kingdoms. Interestingly, ECM species are generally darker in phenotype compared to saprotrophs, and their average assemblage-based color lightness showed a much weaker response to the thermal environment. Our results thus indicate a lifestyle-specific adaption of mushroom lightness to the thermal environment.

3.4.1 Nutritional mode disparity

Even though fungi of both nutritional modes (mutualistic ectomycorrhizal and saprotrophic) have the same fruit body type (mushrooms), they differ significantly in lightness (Figure 3.7, Tables 3.5, 3.4). Indeed, we have shown that our study is consistent with previous studies demonstrating significant differences of morphological traits of the fruit body between these nutritional modes. It has been shown that mutualistic fungi have larger fruit bodies as well as larger and more ornamented spores compared to free-living saprotrophs [Bässler et al., 2014b, Calhim et al., 2018]. Furthermore, the fruit body size versus number of fruit bodies trade-off is less pronounced for mutualistic fungi indicating an overall higher level of reproductive biomass compared to saprotrophic fungi [Bässler et al., 2014b, 2016a]. The production of large and many fruit bodies (reproductive biomass [Halbwachs et al., 2016]) requires carbon acquisition, which is costly for the organism. It has therefore been suggested that the evolution of the mutualistic lifestyle in mushroom-forming fungi increased their reproductive fitness by receiving carbon from the symbiotic host plant which is consistent with mutualism theory [Bässler et al., 2014b, Calhim et al., 2018, Leigh Jr, 2010]. In contrast, saprotrophic fungi have to produce enzymes to gain carbon from the breakdown of organic matter. If the production of pigments is costly and pigments are correlated with reproductive fitness, we would expect that the mutualistic lifestyle could afford a higher level of mushroom pigmentation compared to free living saprotrophs.

However, mutualistic relationships not only provide opportunities but also constraints. For example, environmental selection on ECM fungi can be affected by the hosts' biology and ecology via at least two possible mechanisms: (1) ECM species occur in darker habitats owing to their symbiosis with forest tree species, and because forests are darker and thus colder during the daytime than open fields or grasslands, ECM species might have evolved darker mushroom phenotypes in order to enhance warming by solar radia-

tion. (2) ECM tend to produce fruit bodies towards late autumn (September, October), when the host tree allocates carbon towards the root and ECM species [Kauserud et al., 2010, Boddy et al., 2014]. Late fruiting coincides with lower temperatures, which could also lead to stronger selection for darker mushrooms among ECM species. By contrast, free-living saprotrophs might be less affected by spatial [Kauserud et al., 2010, Boddy et al., 2014] and temporal constraints [Büntgen et al., 2013] and thus avoiding very low temperatures. These additional hypotheses are currently difficult to assess because habitat characteristics are still poorly characterized for most species due to a lack of observational studies.

Our results together suggest thermal melanism for saprotroph fungi but do not indicate that pigmentation of ECM mushrooms is associated with their thermal environment. However, the weaker environmental selection of ECM mushroom color lightness by temperature (Figure 3.8B) may be caused by a generally darker phenotype of ECM fungi (Figure 3.7A).

3.4.2 Climate Change and mushroom color lightness

The main finding of our study is that mushroom color lightness of saprotrophs is darker in cold environments and cold months of the year (Figure 3.8, Table 3.8). We were further interested whether mushroom color lightness has responded to recent climate warming (temperature shift). However, even though the trend was slightly positive for both saprotrophic and ECM fungi, the change in mushroom color lightness was not yet significant (Figure 3.13). Possible explanations for the lack of relationship between climate change and mushroom lightness may be that: (1) species occurrences are stable, but their abundances have changed, which we are not able to track given that our dataset consists of presence/absence entries; (2) species occurrences are stable at the 50 x 50 km grid scale, as they can disperse and find suitable habitats within this scale. For example, it is well known that many species move towards higher altitudes due to climate warming [Chen et al., 2011]; and (3) dark-colored species might still exist by occupying a suitable "cold" niche [Gange et al., 2018]. This phenomenon has been introduced to explain that cold pockets prevent plant species from elevation shifts to track climate warming [Scherrer and Körner, 2011]. Further studies are hence needed to illuminate changes in abundance on a larger scale, based on fine-grained resolution. A local study in Switzerland, for example, showed a recent increase in the number of fruit bodies in the period 1991-2006 compared to 1975-1990 [Büntgen et al., 2013]. Another study demonstrated a drought-induced reduction of sporocarps and species richness since 1995 [Büntgen et al., 2015]. This suggests that global warming can affect mushroom fruiting.

A warmer environment might allow light-colored species to colonize a new habitat. On the other hand, dark-colored species might disappear if physiological constraints are limiting metabolism (e.g., overheating) and may be prone to colonize higher altitudes. However, our results suggest that a shift in the community composition (change of occupancy pattern, not abundance) due to global warming, as a result of pigmentation, is likely a longer-term process.
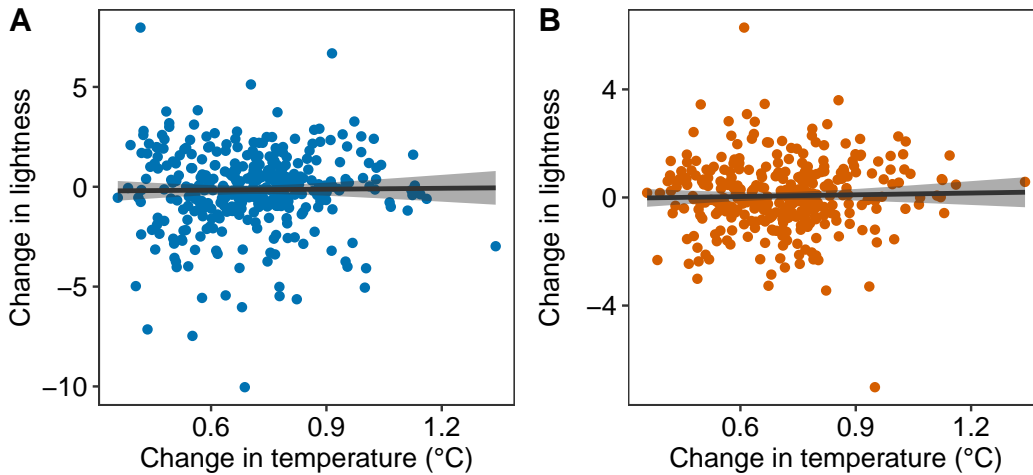
Figure 3.13: Effects of climate warming on change in mushroom color lightness. To test for effects of climate warming on mushroom color lightness, we split our 40-year European dataset into two time intervals: 1970–1990 and 1991–2010. The border between these two time intervals marks the approximate border of accelerated climate warming [Mann et al., 2004]. We calculated the change in temperature as the mean annual temperature of the first time-interval subtracted from the mean annual temperature of the second time-interval; the change in lightness is the mushroom color lightness of the first time-interval subtracted from the mushroom color lightness of the second time- interval. Effect of a change in temperature on a change in mushroom color lightness of (A) saprotrophic fungi (blue) and (B) ectomycorrhizal (orange) between the two time-intervals. Lines are linear model regressions with error bars displaying 95% confidence interval.

3.4.3 Phylogenetic signal

We found a low phylogenetic signal for lightness (Figure 3.10), suggesting that lightness of mushroom-forming fungi is not strongly conserved. The phylogenetic signal only increased slightly but significantly towards the tips of the phylogeny (ca. 25 million years), indicating conserved evolution below the genus level (Figure 3.10). Studies addressing phylogenetic signal in color traits are rare, but one study found low phylogenetic signal in plant fruit colors [Stournaras et al., 2013]. Supporting the general finding of low

phylogenetic signal, the widespread and species-rich genus *Entoloma* demonstrated that lightness shifts also occurred on very small taxonomic scales, resulting in a positive color lightness response with temperature and seasonality, even within this genus (Figure 3.9). Further, the phylogenetic signal in temperature was equally high as lightness, indicating a possible adaptation of lightness to temperature (Figure 3.10). Taxonomically well-sampled fine-scale phylogenomic studies can further elucidate the evolutionary basis of the color trait.

3.4.4 Alternative explanations beyond the thermal environment

Studies addressing the color lightness of insects have often found significant effects of precipitation/humidity or UV radiation [Zeuss et al., 2014, Bishop et al., 2016, Heidrich et al., 2017]. Some studies suggested that UV radiation affects melanin within mycelium [Cordero and Casadevall, 2017]. Furthermore, even though it has not yet been addressed, we found it plausible to assume that the structure of the habitat (microclimate conditions as they entail temperature variability) could also influence mushroom color lightness. Besides temperature we tested the effects of other environmental factors, namely mean annual precipitation, UV radiation, and relative forest cover (a proxy for microclimate conditions), on mushroom color lightness. We found only weak correlations among all variables (r<0.41), suggesting no confounding effects of precipitation, UV radiation, and relative forest cover on temperature (Table 3.9). Further, in the general additive model considering all variables, we found that besides temperature and seasonality, precipitation was a strong predictor of mushroom color lightness for saprotrophs (however, with lower F-values: 10.56 vs. 6.14, Table 3.9). Furthermore, relative forest cover and UV index had no significant effects (Table 3.8). For ECM fungi, UV index, as well as temperature, had small but significant effects on mushroom color lightness (Table 3.8), however, with a positive response, meaning darker assemblages in environments with lower UV index (Figure 3.14). In the following, we will briefly discuss the possible effects of precipitation, UV radiation, and relative forest cover on mushroom color lightness, although these relationships remain speculative without further studies.
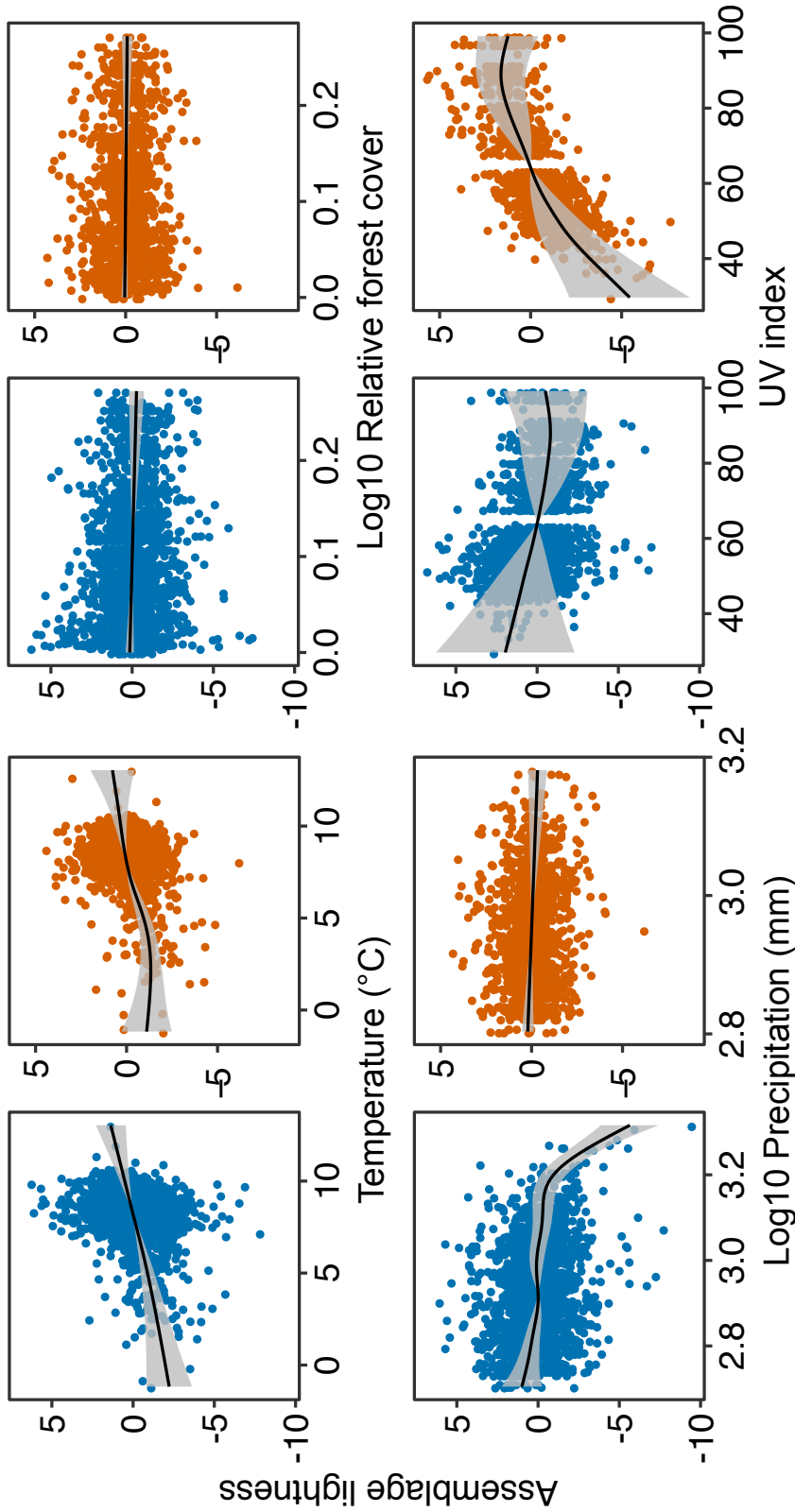
Figure 3.14: Partial effect of temperature, precipitation, relative forest cover and UV index on mushroom color lightness. The left column within each variable displays effects for saprotrophs (blue), the right column for ectomycorrhizal fungi (orange). Plots are based on fits of the generalized additive models (Table 3.9).

Precipitation. A recent study found a strong negative correlation between humidity and Lepidoptera color lightness, suggesting a potential role of melanin in protection against pathogens [Heidrich et al., 2017]. Humid habitats coincide with a higher pathogen (bacterial, fungal) pressure [Reilly et al., 2014, Yin et al., 2016], and melanin-based dark pigments protect insects against pathogens [Wilson et al., 2001]. To the best of our knowledge, such an antimicrobial protection is not known for mushrooms [Cordero and Casadevall, 2017]. Further, impacting rain might cause mechanical damage in light-colored species and especially fragile and soft-fleshed mushrooms (pigments can stabilize cell walls, Figure 3.15).

Abiotic effects	**Phenotype**	**Biotic effects**
- Energy harvesting - Cell development - Metal binding - Resistance to mechanical and chemical stress **- Thermoregulation** (protection against heat or cold) - Protection against desiccation - Photoprotection (e.g. sun- or UV radiation)	Hue Saturation **Lightness** Fluorescence	- Warning colors of specifically protected fungi - Warning colors of defenseless fungi mimicking protected fungi - Attractive colors (e.g., spore dispersal through animals) - Camouflage (e.g., against mushroom-feeding animals) - Microbial resistance (e.g., antibiotic)

Figure 3.15: Overview of possible abiotic and biotic effects on the mushroom color phenotype. Abiotic effects were adapted from [Cordero and Casadevall, 2017]; biotic effects from [Caro, 2017]. The theory of 'thermal melanism' is highlighted (see also Figure 3.3).

UV radiation. Many studies addressing insects have found effects of UV radiation on assemblage lightness, favoring darker assemblages in high UV environments [Trullas et al., 2007]. Melanin also reduces UV-radiation-induced stress in fungal mycelium and spores (photoprotection [Cordero and Casadevall, 2017]). Butterfly color lightness was affected by UV radiation [Heidrich et al., 2017]; this effect was, however, tightly correlated with temperature, which prohibited disentangling their independent effects. These variables were not highly correlated in our dataset (Tables 3.8, 3.6), likely be-

cause of the smaller spatial extent. However, we did not find a significant relationship between mushroom color lightness and UV index for saprotrophs and a positive relationship with ectomycorrhizal assemblages (Figure 3.14, Table 3.9). Further, we found that saprotrophic assemblages were darker in spring, fall and winter and lighter in the warmest months (Figure 3.8). These results together strongly suggest that UV radiation is not a significant driver of (saprotrophic) mushroom color lightness at the scale of our study. One explanation for the contrasting responses of fungi and insects to UV radiation [Bishop et al., 2016, Heidrich et al., 2017] might be that mushrooms have a much shorter existence (hours to days) [Nagy et al., 2017] than butterflies or dragonflies (weeks to months [Resh, 2009]). Thus, the exposure time to radiation is lower for mushrooms, and thus damage caused by UV radiation might cause a lower death rate.

Relative forest cover. Generally, mean annual temperature decreases from temperate to boreal to arctic areas (latitudinal gradient). This macroclimatic temperature gradient, along with seasonality, was the main focus of our study, but temperature may also vary at local-spatial scales due to vegetation properties and/or topographic variation. From local studies we know that canopy cover is a suitable surrogate for microclimate conditions [Bässler et al., 2010], creating more buffered but on average cooler climates underneath the canopy. In our study therefore, grid cells with a high level of forest cover might be cooler on average than those with a low cover. We, therefore, expected to find a negative relationship of mushroom color lightness with forest cover (darker assemblages on grids with a higher level of forest cover). However, even though we found a negative relationship for both nutritional modes (more pronounced for saprotrophic fungi) the effect was not statistically significant (Table 3.8). It is important to note that co-linearity between macro- and microclimate (Table 3.6) is very low. We, therefore, suggest that macroclimate (represented by mean annual temperature across grids) is more important than microclimate (variability in forest cover within grids) in affecting mushroom color lightness. Several studies have followed this approach at smaller grain size and extent [Bässler et al., 2010, Bässler et al., 2016b]. However, relative forest cover might not fully represent temperature variability within grids, which might explain the non-significant negative effect. Forest vs. open-land as proxy for microclimate would further depend on the tree density (denser would mean colder) and the type of tree species (e.g., *Fagus sylvatica* vs. *Pinus sylvestris*). A thorough test of the effect of local microclimatic variability on mushroom color lightness is thus left to further, experimental studies.

Finally, it is important to note that we focused on abiotic factors as drivers of mushroom color lightness; however, biotic factors might likewise play an important role in

structuring fungal assemblages. To our knowledge, only one biotic hypothesis has been addressed so far, namely whether mushroom color can act as a warning to herbivores, but this hypothesis was not supported [Sherratt et al., 2005]. For further hypothesis testing considering abiotic and biotic factors, we provide a conceptual overview within Figure 3.15.

3.4.5 Conclusions

Our results provide the first evidence that a morphological trait – mushroom color – contributes to structuring fungal communities at a continental scale. We demonstrate that dark-colored saprotrophic mushrooms heat up more rapidly than light-colored mushrooms and that dark-colored assemblages are more prevalent in colder environments and seasons of the year. These patterns thus yield further support extending the theory of 'thermal melanism' from the animal to the fungal kingdom and within fungi from unicellular [Cordero et al., 2018] to multicellular fungi. We hypothesize that saprotrophic fungi with dark-colored mushrooms are at an advantage in cold climates via increased reproductive success. Furthermore, this adaptation could play an important role in maintaining the fungal-driven carbon and nutrient cycling in the Holarctic. The low phylogenetic signal of color lightness supports the interpretation as adaptive selection by the thermal environment. Finally, our findings provide intriguing evidence that transitions from saprotrophic to mutualistic lifestyle may have promoted mushroom-darkening. However, we found no indication for thermal melanism in ectomycorrhizal fungi, despite their being significantly darker than saprotrophic species, suggesting that thermal melanism is specific to functional groups. Our results thus indicate a lifestyle-dependent response of mushroom pigmentation to the thermal environment. The study of color has a long tradition in animals and plants, but this study strongly suggests the need for more research efforts to understand the biology of colors in the fungal kingdom.

4 Independent effects of host and environment on the diversity of wood-inhabiting fungi

Abstract

Dead wood is a habitat for numerous fungal species, many of which are important agents of decomposition. Previous studies suggested that wood-inhabiting fungal communities are affected by climate, availability of dead wood in the surrounding landscape and characteristics of the colonized dead-wood object (e.g. host tree species). These findings indicate that different filters structure fungal communities at different scales, but how these factors individually drive fungal fruiting diversity on dead-wood objects is unknown. We conducted an orthogonal experiment comprising 180 plots (0.1 ha) in a random block design and measured fungal fruit body richness and community composition on 720 dead-wood objects over the first four years of succession. The experiment allowed us to disentangle the effects of the host (beech and fir; logs and branches) and the environment (microclimate: sunny and shady plots; local dead wood: amount and heterogeneity of dead wood added to plot). Variance partitioning revealed that the host was more important than the environment for the diversity of wood-inhabiting fungi. A more detailed model revealed that host tree species had the highest independent effect on richness and community composition of fruiting species of fungi. Host size had significant but low independent effects on richness and community composition of fruiting species. Canopy openness significantly affected the community composition of fruiting species. By contrast, neither local amount nor heterogeneity of dead wood significantly affected the fungal diversity measures. Our study identified host tree species as a more important driver of the diversity of wood-inhabiting fungi than the environment, which suggests a host-centred filter of this diversity in the early phase of the decomposition process. For the conservation of wood-inhabiting fungi, a high variety of host species in various microclimates is more important than the availability of dead wood at the stand level.

4.1 Introduction

Many fungal species inhabit dead wood, where they are important agents of decomposition and associated fluxes of carbon and nutrients [Floudas et al., 2012, Bradford et al., 2014]. Although the global number of fungal species living on dead wood is unknown [Boddy et al., 2007], a review study covering Norway, Sweden and Finland documented that more than 2,500 species associated with dead wood exist in this area [Stenlid et al., 2008]. On a single dead-wood log, at least 46 fruiting species can coexist [Heilmann-Clausen and Christensen, 2004]. Despite the importance and diversity of wood-inhabiting fungi, our understanding of the factors driving the spatial and temporal patterns of their diversity is limited. It is has been suggested that characteristics of the colonized dead-wood object (host) and the environment surrounding an object are important drivers of the diversity of wood-inhabiting fungi [Seibold et al., 2015a, Heilmann-Clausen et al., 2016]. However, how the host and the environment individually affect fungal diversity on dead-wood objects is unknown [Bradford et al., 2014]. Untangling and comparing the importance of host versus environmental drivers would yield basic ecological knowledge about wood-inhabiting fungal communities and allow predictions about the influence of silviculture on this important group of fungi in forest ecosystems.

Numerous studies have shown that the host affects the diversity of wood-inhabiting fungi [Hoppe et al., 2015, Baber et al., 2016, Kahl et al., 2017]. The host is the resource and provides energy for metabolism, growth and reproduction [Stokland et al., 2012], which can be depleted [Field et al., 1992]. The host is also the habitat, which is characterized by specific conditions, e.g. pH, moisture and composition of carbon compounds. Especially the host tree species and the size of dead wood are important drivers of fungal diversity (tree species: [Ferrer and Gilbert, 2003, Nordén et al., 2004b, Baber et al., 2016]; tree size: [Heilmann-Clausen and Christensen, 2004, Juutilainen et al., 2011]). Physicochemical properties differ between host species, especially between gymnosperms and angiosperms [Brunow, 2005, Higuchi, 2006], and this difference should contribute to explaining differences in the composition of fungal communities [Hoppe et al., 2015, Kahl et al., 2017].

Furthermore, physicochemical properties and hence habitat conditions change over time and are caused by biotic activity of fungal primary (endophytes) and secondary colonizers (e.g. changes in the composition of carbon compounds [Hoppe et al., 2015]) or non-fungal saproxylic organisms [Saint-Germain et al., 2007]). Both groups of colonizers can affect the colonization success of species arriving later - the so-called 'priority effect'

[Fukami et al., 2010, Dickie et al., 2012, Song et al., 2015, 2017, Hiscox et al., 2015b,a]. With regard to the size of a dead-wood object, a log provides more resources in space and time for fungi than a branch [Heilmann-Clausen and Christensen, 2004, Juutilainen et al., 2011]. Furthermore, logs and branches differ in their anatomical, chemical and physical properties, e.g. the presence of heart wood [Jacobsen et al., 2003]. Therefore, different wood-inhabiting fungal species could prefer different niches represented by different species and sizes of dead-wood objects [Juutilainen et al., 2011].

Beside host properties, the environment of a dead-wood object affects fungal diversity. Among environmental conditions, stand microclimate and the amount and heterogeneity of dead wood in the surroundings seem to be of particular importance. First of all, numerous studies have shown that the diversity of wood-inhabiting fungi is correlated with canopy openness - a proxy for microclimate conditions [Bässler et al., 2010, Bässler et al., 2016b, Lehnert et al., 2013, Horák et al., 2016]. This correlation is not surprising as forest gap dynamics caused by anthropogenic disturbances, e.g. logging, or natural disturbances, e.g. windthrows, insects, fire, or snow, is an important driver influencing the diversity of forest species across numerous taxa at the landscape scale [Swanson et al., 2011]. Variation in canopy openness is physically correlated to changes in moisture and temperature regimes and to fluctuations of these variables also within a dead-wood object [Scharenbroch and Bockheim, 2007, Seibold et al., 2016]. Variation in microclimate within dead wood can therefore have pronounced effects on the fungal community [Boddy and Heilmann-Clausen, 2008, Pouska et al., 2017]. However, current results are inconsistent, and both negative [Bässler et al., 2010, Horák et al., 2016] and neutral effects [Bässler et al., 2016b] of the microclimate on species richness have been reported. Second, the amount and heterogeneity (e.g. different host tree species) of dead wood at and around the stand can effect source populations of fungi [Edman et al., 2004, Nordén et al., 2004b, Norros et al., 2012] . For example, when the amount of dead wood in a forest stand is high, we would expect that more individuals occur in an area owing to the larger dead-wood area (species pool, species-area relationship, [MacArthur and MacArthur, 1961]). Consequently, more species would be found on a nearby object because of increased colonization events due to dense spore rain near existing fruit bodies (e.g. 'random replacement hypothesis' [Coleman, 1981]). This view is supported by one study, which showed that the number of fungal species on freshly cut logs was higher on sites with large local amounts of dead wood than on sites with small amounts [Edman et al., 2004],. The mechanism behind this pattern has been attributed to differences in donor populations caused by differences in resource availability. However, it is not possible to infer from observational studies a causal relationship between dead-wood

amount and fungal diversity because under natural conditions, the amount and heterogeneity of dead wood are often correlated [Müller and Bütler, 2010]; see also 'habitat amount hypothesis' [Fahrig, 2013]). By contrast, other studies observed no differences in the fungal diversity pattern on objects exposed to different amounts of dead wood in the surroundings [Olsson et al., 2011, Rolstad et al., 2004]. In these cases, drivers other than dead-wood amount (e.g. abiotic environment) might have driven the fungal diversity pattern on the logs.

Despite these numerous observational studies of the drivers of the diversity of wood-inhabiting fungi, the relative importance and interaction of the host and environment remain unclear. This lack of knowledge prohibits a deeper understanding of how fungal communities are structured and limits our ability to take measures to maintain fungal diversity and related processes in managed forest ecosystems. Therefore, we set up an orthogonal experiment in which we varied the host and the environment. The host was varied by adding dead wood of different species (fir or beech) and of different size (branches or logs); The environment was varied by varying the stand microclimate (sunny plots in forest gaps or plots under shady canopies) and by varying the local dead wood by adding dead wood in high or low amounts and of low, middle or high heterogeneity (for definitions, see Table 4.1). We considered the number of fruiting species of fungi (hereafter 'number of species') and the community composition of fruiting species (hereafter 'community composition') on dead-wood objects as response variables and addressed the question: Is the host (species and size) more important for fungal diversity than the environment (stand microclimate and local dead wood)?

Table 4.1: Definition of the main variables with their description, measurement and ecological meaning. We defined five variables in two sets of variables.

Variable sets	Variable	Description	Measurement	Ecological meaning
Host	Host size	Size of a dead-wood object	Branches (fine woody debris); logs (coarse woody debris)	Resource availability, habitat (micro-environment)
	Host species	Tree species of a dead-wood object	*Fagus sylvatica* (beech); *Abies alba* (fir)	Habitat (micro-environment)
Environ-ment	Stand microclimate	Proxy for microclimate conditions on the plot level the plot level	Canopy openness (sunny, shady)	Macro-environmental climate stand level
	Local dead-wood amount	High and low amount of dead wood added to the plot	Surface (m^2)	Species pool size
	Local dead-wood heterogeneity	Gradient of dead-wood diversity added to the plot	Siitonen index (low, middle, high)	Species pool diversity

4.2 Methods

4.2.1 Study area and experimental design

The experiment was conducted in the management zone of the Bavarian Forest National Park in south-eastern Germany. The management zone covers an area of ca. 6,000 ha around the ca. 18,000 ha core zone. The former is characterized by montane mixed forest consisting of Norway Spruce (*Picea abies* (L.) H. Karst), European Beech (*Fagus sylvatica* L.) and Silver Fir (*Abies alba* Mill.) [Bässler et al., 2010]. Overall, 180 plots of 0.1 ha were arranged in a random block design of five blocks (Figure 2.3).
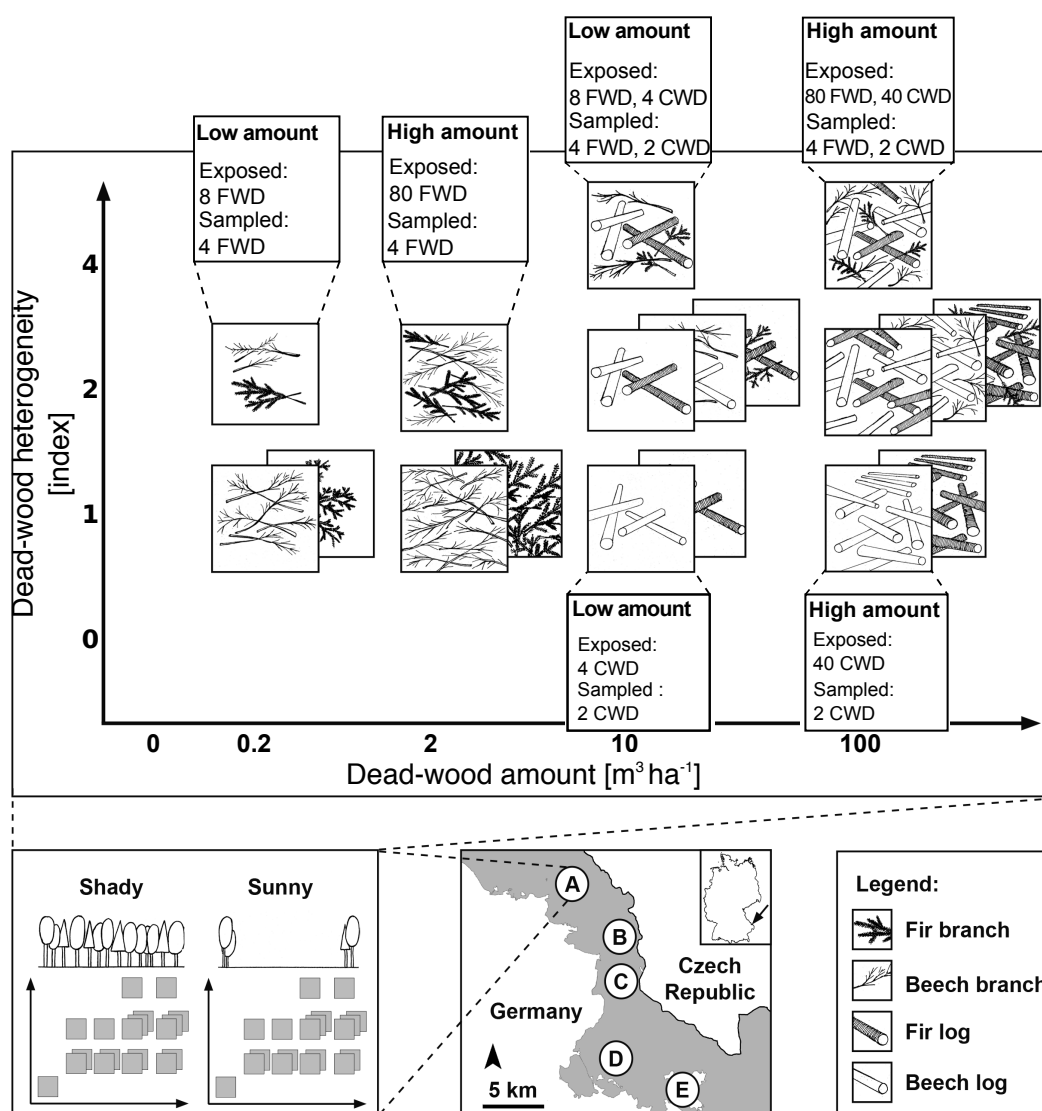
Figure 4.1: Study design for testing the effect of the host (tree species and size) and environment (canopy openness, dead-wood amount and dead-wood heterogeneity) on wood-inhabiting fungi. Dead-wood amount was either low or high; dead-wood heterogeneity was characterized as combinations of different types of dead wood (two host species and two sizes). Host species were Fagus sylvatica (European Beech) and Abies alba (Silver Fir); sizes were branches (fine woody debris; FWD) and logs (coarse woody debris; CWD). All combinations were set up on plots in sunny gaps or under shady canopies (inset bottom left). The experimental set-up was a random block design with five blocks (A-E) on 180 plots (inset bottom middle). On each set plots with low and high amounts of dead wood, a subset of two CWD and/or four FWD objects were sampled.

In autumn 2011, we freshly cut and directly deposited (within less than eight weeks) ca. 7,400 dead-wood objects of four different types: logs (coarse woody debris; mean diameter $\pm$ SD $= 33 \pm 6.5$ cm, length $= 5$ m) and branches (fine woody debris; mean diameter $\pm$ SD $= 3.2 \pm 1.3$ cm, mean length $\pm$ SD $= 2.7 \pm 0.88$ m) of beech and fir. The wood objects were taken from trees of the same age that were harvested from the same forest stand. Each plot contained either fine or coarse woody debris or both and either beech or fir or both (Figure 4.1; see also [Seibold et al., 2016]), creating three levels (low, middle and high) of dead-wood heterogeneity. The lowest level comprised either logs or branches of beech or fir; the intermediate level comprised logs and branches of beech or fir, or logs or branches of beech and fir; and the highest level comprised logs and branches of beech and fir (Figure 2.1). Half of the plots contained a low amount of local dead wood (8 branches of ca. 0.2 m^3 ha^{-1} or 4 logs of ca. 10 m^3 ha^{-1}) and the other half contained a high amount of local dead wood (80 branches of ca. 2 m^3 ha^{-1} or 40 logs of ca. 100 m^3 ha^{-1}). We used canopy openness as a surrogate for stand microclimate [Vodka et al., 2009, Müller et al., 2015, Seibold et al., 2016] and created each combination of dead-wood amount and heterogeneity twice per block, once in a sunny gap and once under a shady canopy (Figure 4.1). The sunny gaps are a result of clearings; an area of 0.1 ha was freed from living or dead trees. Penetration rates of airborne LiDAR (light detection and ranging) differed considerably between sunny and shady plots (ca. seven-fold) on an area of 0.5 ha (Figure 4.2). To avoid shading by a dense grass layer surrounding the logs and branches on sunny plots, each plot was mowed once a year during the growing season (for details, see [Seibold et al., 2016]).
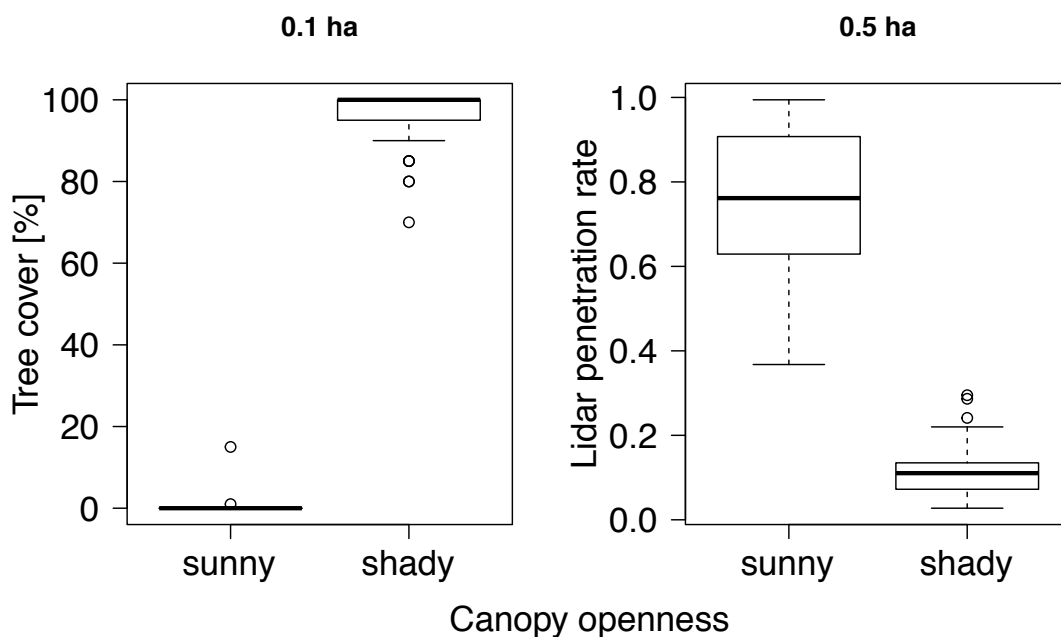
Figure 4.2: Characterization of canopy openness using ground observations (tree cover, 0.1 ha) and LiDAR-based penetration rate (0.5 ha).

We calculated an index of local dead-wood heterogeneity as the number of different substrate types per plot, ranging from low to high (according to the above classification of the heterogeneity set-up; [Siitonen et al., 2000], see Figure 4.1). To precisely characterize the amount of dead wood per plot, we calculated the surface area of each object using the formula for a truncated cone and summed the surface area of all logs and branches and of the sampled objects separately (see below). Surface area was calculated from the length and diameters measured on both ends of each object. We considered surface area as recommended [Heilmann-Clausen and Christensen, 2004], because we sampled fruit bodies on the surface of dead-wood logs and branches and because the surface of an object basically reflects the number of arriving propagules; objects with larger surfaces are more likely to be reached by a spore (airborne dispersal) or mycelium (soilborne dispersal), as as suggested [Edman et al., 2004] and in theory by the random replacement hypothesis leading to a species-area relationship [Coleman, 1981].

4.2.2 Fruit body sampling

We sampled fruit bodies on a subset of two logs and four branches on each plot three times per year for four consecutive years (2012-2015), which led to a total of 720 sampled objects (hosts). The first campaign of each year was in spring (April/May), the second in

summer (July/August) and the third in autumn (September/October), the main season of fruit body development. Fruit bodies were identified in the field or, if necessary, in the laboratory with the aid of a microscope. Voucher specimens were deposited in the herbarium of the Bavarian Forest National Park. The nomenclature followed MycoBank [Crous et al., 2004] (see Table A 2.3 for the complete list of species). We considered all visible species, in contrast to other studies, which restricted investigated fruit bodies to a size threshold of > 1-5 mm [Nordén et al., 2004a] or 10 mm [Ódor et al., 2006] or to a taxonomic group, e.g. polyporoid fungi [Junninen et al., 2006]. A threshold of 1 mm would exclude some of the smallest sporocarps that we observed, e.g. *Hamatocanthoscypha laricionis* (Velen.) Svrcek (145 records), whose fruit bodies do not exceed 0.5 mm [Huhtinen, 1990]. To ensure an effective and non-redundant sampling, we divided logs into seven sectors, two representing the cut edges of the log and five representing the trunk surface (each 1 m long), and sampled fruit bodies within each sector. Each branch was considered as one sector. Based on these data, we calculated a community matrix, within which the abundance of a species on an object is the sum of occupied sectors, summed across the three campaigns per year.

4.2.3 Statistical analysis

To approach our study question, we first used variance partitioning to test for overall effects of host and environment on the number of species and community composition. Then we used a serial model framework to disentangle the individual effects of all main predictors and their interactions on richness of species (for definition see below) and community composition by accounting for sampled surface. For the latter step, we used three approaches: 1) linear mixed effects and generalized linear mixed-effects models for the response variable number of species; 2) linear mixed effects models for the first four axes of a correspondence analysis (LME-CA); and 3) ANOVA-like permutation tests for constrained correspondence analysis (ANOVA-CCA). The ANOVA-CCA integrates the full ordination space (all axes), but does not consider the nested design of our study. By contrast, the LME-CA analysis accounts for the nested design of our study by integrating a random effect.
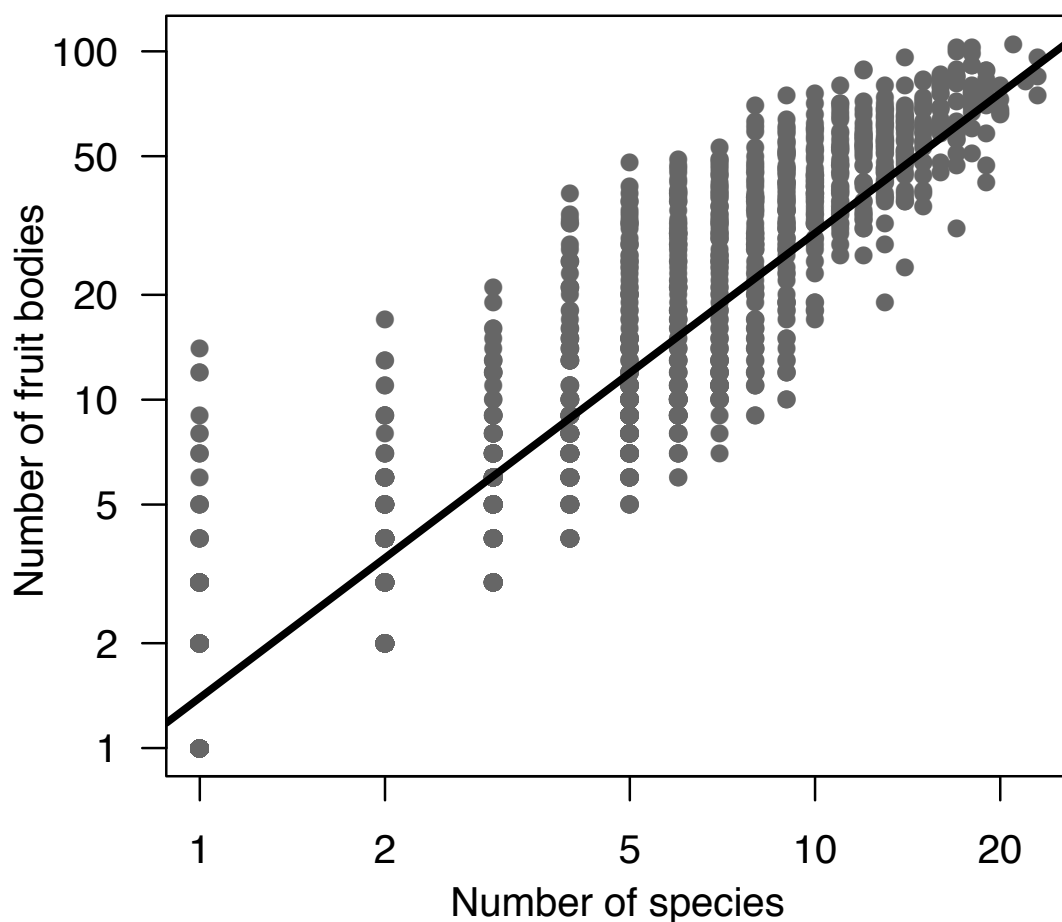
Figure 4.3: Scatterplot of the number of fruiting species of fungi and numbers of fungal fruit bodies. We found a strong correlation (adjusted $R^2 = 0.84$) and thus analysed the number of species as a measure of alpha-diversity. Note that the x- and y-axes are on a log-scale.

4.2.3.1 Data preparation

First, we calculated the number of species for each object and year. This measure was closely correlated with the total abundance on this object of the respective year (sum of the sectors for each object and year summed over three campaigns, adjusted $R^2 = 0.84$, $p < 0.001$; both were $\log_{10}$-transformed; Figure 4.3, see also above for the definition of species abundance on an object). Second, we considered the community composition and used abundance data (square-root transformed) and presence/absence data. We considered only species that occurred on at least five objects in a respective year, and to generate robust communities, we considered only objects with at least three species in a respective year. To increase the explained variance of our final model (described below),

we empirically tested the influence of species that occurred on at least one to six objects in a year and compared the explained variance (R^2) of our final CCA models. This exercise showed that inclusion of species that occurred on at least five objects within a particular year yielded the highest R^2 value; we used this threshold for all subsequent analyses. To test whether the excluded rare species had any effect on our interpretation, we compared the reduced community matrices with the full community matrix based on procrustes rotation using the function protest in the R package 'vegan'. All R^2 values of the comparisons were above 0.99; thus, rare species did not significantly affect our analysis.

4.2.3.2 Variance partitioning

To assess overall effects, we partitioned the variance in the response variables number of species and the community composition between (1) the host set (host species and host size) and the environmental set (stand microclimate, local dead wood), considering year as a covariate. We calculated the individual fractions of the variables sets by using partial (linear) regression [Peres-Neto et al., 2006] for the number of species using the function varpart in the R package 'vegan' [Oksanen, 2015]. For community composition, we used partial constrained correspondence analysis using the function cca in the R package 'vegan'. We report the adjusted R^2 values for individual effects (fractions explained uniquely by each of the two sets and year as covariate) scaled to 100%.

4.2.3.3 Models for the number of species

To assess the main and interacting effects of each predictor on the number of species, we constructed a series of models. Our first model, which we termed the 'sample model' (Table 4.2), included the factorial predictors year and size (logs or branches) and the interacting relationship between year, size and the $\log_{10}$-transformed sampled surface (i.e. the surface area of the sampled logs and branches). This model showed significant interactions between size and sampled surface across years (Figures 4.6, 4.7). We therefore decided to include an interaction term that considered year, size and sampled surface as a covariate in all subsequent models. This approach allowed us to interpret species numbers as species richness because the models accounted for sampling effort (surface) [Gotelli and Colwell, 2011]. We therefore used the term 'species richness' in cases where we controlled for sampling effort in the models.

In the second model, i.e. the 'basic model' (Table 4.2), we added treatment variables (host species, canopy openness, local dead-wood amount and local dead-wood heterogeneity) to the sample model. Based on this model, we systematically checked for interactions among all two-way combinations of predictors, i.e. canopy openness, host species, host size, local dead-wood amount, local dead-wood heterogeneity and year. We iteratively added one of the two-way interactions to the basic model and tested for a significantly better fit of the model using the function anova within the R package 'stats'. If the model with the new interaction yielded a significantly better fit (based on the Chi-square test, as we used models with Poisson error) than the basic model, we added this interaction to the final model.

Our third, 'final model' then consisted of the basic model and significant interacting effects (Table 4.2). We considered only two-way interactions to reduce complexity. We used linear mixed effects models using the functions lmer/glmer within the R package 'lme4' [Bates et al., 2015]. Each model contained 'object' nested within 'plot' nested within 'block' as random effect to account for the nested design and repeated sampling of objects. The number of species is a count variable; therefore, a statistical model using the Poisson error distribution with a log-link function would be an appropriate choice (generalized linear mixed-effects model, GLME). As the results of such models showed over-dispersion, we included a random variable to account for individual-level variability [Elston et al., 2001]. In all models that included such an individual-level factor, the algorithm for estimating the model failed to converge. Therefore, we $\log_{10}$-transformed the number of species and used a linear mixed-effects model (LME). Solutions of the GLME and LME were consistent (Tables 4.2, 4.3). For all comparisons within and among the models, we used standardized effect sizes of the parameter estimates with an expected mean of 0 (z-values = estimates divided by the respective standard error [Bring, 1994], and p-values were inferred using the R package 'multcomp' [Hothorn et al., 2008]. Note that we tested for interactions independent of the significance of main effects as significant factorial interactions can be meaningful without overall significant effects of the individual factors ('crossover interactions', e.g. [VanderWeele and Knol, 2014]).

Table 4.2: Serial model framework. We fitted three models for different response variables. (1) $\log_{10}$-transformed richness of fruiting species of fungi; (2) scores from the first four CA (correspondence analysis) axes and (3) the constrained correspondence analysis (CCA) without random effect. The sample model tests for the interacting relationships between sampled surface, size and year. In the basic model, we added the treatment variable host species and the environmental variables canopy openness and local dead-wood. The final model included all significant two-way interactions among these predictors after all combinations were tested (for details, see Statistical analysis).

Model	Description	Predictors
Sample	Check for co-variation of year, size and sampled surface	year + host size + year : host size : sampled surface + (1|block/plot/object)
Basic	Added treatment variables and systematically checked for interactions among all predictors	year + host size + year : host size : sampled surface + (1|block/plot/object) + host species + local amount + local heterogeneity + canopy openness
Final	Sample model and all variables with significant interactions (tested in basic model) estimated as overall and interacting effects	example: year + size + year : host size : sampled surface + (1|block/plot/object) + significant interactions

4.2.3.4 Models for the community composition

As outlined above, we used two approaches (LME-CA and ANOVA-CCA) to address the main and interacting effects of the predictor variables on the community composition as a response. For the first approach (LME-CA), we subjected the final community matrix to a correspondence analysis (CA) using the function cca in the R package 'vegan'. We used the scores of the first four CA axes for further analysis. We also used presence/absence data to calculate the CA (results not shown) and found a high consistency with the abundance-based results. This consistency was not surprising as we found a strong relationship between these two correspondence analyses ($R^2 = 0.96$, p < 0.001, permutations = 9999, based on procrustes rotation with the function protest from R package 'vegan'). Using the scores of the first four axes from the CA, we applied the same model framework as for the number of species (see above). As the derived axes

from the CA ordination were normally distributed, we used LMEs for these models. Using scores of the CA axes within the LME-CA framework allowed us to specify a random effect to account for the nested design of our study. However, to consider the full ordination space, we fitted in a second approach (ANOVA-CCA) the same series of models (sample, basic and final) as described above using the function cca in the R package 'vegan' and used ANOVA-like permutation tests for constrained correspondence analysis to test for significance of predictors and interactions (function anova.cca within the R package 'vegan'). We interpreted effects as significant in our study if effects were significant across statistical approaches (for species richness LME and GLME; for the community composition LME-CA and ANOVA-CCA).

4.3 Results

A total of 45,992 sectors were occupied by at least one fungal species (we considered an occupied sector as a record). The number of records increased with succession (2012: 3,880; 2013: 9,124; 2014: 15,837 and 2015: 17,151). Across all records, we found 291 species of fungi, including 116 species of Ascomycota and 175 species of Basidiomycota. The most common basidiomycete species was *Cylindrobasidium leave* (Pers.), and the most abundant ascomycete species was *Hypoxylon fragiforme* (Pers.) J.Kickx.f. (for the rank-abundance curve and the 20 most abundant species, see Figure 4.4). The set of host variables (host species, host size) clearly explained more of the partitioned variance of number of species and community composition than the environment (stand microclimate, local amount and local heterogeneity of dead wood, Figure 4.5).
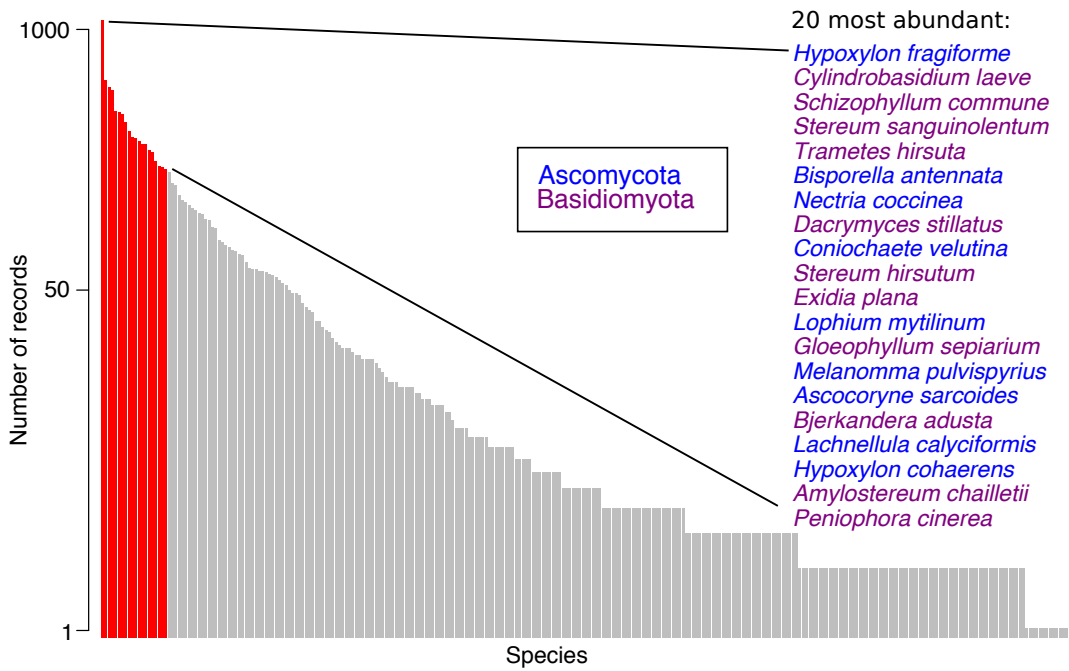
Figure 4.4: Rank-abundance curve based on the number of records. The species names of the 20 most abundant species of Ascomycota and Basidiomycota are given. Note that the y-axis is on a log-scale.
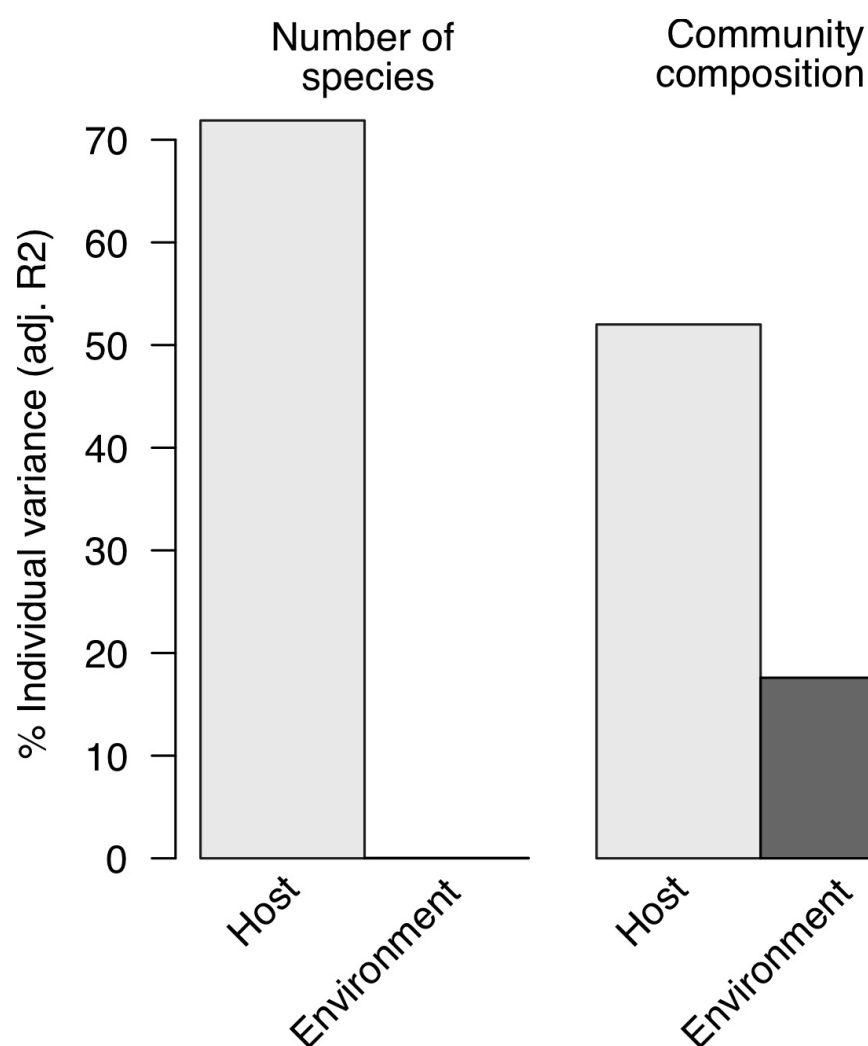
Figure 4.5: Variance partitioning of the number of fruiting species of fungi and community composition of fruiting species between two variables sets. The variance was partitioned between the host set (host species and size) and the environmental set (stand microclimate and local dead wood). The explained variance was 61.6% for fruiting species richness and 9.2% for community composition of fruiting species. Remaining variance was attributed to the year, which was included as covariate.

4.3.1 Species richness

The relationship between the number of species and the sampled surface differed between the two size classes (Figure 4.6). For logs, this relationship was initially negative and became positive with succession (Figure 4.6). For branches, the relationship was consistently positive, and effect sizes were higher than for logs (Figure 4.6; Table 4.3, sample model). The number of species of beech and fir of logs and branches increased

with the first three years and levelled off in the fourth year with one exception — the number of species on fir branches showed no clear trend across years (Figure 4.7).
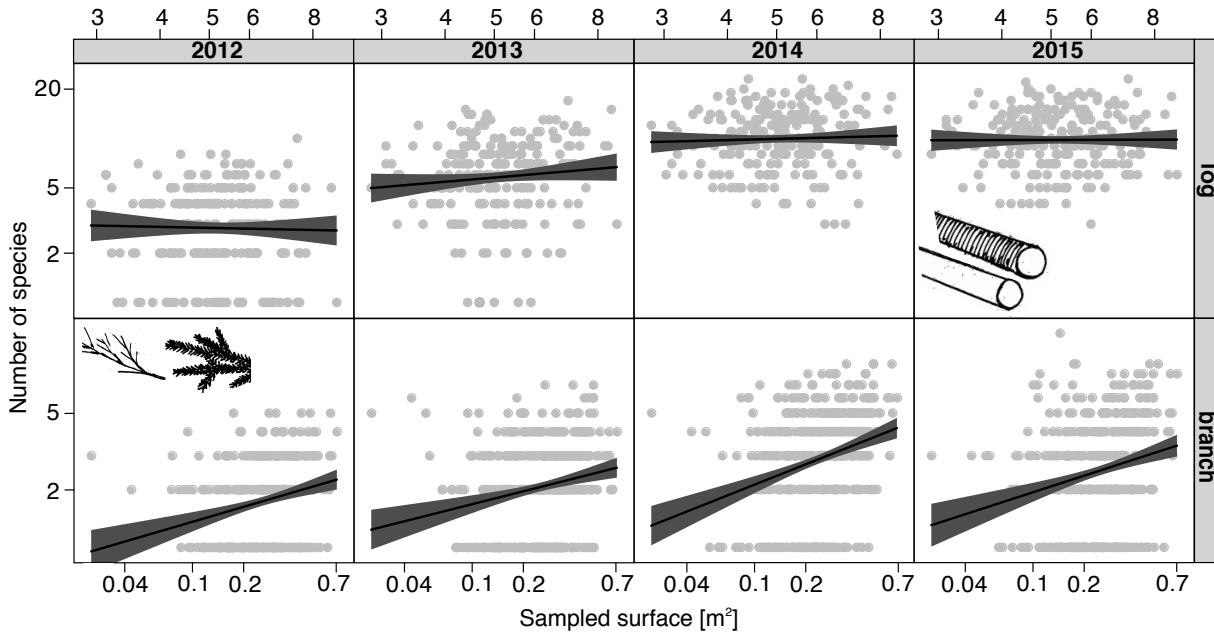
Figure 4.6: Scatterplots of number of fruiting species of fungi in relation to surface sampled by year and size. Note the log-scale of the x- and y-axes. The y-axis for logs is displayed at the top; the y-axis for branches is displayed at the bottom. Shown are raw data for single objects and the line of best fit with the predicted confidence interval.

Our mixed-effects models revealed host species, host size and year as important drivers of species richness (Tables 4.3, 4.4). Beech harbored more species than fir, and logs harboured more species per surface area than branches (Tables 4.3, 4.4). Local dead-wood amount and heterogeneity had no significant effect on species richness (Tables 4.3, 4.4). Canopy openness showed no significant effect in the basic model of the GLME (Tables 4.3, 4.4); therefore, we did not consider this effect as significant.
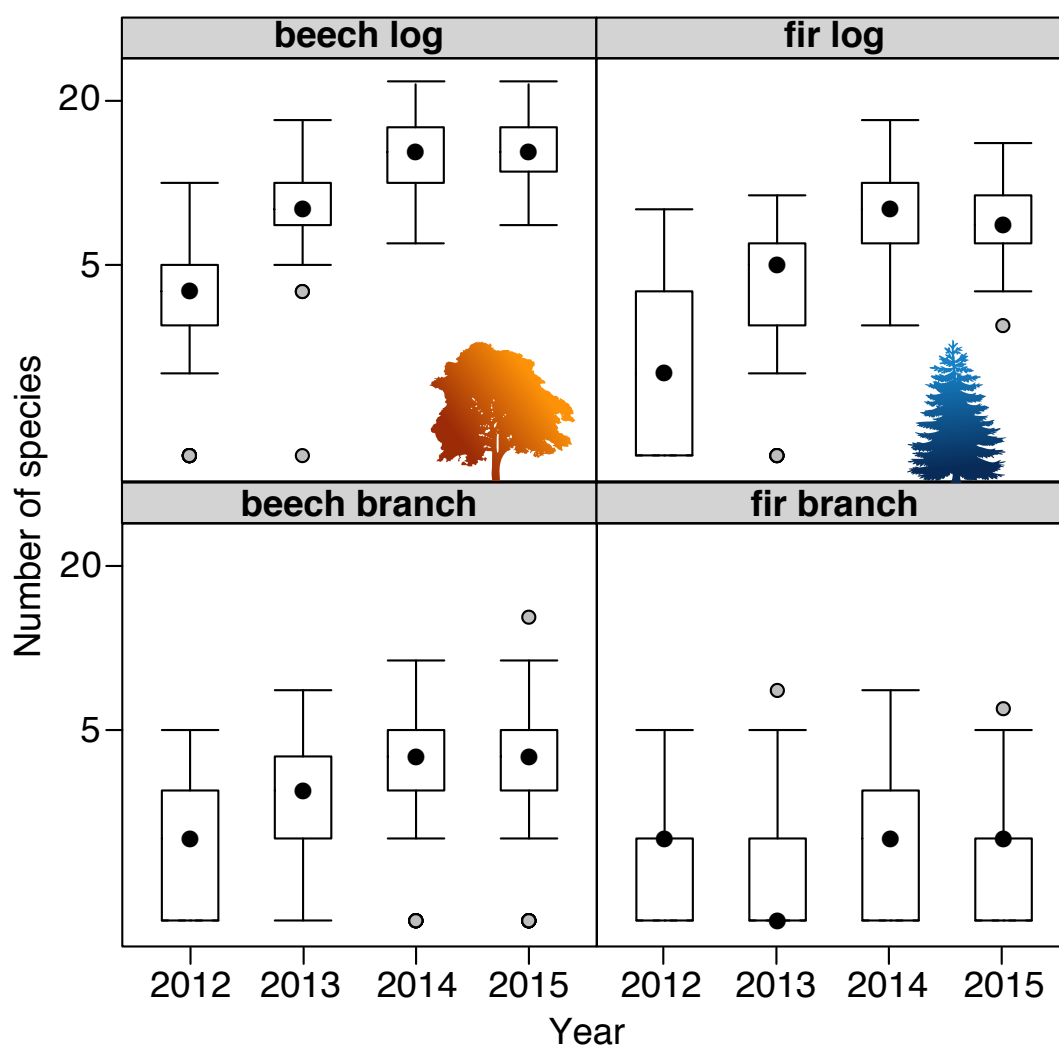
Figure 4.7: Box plots showing number of fruiting species of fungi by years (2012-2015), separate for host species (fir, *Abies alba*; beech, *Fagus sylvatica*) and size classes. Note the log-scale of the y-axis. Black dots indicate the medians; boxes indicate the lower and upper quartiles; grey dots are outliers; and error bars are the minimum and maximum without outliers. Angiosperm tree image by Michele M. Tobias under creative commons (http://phylopic.org, https://creativecommons.org/licenses/by-nc-nd/3.0/).

We found four significant interactions (Tables 4.3, 4.4); between host species and year (the richness increase between 2012 and 2013/2014/2015 was stronger for beech than for fir), between canopy openness and year (the richness difference between 2012 and 2013/2014 was higher under shady canopies than in sunny gaps), between host species and canopy openness (the richness difference between beech and fir was lower under shady canopies than in sunny gaps) and between canopy openness and host size (the

richness difference between logs and branches was lower under shady canopies than in sunny gaps).

Table 4.3: Summary of statistics from the serial model framework with richness of fungal fruit-ing species as response variable using linear mixed effects models (LME). We show the standardized effect sizes of the parameter estimates using an expected mean of 0 (z-values, estimates divided by the respective standard error); boldface indicates significant values. The marginal R^2 (variance explained by fixed factors) is given. Effects in parentheses were not significant in the basic model of the LME or the generalized linear mixed-effects model (GLME, Table 4.6) and were therefore not interpreted. The grey-shaded area represents the main treatment effects (without interaction). The first factor named is the reference factor.

	Sample	Basic	Final
Intercept	7.30	8.45	10.15
Year - 2013 vs 2012	1.90	2.14	1.05
Year - 2014 vs 2012	8.02	8.25	7.13
Year - 2015 vs 2012	5.79	5.99	6.63
Size - branches vs logs	-3.20	-3.24	-3.66
Host species - fir vs beech		-20.07	-9.01
Canopy openness - shady vs sunny		1.97	(-5.48)
Local amount		0.34	
Local heterogeneity - mid vs low		-0.66	(-2.32)
Local heterogeneity - high vs low		-0.90	-1.82
Year 2013 : host species - fir			-6.91
Year 2014 : host species - fir			-6.14
Year 2015 : host species - fir			-8.31
Year 2013 : canopy openness - shady			3.39
Year 2014 : canopy openness - shady			2.43
Year 2015 : canopy openness - shady			-1.27
Host species - fir: canopy openness - shady			7.36
Size - branch : canopy openness - shady			3.33
Canopy openness - open : local heterogeneity - mid			2.52
Canopy openness - open : local heterogeneity - high			1.71
Year 2012 : size logs: sampled surface	-1.65	-0.44	-1.21
Year 2013 : size logs: sampled surface	1.38	3.06	3.64
Year 2014 : size logs: sampled surface	1.34	3.06	3.47
Year 2015 : size logs: sampled surface	2.31	4.21	4.62
Year 2012 : size branches: sampled surface	3.38	1.69	3.64
Year 2013 : size branches: sampled surface	3.55	2.05	1.87
Year 2014 : size branches: sampled surface	6.34	4.94	5.10
Year 2015 : size branches: sampled surface	5.38	3.88	4.20
R^2	0.57	0.66	0.69

Table 4.4: Summary of statistics from the serial model framework using richness of fruiting species of fungi as response variable and generalized linear mixed-effects models (GLME). We show the standardized effect sizes of the parameter estimates using an expected mean of 0 (z-values, estimates divided by the respective standard error); boldface indicates significant values. The marginal R^2 (variance explained by fixed factors) is given. Effects in parentheses were not significant in the basic model of the GLME or the linear mixed effects model (LME) and were therefore not interpreted. The grey-shaded area represents the main treatment effects (without interaction). The first factor named is the reference factor.

	Sample	**Basic**	**Final**
Intercept	8.31	9.55	10.22
Year - 2013 vs 2012	0.91	1.04	0.37
Year - 2014 vs 2012	5.56	5.62	4.62
Year - 2015 vs 2012	4.93	5.00	5.28
Size - branches vs logs	-3.86	-3.85	-4.03
Host species - fir vs beech		-21.06	-6.93
Canopy openness - shady vs sunny		0.01	(-3.45)
Local amount		0.17	
Local heterogeneity - mid vs low		-0.71	
Local heterogeneity - high vs low		-0.71	
Year 2013 : host species - fir			-4.66
Year 2014 : host species - fir			-3.41
Year 2015 : host species - fir			-4.73
Year 2013 : canopy openness - shady			2.03
Year 2014 : canopy openness - shady			2.00
Year 2015 : canopy openness - shady			-1.44
Host species - fir: canopy openness - shady			7.01
Size - branch : canopy openness - shady			2.59
Year 2012 : size logs : sampled surface	-1.48	-0.05	-0.63
Year 2013 : size logs : sampled surface	1.98	4.26	4.74
Year 2014 : size logs : sampled surface	1.58	4.06	4.30
Year 2015 : size logs : sampled surface	1.89	4.41	4.48
Year 2012 : size branches : sampled surface	2.25	1.26	2.22
Year 2013 : size branches: sampled surface	1.97	1.01	0.77
Year 2014 : size branches: sampled surface	4.93	3.85	3.92
Year 2015 : size branches: sampled surface	5.16	4.17	4.48
R^2	0.52	0.61	0.62

4.3.2 Community composition

The community composition was mainly driven by host species (Figure 4.8, Tables 4.5, 4.6). Moreover, canopy openness, host size and year also showed significant relationships with the community composition (Figure 4.8, Tables 4.5, 4.6). We found no significant overall effects of local amount and heterogeneity of dead wood on the community composition (Tables 4.5, 4.6; note that we considered an effect as significant only if the effect was significant in both the ANOVA-CCA and the LME-CA model).

We found four significant interactions (Tables 4.5, 4.6): between host species and year (the difference in the community composition between beech and fir increased with time) and between canopy openness and year (the difference in community composition between 2012 and 2013/2014/2015 was higher under shady canopies than in sunny gaps), between host species and canopy openness (the difference in community composition between beech and fir was higher under shady canopies than in sunny gaps), between host species and host size (the difference in community composition between beech and fir was higher on branches than on logs).
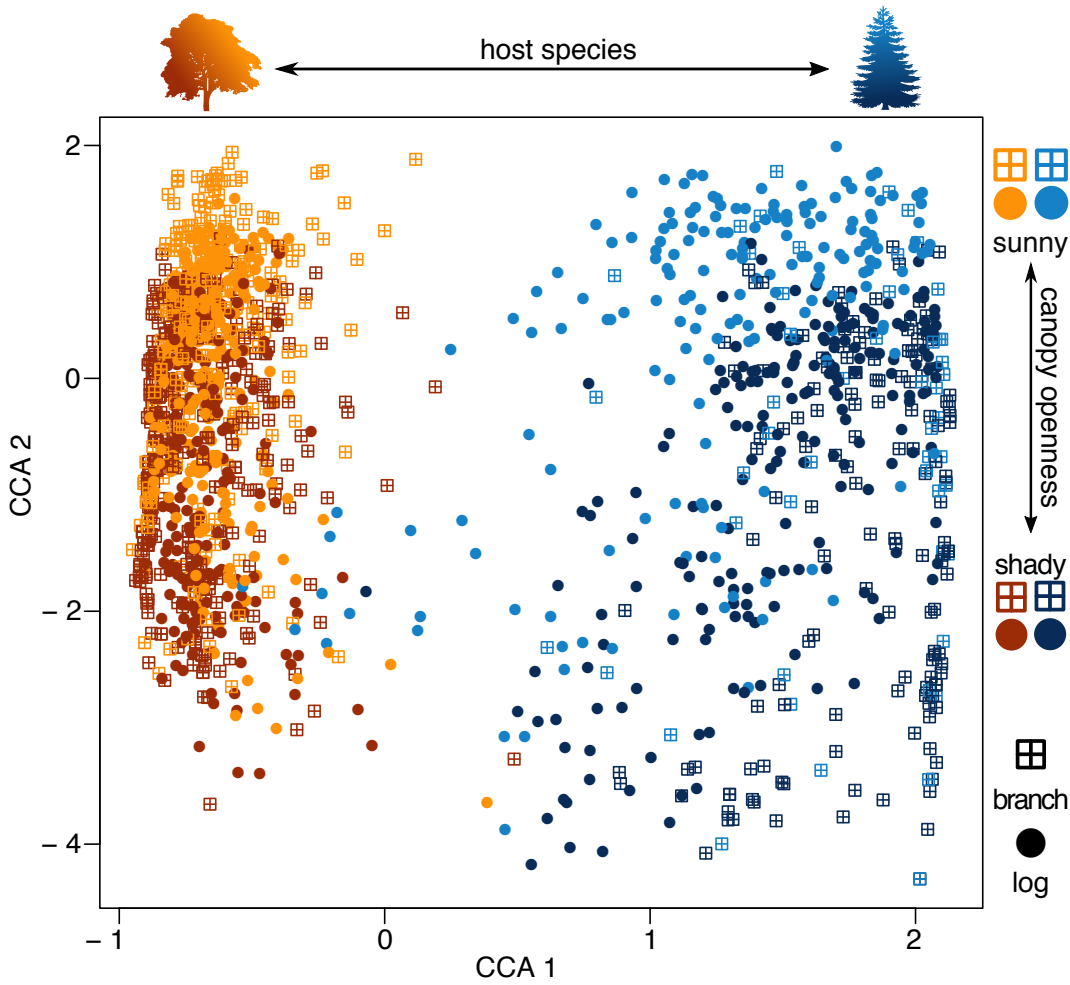
Figure 4.8: Ordination of the community composition of fungal fruiting species based on constrained correspondence analysis (CCA). Abundance data were square-root transformed. We used year, canopy openness, size, local dead-wood amount and local dead-wood heterogeneity as constraint environmental variables. Displayed are the two main drivers of the community composition, namely host species and canopy openness. Size had a minor effect (see Table 4.2). Note that most of our environmental variables are factorial treatments, which cannot be easily displayed as arrows within the CCA. Angiosperm tree image by Michele M. Tobias under creative commons (http://phylopic.org, https://creativecommons.org/licenses/by-nc-nd/3.0/) and the color was changed.

Table 4.5: Summary of statistics from the serial model framework using community composition of fruiting species of fungi as response variable. The serial model was fit using ANOVA-like permutation tests based on constrained correspondence analysis (CCA). Boldface indicates highly significant values ($Chi^2 > 15$). The adjusted R^2 of the CCA is given. The grey-shaded area represents the main treatment effects (without interactions).

	Sample			Basic			Final		
	Chi2	F	Pr(>F)	Chi^2	F	Pr(>F)	Chi^2	F	Pr(>F)
Year	0.49	15.58	0.001	0.49	16.55	0.001	0.49	17.50	0.001
Host size	0.20	18.79	0.001	0.20	19.95	0.001	0.20	21.10	0.001
Host species				0.71	71.89	0.001	0.71	76.04	0.001
Canopy openness				0.29	28.75	0.001	0.29	30.44	0.001
Local amount of dead wood				0.02	1.70	0.002	0.02	1.78	0.002
Local heterogeneity of dead wood				0.03	1.32	0.008	0.03	1.39	0.007
Year : Host species							0.32	11.36	0.001
Year : Canopy openness							0.13	4.79	0.001
Year : Host size							0.13	4.74	0.001
Year : Local amount							0.02	0.86	0.967
Host species : Canopy openness							0.19	20.33	0.001
Host species : Local heterogeneity							0.03	1.51	0.001
Host species : Local amount							0.02	2.44	0.001
Host size : Host species							0.22	23.01	0.001
Host size : Canopy openness							0.05	5.76	0.001
Host size : Local heterogeneity							0.03	1.34	0.004
Host size : Local amount							0.01	1.55	0.006
Canopy openness : Local amount							0.01	1.18	0.134
Local amount : Local heterogeneity						0.03	1.39	0.002	
Year : Host size : Sampled surface	0.24	2.81	0.001	0.22	2.80	0.001	0.11	1.41	0.001
Residual	16.77			15.74			14.66		
adj. R^2	0.04			0.10			0.15		

Table 4.6: Summary of statistics of the serial model framework for the community composition of fruiting species of fungi (see 'Statistical analysis' and Tables 4.1 and 4.2). S = Sample, B = Basic, F = Final model.

	CA 1			CA 2			CA 3			CA 4		
	S	B	F	S	B	F	S	B	F	S	B	F
Intercept	-0.67	-4.20	-3.23	-3.40	-2.65	-3.05	-0.59	-0.04	-0.34	-4.88	-6.56	-5.26
Year - 2013 vs 2012	0.62	0.58	-1.12	3.16	3.12	1.93	0.64	0.71	2.70	1.52	1.39	1.02
Year - 2014 vs 2012	1.36	1.41	-0.40	7.07	7.03	5.11	2.96	2.92	5.15	6.66	6.60	3.13
Year - 2015 vs 2012	0.60	0.82	-1.08	7.52	7.49	5.50	4.98	5.06	6.59	8.08	7.92	3.58
Size - branches vs logs	0.12	-1.70	(-2.19)	-0.34	0.10	0.87	-0.57	-0.28	-1.31	2.10	2.16	3.00
Host species - fir vs beech	92.85	16.83			-10.98	-5.88		8.14	0.59		-0.98	-2.84
Canopy openness - shady vs sunny	2.31	-2.98			-6.22	-2.15		-10.29	-5.64		16.35	-0.01
Local amount	0.50	0.47			-1.31	-0.28		-0.24	-1.30		-0.44	0.37
Local heterogeneity - mid vs low	1.50				-0.19			0.40			0.30	
Local heterogeneity - high vs low	0.76				-0.83			0.40			0.72	
Year 2013 : host species - fir		13.39			5.56			-1.73			1.77	
Year 2014 : host species - fir		18.58			18.80			-6.87			-1.30	
Year 2015 : host species - fir		18.21			23.19			-10.09			-4.93	
Year 2013 : canopy openness - shady					-1.55			-3.58			2.89	
Year 2014 : canopy openness - shady					-0.12			-3.75			10.54	
Year 2015 : canopy openness - shady					0.43			-1.89			12.97	
Host species - fir : canopy openness - shady	6.54			-2.37						9.06		
Host species - fir : local amount			-0.35			-0.72			0.70			-0.76
Size - branch : host species - fir			16.24			-22.78			20.35			3.62
Year 2012 : size logs : sampled surface	0.85	-3.12	-2.32	1.74	2.54	2.21	-2.48	-3.01	-2.91	1.26	1.46	1.65
Year 2013 : size logs: sampled surface	1.07	-2.68	-1.89	1.00	1.87	2.34	-1.61	-2.17	-2.49	2.84	3.17	3.14
Year 2014 : size logs: sampled surface	1.27	-2.13	-1.82	0.73	1.62	0.11	-0.97	-1.43	-0.61	1.88	2.16	3.34
Year 2015 : size logs: sampled surface	1.53	-1.35	-0.86	0.79	1.67	-0.83	-1.36	-1.91	-0.44	1.31	1.62	3.58
Year 2012 : size branches : sampled surface	-3.40	-1.98	-1.84	1.30	1.35	0.38	-2.43	-1.52	-0.25	-0.01	-0.21	0.94
Year 2013 : size branches: sampled surface	-3.12	-1.43	-0.09	0.75	0.87	-0.43	-2.85	-1.76	-0.38	-1.05	-1.61	0.79
Year 2014 : size branches: sampled surface	-3.36	-2.41	0.29	2.52	2.64	1.81	-2.89	-1.77	-0.23	0.41	-0.12	0.82
Year 2015 : size branches: sampled surface	-3.59	-2.23	-0.39	0.80	0.83	-0.18	-1.49	-0.11	0.99	0.96	0.28	-0.03
R^2	0.02	0.91	0.94	0.28	0.40	0.68	0.29	0.41	0.57	0.22	0.48	0.56
Axis explained variance		4.4			3.1			2.4			2.1	

4.4 Discussion

In this study, we quantified the effects of the host (tree species and size) and the environment (stand microclimate: sunny gaps and shady canopies, local dead wood: amount and heterogeneity of dead wood added to a plot) on the fungal richness and community composition on single dead-wood objects over time. Our analysis was based on an orthogonal experiment that allowed identification and quantification of independent effects of these variables, which are usually correlated in observational surveys. Variance partitioning revealed that the host was a more important driver of species richness and community composition than the environment. Among all individual treatment variables, we found that the host species had the highest relative effect on the diversity of wood-inhabiting fungi on a dead-wood object. Canopy openness significantly affected the community composition. The host size had significant but rather small effects on species richness and community composition. By contrast, local amount and heterogeneity of dead wood showed no significant effects on species richness and community composition.

4.4.1 The importance of host species and size

Among the investigated variables, host species was important throughout all models of species richness and explained most of the variation in the community composition (Tables 4.5, 4.4). Specialization of wood-inhabiting fungi on species of a particular host genus and to a lesser extent on a tree species have been documented [Heilmann-Clausen and Christensen, 2005, Baber et al., 2016, Heilmann-Clausen et al., 2016]. Especially wood of gymnosperms and angiosperms differ in numerous properties [Cornwell et al., 2009, Kahl et al., 2017]. and many wood-decaying fungi show preferences for one of these two major plant lineages [Gilbertson, 1980, Hibbett and Donoghue, 2001, Hoppe et al., 2015]. Such clear differences in preference for gymnosperm and angiosperm trees have also been shown for assemblages of phytophagous insects [Brändle and Brandl, 2006]. Furthermore, our results showed that the effect of year differed between host tree species, as indicated by their interaction (Table 4.3). This result points to clear differences between the two host species in their successional trajectories. However, we did not measure decomposition explicitly, and the decomposition process can succeed at very different rates in different tree species [Weedon et al., 2009]; thus, we did not interpret this interaction as a difference in decomposition between tree species.

We are far from having a complete mechanistic understanding of why fungal communities differ between host species and why the communities show different successional trajec-

tories. The differences in fungal communities between beech and fir might be due to both abiotic and biotic factors (filters) and their interactions. It is well known that species of host trees differ considerably in their physicochemical properties and hence in basic habitat conditions for fungi [Cornwell et al., 2009, Kahl et al., 2017, Hoppe et al., 2015]. However, recent studies have also shown the importance of endophytic fungi of wood, which are prevalent even in living trees and are able to switch to a saprophytic lifestyle after the death of the tree [Promputtha et al., 2007, Parfitt et al., 2010, Song et al., 2017]. Activity of this primary colonizer community also potentially influences micro-habitat conditions of the host tree via modification of woody compounds (e.g. lignin, cellulose decay with cell wall density loss; [Schilling et al., 2015, Song et al., 2017]) and related metabolites plus the possible response (production of secondary metabolites) of the host [Hiscox et al., 2015b]. The endophytic community is most likely primarily driven by the identity of the host species, i.e. angiosperm versus gymnosperm, and secondarily by the vitality of the host [Schwarze et al., 2000], which could also contribute in explaining differences in diversity patterns between hosts (Figure 4.8, Table 4.5). However, to the best of our knowledge, no study has demonstrated the differences in wood-endophyte communities of angiosperm and gymnosperm trees. Even though we did not determine the endophytic community at the beginning of the experiment, we detected fruit bodies of 5 of 11 known endophytic species on beech objects (angiosperm wood) (*Biscognauxia nummularia*, *Eutypa spinosa*, *Fomes fomentarius*, *Hypoxylon fragiforme* and *Stereum rugosum*; Figure 4.9). Most species were missing in the fruit body record in the first year after exposure; however, the 5 detected species were found after four years. Interestingly, *Hypoxylon fragiforme* was highly abundant at the start and across all years, and was the most abundant species in our experiment (Table B.1, Figure 4.8). This observation supports the view that species known as endophytes are prevalent after tree death in consecutive years. Experiments have demonstrated that the identity and abundance of primary colonizers can have effects on species communities of later decay stages (known as 'priority effect'), which can differ with tree species [Hiscox et al., 2015b,a, Leopold et al., 2017]. More studies are needed to disentangle the complex interactions between abiotic and biotic effects driving the differences in fungal communities among host species.
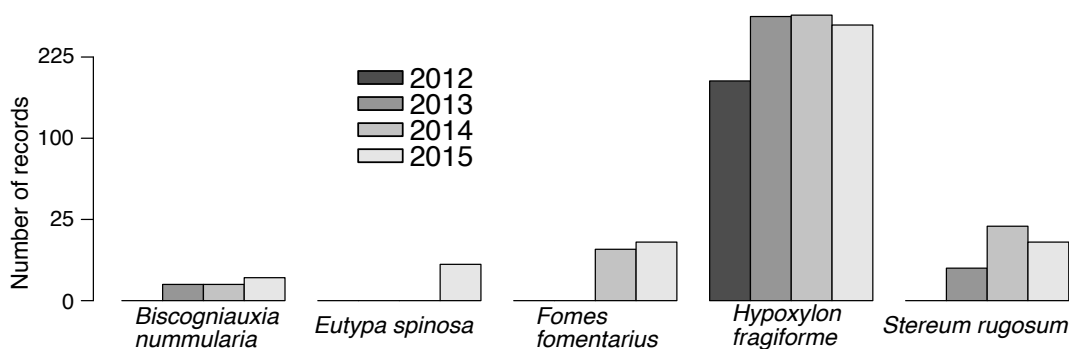
Figure 4.9: Occurrence of fruit bodies of five endophytic fungi in four years of the initial phase of decomposition, given as the number of records (sectors occupied) per year.

Our model framework, which standardized for the sampling effort, revealed a significant negative difference between branches and logs. This means that logs harbor on average a higher number of species per surface area of an object than branches. One possible explanation for the observed pattern might include the more cryptic variation in dead-wood characteristics within a log compared to a branch. For example, temperature, wood density, water content, and decay stage can considerably vary within large logs [Graham, 1924, Saint-Germain et al., 2010, Leather et al., 2014]. Therefore, the effect of dead-wood size might include an increase in the number of habitats (niches), i.e. habitat heterogeneity, which is an important driver of saproxylic beetle richness [Seibold et al., 2016].

4.4.2 The importance of the stand microclimate

Our models consistently revealed a significant effect of microclimate on the community composition. This effect indicates that fungal species differ in their preferences for microclimate conditions and suggests that wood-inhabiting fungi are adapted to different microclimates. Norros and colleagues showed that sunlight and freezing causes severe spore mortality, which supports the view that microclimate is an important environmental filter for wood-inhabiting fungi [Norros et al., 2015]. Moreover, in our models, we found a significant interaction of host species and canopy openness (Tables 4.5, 4.6). Based on a visual inspection of the ordination (Figures 4.8, 4.10) for unconstrained correspondence analysis), this interaction suggests that the community composition of beech and fir are more similar in sunny gaps than under shady canopies (Table 2.1). Beech and fir specialists seem to form more distinct communities under shady canopies, which are characterized, e.g. by microclimatic conditions with fewer and lower temperature amplitudes than in sunny gaps. Sunny gaps are characterized by a harsh microclimate

(e.g. more temperature extremes), which might be unfavorable for host specialists, and thus opportunistic species become predominant and communities become more similar. An example of a host specialist is *Amylostereum chailletii*. This species was recorded only on fir and occurred on 84% of all occupied objects under shady canopies and on only 16% of the objects in sunny gaps. An example of a host opportunistic species that becomes more abundant in sunny gaps is *Coniochaeta pulveracea*. This species was recorded on both beech (74%) and fir (26%) but occurred on 96% of all occupied objects in sunny gaps. Species of the genus *Coniochaeta* consist mainly of very small, black, hard fruit bodies, and it is known that some even survive fires, which are adaptations that suggest that *Coniochaeta sp.* are specialists of harsh microclimate conditions [Wicklow, 1975]. However, at present, we have only a limited understanding of the morphological and physiological adaptations of fungi to environmental conditions [Norros et al., 2015, Pringle et al., 2015] and how they relate to different host species and subsequently influence assembly processes.
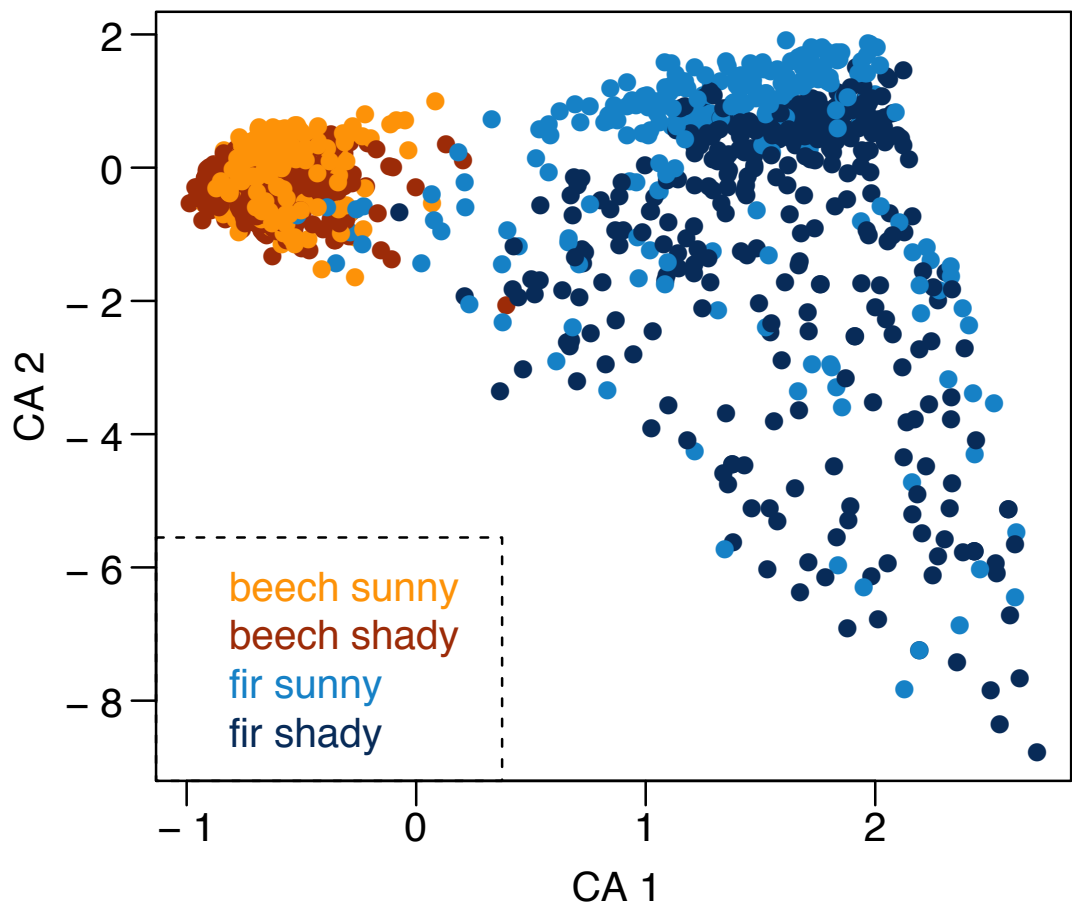
Figure 4.10: Ordination of the community composition of fungal fruiting species based on correspondence analysis (CA). Abundance data were square-root transformed. We colour coded tree species (red: beech, blue: fir) and canopy openness (light: sunny, dark: shady).

Species richness, in contrast to the community composition, was not significantly affected by canopy openness (Table 4.3). Some of the few existing studies have suggested that canopy openness reduces the number of species [Bässler et al., 2010, Horák et al., 2016] and another reported no effect [Bässler et al., 2016b]. One explanation for the conflicting results might be that these studies were based on survey data, in which important drivers of species richness were either unknown or correlated, which leads to confounding effects. In survey studies, the history of the dead-wood objects is usually unknown. The cause of death, however, can have strong effects on the species diversity, which might overlay effects of microclimate [Renvall, 1995, Boddy, 2001, Nordén et al., 2004b]. For example, mortality might be caused by large-scale windthrow or insect-pest disturbance, in contrast to thinning under a dense canopy with patchily distributed dead

wood throughout the year [Fricker et al., 2008]. Thus, different levels of canopy openness (and thus microclimates) are created depending on the cause of death. Furthermore, the way a tree dies affects the chemical and physical properties of the log or branch [Stokland et al., 2012], and consequently, this affects how the subsequent decay succession proceeds [Renvall, 1995, Stokland et al., 2012, Ottosson et al., 2014]. In addition, the amount of dead wood in survey studies is often correlated with microclimate; larger gaps, e.g. caused by a disturbance event, are not only correlated with more dead wood but also alter the stand microclimate. In such a scenario, it is furthermore not possible to disentangle effects of dead-wood amount and dead-wood heterogeneity (see above and [Müller and Bütler, 2010, Seibold et al., 2015a, Bässler et al., 2016b]). Our study overcame such confounding effects by standardizing the history of the hosts (trees of the same history and age harvested from one stand), cause of death (cutting by chainsaw), local dead-wood amount, local dead-wood heterogeneity and one of two microclimate conditions (either sunny gaps or shady canopies). Hence, a similar number of species but a clear difference in the community composition supports the view that fungal species are adapted to different microclimates.

4.4.3 Effects of local amount and heterogeneity of dead wood

Against our expectation, the local amount and heterogeneity of dead wood on a plot had no significant effect on species richness on a single dead-wood object (Tables 4.3, S 4.4). Furthermore, we did not find a tendency for this pattern to change over time (no significant interaction terms). When the amount of dead wood on a plot is high, we expected that more individuals would be able to coexist in an area owing to the larger area (species pool). Clearly, spores can disperse over long distances [Hallenberg and Kuffer, 2001, Brown and Hovmøller, 2002]; however, the probability of colonization decreases with distance, and the majority of sources for successful colonization might be located some hundred meters from the considered object [Norros et al., 2012] or even less [Galante et al., 2011]. Thus, we expected that local dead wood would increase the species richness of an object nearby. Some of earlier studies supported this view [Edman et al., 2004], other studies did not find an effect of local enrichment on the diversity of fungi on a dead-wood object in the surroundings [Rolstad et al., 2004, Olsson et al., 2011]. There was no dispersal limitation at the scale of their studies of similar spatial scale [Rolstad et al., 2004]. Thus, spores and mycelia might be omnipresent at the scale of our study as well (landscape covering ca. 24,000 ha), and wood-inhabiting fungi are not limited in their ability to colonize dead wood, at least in the early successional stage. Another explanation for the mechanism behind this pattern might be that the early

colonization and subsequent species diversity determines the subsequent communities. As outlined above, it has been shown that numerous wood-decay fungi are latently present as endophytes in sapwood of a wide range of still-living angiosperm trees [Parfitt et al., 2010]. The endophyte community might therefore act as a filter and determine the secondary colonizers and subsequent communities independent from local donors or the number of colonization events. Therefore, the lack of a significant effect of the local dead-wood amount might be caused by priority effects [Fukami et al., 2010, Hiscox et al., 2015b]. The priority effect states that the succession of species communities is affected by the predecessor community. However, we aimed at focusing on the very early stage of succession, with species from the endophytic and secondary colonizer communities [Boddy, 2001, Parfitt et al., 2010] (see Table 4.4 for the complete species list). Overall, our study demonstrated that the local dead-wood amount and heterogeneity at the scale of our study are not important for species richness and community composition on single dead-wood objects in the early phases of wood decomposition. Further studies are needed to shed light on the distribution and relevant scale of donor populations affecting the colonization of a dead-wood object within and across landscapes and to untangle these processes from priority effects.

4.4.4 Conclusion

Our study demonstrated that host is a more important driver of the diversity of fruiting species of fungi than the environment. A closer look revealed that the host species had the highest relative effect on the diversity of wood-inhabiting fungi, followed by microclimate and host size, but not local dead wood. We hypothesize that the combined effects of tree species and canopy openness leads to a preponderance of host specialists under shady canopies that shift towards communities dominated by host opportunists or microclimate harshness specialists in sunny gaps. For the conservation of wood-inhabiting fungi, forest managers should provide dead wood of a broad range of tree species, exposed to different microclimatic conditions. This goal can be achieved most efficiently by enriching dead wood of larger sizes during regular logging activities independent of the availability and distribution of existing dead wood in the surroundings.

5 Assembly processes linked to organism size in a dead-wood experiment

Abstract

The study of organism size in ecology has a long history, however, whether assembly processes differ between macro- and microorganisms remains speculative. Important variables are often correlated in survey studies, introducing potential bias into interpretations of niche selection, dispersal limitation and ecological drift. We therefore use an orthogonal dead-wood experiment on landscape scale, to disentangle spatial and environmental effects. We tested whether assembly processes vary with organism size and focus on the niche selection to ecological drift ratio, as the influence of dispersal limitation is negligible on the scale of our study. As size categories we used i) a between-taxon approach based on bacteria, fungi and beetles and ii) a within-taxon approach based on small, medium and large beetles. Variation partitioning and a recent null model framework consistently showed a decreasing niche selection to ecological drift ratio with organism size. Our findings thus suggest that assembly mechanisms differ between wood-inhabiting macro- and microorganisms. In detail, our study supports the "size-demography hypothesis", stating that larger organisms have smaller community sizes, increasing the influence of ecological drift. Our results thus emphasize the role of demographic properties, e.g., community size, as important driver of variation in assembly processes on landscape-scale.

5.1 Introduction

Community ecologists increasingly concur that niche selection, dispersal and ecological drift jointly influence the assembly of natural communities [Farjalla et al., 2012, Stegen et al., 2012, Thompson and Townsend, 2006, Vellend, 2010, Zhou and Ning, 2017]. Most of our current knowledge of assembly processes has been derived from research on animals and plants [Clements, 1916], raising the question whether microorganismal

assembly follows different or similar processes [Barberán et al., 2014]; thus whether assembly is constant for organisms of different size classes [Farjalla et al., 2012]. Organism size is a central measure in various areas of biology, e.g., metabolic theory [McMahon, 1973], biogeography [Bergmann, 1847] or r/K-selection ecology [MacArthur and Levins, 1967]. Although organism size is an integrative trait for differences in dispersal abilities and demographic properties [Farjalla et al., 2012], its role in assembly processes is still poorly understood. Assembly processes differ based on the spatial scale [Leibold and Chase, 2017]. Especially dispersal limitation becomes more influential on regional to global scales [Barberán et al., 2014, Leibold and Chase, 2017]. Previous studies have focused on niche selection and dispersal [Farjalla et al., 2012, Wu et al., 2017], whereas the relative importance of niche selection and ecological drift have rarely been addressed [Zhou and Ning, 2017]. To test whether assembly processes differ between organism of increasing size, our experiment operates at the local to landscape scale to reduce the influence of dispersal limitation.

Differences in demographic properties and life-history traits between macro- and microorganisms lead to two basic expectations relating assembly processes to organism size. First, many microorganisms (e.g., bacteria) were found to be able to survive in various contrasting habitats because of metabolic and phenotypic plasticity ('size-plasticity hypothesis', [Farjalla et al., 2012]), which may decrease the influence of niche selection with decreasing organism size. Second, macroorganisms tend to have smaller community sizes compared to microorganisms [Barberán et al., 2014, De Bie et al., 2012, Savage et al., 2004]. Small community sizes were simulated to be prone to increased ecological drift, because random extinctions have a greater effect on local communities [Barberán et al., 2014, Orrock and Watling, 2010], which may decrease the influence of niche selection with increasing size.

Previous studies have shown increasing influence of niche selection with increasing organism size [Farjalla et al., 2012, Soininen et al., 2013, Wu et al., 2017], whereas other studies found the opposite result [Beisner et al., 2006, De Bie et al., 2012, Zinger et al., 2017]. Some results were based on survey studies, where important variables are often correlated (Chapter 4, [Müller and Bütler, 2010]). The interpretation of partial spatial and environmental effects for independent assembly processes may then introducing potential bias.

Within this study we therefore want to contrast different expectations of size-mediated influences of niche selection and ecological drift (hereafter 'selection' and 'drift') on local spatial scale. We test the following hypothesis relating the influence of selection and drift to organism size: If metabolic plasticity of microorganisms reduces the local habitat to

act as filter, we expect microorganism to be less niche selected than macroorganisms ('size-plasticity hypothesis'). If larger community size reduces the influence of stochasticity, we expect microorganisms to be less influenced by drift than macroorganisms ('size-demography hypothesis') (Figure 5.1).
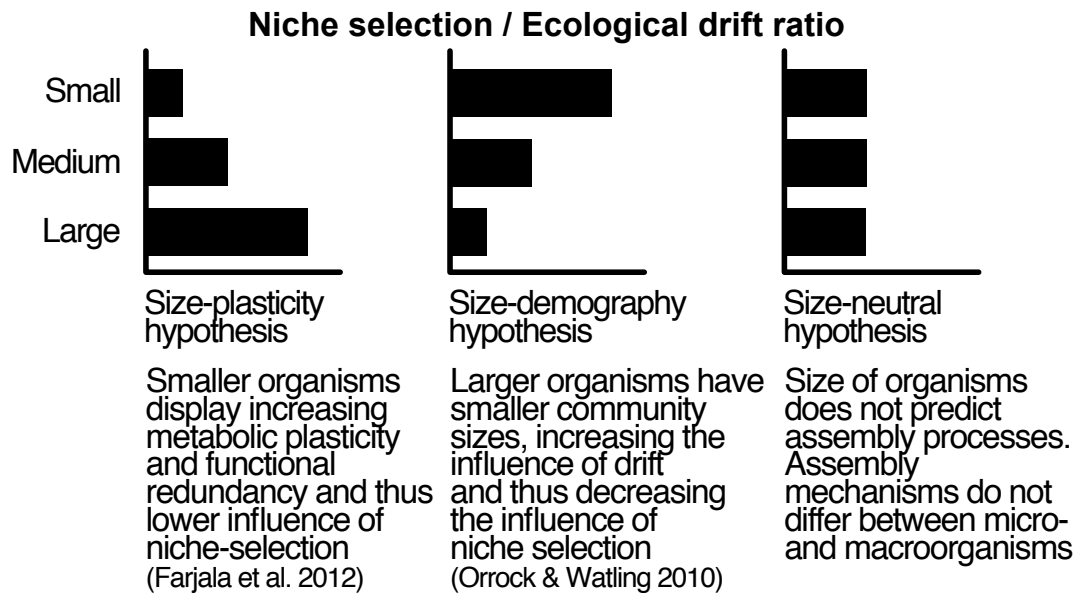
Figure 5.1: Hypotheses relating the selection to drift ratio to organism size. Small (Bacteria and small beetles); medium (Fungi and medium-large beetles); large (Beetles and large beetles); for beetle size classes see Figure 5.5.

Dead wood harbors a high diversity of taxa of various average body sizes [Stokland et al., 2012] within spatially distinct resource units (e.g., dead-wood log), where many different organisms are exposed to the same host and environmental conditions. Therefore, we used a local-scale orthogonal dead-wood experiment to test these hypotheses. Wood-inhabiting bacteria, fungi and beetles were reported to display high dispersal capabilities on local and landscape scales [Forsse and Solbreck, 1985, Komonen and Müller, 2018, Nilssen, 1984]. To test these hypotheses, we use a between-taxon (bacteria, fungi and beetles) and a within-taxon approach (small, medium and large beetles, coding based on average measured body size). We manipulated microclimate (sunny vs. shady plots) and tree species identity (beech vs. fir) (Chapter 4, [Seibold et al., 2016]) (Figure 5.2A). To quantify niche selection vs. ecological drift, we used variation partitioning [McArdle and Anderson, 2001] and a recent null model framework [Stegen et al., 2012], which is based on standardized effect sizes of a phylogenetic turnover and null deviations of a taxonomic turnover (Figure 5.2B).
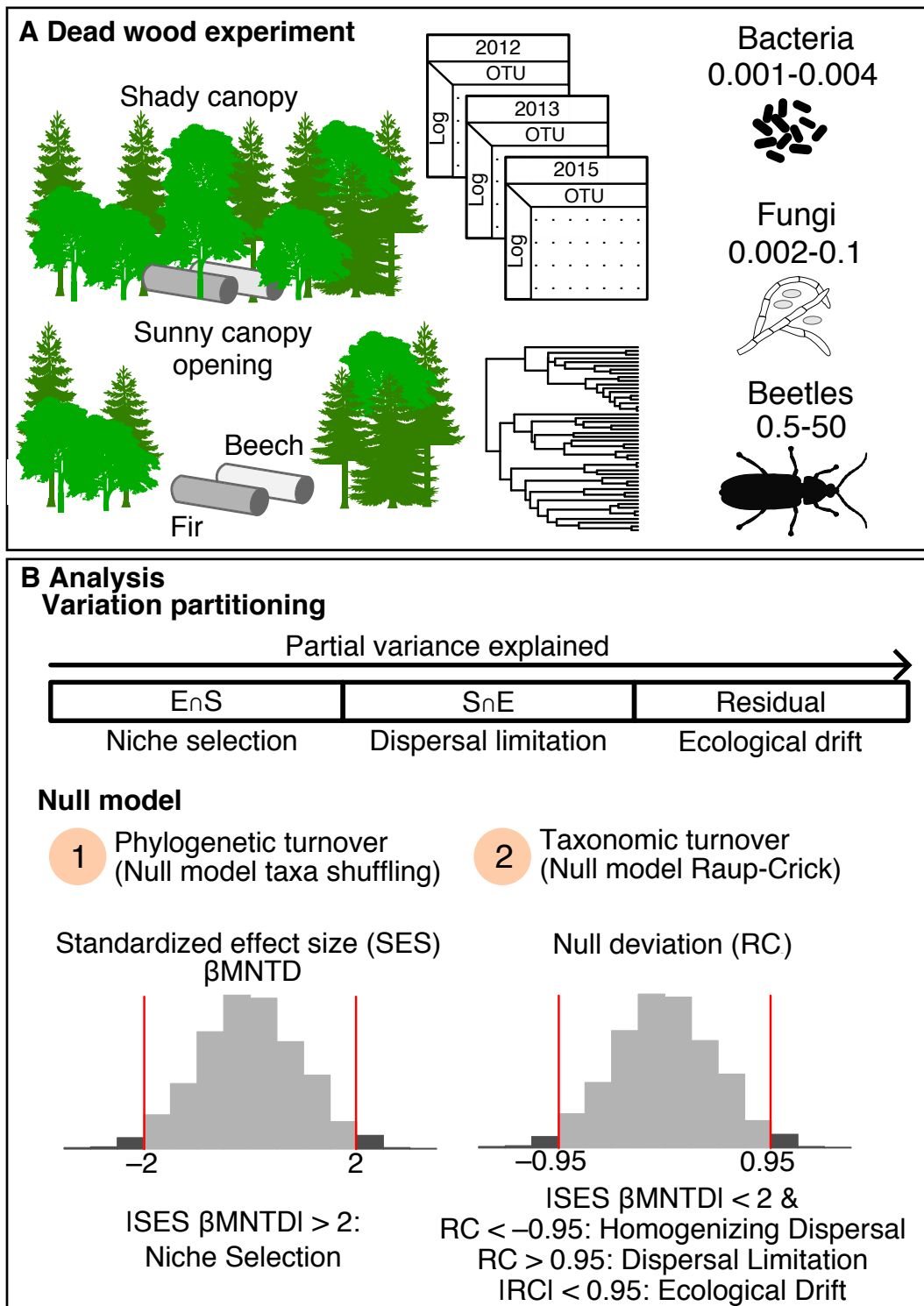
Figure 5.2: Experimental study design and methodological overview. A) Study design of the orthogonal dead-wood experiment and approximate ranges of organism sizes of wood-inhabiting taxa: bacteria, fungi and beetles. Units are in mm. B) Variance partitioning and null model framework developed by [Stegen et al., 2012]. βMNTD = beta mean nearest taxon distance; RCbray = Raup-Crick null model for Bray-Curtis distances; SES = Standardized effect size.

5.2 Material and Methods

5.2.1 Study area, experimental design and sampling

Assembly processes vary with the spatial extend of the study [Barberán et al., 2014, Leibold and Chase, 2017], and thus our experiment operates at the local scale (25.000 ha) to standardize for spatial bias in interpretations (Figure 5.1). On local spatial scales, historical effects (e.g., shared ancestry) and dispersal are less influential, whereas stochasticity (ecological drift) gains importance; niche selection operates on both scales [Barberán et al., 2014].

The experiment was conducted in the Bavarian Forest National Park in south-eastern Germany. This study is part of a large experiment, which was described in detail by (Chapter 4) [Seibold et al., 2016]. Here we used a subset of this experiment, which was described in detail in [Seibold et al., 2018]. In brief, the experiment included 46 and 42 (for beetles) plots of 0.1 ha, which were arranged in a random block design comprising four blocks. In autumn 2011, we freshly cut and directly deposited (within less than eight weeks) 120 dead-wood logs (mean diameter $\pm$ SD = 33 $\pm$ 6.5 cm, length = 5 m) of beech and fir on the plots. The wood objects were taken from trees of the same age, that were harvested within the same region. The same number of plots contained logs of either one and both tree species. We used canopy openness as a surrogate for stand microclimate [Müller et al., 2015, Seibold et al., 2016, Vodka et al., 2009] and placed logs in sunny gaps and under a shady canopy (Figure 5.1A). We sampled bacteria, fungi and beetles on 64 dead-wood logs. We sampled bacteria and fungi on the same 64 logs. 24 plots intersected with the beetle sampling.
Beetles were sampled in 2013, 2014 and 2016 using stem emergence traps, which were installed when snow was melting (within April all years) and operated the end of August in 2013 and 2016, but for technical reasons only until mid-June in 2014. Note that most beetle larvae developed in the wood the year before they emerged, thus sampling years match to sampling of fungi and bacteria. Traps were emptied monthly and beetles were identified to species by taxonomists. All data were pooled to years. Emergence traps were mounted about 1 m away from one end of a log in the first year and moved to the same position near the other end in the second year and in the initial position in the fourth year. Each trap consisted of a 30 cm wide steel sheet bent around and nailed to a log and two strips of lightproof cotton fabric stapled to the log to cover side openings. Each trap had three transparent collecting jars filled with 96% ethanol to preserve beetles [Wikars et al., 2005].

Fungi and bacteria were sampled in September 2012, 2013 and 2015 from 60 logs using a cordless drill (Makita, Anja, Japan) equipped with a 0.8x40 cm wood auger. Each log was drilled four times at log position 0.5 m, 1.5 m, 3.5 m and 4.5 m. In 2013, we shifted the location of the drill ca. 15 cm towards the center of the log. The drill was operated slowly to avoid overheating and introduced at an angle of ~45° to a line perpendicular to the log axis and went through the log. To avoid cross-contamination between samples, the wood auger was flamed and wiped with ethanol after each drilling. Samples were pooled per log and year. The wood samples were stored at -40°C until further processing.

5.2.2 Sequencing of fungi and bacteria

In the laboratory, wood samples were freeze-dried. Dead wood was milled using Ultra Centrifugal Mill ZM 200 (Retsch, Haan, Germany) to fine powder. The resulting fine powder was used for molecular analyses. Total genomic DNA was extracted from 200 mg of material and the fungal community composition was analyzed by high-throughput sequencing based on PCR amplification of the fungal ITS2 region [Ihrmark et al., 2012] as described previously [Baldrian et al., 2016]. Consensus sequences were constructed for each cluster, and the closest hits at the species level was identified using BLASTn against UNITE [Koljalg et al., 2013] and GenBank. Where the best hit showed lower similarity than 97% with 95% coverage, the best genus-level hit was identified. For convenience, we refer to the taxa as 'OTU' (operational taxonomic unit) irrespective if it was an identified species (beetles) or consensus sequences (bacteria and fungi).

5.2.3 Data preparation and community composition analysis

We first assessed potential effects of environmental factors on the community composition. To minimize the effect of sequencing error for fungi and bacteria, we removed singletons and doubletons and OTUs below a sample-based relative abundance threshold of 0.0001 after visual inspection (Figure 5.1). Finally, for all three community matrices we kept only OTUs occurring on at least two logs and logs with at least three OTUs. To assess whether removal of rare OTUs might affect interpretation, we sequentially raised the minimum number of OTUs on a log from 1 to 6 and found mantel correlations above 0.997 for all comparisons with the full matrix. Then we used Bray-Curtis dissimilarity with non-metric multi-dimensional scaling (NMDS) (function metaMDS, R package vegan [Oksanen, 2015]). We set the minimum number of random starts to 50. For bacteria, we were not able to derive meaningful ordinations with this approach and thus

used the function monoMDS (R package vegan) with the method 'hybrid'. To assess the variance explained by each environmental factor on the community composition, we used permutation tests (function envfit, R package vegan) with 999 permutations.
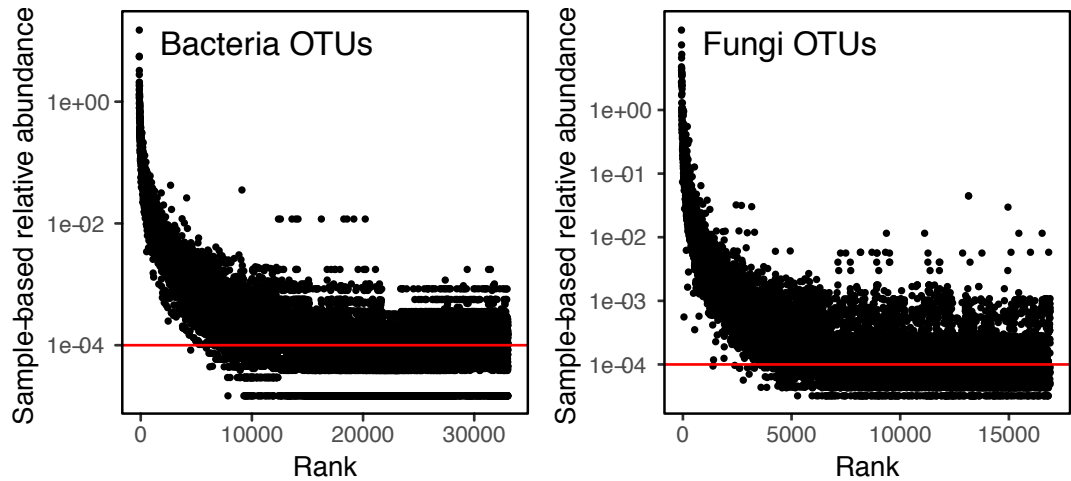
Figure 5.3: Sample-based relative abundance of fungal and bacterial OTUs and threshold (red horizontal line) under which OTUs were removed to reduce potential sequencing error.

5.2.4 Phylogenies

For the bacteria phylogeny, the 16S rRNA gene region was directly used for phylogenetic inference. The sequences were aligned using MAFFT [Katoh and Standley, 2013] and the multiple sequence alignment was then subjected to maximum likelihood tree inference using FastTree [Price et al., 2009] with parameters as in [Kembel et al., 2014]. The beetle phylogeny was taken from [Seibold et al., 2015b] and pruned to recorded species. For fungi, we first removed yeast OTUs based on taxonomy from the OTU list and thus retained only filamentous fungi. Yeasts were not analyzed due to a very small community size. For the fungal phylogeny, we used the BLASTn best hit of the 5.8S rRNA for the phylogeny inference. We aligned the sequences using MAFFT and estimated the topology and branch lengths using RAxML [Stamatakis, 2014] on the CIPRES Science Gateway [Miller et al., 2011]. As the fungal 5.8S rRNA can be uninformative, we also computed averaged taxonomic distances (function taxa2dist, R package vegan) based on taxonomic information. We then computed the beta mean nearest taxon distance (βMNTD) based on a patristic phylogenetic (function cophenetic, R package stats) and taxonomic distance matrix. Procrustes analysis between both βMNTD matrices was

highly correlated (R^2=0.90, p=0.001); we thus presented only the results based on the phylogeny.

5.2.5 Variation partitioning and null model analysis

The main objective of our study was to address differences in assembly processes between wood-inhabiting taxa. To achieve this, we used variation partitioning [McArdle and Anderson, 2001] and a null model framework [Stegen et al., 2012]. Variance partitioning was often used to address assembly mechanisms [Zhou and Ning, 2017]. Here the partial effects of space and environment on the community composition were estimated. Partial environmental effects were often interpreted as niche effects, whereas partial space as dispersal limitation [Wu et al., 2017]. However, space has also been interpreted as unmeasured environmental variables [Langenheder et al., 2012, Wang et al., 2013]. For the calculation of the variance partitioning, we used the partial distance-based two-way permutational multi-variate analyses of variance [Anderson, 2001, Wu et al., 2017]. As spatial input, we used the axis of a principal coordinate analysis (PCoA) based on Euclidian distances of the spatial coordinates between the plots. As environmental input, we used the PCoA axis based on three environmental variables (tree species, canopy openness and time since tree death). This implementation of the variation partitioning estimates the number of included axes (of the PCoA) using the Kaiser–Guttman rule [Wu et al., 2017]. The null model framework provides as stepwise procedure to divide pairwise community comparisons into underlying mechanisms of species niche selection, dispersal limitation, homogenizing dispersal and ecological drift (for a detailed description see Figure 5.1 and [Langenheder et al., 2017, Stegen et al., 2012]). A null model expectation was generated using 999 randomizations. We calculated the abundance weighted version of the βMNTD (beta mean nearest taxon distance) with the null model 'taxa shuffle' and the abundance weighted version of the Raup-Crick null model [Chase, 2010, Stegen et al., 2012]. Using phylogenetic correlograms (function phyloCorrelogram, R package phylosignal [Keck et al., 2016]), we found a significant increase in phylogenetic signal near the tips of the phylogeny (Figure 5.4), supporting the use of the mean nearest taxon distance [Stegen et al., 2012].

To address relative differences in assembly processes between taxa, we compared the ratio between assembly processes, rather than their absolute values [Wu et al., 2017] as the comparison of absolute values was shown to be problematic [Kraft et al., 2011, Stegen et al., 2012]. We define the selection to drift ratio as (i) partial environmental variance divided by residual variance and (ii) niche selection divided by ecological drift within the null model framework. To demonstrate independence of dispersal limitation

we additionally computed the ratios by adding (i) partial spatial variance to residual variance and (ii) dispersal limitation to ecological drift. Besides the comparison of assembly processes between taxa, we also addressed differences in assembly processes within beetles. Therefore, we extracted mean body size from literature [Seibold et al., 2015b] and divided the beetle community into three communities with small, medium and large beetle species. We used the 33% and 66% quantiles as thresholds to separate the beetle communities (Figure 5.5) resulting in three size classes: 0-2.2, 2.2-4.0 and 4.0-23.0 mm. We followed this approach to be able to directly compare the results to the between taxa approach.

5.2.6 OTU richness

To test for differences in OTU richness between taxa, we computed the expected number of OTUs. To account for false singletons potentially due to sequence errors, we applied the approach recently developed by [Chiu and Chao, 2016]. This nonparametric method estimates a true singleton count based on the relationship between the frequency of singletons and doubletons.

5.3 Results

We found 3431 bacterial OTUs, 1333 fungal OTUs and 266 beetle OTUs (for beetles OTUs equals species; 12237 individuals) after preparation of community matrices. Bacteria predominantly belonged to Alphaproteobacteria, Actinobacteria and Gammaproteobacteria; fungi belonged mainly to Agaricomycetes, Leotiomycetes and Sordariomycetes. Most species-rich beetle families were Staphylinidae, Curculionidae and Nitidulidae (Figure 5.6).

5.3.1 Community composition

The community composition of bacteria was significantly affected by time since tree death (R^2=0.94). The community composition of fungi was significantly affected by tree species (R^2=0.23) and time since tree death (R^2=0.60). The community composition of beetles was significantly affected by canopy openness (R^2=0.20) and time since tree death (R^2=0.47, Table 5.1, Figure 5.7). Within beetles, small, medium and large beetle communities were significantly affected by canopy openness and time since tree death (Table 5.1, Figure 5.7).

Table 5.1: Post-hoc environmental fits of tree species identity, canopy openness and time since tree death on the non-metric multi-dimensional scaling (NMDS) of three wood-inhabiting taxa. Ordination was performed using non-metric multi-dimensional scaling. Displayed are adjusted correlation coefficient (R^2) derived from a permutation test with 999 permutations. Significant values are highlighted in bold. Time = Time since tree death (years); Canopy = Canopy openness

| | Between taxa | | | | | |
| | Bacteria | | Fungi | | Beetles | |
Predictor	R^2	p	R^2	p	R^2	p
Tree species	<0.00	0.640	0.23	0.001	0.01	0.429
Canopy openness	<0.00	0.732	<0.00	0.948	0.20	0.001
Time since tree death	0.94	0.001	0.60	0.001	0.47	0.001
	Within taxon					
	Small		Medium		Large beetles	
	R^2	p	R^2	p	R^2	p
Tree species	<0.00	0.749	0.01	0.606	<0.00	0.775
Canopy openness	0.28	0.001	0.50	0.001	0.41	0.001
Time since tree death	0.61	0.001	0.33	0.001	0.23	0.001

5.3.2 Partial variation partitioning and null model analysis

The selection to drift ratio decreased with increasing organism size, from bacteria to fungi to beetle communities based on both variation partitioning and the null model framework (Table 5.2, Figure 5.8A, B; and for raw model output see Figure 5.10). For the variation partition the decrease is stair-like, whereas for the null model framework the effect between bacteria vs. fungi and beetles is almost binary (Figure 5.9). Further beetles have a numerically slightly higher ratio than fungi, however, fungi have a higher ratio than beetles if dispersal limitation was added to drift (Figure 5.11). Within beetles the selection to drift ratio consistently decreased with increasing beetles body size (for the coding see Figure 5.5). This was consistent across the variation partitioning and null model framework; both displayed a stair-like decrease (Figure 5.5C, D). For the results of the individual components see Figure 5.12.
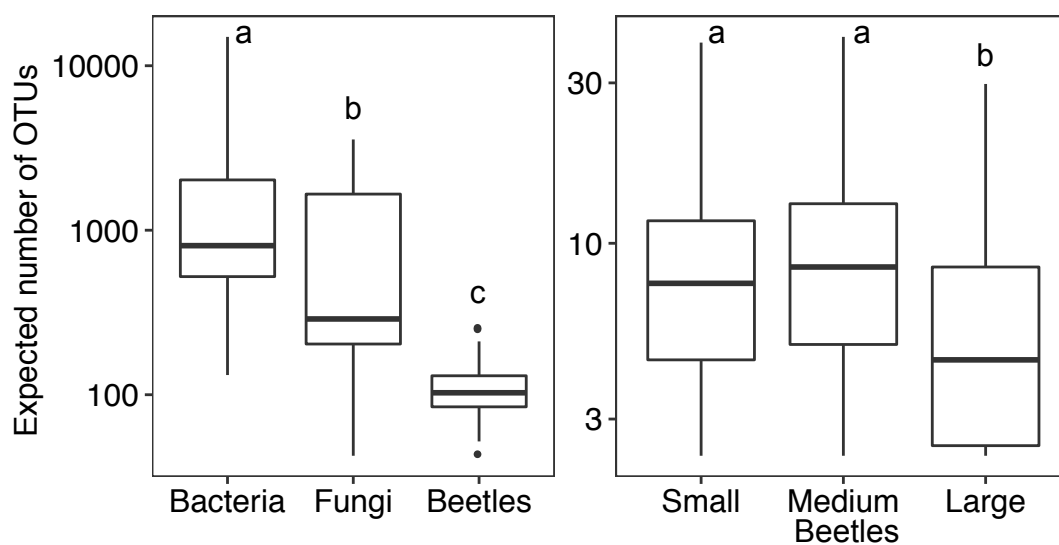
Figure 5.8: Expected number of OTUs [Chiu and Chao, 2016] between bacteria, fungi and beetles and between small, medium and large beetle communities. Significance was tested using linear mixed-effects model (Beetle–Fungi: z=–11.41, p¡0.001; Beetles-Bacteria: z=–17.28, p<0.001; Fungi–Bacteria: z=–7.445, p<0.001; Large–small beetles: z=–7.38, p<0.001; Large-medium beetles: z=–7.97, p<0.001; Medium–small beetles: z=0.88, p=0.656; random effect on log). Significance is indicated by small letters. Boxplots denote the median (horizontal line) and interquartile range (colored box); whiskers show three times the interquartile range; points indicating values outside this range.
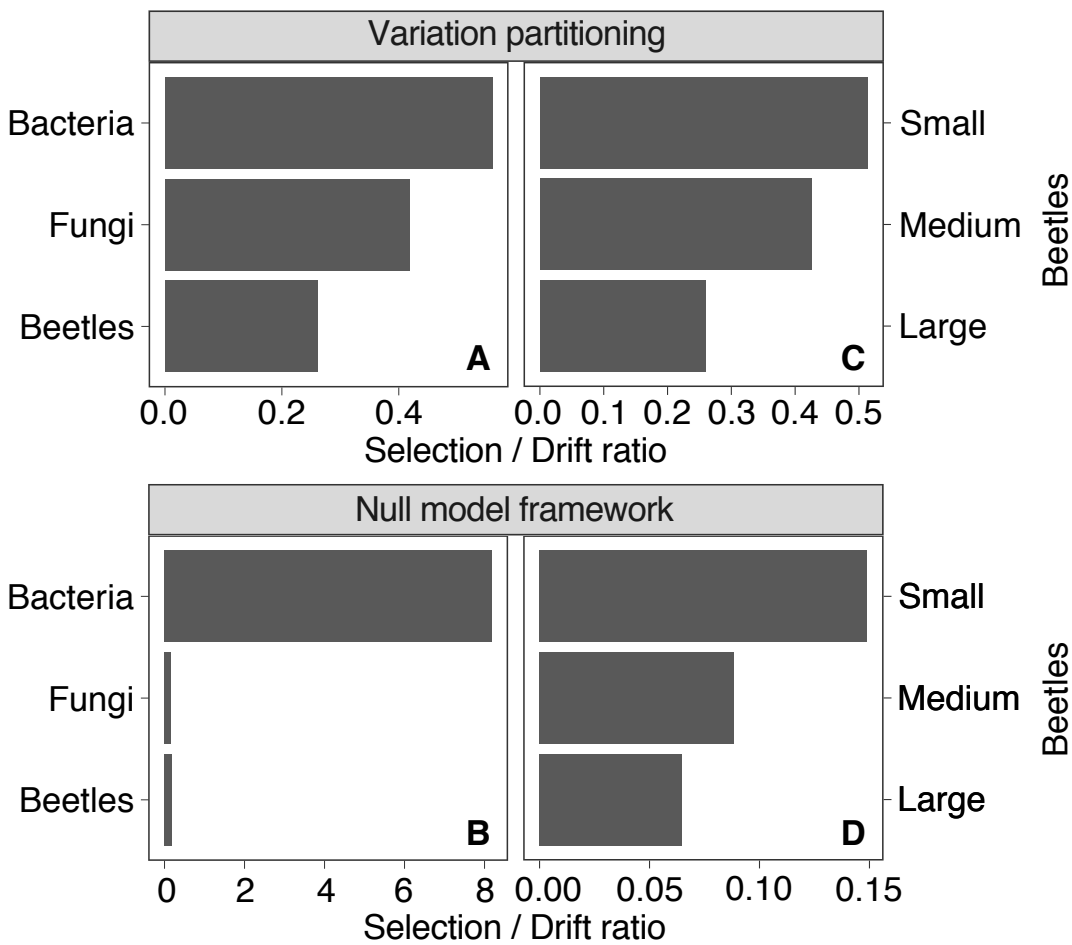
Figure 5.9: Selection to drift ratio of wood-inhabiting taxa based on partial variation and a null model framework. A) Selection to drift ratio inferred based on partial variation analysis between taxa. B) Selection to drift ratio inferred based on a null model framework between taxa. C) Selection to drift ratio inferred based on partial variation analysis between taxa within beetles. D) Selection to drift ratio inferred based on a null model framework between taxa. For individual assembly processes see Figure 5.11

Table 5.2: Variation partition statistics table based on 999 permutations. E∩S = Partial environmental effect; S∩E = Partial spatial effect; E∪S = Intersected partial spatial and environmental effect.

	Between taxa					
	Bacteria		**Fungi**		**Beetles**	
	R^2	p	R^2	p	R^2	p
E∩S	0.34	0.001	0.27	0.001	0.25	0.001
S∩E	<0.01	0.613	0.02	0.070	0.04	0.001
E∪S	0.06	-	0.05	-	0.03	-
Residual	0.61	-	0.66	-	0.67	-
	Within taxon					
	Small		**Medium**		**Large beetles**	
	R^2	p	R^2	p	R^2	p
E∩S	0.32	0.001	0.27	0.001	0.19	0.001
S∩E	0.05	0.004	0.03	0.092	0.07	0.012
E∪S	0.01	-	0.07	-	0.01	-
Residual	0.62	-	0.64	-	0.73	-
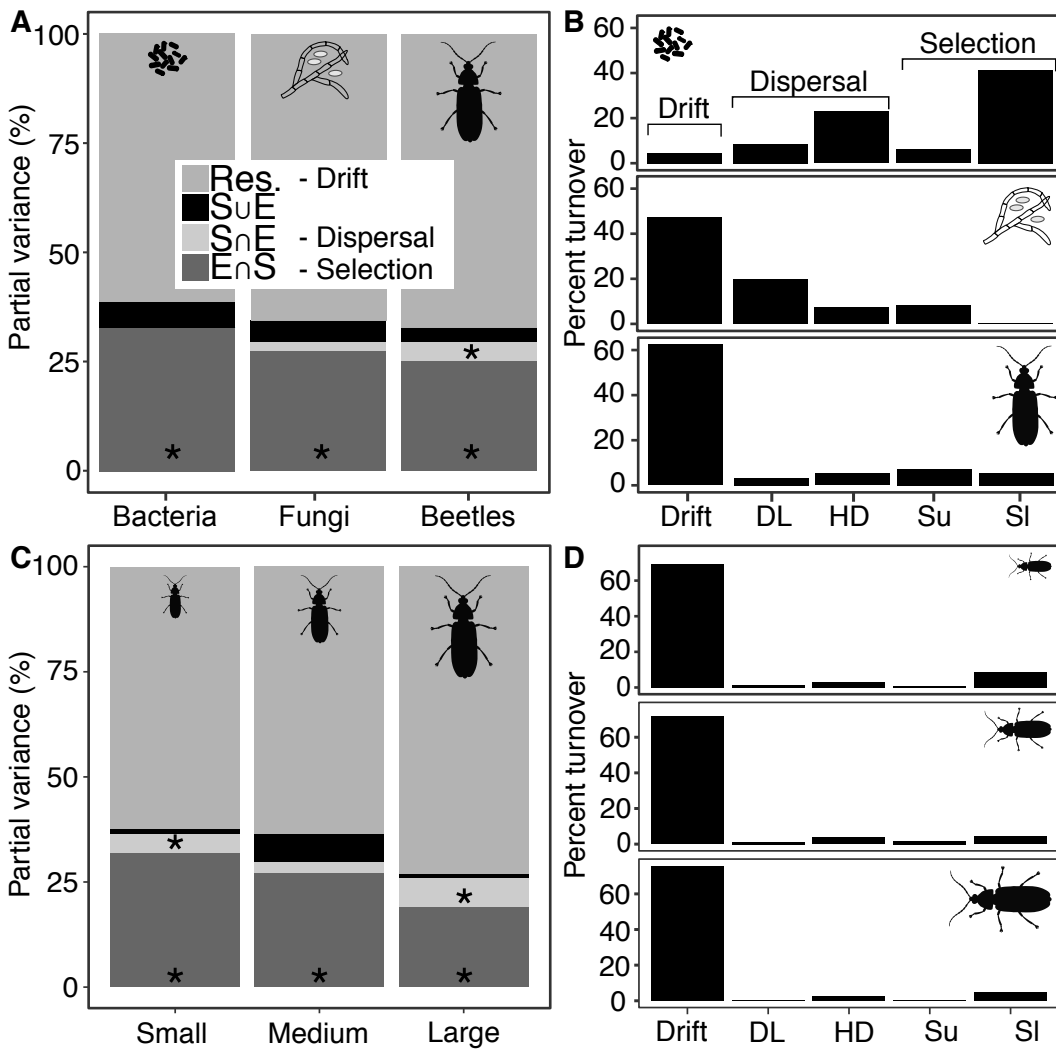
Figure 5.10: Assembly processes inferred using two methods. A) Partial variation partitioning based on Bray-Curtis dissimilarity. S∩E = Partial variance explained by space; E∩S = Partial variance explained by environment; E∪S = Intersecting partial variance explained by both environment and space. Res. = Residuals, unexplained variance. For exact R^2 and p-values see Table 5.2. B) Null model based components of assembly processes. For histograms see Figure 5.11. Drift = Ecological drift; DL = Dispersal limitation; HD = Homogenizing dispersal; Su = Selection upper (SES > 2); Sl = Selection lower (SES < -2). C) Variation partitioning for size classes within beetles Figure 3. D) null model framework for size classes within beetles.
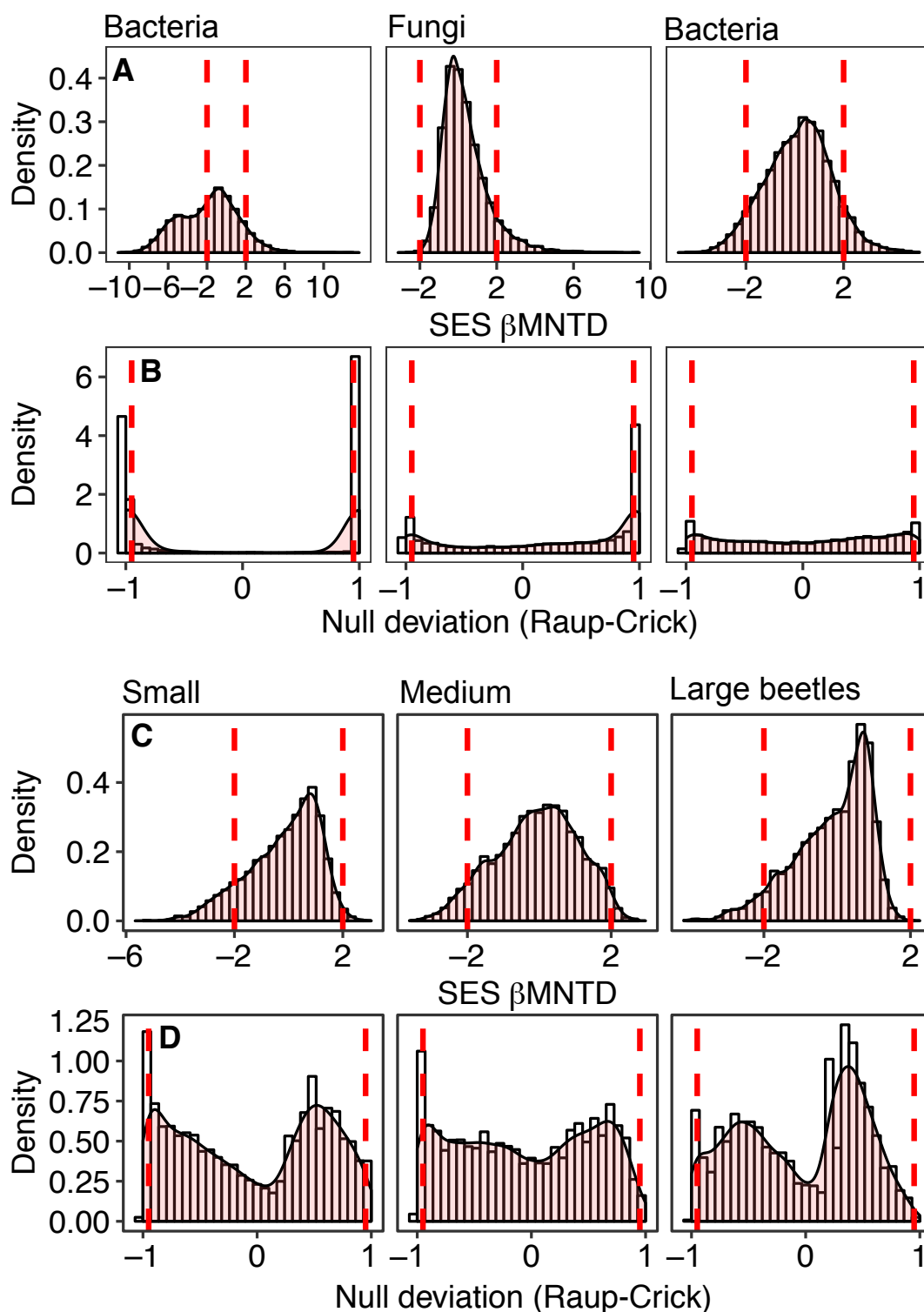
Figure 5.11: Density histograms of the pairwise phylogenetic and taxonomic turnover metrics. A) Standardized effects sizes (SES) for the beta mean nearest taxon distance (βMNTD) with null model 'taxa shuffle'. B) Null deviation based on the Raup-Crick null model. All null models were evaluated based on 999 permutations, between taxa. C) Beta mean nearest taxon distance within beetles. D) Null deviation based on the Raup-Crick within beetles.
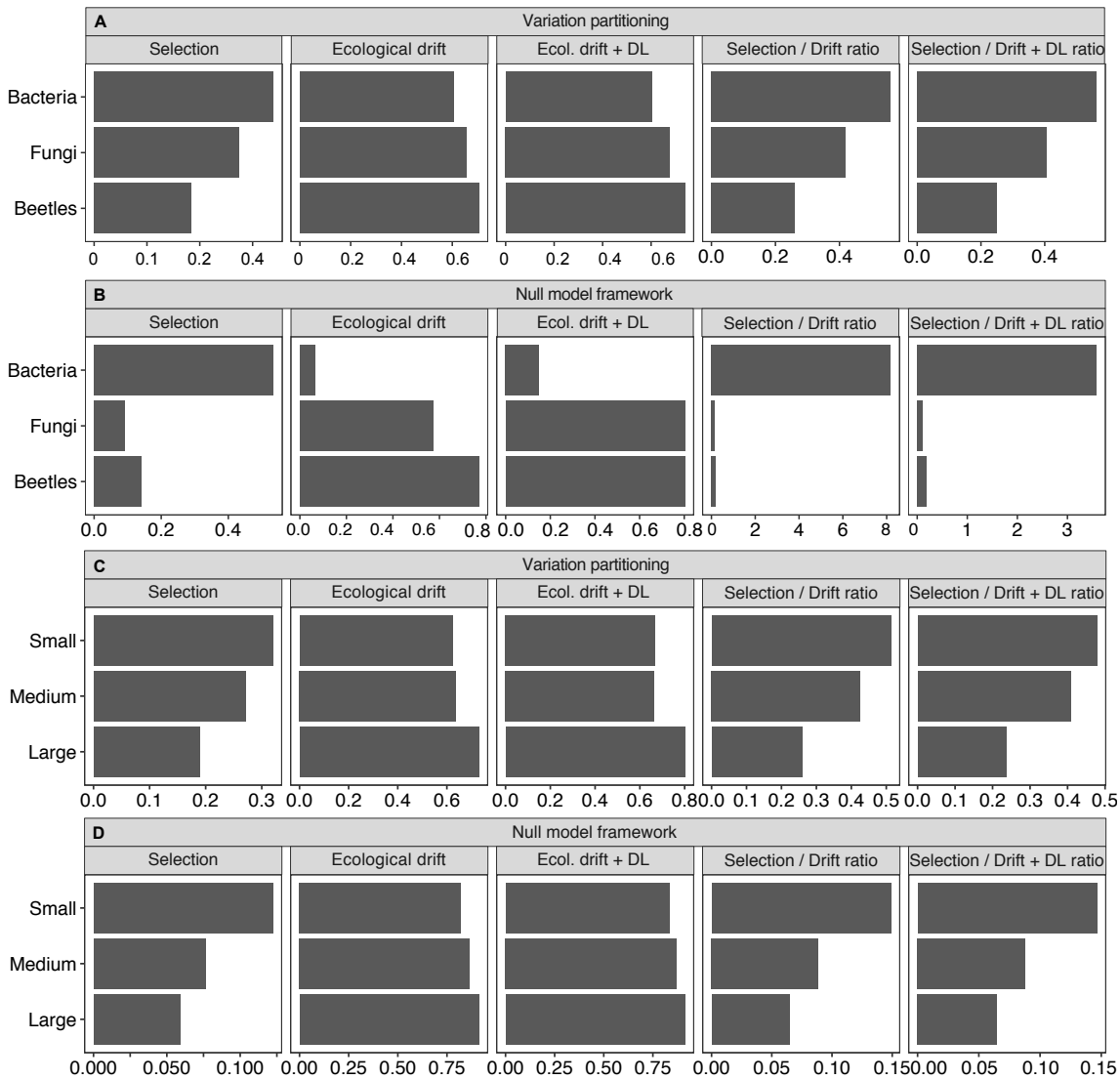
Figure 5.12: Individual components and ratios of assembly processes inferred using variation partitioning and a null model framework. A) Components of assembly processes based on partial variation analysis between taxa. B) Components of assembly processes based on null model framework between taxa. C) Components of assembly processes based on partial variation analysis based within beetles. D) Components of assembly processes based on null model framework within beetles. DL = Dispersal limitation.

5.4 Discussion

In this study we tested different alternative hypotheses how assembly processes expressed by the selection to drift ratio could be relation to organism size (Figure 5.1D). Varia-

tion partitioning as well as null model analysis consistently showed that the selection to drift ratio decreased with organism size between and within taxa. Thus, selection is more relevant for small organisms than for larger ones and contrary drift had a higher relevancy for larger organisms than for small ones. This opens up the opportunity to predict assembly processes by organism size (Figure 5.8) and supports the 'size-demography hypothesis' (Figs. 5.1, 5.8). This hypothesis stats that small community size (typical for larger organisms) leads to increased ecological drift on local scales and thus to reduced niche selection. Based on variation partitioning and a recently developed null model framework we found support for the 'size-demography hypothesis'. Thus, that organism size predicts differences in assembly processes, which was demonstrated across taxa and within beetles. The cross-taxa approach used broad size categories and thus a within-taxon approach was added which was based on measured average body size measurements. Our results thus suggest that assembly processes differ between wood-inhabiting taxa and that those differences are predictable at least partly by the organism size. Further, the 'size-demography hypothesis' states that variability in demographic properties (e.g., community size) is the main underlying driver of assembly processes on local spatial scale (Figure 5.1). From previous studies we know that smaller organism tend to have larger community and population sizes [Savage et al., 2004] and that community size is linked to stochasticity [Orrock and Watling, 2010]. Here we could further show that bacteria have larger community sizes than fungi, and fungi than beetles (Figure 5.8). However, note that we do not have information about the total community and population sizes within the meta-community. A promising approach of such evaluations might be aerial biodiversity assessments to generate a more complete list of the locally occurring fungi (meta-community), but large-scale experiments are still lacking [Abrego et al., 2018]. On the other hand, large communities are typically associated with smaller organism (r-strategy). Large communities might be less prone to ecological drift because high propagule/species numbers can override random death processes, suppressing stochasticity [Leibold and Chase, 2017]. The general phenomenon is known as homogenizing dispersal or 'mass effects' [Leibold et al., 2004, Mouquet and Loreau, 2003] with a steady replacement of local deaths. Without local dispersal limitation the influence of niche selection can thus increase for organism with large community sizes. Here we want to argue that all species have similar dispersal abilities on local scales, however, that organisms with smaller population/community sizes are more prone to ecological drift and thus less niche selection. Thus, ecological drift plays an important role for local-scale community assembly, which may result in a niche selection gradient along the organism size gradient. Alternative explanations for higher influence of niche selection

on smaller organisms might be that i) smaller organism are more specialized than larger organisms and operated in smaller spatial niches; Many bacterial species were indeed found to habitat specialized [Barberán et al., 2014]. Further, a recent experimental transplant study indicates an underestimation of bacteria in their habitat specialization and role in decomposition [Glassman et al., 2018]. Further, we found that bacterial communities displayed high phylogenetic clustering (βMNTD < -2, Figure 5.2), indicating niche specialization [Zhou and Ning, 2017]. Taken these results together, evidence is accumulating that bacteria might be more specialized and less functional redundant than previously assumed. ii) Bacteria are more prone to priority effects than fungi and beetles. Previous studies have suggested that wood-inhabiting bacteria are effected by priority effects of fungal substrate alteration and thus niche-modification [Kielak et al., 2016], however, the current data basis is weak. Especially fungi and bacteria compete for cellulose [De Boer et al., 2005], however, antagonistic as well as synergistic interactions were reported [Johnston et al., 2016]. Fungi and beetles displayed higher phylogenetic overdispersion (βMNTD > 2) than clustering (Figure 5.2), indicating limiting similarity or competitive exclusion [Stegen et al., 2012], whereas bacteria were more structured by phylogenetic clustering. This indicated higher competitive ability by fungi and beetles, which may wood structural niches and therefore bacteria. Given the low amount of secured data we here argue that any interpretation remains speculative, however, suggest that assembly within dead wood can be predicted by traits associated with organism size. Here we assumed equal dispersal abilities between taxa, which is supported by many studies [Forsse and Solbreck, 1985, Komonen and Müller, 2018, Nilssen, 1984, White et al., 2007]. Further, we found overall low partial spatial effects (significant only for beetles with, however, low R^2=0.04) and higher influences of homogenizing dispersal than dispersal limitation in bacteria and beetles (Figure 5.2). For fungi, we found higher dispersal limitation than homogenizing dispersal, but no significant effect of partial spatial variance (Figure 5.2). Nonetheless, to account for potential bias in interpretation we computed the selection/drift ratio and the selection/drift + dispersal limitation ratio. Both showed overall consistent results (Figure 5.11). It is important to note that dispersal limitation within the Stegen null model framework is a purely neutral process [Stegen et al., 2012]. Others proposed that dispersal limitation could also result from variation in dispersal traits (e.g., propagule size). Thus, we yield further suggestive evidence that wood-inhabiting taxa display similar dispersal abilities on local scale between, at least within the early phase of decomposition. Our analysis further revealed the interesting case that fungi reacted more similar to beetles than to bacteria within in the null model analysis (Figure 5.8C). One explanation may be that dispersal events of fungi may be

more similar to beetles than to bacteria. Most fungi reproduce once a year and live as diploid mycelium during most of the lifecycle [Peay et al., 2008]. Single yearly dispersal events may increase the influence of ecological drift on landscape scales. We therefore agree with [Peay et al., 2008] to interpret fungi as 'hybrid' between macro- (mycelium) and microorganisms (spores).

Using classical variation partitioning and a recent null model framework we consistently found that assembly processes were predicted by organism size within a dead-wood experiment. Our study thus provides support that assembly processes differ between macro- and microrganisms. In particular we found support for the 'size-demography hypothesis', emphasizing demographic properties such as community size as important factor in local assembly processes.
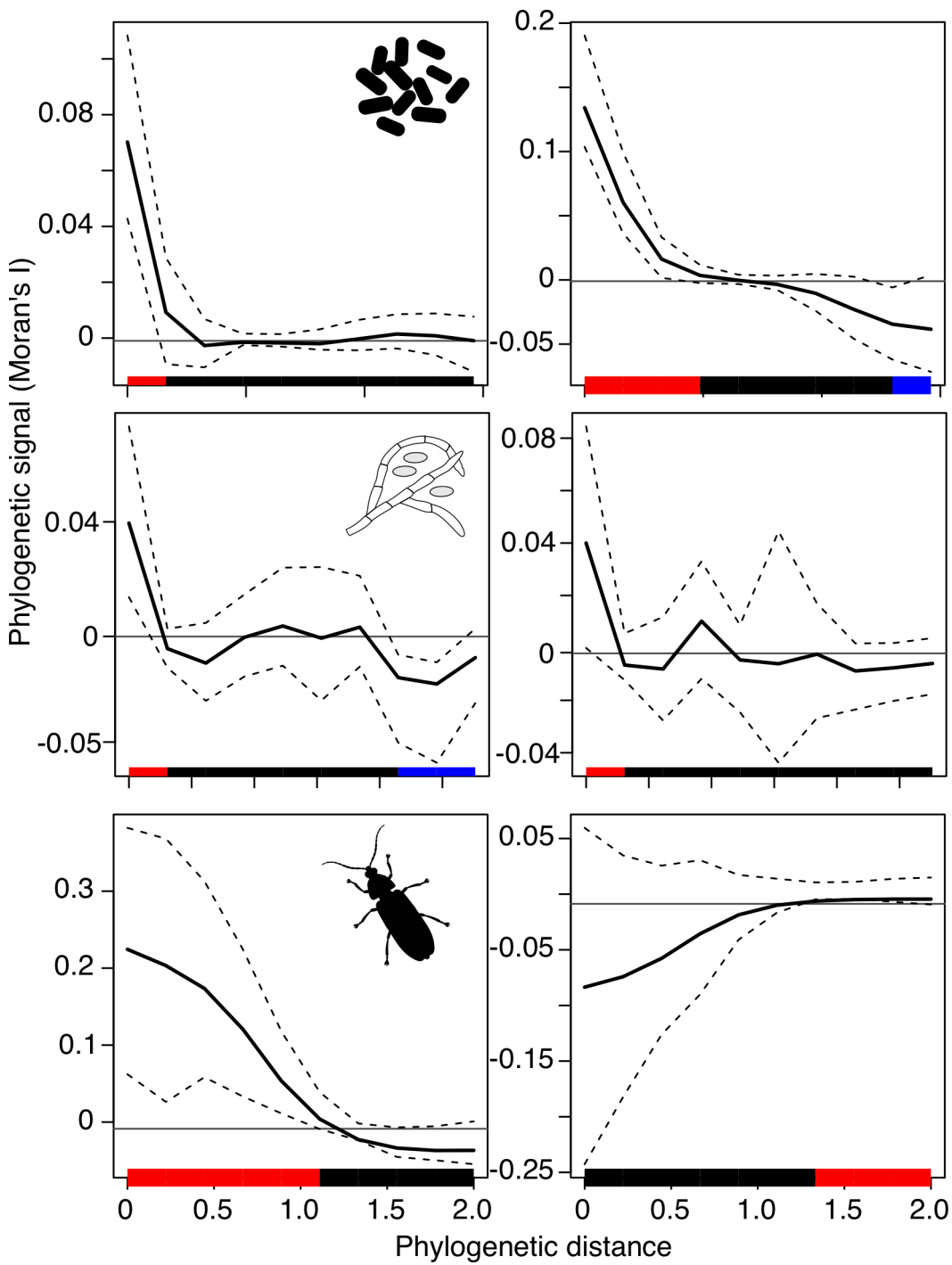
Figure 5.4: Phylogenetic correlograms based on mean values of tree species identity (right column) and canopy openness (left column) for each species. Mean traits were calculated based on at least 10 logs for fungi and bacteria and at least 3 logs for beetle OTUs. Overall phylogenetic signal increased near the tips suggesting the use of the mean nearest taxon distance (MNTD) to measure phylogenetic turnover.
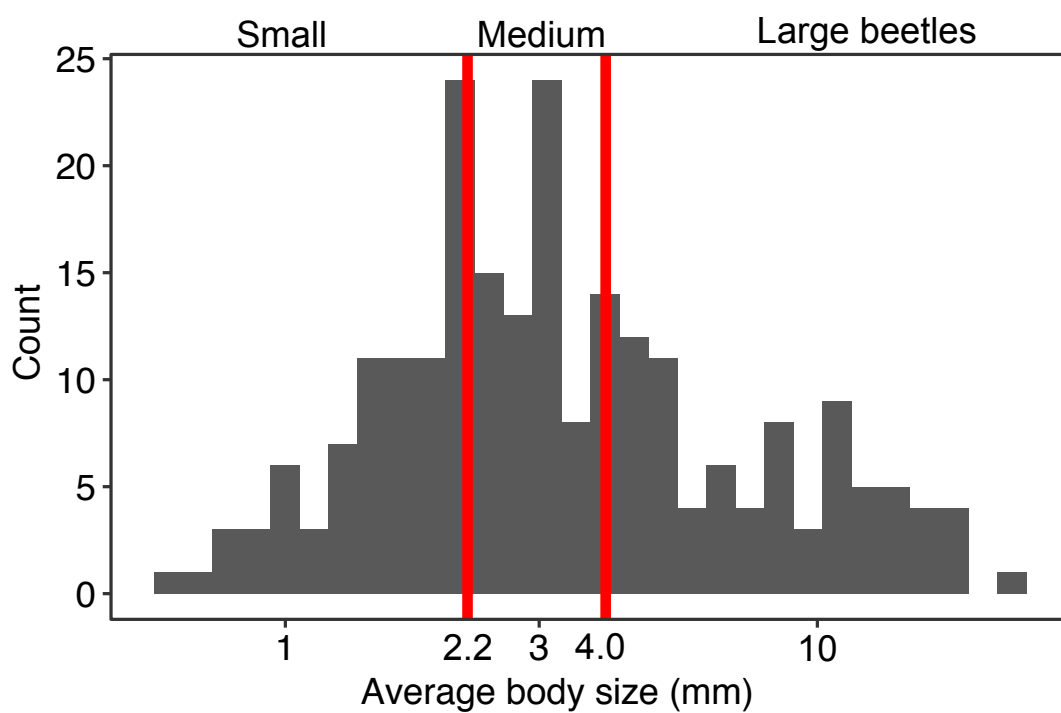
Figure 5.5: Histogram of $\log_{10}$-transformed mean beetle body size. Small, medium and large body size was coded based on the 33% and 66% (indicated by red lines) quantile thresholds to ensure equal number of species within each size class.
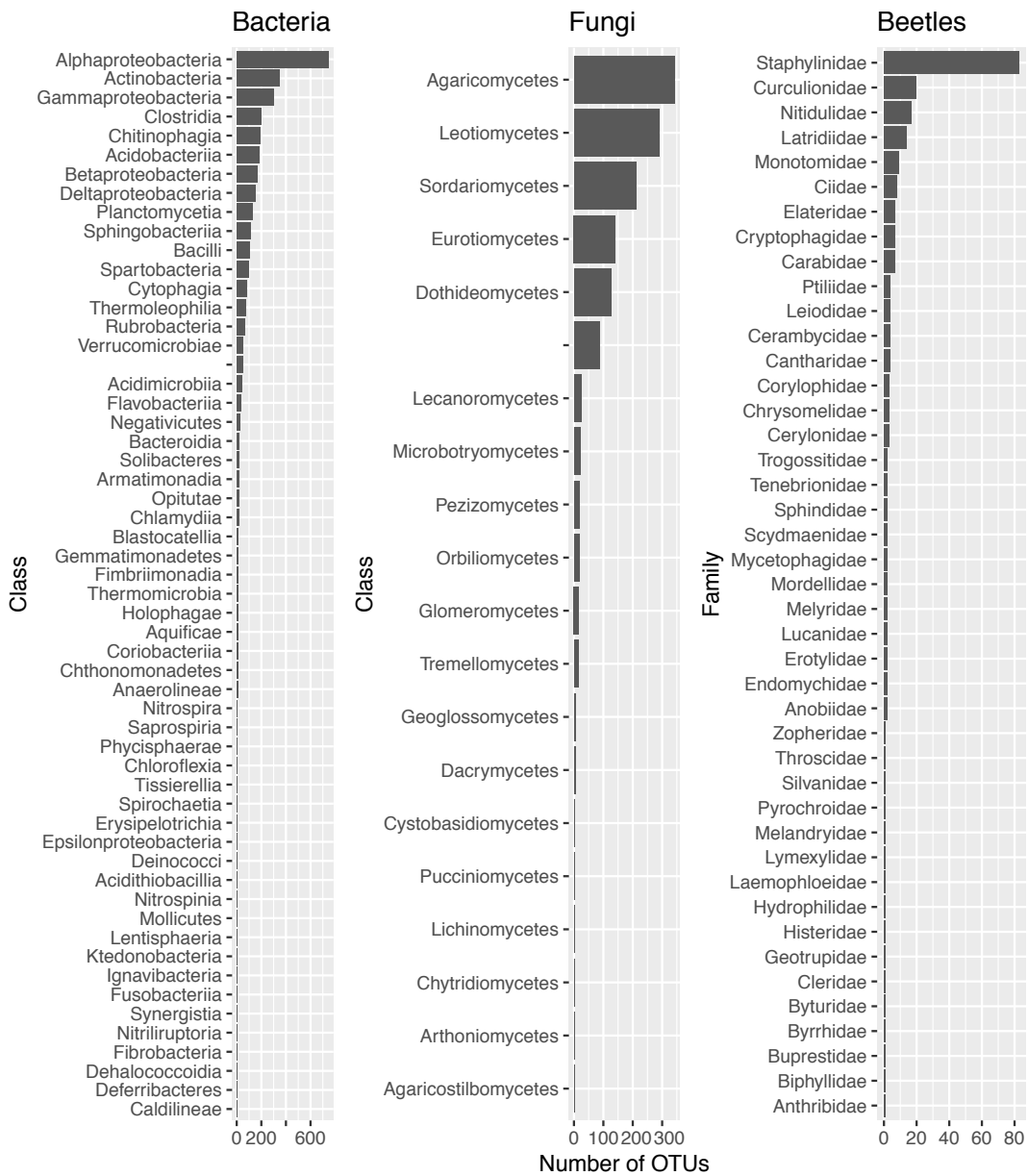
Figure 5.6: Taxonomic overview of the wood-inhabiting bacteria, fungi and beetles of this study. Displayed are the number of OTUs for systematic classes of bacteria and fungi and species abundance (number of individuals) for beetle families.
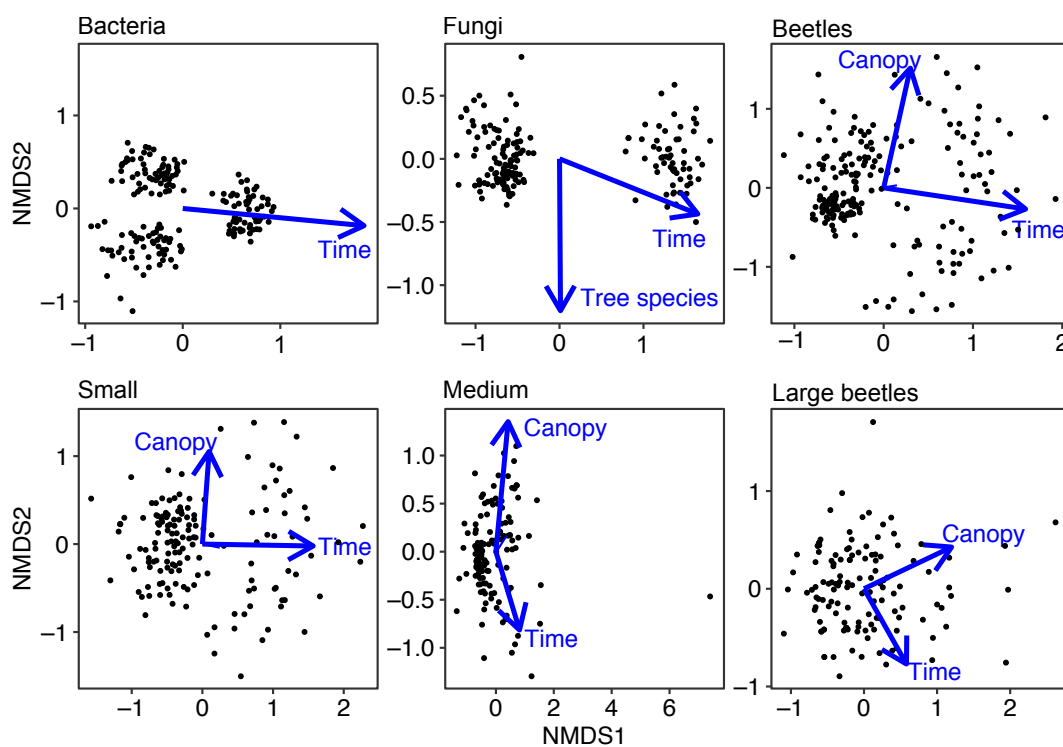
Figure 5.7: Ordination of bacteria, fungi and beetle community composition based on non-metric multi-dimensional scaling (NMDS). Beetle community composition is further presented for small, medium and large beetles, separated according to their mean body size. The effects of canopy openness, tree species and time since tree death were fitted to the ordination using 9999 permutations. Canopy openness and tree species are binaries, with 0 indicating shady canopies and European beech, and 1 indicates sunny canopies and Silver fir. Only significant vectors are displayed as arrows. The length of arrows indicates strength of R^2. For the full statistics table see Table 5.1.

6 rMyCoPortal - an R package to interface with the Mycology Collections Portal

Abstract

The understanding of the biodiversity and biogeographical distribution of fungi is still limited. The small number of online databases and the large effort required to access existing data have prevented their use in research articles. The Mycology Collections Portal was established in 2012 to help alleviate these issues and currently serves data online for over 4.3 million fungal records. However, the current process for accessing the data through the web interface is manual, therefore slow, and precludes the extensive use of the existing datasets. Here we introduce the software package rMyCoPortal, which allows users rapid, automated access to the data. rMyCoPortal makes data readily available for further computations and analyses in the open source statistical programming environment R. We will demonstrate the core functions of the package, and how rMyCoPortal can be employed to obtain fungal data that can be used to address basic research questions. rMyCoPortal is a free and open-source R package, available via GitHub.

6.1 Introduction

Global climate and land-use change are major threats to life on earth, and studies continue to document how animal and plant distributions and phenology have changed due to these factors [Parmesan, 2006]. Although many studies exist that report range and phenological shifts in plant and animals, less is known about inter- and intra-annual shifts of fungal fruiting and occurrence. Large-scale fungal phenology patterns have only recently been addressed [Boddy et al., 2014]. In the last decade, several long-time observational data in Europe were used to study the effects of climate change on fungal fruiting phenology [Andrew et al., 2018, Büntgen et al., 2015, 2012, 2013, Gange et al., 2007, Kauserud et al., 2008, 2010]. The majority of studies were based on herbarium, museum and citizen science fruit body observations of mushroom-forming fungi (reviewed in

[Boddy et al., 2014]). Several studies at different spatial scales found shifts of the average fruiting date later in the year and the fruiting season has expanded in both directions [Boddy et al., 2014, Andrew et al., 2018, Büntgen et al., 2012, 2013, Kauserud et al., 2008, 2012]. However, such phenological shifts have been mainly studied in European and emerging species distribution models (SDM) based on future climate projections have yet to be studied. Open-source data provide an important resource for studying fungal biodiversity [Andrew et al., 2017]. The Mycology Collections data Portal [Miller and Bates, 2017] has made great efforts to compile fungal specimen metadata that document distributions of fungi, with 42% of the records therein being georeferenced (Table 6.1) [Miller and Bates, 2017]. MyCoPortal is built on the open-source Symbiota platform [Gries et al., 2014], and currently serves over 4.3 million unique fungal records, these being primarily specimen-based [Miller and Bates, 2017]. Although the MyCoPortal has been widely used and highly cited (>30 citations since 2015), data from this portal, however, is not readily accessible and requires users to download the data manually through a web interface. This procedure is very time consuming, especially when working with complex queries and building large datasets. After download, the data then needs to be further processed before basic exploration can be undertaken.

Here we wish to highlight three important data analysis techniques that are facilitated by rMyCoPortal:

1. Visualization of fungal species ranges

2. Creation of heatmaps of fungal biodiversity throughout the world, and

3. Modelling of habitat suitability

To this end, the first author has developed software that allows rapid and automated access to a large global database of fungal distribution records, eliminating the need to use the existing web interface. rMyCoPortal is written as a package for the popular R open-source statistical software [R Core Team, 2015] to make data contained in MyCoPortal accessible in the R programming environment. In this publication we introduce the core functionality of the R package and briefly demonstrate the potential uses of the data to address the data analysis techniques mentioned above.

Table 6.1: Collection statistics retrieved in November 2018 via http://mycoportal.org/portal/collections/misc/collstats.php.

Collection Statistic	Number
Occurrence records	4,369,313
Georeferenced	1,843,633 (42%)
Imaged	1,913,838 (44%)
Identified to species	3,302,781 (76%)
Families	1,693
Genera	8,314
Species	113,811
Total taxa (including subsp. and var.)	120,275

6.2 Installation

The package can be downloaded and installed using the R package 'devtools' [Wickham et al., 2018], using the following code:

```
## Install R package rMyCoPortal
install.packages("devtools")
devtools::install.github("FranzKrah/rMyCoPortal")
library("rMyCoPortal")
# Now you will also need to install Docker.
```

The download and usage of the package does not require a GitHub account. An account is, however, required if the user would like to actively contribute to functions of the package or launch an issue.

6.3 Usage

6.3.1 Core package function

Here, we present the core functions of the rMyCoPortal package. rMyCoPortal makes use of several R packages that allow interaction with web data content, including 'RSelenium' [Harrison, 2018], 'XML' [Lang and the CRAN Team, 2018], and 'httr' [Wickham, 2017]; but also plotting packages such as 'ggplot2' [Wickham, 2016]. rMyCoPortal further relies on Docker (https://docs.docker.com), which performs virtualization, also known as 'containerization'. Lastly, rMyCoPortal also provides the class 'records', especially

introduced to provide user-friendly interaction with the downstream data analysis (e.g., plotting).

6.3.2 Querying the database

At the core of rMyCoPortal is the function mycoportal. Using mycoportal, queries can be made to find all records of a known fungal species. Further, all input specifications (i.e., query modifiers) that are present on the website can be adjusted within said function. Some important modifiers are the inclusion of synonyms or the geographic area. The user may also input a higher taxon, e.g., genus or family. The records are then stored in an S4 class object which can be directly subjected to a variety of plotting functions. The functions plot_distmap and plot_datamap can be used to visualize species distributions and heatmaps of species diversity, respectively (Figure 6.1). The downloaded data records can then further be used for subsequent statistical analysis, for example climate suitability modelling (Figure 6.1, R code in vignette of the R package), changes in phenology or to create species lists for a given locality.

```r
## Download data for Amanita muscaria
am.rec <- mycoportal(taxon = "Amanita_muscaria")

## Plot species distribution
plot_distmap(x = am.rec , mapdatabase = "state", interactive = FALSE)

## Plot records heatmap for states of USA
plot_datamap(x = am.rec , mapdatabase = "state", index = "rec")
```

The download and usage of the package does not require a GitHub account. An account is, however, required if the user would like to actively contribute to functions of the package or launch an issue.

6.3.3 Species distribution modeling

The above code demonstrates the core functionality of the rMyCoPortal package for querying fungal records and also for basic data exploration. Using the mycoportal function, we queried the database for all observations for the mushroom-forming fungus *Amanita muscaria* (fly agaric) and modeled the current and future projected habitat suitability (Figure 6.1) using the 'biomod2' R package [Thuiller et al., 2016]. Detailed code to create the species distribution models (SDMs) is provided in the vignettes in the R package.
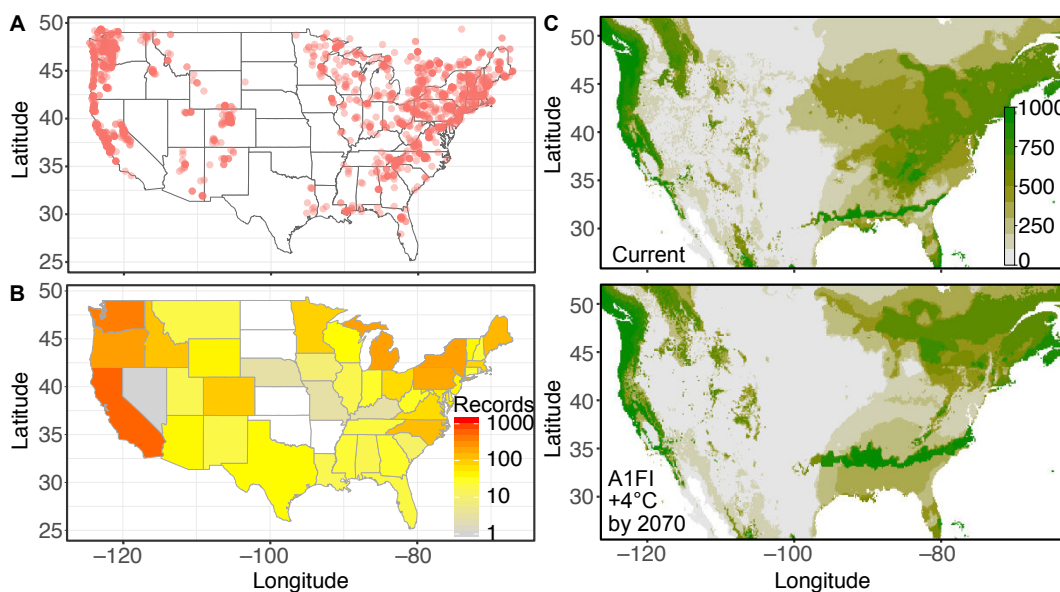
Figure 6.1: Three data analysis techniques enabled by the 'rMyCoPortal' R package. A) A map made with georeferenced records available from MyCoPortal showing the species distribution of *Amanita muscaria* throughout the lower 48 contiguous states (using function plot_distmap). B) A heatmap showing the number of records of *Amanita muscaria* for the lower 48 contiguous states (using function plot_datamap). This function can also be used to plot the number of species if higher taxa are queried. C) The lower two plots show the projected habitat suitability given the current climate, and the projected habitat suitability based on future climate, as predicted by the global climate change model CCSM4 and the A1F1 scenario which predicts an increase of 4°C at the end of the century (R code provided in the vignette in the R package).

6.3.4 Data limitations

The data contained in the MyCoPortal database is an important resource to address ecological research questions, however there are some limitations to be considered. First, the majority of the data within the database is localized within North America. Second, currently only 42% of the records are georeferenced with longitude/latitude values (Table 6.1), which limits their application. However, most observations are georeferenced to the county level, which allows further localization e.g., via U.S. Gazetteer files. Third, the meta-data for each specimen is limited and only provides basic information such as the collector and collection date or the location. For example, the host plant species is often not available (30% has host data) within the meta-data, however, these data could often be accessed and extended via the herbarium labels, which can be loaded into R via the function details.

6.4 Conclusion

In this paper, we have shown how the R package 'rMyCoPortal' can be utilized to access the Mycology Collections data Portal. This package allows for easy and rapid access to MyCoPortal fungal data, speeding up a process that would otherwise be tedious and slow. Connecting the MyCoPortal database to the R statistical interface opens a wide range of research possibilities, where queried data can be efficiently processed and used to address scientific questions. Further, the 'rMyCoPortal' package has the potential to be modified to access other data portals, such as those for vascular plants (http://swbiodiversity.org/seinet/) or arthropods (http://symbiota4.acis.ufl.edu/scan/portal/), which are also built on the Symbiota platform. We hope this R package inspires scientists to conduct studies related to how fungal biodiversity and biogeography responds to global climate change.

7 General discussion

This thesis followed two basic approaches to understand assembly processes of saprotrophic fungi. A first approach focused on the evolution of an assembly relevant trait (host specificity) and how a morphological trait affects the prevalence of species along an environmental gradient. A basic understanding of the evolution of traits can yield a mechanistic link to the selective forces that have shaped the trait distribution across the tree of life and ultimately why species differ with respect to a given trait [Webb et al., 2002]. Further, how traits change along environmental gradients can yield a basic understanding of the mechanistic link between traits and the habitat that selects for species [Cadotte and Tucker, 2017]. Understanding the trait evolution and responses of traits to environmental variables can yield a first basic understanding of the relevant drivers of community ecology. Although the integration of phylogenetic- and trait-information into community ecology can yield first insights into assembly processes, many environmental quantities are correlated, restricting a detailed mechanistic understanding [Graham, 2003, Müller and Bütler, 2010]. A second approach, thus used a dead-wood experiment to disentangle the relative and independent effects of various important drivers of fungal community assembly. Both approaches can yield complementary information of saprotrophic fungal assembly processes. The importance of the host tree identity for saprotrophic wood-inhabiting fungal diversity became apparent within both approaches. In detail, this was demonstrated by vast differences in host specialization between fungal functional groups as well as overwhelmingly large effects of the host tree species on fungal community composition. Further, this thesis is the first to find that saprotroph assemblages are affected by the morphology of their reproductive organ (mushroom) on continental scales. Species with dark-colored mushrooms are more prevalent in cold environments than light-colored species. This thesis thus demonstrated that the theory of thermal melanism [Trullas et al., 2007] can be expanded to multicellular fungi and thus towards a large group of ectotherm organisms [Cordero et al., 2018, Pinkert and Zeuss, 2018]. Finally, integrating the dead-wood experiment, phylogenetic- and trait-information as well as prevalence of three wood-inhabiting organism groups, this thesis could show that assembly processes differ between macro- and microorganisms. From a

fungal perspective, the host tree identity acts as a strong filter on the assembly of communities, whereas the climate has relatively smaller effects. However, climate, especially temperature, likely affects fungal assembly via the color of mushrooms. Further, demographic properties of fungi – small spores and large mycelium – may further determine the relative role of ecological drift for their assembly. The results of the chapters 2 to 5 will be discussed in more detail in the following sections.
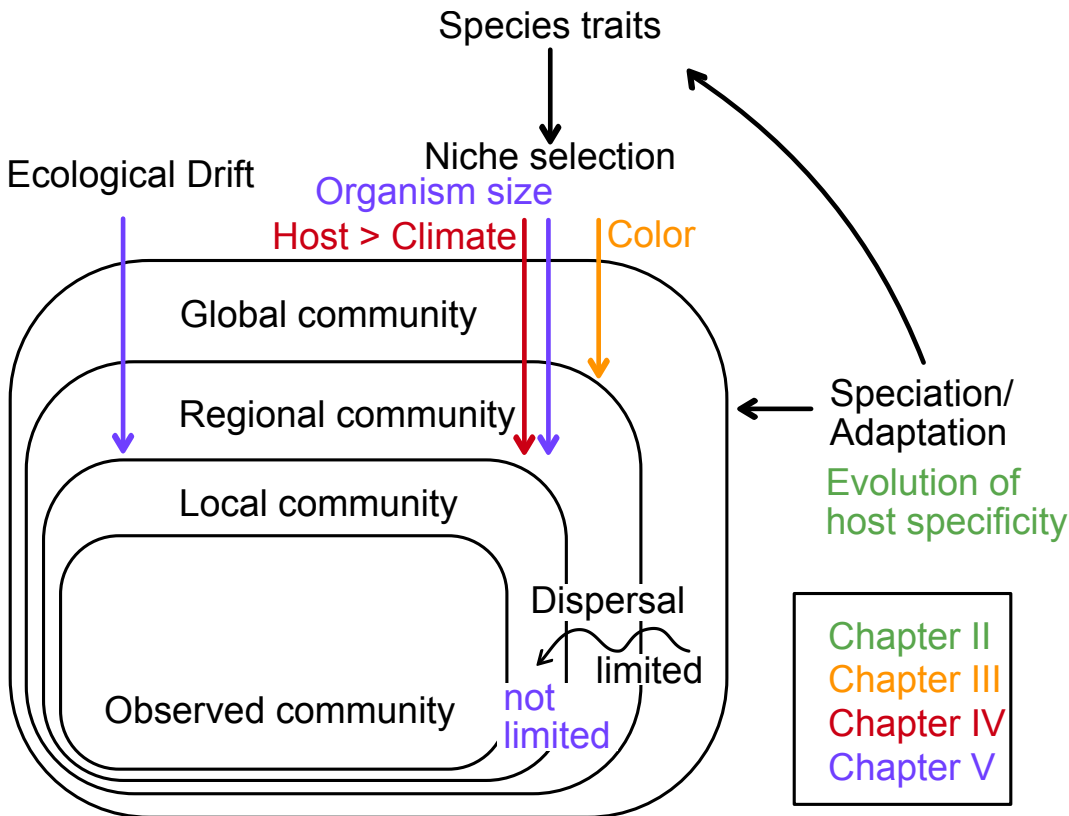
Figure 7.1: Overview of the results within the conceptual model overview from Figure 1.1. The colors denote the chapters and at which level the chapters contribute to a deeper understanding of assembly processes.

Chapter 2 showed that two functional groups (white and brown rot) of wood-decay fungi differ considerably in their host specialization. Whereas white rot fungi are primarily angiosperm specialists, brown rot fungi are primarily generalists and conifer specialists. Radiations of the angiosperm clade were followed by radiations of most clades of wood-decaying fungal species. However, white rot fungi display a higher species diversity compared to brown rot fungi, suggesting that white rot fungi had advantages exploiting angiosperm substrates. A recent study explored possible molecular mechanisms of

substrate specificity. A recent study grew *Fomitopsis pinicola*, a brown rot fungus, on various substrates and found differentially expressed wood-degrading genes (DEGs) as well as differentially expressed RNA-editing genes [Wu et al., 2018]. Both could provide an understanding of how species degrade different substrates (generalism). One explanation might be that wood-decay fungi can change their decay apparatus relative to the substrate [Wu et al., 2018]. More studies with a broad set of fungal species and substrate combinations are, however, needed to show that differential gene expression and RNA editing can explain the host specificity observed among wood-inhabiting fungi. Further, it is currently unclear how the fungus can recognize the substrate. It will be interesting to see whether generalists vs. specialists as well as white rot vs. brown rot fungi differ in the number of DEGs. Based on the results of Chapter 2 one would expect to find a low level of DEGs in white rot specialists and a high level of DEGs in brown rot generalists. Besides a deeper mechanistic understanding of the molecular basis of substrate specificity, further macroevolutionary studies could increase our understanding of how host specificity affects fungal assembly. Chapter 2 of this thesis focused on a rough classification of specificity, namely angio- and gymnosperm specialism between two functional groups. A more fine-grained analysis of the evolutionary history of fungi and their hosts, together with a consideration of the paleoclimate would increase our understanding of the evolution of wood-decay fungi. For example, whether radiations of wood-decay fungal clades coincided with host expansions vs. shifts in the paleoclimate.

Chapter 3 showed, for the first time, significant effects of a morphological trait of mushrooms on the prevalence of species along an environmental gradient on continental scale. Interestingly, color has so far gained little to no attention in mushroom-forming fungi [Sherratt et al., 2005, Cuthill et al., 2017]. Previous studies found that ectothermic animals and yeasts with dark-colored bodies are more frequently found in cold environments than those with light-colored bodies [Kalmus, 1941, Bogert, 1949, Willmer and Unwin, 1981, Kingsolver, 1995, Trullas et al., 2007, Cordero et al., 2018]. In particular, Chapter 3 found that the average assemblage-based lightness of saprotrophs increased with increasing temperature, thus that assemblages in cold climates show a prevalence of saprotrophic species with dark-colored mushrooms. These results suggest the theory of thermal melanism (TTM) for multicellular mushroom-forming fungi and thus expand the TTM from animals and unicellular fungi [Cordero et al., 2018] to multicellular fungi. These findings further strongly suggest adaptation of mushrooms towards the thermal environment. However, to confirm the theory of thermal melanism for mushroom-forming fungi, further experiments are needed to show a fitness benefit of dark-colored species

under cold environments. Such a fitness advantage is most likely linked to a reproductive quantity such as the number of spores produced or the maximum mushroom size [Aguilar-Trigueros et al., 2015]. I suggest a series of experiments to expose fungi with dark and light mushroom color under cold conditions and apply artificial solar radiation to finally quantify and compare growth rates and spores produced. Besides saprotrophic fungi, Chapter 3 also tested the TTM for mutualistic ectomycorrhizal fungi (ECMs). ECMs color lightness showed only weak responses towards the latitudinal and seasonal temperature gradient. This suggests that the TTM is lifestyle-dependent. Free-living saprotrophs and mutualistic ectomycorrhizal fungi thus differed in their responses of the color trait with temperature. The following discussion must remain speculative, however, may provide hypotheses to be tested. Mutualism theory predicts that both partners of the relationship are at a fitness advantage [Connnor, 1995, Leigh Jr, 2010]. Such a fitness benefit for mutualistic ECMs might be an advantage in the trade-off between mycelial growth (to reach new resources) and pigmentation of mushrooms (to increase reproductive success). ECM fungi might need to invest less carbon into additional vegetative mycelium because of a carbon supply by their host plant [Högberg et al., 2010] and thus may invest more into pigment expression. In other words, I propose that ectomycorrhizal individuals were favored by natural selection that increased pigment expression rather than mycelial growth. Saprotrophs, on the other hand, depend on the decomposition of dead organic matter (e.g., dead wood) [Worrall et al., 1997, Floudas et al., 2012]. Thus, an extended mycelium is needed to reach new or exploit current resources, which might be more important than securing reproductive success. In other words, I propose that natural selection favored individuals with extended mycelial growth rather than pigmentation, and thus reproductive success. Such a trade-off could be studied by growing saprotrophs on standardized substrates and first of all testing, whether a higher substrate amount yields more mycelium or more mushroom biomass.

Chapter 4 showed that the host was more important in structuring the diversity of wood-inhabiting fungi than the environment. In detail, the host tree species affected the species richness and community composition more than the other variables. This suggests niche selection of fungi adapted to the contrasting substrate of angio- and gymnosperm wood. Both differ in numerous properties [Cornwell et al., 2009, Kahl et al., 2017], and many wood-decaying fungi were shown to preferentially grow on either of the two major plant lineages [Gilbertson, 1980, Hibbett and Donoghue, 2001, Hoppe et al., 2015] (Chapter 2). However, we still have a limited understanding of the host specificity and the underlying mechanism that regulate host specificity (see also discussion

for Chapter 2). However, Chapter 2 and 4 showed that functional groups differ in host specificity, which may explain some of the observed differences in community composition between angiosperm and gymnosperm hosts found in Chapter 4. Chapter 4 found that the community composition differed strongly between the angiosperm and gymnosperm tree species (Figure 4.8). Further, the variation in the community composition was lower on angiosperms than on gymnosperms (Figure 4.8). This may be explained by the divergence in host specificity of white and brown rot fungi found in Chapter 2. The community composition on angiosperm trees might be more similar to each other than the community composition on conifer trees, because more species are specialized towards angiosperms whereas most species occurring on conifers are generalists (Chapter 2). A preponderance of white rot angiosperm specialists would then lead to an observed specific niche selection on beech and thus more similar communities. Whereas a preponderance of brown rot generalists would then lead to an observed unspecific establishment and niche selection on fir and thus more random and dissimilar communities. A potential weakness of the dead-wood experiment, however, is the low number of host tree species (two), which prevents from generalizing the results to a general host filter hypothesis. Nonetheless, the two tree species used were of two highly diverged lineages, angio- and gymnosperm tree species. Thus, the host identity treatment created a strong binary gradient. Further, a previous study showed that a preponderance of species grow on either of the two substrates [Hibbett and Donoghue, 2001] (Chapter 2). Another dead-wood experiment, however, without climate standardization, used 11 tree species and consistently found a high effect by host identity compared with other variables [Baber et al., 2016, Purahong et al., 2018]. Besides the host tree identity, we also found significant effects of the stand microclimate and further a significant interaction of host identity and microclimate. This result suggests that host specialization might not be seen independent from climatic adaptations. In general host specificity may be driven by (i) capabilities of the fungus to degrade the hosts woody compounds (ii) shared geographical range and thus climatic requirements of the fungus and the host; (iii) and similar dispersal abilities between host and fungus (at least over evolutionary timescales). Climate affects the occurrence of the host and the fungus and thus fungal diversity on dead-wood is affected directly as well as indirectly by climate. Especially strong climatic shifts may lead to rapid contractions or expansions of tree species distributions and thus affect fungal evolution [Thuiller et al., 2005, 2011]. Such effects have been found for leaf-mining flies [Winkler et al., 2009], however, similar studies are lacking for wood-inhabiting fungi. A research focus on the interaction between fungus-host-climate both on evolutionary as well as ecological scales may further elucidate underlying mechanisms

of fungal community assembly.

Chapter 5 used phylogenetic and trait information together with a recently developed null model framework to disentangle different assembly processes [Stegen et al., 2012]. The null model is based on the conceptual synthesis [Vellend, 2010] and was used to test for the relative influence of niche selection and ecological drift on fungal assembly. Fungal community turnover was explained mainly by ecological drift, then dispersal limitation and homogenizing dispersal, then niche selection. Thus, niche selection surprisingly had the smallest influence on fungal assembly, which was in contrast to the expectation that the host would act as a strong filter structuring fungal communities. A high degree of drift suggests the influence of demographic properties, e.g. random birth/deaths in local communities [Hubbell, 2001]. To further understand this result, the analysis was expanded to include bacteria and beetles. Bacteria, fungi and beetles differ in organism size, which is one of the most basic properties of organisms [Blackburn et al., 1990, White et al., 2007]. Size is an integral trait with important implications for demographic properties and dispersal capabilities [Farjalla et al., 2012]. Thus, it was hypothesized that organism size predicts the influence of niche selection vs. ecological drift on local scale. An assumption of the study was, that on local scale all three taxa are not dispersal limited, which is supported by previous studies [Nilssen, 1984, Forsse and Solbreck, 1985, Komonen and Müller, 2018] and results of Chapter 5. The main result of Chapter 5 was that organism size predicts the selection to drift ratio, suggesting different assembly processes among wood-inhabiting macro- and microorgansisms. The study showed an increasing selection to drift ratio with decreasing organism size, both across bacteria, fungi and beetles and with beetles of decreasing average body size (measured trait). The results supported the 'size-demography hypothesis', that assembly processes on local scales could be explained by differences in their community sizes. Larger organisms tend to have smaller community sizes [Savage et al., 2004, White et al., 2007], which were shown to be more prone to ecological drift [Orrock and Watling, 2010]. Niche selection influences community assembly but it is probably partly overwhelmed by ecological drift stemming from small community sizes, within which local random extinctions are more effective in structuring local communities. Although niche selection via host specificity influences fungal communities on dead wood (Chapter 2 and 4), small local community sizes may introduce substantial ecological drift (Chapter 5). These findings raise the questions: why does the community composition (Chapter 4) display such strong differences between the host trees if drift has such a high relative influence compared to niche selection (Chapter 5)? This might first of all be a methodological artefact of

one or both of the methods. Community composition might overestimate dissimilarity, whereas the null model approach might underestimate the influence of niche selection. Niche selection within the null model framework is defined as significant difference of the beta mean nearest taxon distance (βMNTD) from a random expectation. Thus, pairwise community comparisons which are more or less phylogenetically similar than expect by chance are considered significant and thus interpreted as niche selection. The underlying assumption is that more closely related species share more similar traits and thus react more similar to environmental gradients [Stegen et al., 2012]. However, if a trait under consideration, e.g., host specificity displays convergence of a trait (e.g., brown rot decay mode) this assumption partly is invalidated (Chapter 2). In a case of repeated evolution of a trait, very phylogenetically distant species can share very similar traits. In the case of fungi, we know that brown rot fungi evolved repeatedly at least 5-7 times (Chapter 2) and that more than one brown rot clade is consisting mainly of generalists (Chapter 2). This could lead to an underestimation of niche selection if it is interpreted based on the mean nearest taxon distance. The absence of a consideration of phylogenetic relatedness, as in measures of community composition, such as community dissimilarity, could lead to an overestimation of dissimilarity. Communities which consist of two species, which are exclusively only found in one of the communities, would result in a high degree of observed dissimilarity. However, if the two species are closely related, e.g., sister species and habitats are equal, then the two species may not coexist because of competitive exclusion or similarity [MacArthur and Levins, 1967], and not because of differential abiotic habitat filtering. In other words, the two communities would be more similar than expected from the occurrence alone. Thus, measures of community composition might overestimate dissimilarity of communities. It might thus be problematic to use quantities of community composition without phylogenetic information, however, also quantities which consider phylogenetic relatedness may bias interpretations. Further studies are needed to test the methods for such interpretation biases.

Finally, understanding biodiversity – both the pattern of their occurrence and processes underlying these patterns - is critical to gain a mechanistic understanding of assembly processes. Such knowledge will increase our ability to implement evidence-based management and conservation strategies to protect species and ecosystems and to predict future responses to e.g., habitat loss and climate change. Both, habitat loss and climate change, are major threads to fungal species occurrence and abundance [Heilmann-Clausen et al., 2015]. Dead-wood reduction due to modern forest management is causing habitat loss for wood-inhabiting fungi. Global climate change affects host tree species distributions [Iverson and Prasad, 1998, Parmesan, 2006, Fei et al., 2017, Chen

et al., 2011] and thus will likely affect availability of resources for wood-inhabiting fungi. However, most studies addressing biodiversity focus on the description of pattern (e.g., species richness and community composition) rather than on mechanistic explanations. In a meta-analysis, it was found that the majority of studies addressing climate change did not provide any mechanistic explanation for the observed pattern [Urban et al., 2016] and similar numbers could be expected from community ecology as a whole. Although many survey-based studies accumulated, so far fungi and particular wood-inhabiting fungi have been rarely studied within experiments [Heilmann-Clausen et al., 2015, Seibold et al., 2015a] or evolutionary studies, although they are the main agents of wood decomposition and thus play important roles in global carbon and nutrient cycling [Stokland et al., 2012]. Thus, here I want to demonstrate how results based on a mechanistic understanding of the community assembly of species can be used to predict the effect of climate change on fungal diversity. A key aspect of climate change is an increasing average temperature [IPCC, 2014]. Increasing average temperature will have direct as well as indirect effects on the diversity of wood-inhabiting fungi. Direct effects of climate change will mainly affect the community composition (Chapter 4) and assembly processes via morphological traits such as color lightness, which is linked to the thermal environment (Chapter 3). Climate change will further affect host availability [Thuiller et al., 2005, Parmesan, 2006] and thus indirectly fungal diversity, given the stronger experimental effects of host vs. environment (Chapter 4) and especially the strongly host specialized white rot fungi (Chapter 2). Climate change is predicted to further change precipitation regimes which will, together with climate warming, increase drought occurrences [Allen et al., 2010, IPCC, 2014]. Variation in water content within dead-wood may further affect demographic properties (abundance, stochastic birth/death processes) and thus affect stochastic processes. Chapter 5 revealed significant influence of drift on local assembly processes. Reduced local abundances, for example, may reduce the effect of drift, leading to an increase of niche selection or changed dispersal limitation. It is important to emphasize that studies purely based on diversity pattern recently found inconsistent effects of e.g., dead-wood resource (host) vs. climate [Bässler et al., 2010, Bässler et al., 2016b]. In summary, climate may affect fungi indirectly via change in host tree availability or directly via changed (micro-) climatic conditions (Chapter 4), e.g., via thermal adaptations such as color (Chapter 3). This effect might be especially critical for highly specialized white rot fungi (Chapter 2).

Based on two fundamental approaches to study potential mechanisms of fungal assembly, this thesis could increase our understanding of how evolutionary constraints together with species traits structures fungal assemblages. Fungal adaptations towards

the host tree species as well as morphological traits and life-history traits influence the assembly of saprotrophic fungal communities. Further, besides niche selection, demographic differences due to community sizes may play an important role in structuring fungal assemblages by regulating the influence of stochasticity.

8 Future directions

In general, future directions should address the question whether the climate or the host are more important for fungal evolution and community ecology. To reach this goal, to further advance the understanding of assembly processes and to further expand the findings of this thesis, research effort should be directed into 1) broadening data-acquisition methods and 2) utilizing newly developed data-analysis methods. Within the general research field of fungal community ecology, involving e.g., host specificity, currently only few studies are utilizing high-throughput sequencing approaches. Although meta-barcoding has recently gained some attention within fungal ecology studies [Hibbett et al., 2009], other 'OMICS' (transcript-, gen-, proteomics) approaches have rarely been used and 'METAOMICS' (metatranscript-, metagenomics) are especially rare [Yadav et al., 2016]. Here I will thus propose an experimental approach involving transcriptome analysis to study responses of mushrooms to environmental stress on a molecular level to complement existing approaches addressing the molecular underpinnings of substrate specificity [Wu et al., 2018]. Further, comparative genomics could be used to study the genomic basis for the observed color diversity even within single genera. Besides exploiting novel sequencing methods to study fungal adaptations and genome evolution, novel data-analysis methods should be used to (re)analyze existing and newly generated data. Currently many analytical approaches within fungal community ecology are based on descriptive statistics [Ovaskainen et al., 2017] or null models [Ulrich and Gotelli, 2010]. Null models iteratively produce stochastic expectations of ecological patterns by randomly permutation of the data by excluding certain processes (e.g., species interactions) of interest [Gotelli, 2000]. However, null models display several statistical challenges, e.g., the strength of randomization has direct effects on the type-I error rate [Zhou and Ning, 2017]. Thus, there is a need to build parametric models where such uncertainties can be estimated with the parameters of interest. Here I will propose the use of such a novel framework to study assembly processes based on the described local-scale dead-wood experiment (general understanding of assembly processes) and continental-scale European fungal dataset (prediction of effects of future host distributions and climate change).

Effects of host, climate and drift on fungal assembly processes

Fungal community assembly is driven by the abiotic environment and the host (Chapter 2, 4), neutral processes (Chapter 5) as well as niche selection through e.g., morphological traits (Chapter 3). Another important factor is competition (competitive exclusion, limiting similarity), which becomes more influential on local spatial scales [Barberán et al., 2014, Leibold and Chase, 2017]. Finally species share evolutionary history, and thus species are not statistically independent [Felsenstein, 1985] but also that more closely related species are more likely to show similar traits and functional responses ('niche conservatism', [Losos, 2008]). To better understand the interplay of abiotic and biotic filtering, niche conservatism and traits as well as neutral processes on local assembly processes, I propose to use hierarchical modelling of species communities (HMSC). This method has only recently been developed with the advantage of being a parametric model framework. The currently used null model framework used in Chapter 5 [Stegen et al., 2012] allows to infer similar quantities, however, a parametric modelling framework comes with advantages over null model approaches. The advantages are listed in Box 1 within [Ovaskainen et al., 2017], however, one important feature is model validation and prediction. This framework thus allows to predict inferred relations into future climate scenarios, which allows to more directly present predicted future effects with confidence estimation given the data and model. A null model approach does not allow parametric predictions and thus remains entirely speculative about future developments. Figure 2.5 presents a conceptual framework, how the dead-wood experiment can be used to build a HMSC model. The central research objective could be whether the host or environment filter more on fruit body traits or whether assembly processes are neutral regarding trait distributions. Given the effects of the climate on community composition within Article I and the high influence of drift found within Chapter 2 it can be expected to find a combination of niche selection by climate which affects morphological trait composition (e.g., fruit body size or color) alongside high influence of neutral processes.

This approach allows to disentangle various assembly processes in a model framework, given the data is derived from an experimental setup. As highlighted above, this model allows to make predictions given future climate scenarios. Environmental change, however, does not act unidirectional on fungal assemblages only, but also on trophic-interactions fungi are involved in. Climate-induced range- as well as phenological shifts have been reported for plant and fungal species [Parmesan and Yohe, 2003, Thomas et al., 2004, Lenoir et al., 2008, Harsch et al., 2009, Chen et al., 2011, Gottfried et al., 2012, Kauserud et al., 2012, Boddy et al., 2014]. Thus, on large-scale spatial scales as
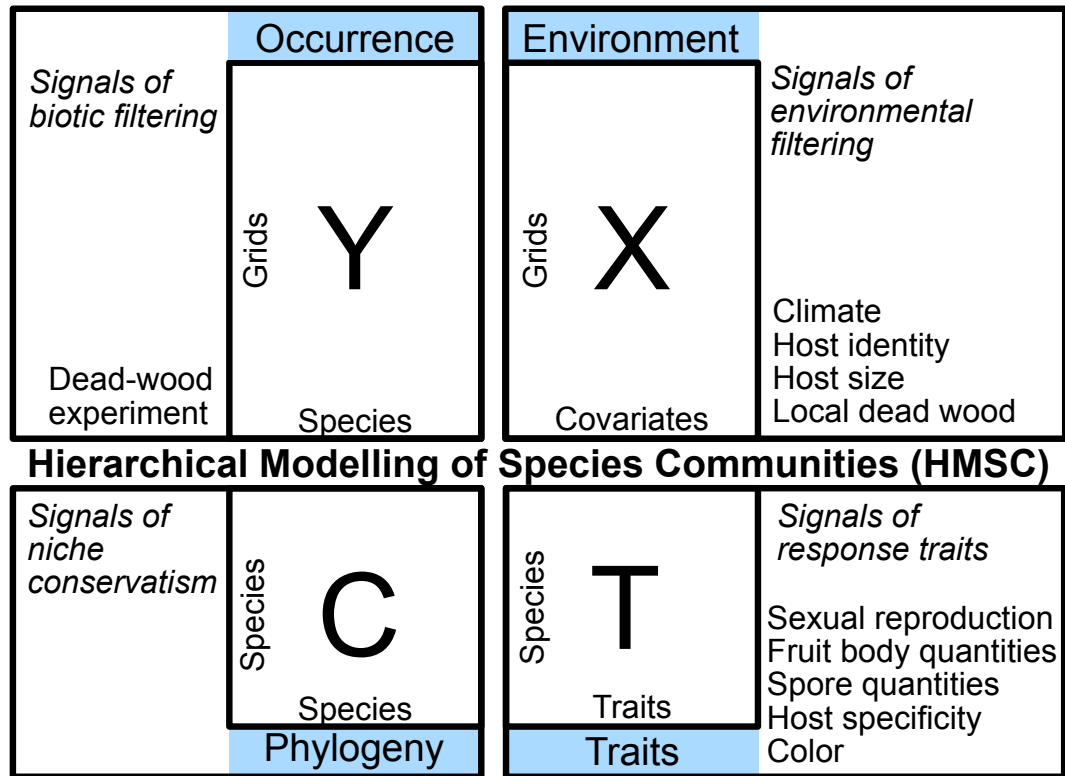
Figure 8.1: Conceptual framework to test for signals of environmental filtering (niche selection) vs. random processes on wood-inhabiting assembly. Graphical representation adapted from [Ovaskainen et al., 2017].

well as temporal (seasonal) scales it can be expected that climate affects both plant host as well as fungal occurrence/ abundance simultaneously. The above proposed model framework allows predictions and thus I propose to use HMSC modeling on large-spatial scales to test whether the host (diversity) is more important for fungal diversity than the macroclimate (controlling for other environmental effects). Such a model can once be fit for fungi and once for host tree species across Europe. Then future host distributions can be modelled given future climate scenarios, which can then be used as input alongside future climate into the fungal model for further predictions. Such a framework is displayed in Figure 8.2. As data basis one could use the fungal species distributions and phylogeny from Article 4 together with host data derived from GBIF [Gbif, 2017].

Beyond tree species identity (host), the climate had significant effects on the community composition of mushroom-forming fungi (Chapter 4). To gain a more mechanistic understanding of how climate affect fungi, I propose to perform experimental treatment of mushrooms to test for their responses to environmental stress. It is cur-

rently unknown whether mushrooms are able to react to environmental stress, e.g., to secure spore production even under harsh conditions. Therefore, a first approach could be laboratory experiments where cultured mushrooms (e.g., *Lentinula eodes*) are exposed to heat, drought and frost stress and subsequent transcriptome analysis to test for differences in gene expression levels between treatments and controls. Using such experimental approaches, it could be tested whether mushrooms react to environmental stress independently from a mycelial response and if yes, what are specific responses on a molecular level, e.g., upregulation of heat-shock or metabolism-related proteins [Liu et al., 2017]. A previous study demonstrated 577 differentially expressed genes only in the mature fruit body of *Lentinula eodes* [Song et al., 2018], suggesting a potential for mushroom-exclusive responses to environmental stress.
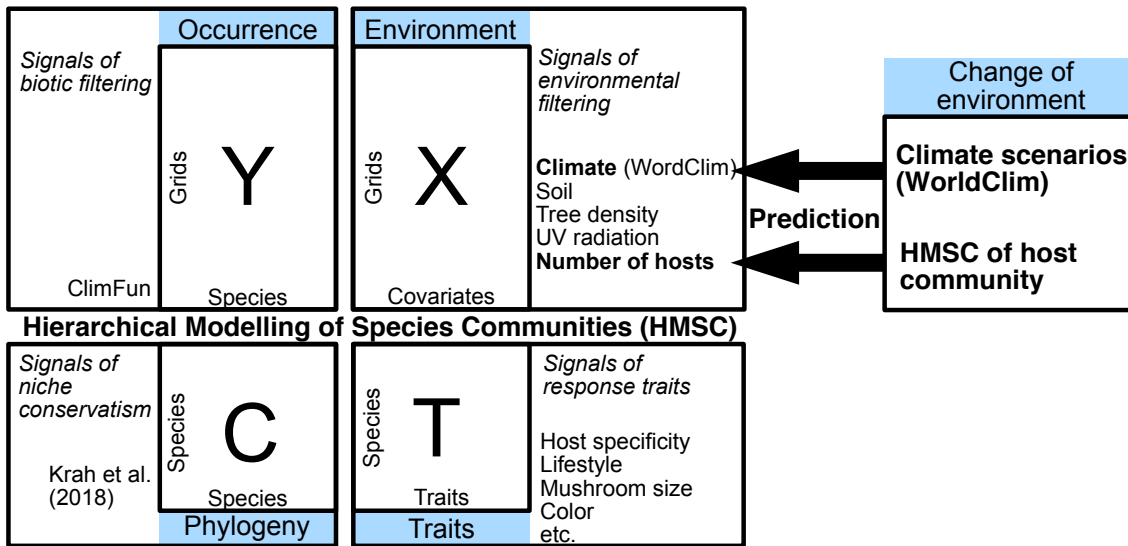
Figure 8.2: Conceptual framework to test for signals of environmental filtering (niche selection) vs. random processes on wood-inhabiting assembly and their effects under future climate szenarios.

Effects of morphological traits on fungal assembly processes

Fitness advantage of dark-colored mushrooms in cold environments

A key finding of this thesis was a significant effect of temperature and seasonality on color lightness of saprotroph mushrooms assemblies (Chapter 4). Saprotroph assemblages are darker in cold environments and seasons of the year. This result suggests the theory of thermal melanism (TTM) for mushrooms. As a recent study pointed out, for full

support of the TTM three conditions must be met, demonstrating that color variation: (1) displays a geographic pattern with the thermal environment (2) affects the temperature of the organism and (3) increases fitness [Cordero et al., 2018]. Chapter 3 could sufficiently demonstrate support for (1) and (2), however, additional experiments are needed to demonstrate condition (3). Such experiments should define basic parameters of mushroom fitness [Pringle and Taylor, 2002] (e.g., total biomass, number of viable spores, fruiting duration) and compare dark- vs. light-colored individuals in cold environments. The expectation is that dark-colored mushrooms are at a fitness advantage in cold environments.

Genomic basis of mushroom color diversity

Mushroom-forming fungi display tremendous color diversity within their reproductive organs known as mushrooms (Chapter 3). However, we are only beginning do understand the ecological and evolutionary causes of this color diversity. Interestingly even genera display a high amount of color variability, e.g., within the genus *Amanita*. One explanation might be that color in mushroom is under rapid adaptive selection by the environment (e.g. macroclimate). Thus, further ecological and evolutionary studies will help to further understand the underlying causes of color in mushrooms. Here I propose to study the genetic underpinnings of the high color diversity at the genomic level, that is finding the genes under strong selection, and the evolutionary mechanisms by which genetic diversity may be generated (gene duplication, deletions/insertions, changes in gene network). One potential approach is to draw on published genomes of *Amanita* and to sequence additional *Amanita* genomes to generate genomes of the full color palette. *Amanita* is a well-studied genus and important to the nutrition of many forest tree species (ectomycorrhizal species). The phylogenetic relationships are well known [Wolfe et al., 2012] and recently, the first genomes in this genus have become available [Kohler et al., 2015].

Fungal pigments share many chemical structures with pigments found in plants and animals, e.g., melanin, betalains, quinones and carotenoids. Thus, assembled genomes and transcriptomes from other *Amanita* species could be used to annotate genome assemblies. Once the genes within the assemblies have been identified one could proceed to identify homologs to pigment-related genes in plants and animals and perform comparative genomic analysis. The main hypothesis would be that gene duplications led to an increased mutation rate of pigment related genes, which then led to an increased diversity in the color phenotype.

Bibliography

Andre J Aberer, Kassian Kobert, and Alexandros Stamatakis. ExaBayes: Massively Parallel Bayesian Tree Inference for the Whole-Genome Era. *Molecular Biology and Evolution*, 31(10):2553–2556, 2014.

Nerea Abrego, Anna Norberg, and Otso Ovaskainen. Measuring and predicting the influence of traits on the assembly processes of wood-inhabiting fungi. *Journal of Ecology*, 105(4):1070–1081, 2017.

Nerea Abrego, Veera Norros, Panu Halme, Panu Somervuo, Heini Ali-Kovero, and Otso Ovaskainen. Give me a sample of air and I will tell which species are found from your region–molecular identification of fungi from airborne spore samples. *Molecular ecology resources*, 18(3):381–728, 2018.

Carlos A Aguilar-Trigueros, Stefan Hempel, Jeff R Powell, Ian C Anderson, Janis Antonovics, Joana Bergmann, Timothy R Cavagnaro, Baodong Chen, Miranda M Hart, John Klironomos, , Jana S Petermann, Erik Verbruggen, Stavros D Veresoglou, and Matthias C Rillig. Branching out: towards a trait-based understanding of fungal ecology. *Fungal Biology Reviews*, 29(1):34–41, 2015.

Hirotugu Akaike. A new look at the statistical model identification. *IEEE Transactionson Automatic Control*, 19(6):716–723, 1974.

Josu G Alday, Juan Martínez De Aragón, Sergio de Miguel, and José Antonio Bonet. Mushroom biomass and diversity are driven by different spatio-temporal scales along mediterranean elevation gradients. *Scientific reports*, 7:45824, 2017.

Craig D Allen, Alison K Macalady, Haroun Chenchouni, Dominique Bachelet, Nate Mc-Dowell, Michel Vennetier, Thomas Kitzberger, Andreas Rigling, David D Breshears, E H (Ted) Hogg, Patrick Gonzalez, Rod Fensham, Zhen Zhang, Jorge Castro, Natalia Demidova, Jong Hwan Lim, Gillian Allard, Steven W Running, Akkin Semerci, and Neil Cobb. A global overview of drought and heat-induced tree mortality reveals emerging climate change risks for forests. *Forest Ecology and Management*, 259(2): 660–684, 2010.

Bibliography

Marti J Anderson. A new method for non-parametric multivariate analysis of variance. *Austral Ecology*, 26(1):32–46, 2001.

Carrie Andrew, Einar Heegaard, Paul M Kirk, Claus Bässler, Jacob Heilmann-Clausen, Irmgard Krisai-Greilhuber, Thomas W Kuyper, Beatrice Senn-Irlet, Ulf Büntgen, Jeffrey Diez, Simon Egli, Alan C Gange, Rune Halvorsen, Klaus Høiland, Jenni Nordén, Frederik Rustø en, Lynne Boddy, and Håvard Kauserud. Big data integration: Pan-european fungal species observations' assembly for addressing contemporary questions in ecology and global change biology. *Fungal Biology Reviews*, 31(2):88–98, 2017.

Carrie Andrew, Einar Heegaard, Klaus Høiland, Beatrice Senn-Irlet, Thomas W. Kuyper, Irmgard Krisai-Greilhuber, Paul M. Kirk, Jacob Heilmann-Clausen, Alan C. Gange, Simon Egli, Claus Bässler, Ulf Büntgen, Lynne Boddy, and Håvard Kauserud. Explaining European fungal fruiting phenology with climate variability. *Ecology*, 99 (6):1306–1315, 2018.

Maria Anisimova, Manuel Gil, Jean-François Dufayard, Christophe Dessimoz, and Olivier Gascuel. Survey of branch support methods demonstrates accuracy, power, and robustness of fast likelihood-based approximation schemes. *Systematic biology*, 60 (5):685–699, 2011.

Colin Averill, Benjamin L. Turner, and Adrien C. Finzi. Mycorrhiza-mediated competition between plants and decomposers drives soil carbon storage. *Nature*, 505(7484): 543–545, 2014.

Kristin Baber, Peter Otto, Tiemo Kahl, Martin M. Gossner, Christian Wirth, Andreas Gminder, and Claus Bässler. Disentangling the effects of forest-stand type and deadwood origin of the early successional stage on the diversity of wood-inhabiting fungi. *Forest Ecology and Management*, 177:161 – 169, 2016.

Petr Baldrian, Petra Zrůstová, Vojtěch Tláskal, Anna Davidová, Věra Merhautová, and Tomáš Vrška. Fungi associated with decomposing deadwood in a natural beech-dominated forest. *Fungal Ecology*, 23:109–122, 2016.

Albert Barberán, Emilio O Casamayor, and Noah Fierer. The microbial contribution to macroecology. *Frontiers in microbiology*, 5:203, 2014.

José María Barrasa, Fernando Esteve-Raventós, and Rose Marie Dähncke. Clitocybula canariensis (tricholomataceae), a new brown-rot fungus from the canary islands (spain). *Fungal diversity*, 22:1–11, 2006.

Claus Bässler, Jörg Müller, Frank Dziock, and Roland Brandl. Effects of resource availability and climate on the diversity of wood-decaying fungi. *Journal of Ecology*, 98 (4):822–832, 2010.

Claus Bässler, Jutta Stadler, Jörg Müller, Bernhard Förster, Axel Göttlein, and Roland Brandl. LiDAR as a rapid tool to predict forest habitat types in Natura 2000 networks. *Biodiversity and Conservation*, 20(3):465–481, December 2010.

Claus Bässler, Raffael Ernst, Marc Cadotte, Christoph Heibl, and Jörg Müller. Near-to-nature logging influences fungal community assembly processes in a temperate forest. *Journal of Applied Ecology*, 51(4):939–948, 2014a.

Claus Bässler, Jacob Heilmann-Clausen, Peter Karasch, Roland Brandl, and Hans Halbwachs. Ectomycorrhizal fungi have larger fruit bodies than saprotrophic fungi. *Fungal Ecology*, 17:205–212, 2014b.

Claus Bässler, Hans Halbwachs, Peter Karasch, Heinrich Holzer, Andreas Gminder, Lothar Krieglsteiner, Ramiro Silveyra Gonzalez, Jörg Müller, and Roland Brandl. Mean reproductive traits of fungal assemblages are correlated with resource availability. *Ecology and evolution*, 6(2):582–592, 2016a.

Claus Bässler, Jörg Müller, Marc W Cadotte, Christoph Heibl, Johannes H Bradtka, Simon Thorn, and Hans Halbwachs. Functional response of lignicolous fungal guilds to bark beetle deforestation. *Ecological Indicators*, 65:149–160, 2016b.

Douglas Bates, Martin Maechler, Ben Bolker, and Steve Walker. Fitting Linear Mixed-Effects Models using lme4. *Journal of Statistical Software*, 67(1):1–48, 2015.

Jeremy M Beaulieu and Michael J Donoghue. Fruit evolution and diversification in campanulid angiosperms. *Evolution*, 67(11):3132–3144, 2013.

Jeremy M Beaulieu, Jeffrey C Oliver, and Brian O'Meara. Package 'corhmm'. 2014.

Jan Beck, Liliana Ballesteros-Mejia, Carsten M Buchmann, Jürgen Dengler, Susanne A Fritz, Bernd Gruber, Christian Hof, Florian Jansen, Sonja Knapp, Holger Kreft, Anne-Kathrin Schneider, Marten Winter, and Carsten F Dormann. What's on the horizon for macroecology? *Ecography*, 35(8):673–683, 2012.

Emily Beech, Malin C Rivers, Sara Oldfield, and PP Smith. GlobalTreeSearch: The first complete global database of tree species and country distributions. *Journal of Sustainable Forestry*, 36(5):454–489, 2017.

Bibliography

Beatrix E Beisner, Pedro R Peres-Neto, Eva S Lindström, Allain Barnett, and Maria Lorena Longhi. The role of environmental and spatial processes in structuring lake communities from bacteria to fish. *Ecology*, 87(12):2985–2991, 2006.

Dennis A. Benson, Mark Cavanaugh, Karen Clark, Ilene Karsch-Mizrachi, David J. Lipman, James Ostell, and Eric W. Sayers. Genbank. *Nucleic acids research*, 2012.

Zachary T Bergeron and Rebecca C Fuller. Using Human Vision to Detect Variation in Avian Coloration: How Bad Is It? *The American Naturalist*, 191(2):269–276, 2018.

Carl Bergmann. *Ueber die Verhältnisse der Wärmeökonomie der Thiere zu ihrer Grösse*. Vandenhoeck und Ruprecht, 1847.

Manfred Binder, David S. Hibbett, Karl-Henrik Larsson, Ellen Larsson, Ewald Langer, and Gitta Langer. The phylogenetic distribution of resupinate forms across the major clades of mushroom-forming fungi (homobasidiomycetes). *Systematics and Biodiversity*, 3(02):113–157, 2005.

Manfred Binder, Alfredo Justo, Robert Riley, Asaf Salamov, Francesc Lopez-Giraldez, Elisabet Sjökvist, Alex Copeland, Brian Foster, Hui Sun, Ellen Larsson, Karl Henrik Larsson, Jeffrey P Townsend, Igor V Grigoriev, and David S Hibbett. Phylogenetic and phylogenomic overview of the polyporales. *Mycologia*, 105(6):1350–1373, 2013.

Tom R Bishop, Mark P Robertson, Heloise Gibb, Berndt J van Rensburg, Brigitte Braschler, Steven L Chown, Stefan H Foord, Thinandavha C Munyai, Iona Okey, Pfarelo G Tshivhandekano, Victoria Werenkraut, and Catherine L Parr. Ant assemblages have darker and larger members in cold environments. *Global Ecology and Biogeography*, 25(12):1489–1499, 2016.

Tim M Blackburn, Paul H Harvey, and Mark D Pagel. Species number, population density and body size relationships in natural communities. *Journal of Animal Ecology*, 59(1):335–345, 1990.

Robert A Blanchette. Delignification by wood-decay fungi. *Annual review of phytopathology*, 29(1):381–403, 1991.

Lynne Boddy. Fungal community ecology and wood decomposition processes in angiosperms: from standing tree to complete decay of coarse woody debris. *Ecological Bulletins*, pages 43–56, 2001.

176

Lynne Boddy and Jacob Heilmann-Clausen. Chapter 12 Basidiomycete community development in temperate angiosperm wood. *British Mycological Society Symposia Series*, 28(C):211–237, 2008.

Lynne Boddy, Juliet Frankland, and Pieter Van West. *Ecology of saprotrophic basidiomycetes*, volume 28. Academic Press, 2007.

Lynne Boddy, Ulf Büntgen, Simon Egli, Alan C Gange, Einar Heegaard, Paul M Kirk, Aqilah Mohammad, and Håvard Kauserud. Climate variation effects on fungal fruiting. *Fungal Ecology*, 10:20–33, 2014.

Charles M Bogert. Thermoregulation in reptiles, a factor in evolution. *Evolution*, 3(3): 195–211, 1949.

Mark A Bradford, Robert J Warren, Petr Baldrian, Thomas W Crowther, Daniel S Maynard, Emily E Oldfield, William R Wieder, Stephen A Wood, and Joshua R King. Climate fails to predict wood decomposition at regional scales. *Nature Climate Change*, 4(7):625–630, 2014.

Martin Brändle and Roland Brandl. Is the composition of phytophagous insects and parasitic fungi among trees predictable? *Oikos*, 113(2):296–304, 2006.

Johan Bring. How to standardize regression coefficients. *The American Statistician*, 48 (3):209–213, 1994.

James KM Brown and Mogens S Hovmøller. Aerial dispersal of pathogens on the global and continental scales and its impact on plant disease. *Science*, 297(5581):537–541, 2002.

Gösta Brunow. Methods to reveal the structure of lignin. *Biopolymers Online: Biology* Chemistry* Biotechnology* Applications*, 1, 2005.

Timothy DH Bugg, Mark Ahmad, Elizabeth M Hardiman, and Rahman Rahmanpour. Pathways for degradation of lignin in bacteria and fungi. *Natural product reports*, 28 (12):1883–1896, 2011.

Ulf Büntgen, Håvard Kauserud, and Simon Egli. Linking climate variability to mushroom productivity and phenology. *Frontiers in Ecology and the Environment*, 10(1):14–19, 2012.

Bibliography

Ulf Büntgen, Martina Peter, Håvard Kauserud, and Simon Egli. Unraveling environmental drivers of a recent increase in swiss fungi fruiting. *Global change biology*, 19 (9):2785–2794, 2013.

Ulf Büntgen, Simon Egli, J Diego Galván, Jeffrey M Diez, Jorge Aldea, Joaquin Latorre, and Fernando Martínez-Peña. Drought-induced changes in the phenology, productivity and diversity of spanish fungi. *Fungal Ecology*, 16:6–18, 2015.

Harold H Burdsall, Meredith Blackwell, and Karen K Nakasone. Robert lee gilbertson, 1925–2011. *Mycologia*, 104(6):1521–1524, 2012.

Kenneth P Burnham and David R Anderson. *Model Selection and Multimodel Inference: A Practical Information-Theoretic Approach*, volume 172. 2002.

Sarah E Bush, Jason D Weckstein, Daniel R Gustafsson, Julie Allen, Emily DiBlasi, Scott M Shreve, Rachel Boldt, Heather R Skeen, and Kevin P Johnson. Unlocking the black box of feather louse diversity: A molecular phylogeny of the hyper-diverse genus brueelia. *Molecular phylogenetics and evolution*, 94:737–751, 2016.

Marc W Cadotte and Caroline M Tucker. Should environmental filtering be abandoned? *Trends in ecology & evolution*, 32(6):429–437, 2017.

Sara Calhim, Panu Halme, Jens H Petersen, Thomas Læssøe, Claus Bässler, and Jacob Heilmann-Clausen. Fungal spore diversity reflects substrate-specific deposition challenges. *Scientific reports*, 8(1):5356, 2018.

Tim Caro. Wallace on coloration: Contemporary perspective and unresolved insights. *Trends in Ecology & Evolution*, 32(1):23–30, 2017.

Jonathan M Chase. Stochastic community assembly causes higher biodiversity in more productive environments. *Science*, 328(5984):1388–1391, 2010.

I-Ching Chen, Jane K Hill, Ralf Ohlemüller, David B Roy, and Chris D Thomas. Rapid range shifts of species associated with high levels of climate warming. *Science*, 333 (6045):1024–1026, 2011.

Olga Chernomor, Arndt von Haeseler, and Bui Quang Minh. Terrace aware data structure for phylogenomic inference from supermatrices. *Systematic biology*, 65(6):997–1008, 2016.

Chun-Huo Chiu and Anne Chao. Estimating and comparing microbial diversity in the presence of sequencing errors. *PeerJ*, 4:e1634, 2016.

Frederic Edward Clements. *Plant succession: an analysis of the development of vegetation.* Number 242. Carnegie Institution of Washington, 1916.

Karina E Clemmensen, Adam Bahr, Otso Ovaskainen, Anders Dahlberg, Alf Ekblad, Håkan Wallander, Jan Stenlid, Roger D Finlay, David A Wardle, and Björn D Lindahl. Roots and associated fungi drive long-term carbon sequestration in boreal forest. *Science*, 340(6127):1615–1618, 2013.

Bernard D Coleman. On random placement and species-area relations. *Mathematical Biosciences*, 54(3-4):191–215, 1981.

Richard C Connnor. The Benefits of Mutualism: A Conceptual Framework. *Biological Reviews*, 70(3):427–457, 1995.

Radames J B Cordero, Vincent Robert, Gianluigi Cardinali, Ebuka S Arinze, Susanna M Thon, and Arturo Casadevall. Impact of Yeast Pigmentation on Heat Capture and Latitudinal Distribution. *Current Biology*, 28(16):2657–2664.e3, 2018.

Radames JB Cordero and Arturo Casadevall. Functions of fungal melanin beyond virulence. *Fungal Biology Reviews*, 31(2):99–112, 2017.

William K Cornwell, Johannes HC Cornelissen, Steven D Allison, Juergen Bauhus, Paul Eggleton, Caroline M Preston, Fiona Scarff, James T Weedon, Christian Wirth, and Amy E Zanne. Plant traits and wood fates across the globe: rotted, burned, or consumed? *Global Change Biology*, 15(10):2431–2449, 2009.

Pedro W Crous, Walter Gams, Joost A Stalpers, Vincent Robert, and Gerrit Stegehuis. Mycobank : an online initiative to launch mycology into the 21st century. *Studies in Mycology*, 50(1):19–22, 2004.

Innes C Cuthill, William L Allen, Kevin Arbuckle, Barbara Caspers, George Chaplin, Mark E Hauber, Geoffrey E Hill, Nina G Jablonski, Chris D Jiggins, Almut Kelber, Johanna Mappes, Justin Marshall, Richard Merrill, Daniel Osorio, Richard Prum, Nicholas W Roberts, Alexandre Roulin, Hannah M Rowland, Thomas N Sherratt, John Skelhorn, Michael P Speed, Martin Stevens, Mary Caswell Stoddard, Devi Stuart-Fox, Laszlo Talas, Elizabeth Tibbetts, and Tim Caro. The biology of color. *Science*, 357(6350):eaan0221, 2017.

Charles R Darwin. *On the origin of species by means of natural selection, or the preservation of favoured races in the struggle for life.* Murray, London, 1859.

Bibliography

Tom De Bie, Luc De Meester, Luc Brendonck, Koenraad Martens, Boudewijn Goddeeris, Dirk Erkeen, Henrietta Hampel, Luc Denys, Leo Vanhecke, Katkeen van der Gucht, Wim Vyerman, and Steven Declerk. Body size and dispersal mode as key traits determining metacommunity structure of aquatic organisms. *Ecology letters*, 15(7): 740–747, 2012.

Wietse De Boer, Larissa B. Folman, Richard C. Summerbell, and Lynne Boddy. Living in a fungal world: Impact of fungi on soil bacterial niche development. *FEMS Microbiology Reviews*, 29:795–811, 2005.

Ian A Dickie, Tadashi Fukami, J Paula Wilkie, Robert B Allen, and Peter K Buchanan. Do assembly history effects attenuate from species to ecosystem properties? A field test with wood-inhabiting fungi. *Ecology Letters*, 15(2):133–141, 2012.

Alexei J Drummond and Remco R Bouckaert. Bayesian evolutionary analysis with BEAST 2. *Bayesian Evolutionary Analysis with BEAST*, (Mcmc):249, 2015.

Alexei J Drummond, Marc A Suchard, Dong Xie, and Andrew Rambaut. Bayesian phylogenetics with BEAUti and the BEAST 1.7. *Molecular Biology and Evolution*, 29 (8):1969–1973, 2012.

Mattias Edman, Nicholas Kruys, and Bengt Gunnar Jonsson. Local dispersal sources strongly affect colonization patterns of wood-decaying fungi on spruce logs. *Ecological Applications*, 14(3):893–901, 2004.

David A Elston, Robert Moss, Thierry Boulinier, Claire Arrowsmith, and Xavier Lambin. Analysis of aggregation, a worked example: Numbers of ticks on red grouse chicks. *Parasitology*, 122(5):563–569, 2001.

Lenore Fahrig. Rethinking patch size and isolation effects: the habitat amount hypothesis. *Journal of Biogeography*, 40(9):1649–1663, 2013.

Vinicius F Farjalla, Diane S Srivastava, Nicholas AC Marino, Fernanda D Azevedo, Viviane Dib, Paloma M Lopes, Alexandre S Rosado, Reinaldo L Bozelli, and Francisco A Esteves. Ecological determinism increases with organism size. *Ecology*, 93(7): 1752–1759, 2012.

David F Farr, Amy Y Rossman, Marry E Palm, and E.B. McCray. Fungal databases, systematic mycology and microbiology laboratory, ars, usda. retrieved february 2017, 2017.

Songlin Fei, Johanna M Desprez, Kevin M Potter, Insu Jo, Jonathan A Knott, and Christopher M Oswalt. Divergence of species responses to climate change. *Science advances*, 3(5):e1603055, 2017.

Joseph Felsenstein. Phylogenies and the comparative method. *American Naturalist*, 125 (1):1–15, 1985.

Astrid Ferrer and Gregory S Gilbert. Effect of tree host species on fungal community composition in a tropical rain forest in panama. *Diversity and Distributions*, 9(6): 455–468, 2003.

Christopher B Field, F Stuart Chapin III, Pamela A Matson, and Harold A Mooney. Responses of terrestrial ecosystems to the changing atmosphere: a resource-based approach. *Annual Review of Ecology and Systematics*, 23(1):201–235, 1992.

Richard G FitzJohn, Matthew W Pennell, Amy E Zanne, Peter F Stevens, David C Tank, and William K Cornwell. How much of the world is woody? *Journal of Ecology*, 102 (5):1266–1272, 2014.

D Floudas, M Binder, R Riley, K Barry, R A Blanchette, Bernard Henrissat, A T Martinez, Robert Otillar, Joseph W Spatafora, Jagjit S Yadav, A Aerts, I Benoit, A Boyd, A Carlson, A Copeland, Pedro M Coutinho, R P de Vries, Patricia Ferreira, Keisha Findley, Brian Foster, J Gaskell, D Glotzer, P Gorecki, J Heitman, C Hesse, C Hori, K Igarashi, J A Jurgens, N Kallen, P Kersten, A Kohler, U Kues, T K A Kumar, A Kuo, K LaButti, L F Larrondo, E Lindquist, A Ling, V Lombard, S Lucas, T Lundell, R Martin, D J McLaughlin, I Morgenstern, E Morin, C Murat, L G Nagy, M Nolan, R A Ohm, A Patyshakuliyeva, A Rokas, F J Ruiz-Duenas, G Sabat, A Salamov, M Samejima, J Schmutz, J C Slot, F St John, J Stenlid, H Sun, S Sun, K Syed, A Tsang, A Wiebenga, D Young, A Pisabarro, D C Eastwood, F Martin, D Cullen, I V Grigoriev, and D S Hibbett. The Paleozoic Origin of Enzymatic Lignin Decomposition Reconstructed from 31 Fungal Genomes. *Science*, 336(6089):1715–1719, 2012.

E. Forsse and CH Solbreck. Migration in the bark beetle Ips typographus L.: duration, timing and height of flight. *Zeitschrift für Angewandte Entomologie*, 100(1-5):47–57, 1985.

Mark D Fricker, Dan Bebber, and Lynne Boddy. Mycelial networks: structure and dynamics. In *British Mycological Society Symposia Series*, volume 28, pages 3–18. Elsevier, 2008.

Bibliography

Susanne A Fritz and Andy Purvis. Selectivity in mammalian extinction risk and threat types: a new measure of phylogenetic signal strength in binary traits. *Conservation Biology*, 24(4):1042–1051, 2010.

Tadashi Fukami, Ian A Dickie, J Paula Wilkie, Barbara C Paulus, Duckchul Park, Andrea Roberts, Peter K Buchanan, and Robert B Allen. Assembly history dictates ecosystem functioning: evidence from wood decomposer communities. *Ecology Letters*, 13(6):675–684, 2010.

Tera E Galante, Thomas R Horton, and Dennis P Swaney. 95% of basidiospores fall within 1 m of the cap: a field-and modeling-based study. *Mycologia*, 103(6):1175–1183, 2011.

AC Gange, EG Gange, TH Sparks, and L Boddy. Rapid and recent changes in fungal fruiting patterns. *Science*, 316(5821):71–71, 2007.

Alan C Gange, Einar Heegaard, Lynne Boddy, Carrie Andrew, Paul M Kirk, Rune Halvorsen, Thomas W W. Kuyper, Claus Bässler, Jeffrey Diez, Jacob Heilman-Clausen, Klaus Høiland, Ulf Büntgen, and Hå vard Kauserud. Trait-dependent distributional shifts in fruiting of common British fungi. *Ecography*, 41(1):51–61, 2018.

G F Gause. The struggle for existence. 1934. *Williams and Wilkins, Baltimore, MD*, 1964.

Gbif. Global Biodiversity Information Facility (GBIF). *Natural History*, 2017.

Roy Genders. *Mushroom growing for everyone.* Faber and Faber., 1982.

Benjamin Gilbert and Martin J Lechowicz. Neutrality, niches, and dispersal in a temperate forest understory. *Proceedings of the National Academy of Sciences*, 101(20): 7651–7656, 2004.

Robert L Gilbertson. Wood-rotting fungi of north america. *Mycologia*, pages 1–49, 1980.

Robert L Gilbertson, KJ Martin, and J Page Lindsey. Annotated check list and host index for arizona wood-rotting fungi. *Journal of the Arizona-Nevada Academy of Science*, 1974.

M Gill and W Steglich. Pigments of fungi (macromycetes). In *Fortschritte der Chemie organischer Naturstoffe/Progress in the Chemistry of Organic Natural Products*, pages 1–297. Springer, 1987.

Sydney I Glassman, Claudia Weihe, Junhui Li, Michaeline BN Albright, Caitlin I Looby, Adam C Martiny, Kathleen K Treseder, Steven D Allison, and Jennifer BH Martiny. Decomposition responses to climate depend on microbial community composition. *Proceedings of the National Academy of Sciences*, 115(47):11994–11999, 2018.

Henry Allan Gleason. On the relation between species and area. *Ecology*, 3(2):158–162, 1922.

Nicholas J Gotelli. Null model analysis of species co-occurrence patterns. *Ecology*, 81 (9):2606–2621, 2000.

Nicholas J Gotelli and Robert K Colwell. Estimating species richness. In *Biological Diversity. Frontiers in Measurement and Assessment*, volume 12, pages 39–54. Oxford University Press Oxford, 2011.

Michael Gottfried, Harald Pauli, Andreas Futschik, Maia Akhalkatsi, Peter Barančok, José Luis Benito Alonso, Gheorghe Coldea, Jan Dick, Brigitta Erschbamer, María Rosa Fernández Calzado, George Kazakis, Ján Krajči, Per Larsson, Martin Mallaun, Ottar Michelsen, Dmitry Moiseev, Pavel Moiseev, Ulf Molau, Abderrahmane Merzouki, Laszlo Nagy, George Nakhutsrishvili, Bård Pedersen, Giovanni Pelino, Mihai Puscas, Graziano Rossi, Angela Stanisci, Jean Paul Theurillat, Marcello Tomaselli, Luis Villar, Pascal Vittoz, Ioannis Vogiatzakis, and Georg Grabherr. Continent-wide response of mountain vegetation to climate change. *Nature Climate Change*, 2(2): 111–115, 2012.

Alan Grafen. The phylogenetic regression. *Philosophical Transactions of the Royal Society of London. Series B, Biological Sciences*, 326(1233):119–157, 1989.

Michael H Graham. Confronting multicollinearity in ecological multiple regression. *Ecology*, 84(11):2809–2815, 2003.

Samuel A Graham. Temperature as a limiting factor in the life of subcortical insects. *Journal of economic entomology*, 17(3):377–383, 1924.

Dominique Gravel, Charles D Canham, Marilou Beaudet, and Christian Messier. Reconciling niche and neutrality: the continuum hypothesis. *Ecology letters*, 9(4):399–409, 2006.

Corinna Gries, Edward E. Gilbert, and Nico M. Franz. Symbiota–a virtual platform for creating voucher-based biodiversity information communities. *Biodiversity Data Journal*, (2), 2014.

Bibliography

Simon J Grove. Saproxylic insect ecology and the sustainable management of forests. *Annual review of ecology and systematics*, pages 1–23, 2002.

Richard M Gunton, Chiara Polce, and William E Kunin. Predicting ground temperatures across european landscapes. *Methods in Ecology and Evolution*, 6(5):532–542, 2015.

Hans Halbwachs, Roland Brandl, and Claus Bässler. Spore wall traits of ectomycorrhizal and saprotrophic agarics may mirror their distinct lifestyles. *Fungal Ecology*, 17:197–204, 2015.

Hans Halbwachs, Josef Simmel, and Claus Bässler. Tales and mysteries of fungal fruiting: How morphological and physiological traits affect a pileate lifestyle. *Fungal Biology Reviews*, 30(2):36–61, 2016.

Nils Hallenberg and Nicolas Kuffer. Long-distance spore dispersal in wood-inhabiting basidiomycetes. *Nordic journal of botany*, 21(4):431–436, 2001.

John Laker Harley. Fungi in ecosystems. *Journal of Applied Ecology*, pages 627–642, 1971.

Frank E Harrell Jr and Many others. Hmisc: Harrell Miscellaneous, 2017.

John Harrison. *RSelenium: R Bindings for 'Selenium WebDriver'*, 2018. R package version 1.7.4.

Melanie A Harsch, Philip E Hulme, Matt S McGlone, and Richard P Duncan. Are treelines advancing? a global meta-analysis of treeline response to climate warming. *Ecology letters*, 12(10):1040–1049, 2009.

Stephan Hättenschwiler, Sylvain Coq, Sandra Barantal, and Ira Tanya Handa. Leaf traits and decomposition in tropical rainforests: revisiting some commonly held views and towards a new hypothesis. *The New Phytologist*, 189(4):950–65, 2011.

David L Hawksworth and Robert Luecking. Fungal diversity revisited: 2.2 to 3.8 million species. *Microbiology spectrum*, 5(4), 2017.

M R. Haylock, Nynke Hofstra, AMG Klein Tank, E J Klok, Peter G D Jones, and Mark New. A European daily high-resolution gridded data set of surface temperature and precipitation for 1950-2006. *Journal of Geophysical Research Atmospheres*, 113(20), 2008.

Christoph Heibl. The megapera package: Large phylogenetic dataset assembly in r. Modern Phylogenetic Comparative Methods and their application in evolutionary biology. Seville, Spain, 11-15.11.2014.

Christoph Heibl. Package 'megaptera'. 2014.

Lea Heidrich, Nicolas Friess, Konrad Fiedler, Martin Brändle, Axel Hausmann, Roland Brandl, and Dirk Zeuss. The dark side of lepidoptera: Colour lightness of geometrid moths decreases with increasing latitude. *Global Ecology and Biogeography*, 27(4): 407–416, 2017.

Jacob Heilmann-Clausen and Morten Christensen. Does size matter?: On the importance of various dead wood fractions for fungal diversity in danish beech forests. *Forest Ecology and Management*, 201(1):105–117, 2004.

Jacob Heilmann-Clausen and Morten Christensen. Wood-inhabiting macrofungi in danish beech-forests–conflicting diversity patterns and their implications in a conservation perspective. *Biological Conservation*, 122(4):633–642, 2005.

Jacob Heilmann-Clausen and Jan Vesterholt. Conservation: selection criteria and approaches. In *British Mycological Society Symposia Series*, volume 28, pages 325–347. Elsevier, 2008.

Jacob Heilmann-Clausen, Elizabeth S Barron, Lynne Boddy, Anders Dahlberg, Gareth W Griffith, Jenni Nordén, Otso Ovaskainen, Claudia Perini, Beatrice Senn-Irlet, and Panu Halme. A fungal perspective on conservation biology. *Conservation Biology*, 29(1):61–68, 2015.

Jacob Heilmann-Clausen, Pietro K Maruyama, Hans Henrik Bruun, Dimitar Dimitrov, Thomas Læssøe, Tobias Guldberg Frøslev, and Bo Dalsgaard. Citizen science data reveal ecological, historical and evolutionary factors shaping interactions between woody hosts and wood-inhabiting fungi. *New Phytologist*, 212(4):1072–1082, 2016.

Martin Heimann and Markus Reichstein. Terrestrial ecosystem carbon dynamics and climate feedbacks. *Nature*, 451(7176):289–292, 2008.

David S Hibbett and Michael J Donoghue. Analysis of character correlations among wood decay mechanisms, mating systems, and substrate ranges in homobasidiomycetes. *Systematic biology*, 50(2):215–242, 2001.

Bibliography

David S Hibbett, David Grimaldi, and Michael J Donoghue. Fossil mushrooms from miocene and cretaceous ambers and the evolution of homobasidiomycetes. *American Journal of Botany*, 84(7):981–981, 1997.

David S Hibbett, Manfred Binder, Joseph F Bischoff, Meredith Blackwell, Paul F Cannon, Ove E Eriksson, Sabine Huhndorf, Timothy James, Paul M Kirk, Robert Lücking, H Thorsten Lumbsch, François Lutzoni, P Brandon Matheny, David J McLaughlin, Martha J Powell, Scott Redhead, Conrad L Schoch, Joseph W Spatafora, Joost a Stalpers, Rytas Vilgalys, M Catherine Aime, André Aptroot, Robert Bauer, Dominik Begerow, Gerald L Benny, Lisa a Castlebury, Pedro W Crous, Yu-Cheng Dai, Walter Gams, David M Geiser, Gareth W Griffith, Cécile Gueidan, David L Hawksworth, Geir Hestmark, Kentaro Hosaka, Richard a Humber, Kevin D Hyde, Joseph E Ironside, Urmas Kõljalg, Cletus P Kurtzman, Karl-Henrik Larsson, Robert Lichtwardt, Joyce Longcore, Jolanta Miadlikowska, Andrew Miller, Jean-Marc Moncalvo, Sharon Mozley-Standridge, Franz Oberwinkler, Erast Parmasto, Valérie Reeb, Jack D Rogers, Claude Roux, Leif Ryvarden, José Paulo Sampaio, Arthur Schüssler, Junta Sugiyama, R Greg Thorn, Leif Tibell, Wendy a Untereiner, Christopher Walker, Zheng Wang, Alex Weir, Michael Weiss, Merlin M White, Katarina Winka, Yi-Jian Yao, and Ning Zhang. A higher-level phylogenetic classification of the Fungi. *Mycological research*, 111(Pt 5):509–47, May 2007.

David S Hibbett, Anders Ohman, and Paul M Kirk. Fungal ecology catches fire. *New Phytologist*, 184:282–284, 2009.

David S Hibbett, Robert Bauer, Manfred Binder, Admir J. Giachini, Kentaro Hosaka, Alfredo Justo, Ellen Larsson, Karl-Henrik Larsson, James D. Lawrey, Otto Mietinnen, László G Nagy, R Henrik Nilsson, Michael Weiss, and R Greg Thorn. Agaricomycetes. In Karl Esser, editor, *The Mycota: A Comprehensive Treatise on Fungi as Experimental Systems for Basic and Applied Research*, chapter 14, pages 373–429. Springer, 2014.

Takayoshi Higuchi. Look back over the studies of lignin biochemistry. *Journal of Wood Science*, 52(1):2–8, 2006.

Robert J Hijmans, Susan E Cameron, Juan L Parra, Peter G Jones, and Andy Jarvis. Very high resolution interpolated climate surfaces for global land areas. *International Journal of Climatology*, 25(15):1965–1978, 2005.

Cody E Hinchliff, Stephen A Smith, James F Allman, J Gordon Burleigh, Ruchi Chaudhary, Lyndon M Coghill, Keith A Crandall, Jiabin Deng, Bryan T Drew, Romina

Gazis, Karl Gude, David S Hibbett, Laura A Katz, H Dail Laughinghouse, Emily Jane McTavish, Peter E Midford, Christopher L Owen, Richard H Ree, Jonathan A Rees, Douglas E Soltis, Tiffani Williams, and Karen A Cranston. Synthesis of phylogeny and taxonomy into a comprehensive tree of life. *Proceedings of the National Academy of Sciences*, 112(41):12764–12769, 2015.

Jennifer Hiscox, Melanie Savoury, Sarah R Johnston, David Parfitt, Carsten T Müller, Hilary J Rogers, and Lynne Boddy. Location, location, location: priority effects in wood decay communities may vary between sites. *Environmental microbiology*, 18(6): 1954–1969, 2015a.

Jennifer Hiscox, Melanie Savoury, Carsten T Müller, Björn D Lindahl, Hilary J Rogers, and Lynne Boddy. Priority effects during fungal community establishment in beech wood. *The ISME journal*, 2015b.

Lam Si Tung Ho and Cécile Ané. A linear-time algorithm for gaussian and non-gaussian trait evolution models. *Systematic biology*, 63(3):397–408, 2014.

Martin Hofrichter, René Ullrich, Marek J Pecyna, Christiane Liers, and Taina Lundell. New and classic families of secreted fungal heme peroxidases. *Applied microbiology and biotechnology*, 87(3):871–897, 2010.

Mona N Högberg, Maria JI Briones, Sonja G Keel, Daniel B Metcalfe, Catherine Campbell, Andrew J Midwood, Barry Thornton, Vaughan Hurry, Sune Linder, Torgny Näsholm, and Peter Högberg. Quantification of effects of season and nitrogen supply on tree below-ground carbon transfer to ectomycorrhizal fungi and other soil organisms in a boreal pine forest. *New Phytologist*, 187(2):485–493, 2010.

Björn Hoppe, Witoon Purahong, Tesfaye Wubet, Tiemo Kahl, Jürgen Bauhus, Tobias Arnstadt, Martin Hofrichter, François Buscot, and Dirk Krüger. Linking molecular deadwood-inhabiting fungal diversity and community dynamics to ecosystem functions and processes in central european forests. *Fungal Diversity*, 77(1):367–379, 2015.

Jakub Horák, Jiří Kout, Štěpán Vodka, and Daniel C Donato. Dead wood dependent organisms in one of the oldest protected forests of europe: Investigating the contrasting effects of within-stand variation in a highly diversified environment. *Forest Ecology and Management*, 363:229–236, 2016.

William Horwath. Carbon cycling and formation of soil organic matter. In *Soil Microbiology, Ecology and Biochemistry*, pages 303–339. Elsevier, 2007.

Bibliography

Torsten Hothorn, Frank Bretz, and Peter Westfall. Simultaneous inference in general parametric models. *Biometrical journal*, 50(3):346–363, 2008.

Stephen P Hubbell. *The Unified Neutral Theory of Biodiversity and Biogeography*. Princeton University Press, 2001.

Seppo Huhtinen. *A monograph of Hyaloscypha and allied genera*. Suomen sieniseura Helsinki, 1990.

George Evelyn Hutchinson. Concluding remarks. population studies: animal ecology and demography. In *Cold Spring Harbor Symposia on Quantative Biology*, volume 22, pages 415–427, 1957.

Julian Huxley. *Evolution the modern synthesis*. George Allen and Unwin, 1942.

Katarina Ihrmark, Inga TM Bodeker, Karelyn Cruz-Martinez, Hanna Friberg, Ariana Kubartova, Jessica Schenck, Ylva Strid, Jan Stenlid, Mikael Brandstrom-Durling, Karina E Clemmensen, and Björn D Lindahl. New primers to amplify the fungal ITS2 region - evaluation by 454-sequencing of artificial and natural communities. *FEMS Microbiology Ecology*, 82(3):666–677, 2012.

IPCC. *Summary for Policymakers*. Cambridge University Press, 2014.

Louis R Iverson and Anantha M Prasad. Predicting abundance of 80 tree species following climate change in the eastern united states. *Ecological Monographs*, 68(4):465–485, 1998.

Carsten Jacobsen, Peter Rademacher, Henning Meesenburg, and Karl Josef Meiwes. Gehalte chemischer Elemente in Baumkompartimenten. Literaturstudie und Datensammlung. In *Berichte des Forschungszentrums Waldökosysteme*, volume 69, 2003.

Sarah R Johnston, Lynne Boddy, and Andrew J Weightman. Bacteria in decomposing wood and their interactions with wood-decay fungi. *FEMS microbiology ecology*, 92 (11):fiw179, 2016.

Kaisa Junninen, Maarit Similä, Jari Kouki, and Heikki Kotiranta. Assemblages of wood-inhabiting fungi along the gradients of succession and naturalness in boreal pine-dominated forests in fennoscandia. *Ecography*, 29(1):75–83, 2006.

Katja Juutilainen, Panu Halme, Heikki Kotiranta, and Mikko Mönkkönen. Size matters in studies of dead wood and wood-inhabiting fungi. *Fungal Ecology*, 4(5):342–349, 2011.

Tiemo Kahl, Tobias Arnstadt, Kristin Baber, Claus Bässler, Jürgen Bauhus, Werner Borken, François Buscot, Andreas Floren, Christoph Heibl, Dominik Hessenmöller, Martin Hofrichterchter, Björn Hoppe, Harald Kellner, Dirk Krüger, Eduard Karl Linsenmair, Egbert Matzner, Peter Otto, Witoon Purahongg, Claudia Seilwinder, Ernst-Detlef Schulze, Beate Wende, Wolfgang W. Weisser, and Martin M. Gossner. Wood decay rates of 13 temperate tree species in relation to wood properties, enzyme activities and organismic diversities. *Forest Ecology and Management*, 391:86–95, 2017.

Hans Kalmus. Physiology and ecology of cuticle colour in insects. *Nature*, 148(3762): 693, 1941.

Kazutaka Katoh and Daron M. Standley. MAFFT multiple sequence alignment software version 7: Improvements in performance and usability. *Molecular Biology and Evolution*, 30(4):772–780, 2013.

Håvard Kauserud, Leif Christian Stige, Jon Olav Vik, Rune H Okland, Klaus Høiland, and Nils C Stenseth. Mushroom fruiting and climate change. *Proceedings of the National Academy of Sciences of the United States of America*, 105(10):3811–3914, 2008.

Håvard Kauserud, Einar Heegaard, Mikhail a Semenov, Lynne Boddy, Rune Halvorsen, Leif Chr Stige, Tim H Sparks, Alan C Gange, and Nils C Stenseth. Climate change and spring-fruiting fungi. *Proceedings. Biological sciences*, 277(1685):1169–1177, apr 2010.

Håvard Kauserud, Einar Heegaard, Ulf Buntgen, Rune Halvorsen, Simon Egli, Beatrice Senn-Irlet, Irmgard Krisai-Greilhuber, Wolfgang Damon, Tim Sparks, Jenni Norden, Klaus Høiland, Paul Kirk, Mikhail Semenov, Lynne Boddy, and Nils C Stenseth. Warming-induced shift in European mushroom fruiting phenology. *Proceedings of the National Academy of Sciences*, 109(36):14488–14493, 2012.

François Keck, Frédéric Rimet, Agnes Bouchez, and Alain Franc. phylosignal: an r package to measure, test, and explore the phylogenetic signal. *Ecology and evolution*, 6(9):2774–2780, 2016.

Sally A Keith, Tom J Webb, Katrin Böhning-Gaese, Sean R Connolly, Nicholas K Dulvy, Felix Eigenbrod, Kate E Jones, Trevor Price, David W Redding, Ian PF Owens, and Nick J.B. Isaac. What is macroecology? The Royal Society, 2012.

Bibliography

Steven W Kembel, Timothy K O'Connor, Holly K Arnold, Stephen P Hubbell, S Josef Wright, and Jessica L Green. Relationships between phyllosphere bacterial communities and plant functional traits in a neotropical forest. *Proceedings of the National Academy of Sciences*, 111(38):13715–13720, 2014.

Anna M Kielak, Tanja R Scheublin, Lucas W Mendes, Johannes A Van Veen, and Eiko E Kuramae. Bacterial community succession in pine-wood decomposition. *Frontiers in microbiology*, 7(231), 2016.

SY Kim, SY Park, Soo Ko Ko, and Hyun Suk Jung. Phylogenetic analysis of antrodia and related taxa based on partial mitochondrial ssu rdna sequences. *Antonie Van Leeuwenhoek*, 83(1):81–88, 2003.

Joel G Kingsolver. Fitness consequences of seasonal polyphenism in western white butterflies. *Evolution*, 49(5):942–954, 1995.

Annegret Kohler, Alan Kuo, Laszlo G Nagy, Emmanuelle Morin, Kerrie W Barry, Francois Buscot, Björn Canbäck, Cindy Choi, Nicolas Cichocki, Alicia Clum, Jan Colpaert, Alex Copeland, Mauricio D Costa, Jeanne Doré, Dimitrios Floudas, Gilles Gay, Mariangela Girlanda, Bernard Henrissat, Sylvie Herrmann, Jaqueline Hess, Nils Högberg, Tomas Johansson, Hassine-Radhouane Khouja, Kurt LaButti, Urs Lahrmann, Anthony Levasseur, Erika A Lindquist, Anna Lipzen, Roland Marmeisse, Elena Martino, Claude Murat, Chew Y Ngan, Uwe Nehls, Jonathan M Plett, Anne Pringle, Robin A Ohm, Silvia Perotto, Martina Peter, Robert Riley, Francois Rineau, Joske Ruytinx, Asaf Salamov, Firoz Shah, Hui Sun, Mika Tarkka, Andrew Tritt, Claire Veneault-Fourrey, Alga Zuccaro, Mycorrhizal Genomics Initiative Consortium, Anders Tunlid, Igor V Grigoriev, David S Hibbett, and Francis Martin. Convergent losses of decay mechanisms and rapid turnover of symbiosis genes in mycorrhizal mutualists. *Nature Genetics*, 47(4):410–415, 2015.

Urmas Koljalg, R Henrik Nilsson, Kessy Abarenkov, Leho Tedersoo, Andy FS Taylor, Mohammad Bahram, Scott Thomas Bates, Thomas D Bruns, Johan Bengtsson-Palme, Tony M Callaghan, Brian Douglas, Tiia Drenkhan, Ursula Eberhardt, Margarita Duenas, Tine Grebenc, Gareth W Griffith, Martin Hartmann, Paul M Kirk, Petr Kohout, Ellen Larsson, Björn D Lindahl, Robert Luecking, Maria P Martin, P Brandon Matheny, Nhu H Nguyen, Tuula Niskanen, Jane Oja, Kabir G Peay, Ursula Peintner, Marko Peterson, Kadri Poldmaa, Lauri Saag, Irja Saar, Arthur Schuessler, James A Scott, Carolina Senes, Matthew E Smith, Ave Suija, D Lee Taylor, M Teresa Telleria,

Michael Weiss, and Karl Henrik Larsson. Towards a unified paradigm for sequence-based identification of fungi. *Molecular Ecology*, 22(21):5271–5277, 2013.

Atte Komonen and Jörg Müller. Dispersal ecology of deadwood organisms and connectivity conservation. *Conservation Biology*, 32(3):535–545, 2018.

Nathan JB Kraft, Liza S Comita, Jonathan M. Chase, Nathan J. Sanders, Nathan G Swenson, Thomas O Crist, James C Stegen, Mark Vellend, Brad Boyle, Marti J Anderson, Howard V Cornell, Kendi F Davies, Amy L Freestone, Brian D Inouye, Susan P Harrison, and Jonathan A Myers. Disentangling the drivers of β diversity along latitudinal and elevational gradients. *Science*, 333(6050):1755–1758, 2011.

Franz-Sebastian Krah, Claus Bässler, Christoph Heibl, John Soghigian, Hanno Schaefer, and David S Hibbett. Evolutionary dynamics of host specialization in wood-decay fungi. *BMC Evolutionary Biology*, 18(1):119–132, 2018a.

Franz-Sebastian Krah, Sebastian Seibold, Roland Brandl, Petr Baldrian, Jörg Müller, and Claus Bässler. Independent effects of host and environment on the diversity of wood-inhabiting fungi. *Journal of Ecology*, 106(4):1428–1442, 2018b.

Franz-Sebastian Krah, Scott T. Bates, and Andrew N. Miller. rmycoportal - an r package to interface with the mycology collections portal. *Biodiversity Data Journal*, 7:e31511, 2019.

Giddy Landan and Dan Graur. Local reliability measures from sets of co-optimal multiple sequence alignments. In *Pacific Symposium on Biocomputing*, volume 13, pages 15–24, 2008.

Duncan Temple Lang and the CRAN Team. *XML: Tools for Parsing and Generating XML Within R and S-Plus*, 2018. R package version 3.98-1.16.

Silke Langenheder, Mercè Berga, Örjan Östman, and Anna J Székely. Temporal variation of β-diversity and assembly mechanisms in a bacterial metacommunity. *The ISME journal*, 6(6):1107, 2012.

Silke Langenheder, Jianjun Wang, Satu Maaria Karjalainen, Tiina M Laamanen, Kimmo T Tolonen, Annika Vilmi, and Jani Heino. Bacterial metacommunity organization in a highly connected aquatic system. *FEMS microbiology ecology*, 93(4), 2017.

Bibliography

Brendan B Larsen, Elizabeth C Miller, Matthew K Rhodes, and John J Wiens. Inordinate fondness multiplied and redistributed: the number of species on earth and the new pie of life. *The Quarterly Review of Biology*, 92(3):229–265, 2017.

Karl-Henrik Larsson. Re-thinking the classification of corticioid fungi. *Mycological research*, 111(9):1040–1063, 2007.

John H Lawton. Are there general laws in ecology? *Oikos*, pages 177–192, 1999.

Simon R Leather, Eligiusz A Baumgart, Hugh F Evans, and Donald LJ Quicke. Seeing the trees for the wood - beech (Fagus sylvatica) decay fungal volatiles influence the structure of saproxylic beetle communities. *Insect Conservation and Diversity*, 7(4): 314–326, 2014.

Lukas W Lehnert, Claus Bässler, Roland Brandl, Philip J Burton, and Jörg Müller. Highest number of indicator species is found in the early successional stages after bark beetle attack. *Journal for Nature Conservation*, 21:97–104, 2013.

M A Leibold, M Holyoak, N Mouquet, P Amarasekare, J M Chase, M F Hoopes, R D Holt, J B Shurin, R Law, D Tilman, M Loreau, and A Gonzalez. The metacommunity concept: A framework for multi-scale community ecology. *Ecology Letters*, 7(7):601–613, 2004.

Mathew A Leibold and Jonathan M Chase. *Metacommunity ecology*, volume 59. Princeton University Press, 2017.

Egbert Giles Leigh Jr. The evolution of mutualism. *Journal of evolutionary biology*, 23 (12):2507–2528, 2010.

Jonathan Lenoir, Jean-Claude Gégout, PA Marquet, P De Ruffray, and H Brisse. A significant upward shift in plant species optimum elevation during the 20th century. *science*, 320(5884):1768–1771, 2008.

Devin R Leopold, J Paula Wilkie, Ian A Dickie, Robert B Allen, Peter K Buchanan, and Tadashi Fukami. Priority effects are interactively regulated by top-down and bottom-up forces: evidence from wood decomposer communities. *Ecology Letters*, 20 (8):1054–1063, 2017.

Ben A LePage, Randolph S Currah, A Ruth Stockey, and Gar W Rothwell. Fossil ectomycorrhizae from the middle eocene. *American Journal of Botany*, 84(3):410–410, 1997.

192

Eva S Lindström and Silke Langenheder. Local and regional factors influencing bacterial community assembly. *Environmental Microbiology Reports*, 4(1):1–9, 2012.

Jing-Yu Liu, Jun-long Men, Ming-chang Chang, Cui-ping Feng, and Ling-Gang Yuan. itraq-based quantitative proteome revealed metabolic changes of flammulina velutipes mycelia in response to cold stress. *Journal of proteomics*, 156:75–84, 2017.

Vincent Lombard, Hemalatha Golaconda Ramulu, Elodie Drula, Pedro M. Coutinho, and Bernard Henrissat. The carbohydrate-active enzymes database (CAZy) in 2013. *Nucleic Acids Research*, 42(D1):D490–D495, 2014.

Jonathan B Losos. Phylogenetic niche conservatism, phylogenetic signal and the relationship between phylogenetic relatedness and ecological similarity among species. *Ecology letters*, 11(10):995–1003, 2008.

Taina K Lundell, Miia R Mäkelä, and Kristiina Hildén. Lignin-modifying enzymes in filamentous basidiomycetes–ecological, functional and phylogenetic review. *Journal of basic microbiology*, 50(1):5–20, 2010.

Taina K Lundell, Miia R Mäkelä, Ronald P de Vries, and Kristiina S Hildén. Genomics, lifestyles and future prospects of wood-decay and litter-decomposing basidiomycota. In *Advances in botanical research*, volume 70, pages 329–370. Elsevier, 2014.

Robert MacArthur and Richard Levins. The limiting similarity, convergence, and divergence of coexisting species. *The american naturalist*, 101(921):377–385, 1967.

Robert H MacArthur and John W MacArthur. On bird species diversity. *Ecology*, 42 (3):594–598, 1961.

P Maijala, KV Fagerstedt, and M Raudaskoski. Detection of extracellular cellulolytic and proteolytic activity in ectomycorrhizal fungi and Heterobasidion annosum (Fr.) Bref. *New Phytologist*, 117(4):643–648, 1991.

Michael E Mann, Raymond S Bradley, and Malcolm K Hughes. Global-scale temperature patterns and climate forcing over the past six centuries. *Nature*, 392(6678):105, 2004.

Brian H McArdle and Marti J Anderson. Fitting multivariate models to community data: a comment on distance-based redundancy analysis. *Ecology*, 82(1):290–297, 2001.

Bruce A McCarl, F Blaine Metting, and Charles Rice. Soil carbon sequestration. *Climatic Change*, 80(1):1–3, 2007.

Bibliography

Brian J McGill, Brian J Enquist, Evan Weiher, and Mark Westoby. Rebuilding community ecology from functional traits. *Trends in ecology & evolution*, 21(4):178–185, 2006.

Thomas McMahon. Size and shape in biology. *Science*, 179(4079):1201–1204, 1973.

Felix M Medie, Gideon J Davies, Michel Drancourt, and Bernard Henrissat. Genome analyses highlight the different biological roles of cellulases. *Nature Reviews Microbiology*, 10(3):227–234, 2012.

Andrew N Miller and Scott T Bates. The mycology collections portal (mycoportal). *Cryptogamie Mycologie*, 37:15–36, 2017.

Mark A Miller, Wayne Pfeiffer, and Terri Schwartz. The cipres science gateway: A community resource for phylogenetic analyses. In *Proceedings of the 2011 TeraGrid Conference: Extreme Digital Discovery*, TG '11, pages 41:1–41:8. ACM, 2011.

Francis I Molina, Peng Shen, Shung-Chang Jong, and Kazuhiko Orikono. Molecular Evidence Supports the Separation of Lentinula edodes from Lentinus and Related Genera. *Canadian Journal of Botany-Revue Canadienne De Botanique*, 70(12):2446–2452, 1992.

Nicolas Mouquet and Michel Loreau. Community Patterns in Source-Sink Metacommunities. *The American Naturalist*, 162(5):544–557, 2003.

Jörg Müller and Rita Bütler. A review of habitat thresholds for dead wood: a baseline for management recommendations in european forests. *European Journal of Forest Research*, 129(6):981–992, 2010.

Jörg Müller, Herve Brustel, Antoine Brin, Heinz Bussler, Christophe Bouget, Elisabeth Obermaier, Ina MM Heidinger, Thibault Lachat, Bernhard Förster, Jakub Horak, Jiří Procházka, Frank Köhler, Laurent Larrieu, Ulrich Bense, Gunnar Isacsson, Livia Zapponi, and Martin M Gossner. Increasing temperature may compensate for lower amounts of dead wood in driving richness of saproxylic beetles. *Ecography*, 38(5): 499–509, 2015.

Staffan Müller-Wille. Linnaeus' herbarium cabinet: a piece of furniture and its function, 2006.

Tamara Münkemüller, Sebastien Lavergne, Bruno Bzeznik, Stéphane Dray, Thibaut Jombart, Katja Schiffers, and Wilfried Thuiller. How to measure and test phylogenetic signal. *Methods in Ecology and Evolution*, 3(4):743–756, 2012.

László G Nagy, Robin A Ohm, Gábor M Kovács, Dimitrios Floudas, Robert Riley, Attila Gácser, Mátyás Sipiczki, John M Davis, Sharon L Doty, G Sybren De Hoog, B Franz Lang, Joseph W Spatafora, Francis M Martin, Igor V Grigoriev, and David S Hibbett. Latent homology and convergent regulatory evolution underlies the repeated emergence of yeasts. *Nature communications*, 5, 2014.

László G Nagy, Robert Riley, Andrew Tritt, Catherine Adam, Chris Daum, Dimitrios Floudas, Hui Sun, Jagjit S Yadav, Jasmyn Pangilinan, Karl-Henrik Larsson, Kenji Matsuura, Kerrie Barry, Kurt Labutti, Rita Kuo, Robin A Ohm, Sukanta S Bhattacharya, Takashi Shirouzu, Yuko Yoshinaga, Francis M Martin, Igor V Grigoriev, and David S Hibbett. Comparative Genomics of Early-Diverging Mushroom-Forming Fungi Provides Insights into the Origins of Lignocellulose Decay Capabilities. *Molecular biology and evolution*, 33(4):959–970, 2015.

Laszlo G Nagy, Renata Toth, Eniko Kiss, Jason Slot, Attila Gacser, and Gabor M Kovacs. Six key traits of fungi: Their evolutionary origins and genetic bases. *Microbiology spectrum*, 5(4), 2017.

LG Nagy, D Floudas, R Riley, K Barry, IV Grigoriev, and DS Hibbett. Diversification of wood decay systems in early evolution of agaricomycotina. In *Phytopathology*, volume 103, pages 181–181, 2013.

Diana R Nemergut, Steven K Schmidt, Tadashi Fukami, Sean P O'Neill, Teresa M Bilinski, Lee F Stanish, Joseph E Knelman, John L Darcy, Ryan C Lynch, Phillip Wickey, and Scott Ferrenberg. Patterns and processes of microbial community assembly. *Microbiology and Molecular Biology Reviews*, 77(3):342–356, 2013.

Paul A Newman and Richard McKenzie. Uv impacts avoided by the montreal protocol. *Photochemical & photobiological sciences : Official journal of the European Photochemistry Association and the European Society for Photobiology*, 10(7):1152–1160, 2011.

Lam Tung Nguyen, Heiko A. Schmidt, Arndt Von Haeseler, and Bui Quang Minh. IQ-TREE: A fast and effective stochastic algorithm for estimating maximum-likelihood phylogenies. *Molecular Biology and Evolution*, 32(1):268–274, 2015.

Arne C Nilssen. Long-range aerial dispersal of bark beetles and bark weevils (Coleoptera, Scolytidae and Curculionidae) in northern Finland. *Annales Entomologici Fennici*, 50: 37–42, 1984.

Bibliography

Björn Nordén, Frank Götmark, Marie Tönnberg, and Martin Ryberg. Dead wood in semi-natural temperate broadleaved woodland: contribution of coarse and fine dead wood, attached dead wood and stumps. *Forest Ecology and Management*, 194(1): 235–248, 2004a.

Björn Nordén, Martin Ryberg, Frank Götmark, and Bettina Olausson. Relative importance of coarse and fine woody debris for the diversity of wood-inhabiting fungi in temperate broadleaf forests. *Biological conservation*, 117(1):1–10, 2004b.

Jenni Nordén, Reijo Penttilä, Juha Siitonen, Erkki Tomppo, and Otso Ovaskainen. Specialist species of wood-inhabiting fungi struggle while generalists thrive in fragmented boreal forests. *Journal of Ecology*, 101(3):701–712, 2013.

Veera Norros, Reijo Penttilä, Mai Suominen, and Otso Ovaskainen. Dispersal may limit the occurrence of specialist wood decay fungi already at small spatial scales. *Oikos*, 121(6):961–974, 2012.

Veera Norros, Üllar Rannik, Tareq Hussein, Tuukka Petäjä, Timo Vesala, and Otso Ovaskainen. Do small spores disperse further than large spores? *Ecology*, 95(6): 1612–1621, 2014.

Veera Norros, Elina Karhu, Jenni Nordén, Anssi V Vähätalo, and Otso Ovaskainen. Spore sensitivity to sunlight and freezing can restrict dispersal in wood-decay fungi. *Ecology and evolution*, 5(16):3312–3326, 2015.

Péter Ódor, J Heilmann-Clausen, Morten Christensen, E Aude, KW Van Dort, Andrej Piltaver, I Siller, MT Veerkamp, R Walleyn, T Standovár, AFM Hess, Jože Kosec, Neven Matočec, Hojka Kraigher, and Tine Grebnec. Diversity of dead wood inhabiting fungi and bryophytes in semi-natural beech forests in Europe. *Biological Conservation*, 131(1):58–71, 2006.

Jari Oksanen. Multivariate analysis of ecological communities in R: vegan tutorial. *R documentation*, page 43, 2015.

Jörgen Olsson, Bengt Gunnar Jonsson, Joakim Hjältén, and Lars Ericson. Addition of coarse woody debris–the early fungal succession on picea abies logs in managed forests and reserves. *Biological Conservation*, 144(3):1100–1110, 2011.

David Orme. The caper package : comparative analysis of phylogenetics and evolution in R. *R package version 0.5, 2*, pages 1–36, 2013.

196

John L Orrock and James I Watling. Local community size mediates ecological drift and competition in metacommunities. *Proceedings of the Royal Society of London B: Biological Sciences*, 277(1691):2185–2191, 2010.

Elisabet Ottosson, Jenni Nordén, Anders Dahlberg, Mattias Edman, Mari Jönsson, Karl Henrik Larsson, Jörgen Olsson, Reijo Penttilä, Jan Stenlid, and Otso Ovaskainen. Species associations during the succession of wood-inhabiting fungal communities. *Fungal Ecology*, 11:17–28, 2014.

Otso Ovaskainen, Gleb Tikhonov, Anna Norberg, F Guillaume Blanchet, Leo Duan, David Dunson, Tomas Roslin, and Nerea Abrego. How to make more out of community data? a conceptual framework and its implementation as models and software. *Ecology Letters*, 20(5):561–576, 2017.

M Pagel. Inferring the historical patterns of biological evolution. *Nature*, 401(6756): 877–884, 1999.

Stephen G. Pallardy. *Physiology of Woody Plants.* 2008.

Emmanuel Paradis. Molecular dating of phylogenies by likelihood methods: a comparison of models and a new information criterion. *Molecular phylogenetics and evolution*, 67(2):436–444, 2013.

Emmanuel Paradis, Ben Bolker, Julien Claude, Hoa Sien Cuong, Richard Desper, Julien Dutheil, Olivier Gascuel, Gangolf Jobb, Christoph Heibl, Vincent Lefort, Yvonnick Noel, Johan Nylander, Rainer Opgen-rhein, Korbinian Strimmer, and Damien De. The ape Package, 2008.

David Parfitt, Julie Hunt, David Dockrell, Hilary J Rogers, and Lynne Boddy. Do all trees carry the seeds of their own destruction? PCR reveals numerous wood decay fungi latently present in sapwood of a wide range of angiosperm trees. *Fungal Ecology*, 3(4):338–346, 2010.

Camille Parmesan. Ecological and evolutionary responses to recent climate change. *Annu. Rev. Ecol. Evol. Syst.*, 37:637–669, 2006.

Camille Parmesan and Gary Yohe. A globally coherent fingerprint of climate change impacts across natural systems. *Nature*, 421(6918):37, 2003.

Kabir G Peay, Peter G Kennedy, and Thomas D Bruns. Fungal community ecology: a hybrid beast with a molecular master. *AIBs Bulletin*, 58(9):799–810, 2008.

Bibliography

Anssi Pekkarinen, Lucia Reithmaier, and Peter Strobl. Pan-European forest/non-forest mapping with Landsat ETM+ and CORINE Land Cover 2000 data. *ISPRS Journal of Photogrammetry and Remote Sensing*, 64(2):171–183, 2009.

Osnat Penn, Eyal Privman, Giddy Landan, Dan Graur, and Tal Pupko. An alignment confidence score capturing robustness to guide tree uncertainty. *Molecular Biology and Evolution*, 27(8):1759–1767, 2010.

Pedro R Peres-Neto, Pierre Legendre, Stéphane Dray, and Daniel Borcard. Variation partitioning of species data matrices: Estimation and comparison of fractions. *Ecology*, 87(10):2614–2625, 2006.

Ronald H Petersen. Gloeomucro and a note on physalacria concinna. *Mycologia*, pages 301–311, 1980.

Eran Pichersky and David R. Gang. Genetics and biochemistry of secondary metabolites in plants: An evolutionary perspective, 2000.

Stefan Pinkert and Dirk Zeuss. Thermal biology: Melanin-based energy harvesting across the tree of life. *Current Biology*, 28(16):R887–R889, 2018.

Stefan Pinkert, Roland Brandl, and Dirk Zeuss. Colour lightness of dragonfly assemblages across north america and europe. *Ecography*, 40(9):1110–1117, 2017.

Václav Pouska, Petr Macek, Lucie Zíbarová, and Harald Ostrow. How does the richness of wood-decaying fungi relate to wood microclimate? *Fungal Ecology*, 27:178–181, 2017.

Hans Pretzsch, Peter Biber, Gerhard Schütze, Enno Uhl, and Thomas Rötzer. Forest stand growth dynamics in central europe have accelerated since 1870. *Nature communications*, 5, 2014.

Morgan N Price, Paramvir S Dehal, and Adam P Arkin. Fasttree: Computing large minimum evolution trees with profiles instead of a distance matrix. *Molecular Biology and Evolution*, 26(7):1641–1650, 2009.

Anne Pringle and John W Taylor. The fitness of filamentous fungi. *Trends in microbiology*, 10(10):474–481, 2002.

Anne Pringle, Else Vellinga, and Kabir Peay. The shape of fungal ecology: does spore morphology give clues to a species' niche? *Fungal Ecology*, (17):213–216, 2015.

Itthayakorn Promputtha, Saisamorn Lumyong, Vijaykrishna Dhanasekaran, Eric Huge Charles McKenzie, Kevin David Hyde, and Rajesh Jeewon. A phylogenetic evaluation of whether endophytes become saprotrophs at host senescence. *Microbial Ecology*, 53(4):579–590, 2007.

Witoon Purahong, Tesfaye Wubet, Guillaume Lentendu, Björn Hoppe, Katalee Jariyavidyanont, Tobias Arnstadt, Kristin Baber, Peter Otto, Harald Kellner, Martin Hofrichter, Jürgen Bauhus, Wolfgang W Weisser, Dirk Krüger, Ernst-Detlef Schulze, Tiemo Kahl, and Francois Buscot. Determinants of deadwood-inhabiting fungal communities in temperate forests: molecular evidence from a large scale deadwood decomposition experiment. *Frontiers in Microbiology*, 9:2120, 2018.

R Core Team. *R: A Language and Environment for Statistical Computing*. R Foundation for Statistical Computing, Vienna, Austria, 2015.

Eduardo H Rapoport. Gloger's rule and pigmentation of collembola. *Evolution*, 23(4): 622–626, 1969.

Mulchand M Rathod. Taxonomic Studies on the Daedaloid and Hexagonoid Polypores Form the Forest of Western Maharasta. *Recent Research in Science and Technology*, 3(5), 2011.

James R Reilly, Ann E Hajek, Andrew M Liebhold, and Ruth Plymale. Impact of entomophaga maimaiga (entomophthorales: Entomophthoraceae) on outbreak gypsy moth populations (lepidoptera: Erebidae): The role of weather. *Environmental Entomology*, 43(3):632–641, 2014.

Pertti Renvall. Community structure and dynamics of wood-rotting basidiomycetes on decomposing conifer trunks in northern finland. *Karstenia*, 35:1–51, 1995.

Vincent H Resh. *Encyclopedia of Insects*. Elsevier Academic Press, Oxford, 2009.

Liam J Revell. phytools: An R package for phylogenetic comparative biology (and other things). *Methods in Ecology and Evolution*, 3(2):217–223, 2012.

Liam J Revell, D Luke Mahler, Pedro R Peres-Neto, and Benjamin D Redelings. A new phylogenetic method for identifying exceptional phenotypic diversification. *Evolution*, 66(1):135–146, 2012.

Robert Riley, Asaf A Salamov, Daren W Brown, Laszlo G Nagy, Dimitrios Floudas, Benjamin W Held, Anthony Levasseur, Vincent Lombard, Emmanuelle Morin, Robert

Bibliography

Otillar, Erika A Lindquist, Hui Sun, Kurt M LaButti, Jeremy Schmutz, Dina Jabbour, Hong Luo, Scott E Baker, Antonio G Pisabarro, Jonathan D Walton, Robert A Blanchette, Bernard Henrissat, Francis Martin, Dan Cullen, David S Hibbett, and Igor V Grigoriev. Extensive sampling of basidiomycete genomes demonstrates inadequacy of the white-rot/brown-rot paradigm for wood decay fungi. *Proceedings of the National Academy of Sciences of the United States of America*, 111(27):9923–8, 2014.

A C Rinaldi, O Comandini, and T W Kuyper. Ectomycorrhizal fungal diversity: seperating the wheat from the chaff. *Fungal Diversity*, 33:1–45, 2008.

Francois Rineau, Firoz Shah, Mark M Smits, Par Persson, Tomas Johansson, Robert Carleer, Carl Troein, and Anders Tunlid. Carbon availability triggers the decomposition of plant litter and assimilation of nitrogen by an ectomycorrhizal fungus. *ISME Journal*, 7(10):2010–2022, 2013.

Clare H Robinson. Cold adaptation in arctic and antarctic fungi. *New phytologist*, 151 (2):341–353, 2001.

Jørund Rolstad, Magne Sætersdal, Ivar Gjerde, and Ken Olaf Storaunet. Wood-decaying fungi in boreal forest: are species richness and abundances influenced by small-scale spatiotemporal distribution of dead wood? *Biological Conservation*, 117(5):539–555, 2004.

Michel Saint-Germain, Pierre Drapeau, and Christopher M. Buddle. Host-use patterns of saproxylic phloeophagous and xylophagous Coleoptera adults and larvae along the decay gradient in standing dead black spruce and aspen. *Ecography*, 30(6):737–748, 2007.

Michel Saint-Germain, Christopher M. Buddle, and Pierre Drapeau. Substrate selection by saprophagous wood-borer larvae within highly variable hosts. *Entomologia Experimentalis et Applicata*, 134(3):227–233, 2010.

Van M Savage, James F Gillooly, James H Brown, Geoffrey B West, and Eric L Charnov. Effects of body size and temperature on population growth. *The American Naturalist*, 163(3):429–441, 2004.

Douglas Barton Osborne Savile. Arctic adaptations in plants. *Canada Dept. Agric., Res. Branch, Mon*, (6), 1972.

Kamran Schalchian-Tabrizi, Marianne A. Minge, Mari Espelund, Russell Orr, Torgeir Ruden, Kjetill S. Jakobsen, and Thomas Cavalier-Smith. Multigene phylogeny of Choanozoa and the origin of animals. *PLoS ONE*, 2008.

Bryant C Scharenbroch and James G Bockheim. Impacts of forest gaps on soil properties and processes in old growth northern hardwood-hemlock forests. *Plant and Soil*, 294 (1-2):219–233, 2007.

Daniel Scherrer and Christian Körner. Topographically controlled thermal-habitat differentiation buffers alpine plant diversity against climate warming. *Journal of biogeography*, 38(2):406–416, 2011.

Jonathan S Schilling, Justin T Kaffenberger, Feng Jin Liew, and Zewei Song. Signature wood modifications reveal decomposer community history. *PloS one*, 10(3):e0120679, 2015.

Thomas Schneider, Katharina M Keiblinger, Emanuel Schmid, Katja Sterflinger-Gleixner, Günther Ellersdorfer, Bernd Roschitzki, Andreas Richter, Leo Eberl, Sophie Zechmeister-Boltenstern, and Kathrin Riedel. Who is who in litter decomposition? metaproteomics reveals major microbial players and their biogeochemical functions. *The ISME journal*, 6(9):1749–1762, 2012.

F. Schwarze, J. Engels, and C. Mattheck. *Fungal Strategies of Wood Decay in Trees.* 2000.

Sebastian Seibold, Claus Bässler, Roland Brandl, Martin M Gossner, Simon Thorn, Michael D Ulyshen, and Jörg Müller. Experimental studies of dead-wood biodiversity—a review identifying global gaps in knowledge. *Biological Conservation*, 191:139–149, 2015a.

Sebastian Seibold, Roland Brandl, Jörn Buse, Torsten Hothorn, Jürgen Schmidl, Simon Thorn, and Jörg Müller. Association of extinction risk of saproxylic beetles with ecological degradation of forests in europe. *Conservation Biology*, 29(2):382–390, 2015b.

Sebastian Seibold, Claus Bässler, Roland Brandl, Boris Büche, Alexander Szallies, Simon Thorn, Michael D Ulyshen, and Jörg Müller. Microclimate and habitat heterogeneity as the major drivers of beetle diversity in dead wood. *Journal of Applied Ecology*, 53 (3):934–943, 2016.

Sebastian Seibold, Jörg Müller, Petr Baldrian, Marc W Cadotte, Martina Štursová, Peter HW Biedermann, Franz-Sebastian Krah, and Claus Bässler. Fungi associated

with beetles dispersing from dead wood – let's take the beetle bus! *Fungal Ecology*, 2018.

Itamar Sela, Haim Ashkenazy, Kazutaka Katoh, and Tal Pupko. Guidance2: accurate detection of unreliable alignment regions accounting for the uncertainty of multiple parameters. *Nucleic acids research*, 43(W1):W7–W14, 2015.

Thomas N Sherratt, David M Wilkinson, and Roderick S Bain. Explaining dioscorides'"double difference": why are some mushrooms poisonous, and do they signal their unprofitability? *The American Naturalist*, 166(6):767–775, 2005.

Urs Siegenthaler and Jimena L. Sarmiento. Atmospheric carbon dioxide and the ocean. *Nature*, 365(6442):119–125, 1993.

Juha Siitonen, Petri Martikainen, Pekka Punttila, and Josef Rauh. Coarse woody debris and stand characteristics in mature managed and old-growth boreal mesic forests in southern finland. *Forest Ecology and Management*, 128(3):211–225, 2000.

Daniel Simberloff. Community ecology: Is it time to move on? (an american society of naturalists presidential address). *The American Naturalist*, 163(6):787–799, 2004.

Eero Sjöström. *Wood Chemistry Fundamentals and Applications*. Number 1838. 1981.

Sally E Smith and David J Read. *Mycorrhizal symbiosis*. Academic press, 2010.

Stephen A Smith and Michael J Donoghue. Rates of molecular evolution are linked to life history in flowering plants. *Science*, 322(5898):86–9, 2008.

Stephen A Smith, Jeremy M Beaulieu, and Michael J Donoghue. Mega-phylogeny approach for comparative biology: an alternative to supertree and supermatrix approaches. *BMC evolutionary biology*, 9(1):37, 2009.

Stephen A Smith, Jeremy M Beaulieu, and Michael J Donoghue. An uncorrelated relaxed-clock analysis suggests an earlier origin for flowering plants. *Proceedings of the National Academy of Sciences*, 107(13):5897–5902, 2010.

Janne Soininen, Jenni J Korhonen, and Miska Luoto. Stochastic species distributions are driven by organism size. *Ecology*, 94(3):660–670, 2013.

Ha-Yeon Song, Dae-Hyuk Kim, and Jung-Mi Kim. Comparative transcriptome analysis of dikaryotic mycelia and mature fruiting bodies in the edible mushroom lentinula edodes. *Scientific reports*, 8(1):8983, 2018.

Zewei Song, Andrew Vail, Michael J Sadowsky, and Jonathan S Schilling. Influence of hyphal inoculum potential on the competitive success of fungi colonizing wood. *Microbial ecology*, 69(4):758–767, 2015.

Zewei Song, Peter G Kennedy, Feng J Liew, and Jonathan S Schilling. Fungal endophytes as priority colonizers initiating wood decomposition. *Functional Ecology*, 31(2):407–418, 2017.

Alexandros Stamatakis. RAxML version 8: a tool for phylogenetic analysis and post-analysis of large phylogenies. *Bioinformatics*, 30(9):1312–1313, 2014.

Alexandros Stamatakis, Paul Hoover, and Jacques Rougemont. A rapid bootstrap algorithm for the raxml web servers. *Systematic biology*, 57(5):758–771, 2008.

William T Stearn. The Background of Linnaeus's Contributions to the Nomenclature and Methods of Systematic Biology. *Systematic Zoology*, 8:4–22, 1959.

James C Stegen, Xueju Lin, Allan E Konopka, and James K Fredrickson. Stochastic and deterministic assembly processes in subsurface microbial communities. *The ISME journal*, 6(9):1653, 2012.

Jan Stenlid, Reijo Penttilä, and Anders Dahlberg. Wood-decay basidiomycetes in boreal forests: distribution and community development. In *British Mycological Society Symposia Series*, volume 28, pages 239–262. Elsevier, 2008.

Jogeir N Stokland, Juha Siitonen, and Bengt Gunnar Jonsson. *Biodiversity in dead wood*. Cambridge University Press, 2012.

Kalliope E Stournaras, Eugenia Lo, Katrin Böhning-Gaese, Eliana Cazetta, D Matthias Dehling, Matthias Schleuning, Mary Caswell Stoddard, Michael J Donoghue, Richard O Prum, and H Martin Schaefer. How colorful are fruits? limited color diversity in fleshy fruits on local and global scales. *New Phytologist*, 198(2):617–629, 2013.

Mark E Swanson, Jerry F Franklin, Robert L Beschta, Charles M Crisafulli, Dominick A DellaSala, Richard L Hutto, David B Lindenmayer, and Frederick J Swanson. The forgotten stage of forest succession: Early-successional ecosystems on forest sites. *Frontiers in Ecology and the Environment*, 9(2):117–125, 2011.

Ge Tan, Matthieu Muffato, Christian Ledergerber, Javier Herrero, Nick Goldman, Manuel Gil, and Christophe Dessimoz. Current methods for automated filtering of

multiple sequence alignments frequently worsen single-gene phylogenetic inference. *Systematic biology*, 64(5):778–791, 2015.

Leho Tedersoo, Tom W May, and Matthew E Smith. Ectomycorrhizal lifestyle in fungi: global diversity, distribution, and evolution of phylogenetic lineages. *Mycorrhiza*, 20 (4):217–263, 2010.

Leho Tedersoo, Mohammad Bahram, Sergei Põlme, Urmas Kõljalg, Nourou S Yorou, Ravi Wijesundera, Luis Villarreal Ruiz, Aída M Vasco-Palacios, Pham Quang Thu, Ave Suija, Matthew E Smith, Cathy Sharp, Erki Saluveer, Alessandro Saitta, Miguel Rosas, Taavi Riit, David Ratkowsky, Karin Pritsch, Kadri Põldmaa, Meike Piepenbring, Cherdchai Phosri, Marko Peterson, Kaarin Parts, Kadri Pärtel, Eveli Otsing, Eduardo Nouhra, André L Njouonkou, R Henrik Nilsson, Luis N Morgado, Jordan Mayor, Tom W May, Luiza Majuakim, D Jean Lodge, Su See Lee, Karl-Henrik Larsson, Petr Kohout, Kentaro Hosaka, Indrek Hiiesalu, Terry W Henkel, Helery Harend, Liang-dong Guo, Alina Greslebin, Gwen Grelet, Jozsef Geml, Genevieve Gates, William Dunstan, Chris Dunk, Rein Drenkhan, John Dearnaley, André De Kesel, Tan Dang, Xin Chen, Franz Buegger, Francis Q Brearley, Gregory Bonito, Sten Anslan, Sandra Abell, and Kessy Abarenkov. Fungal biogeography. global diversity and geography of soil fungi. *Science*, 346(6213):1256688, Nov 2014.

Vijay Kumar Thakur and Manju Kumari Thakur. Processing and characterization of natural cellulose fibers/thermoset polymer composites. *Carbohydrate Polymers*, 109: 102–117, 2014.

Chris D. Thomas, Alison Cameron, Rhys E. Green, Michel Bakkenes, Linda J. Beaumont, Yvonne C. Collingham, Barend F.N. Erasmus, Marinez Ferreira De Siqueira, Alan Grainger, Lee Hannah, Lesley Hughes, Brian Huntley, Albert S. Van Jaarsveld, Guy F. Midgley, Lera Miles, Miguel A. Ortega-Huerta, A. Townsend Peterson, Oliver L. Phillips, and Stephen E. Williams. Extinction risk from climate change. *Nature*, 427(6970):145–148, 2004.

Ross Thompson and Colin Townsend. A truce with neutral theory: Local deterministic factors, species traits and dispersal limitation together determine patterns of diversity in stream invertebrates. *Journal of Animal Ecology*, 75(2):476–484, 2006.

Wilfried Thuiller, Sandra Lavorel, Miguel B Araújo, Martin T Sykes, and I Colin Prentice. Climate change threats to plant diversity in europe. *Proceedings of the National Academy of Sciences*, 102(23):8245–8250, 2005.

Wilfried Thuiller, Sébastien Lavergne, Cristina Roquet, Isabelle Boulangeat, Bruno Lafourcade, and Miguel B Araujo. Consequences of climate change on the tree of life in europe. *Nature*, 470(7335):531, 2011.

Wilfried Thuiller, Damien Georges, Robin Engler, Frank Breiner, Maintainer Damien Georges, and Contact Wilfried Thuiller. Package 'biomod2', 2016.

Susana Clusella Trullas, Johannes H van Wyk, and James R Spotila. Thermal melanism in ectotherms. *Journal of Thermal Biology*, 32(5):235–245, 2007.

Werner Ulrich and Nicholas J Gotelli. Null model analysis of species associations using abundance data. *Ecology*, 91(11):3384–3397, 2010.

Mark C Urban, Greta Bocedi, Andrew P Hendry, J-B Mihoub, Guy Pe'er, Alex Singer, JR Bridle, LG Crozier, Luc De Meester, William Godsoe, Andrew Gonzalez, Jessica J Hellmann, RD Holt, A Huth, Karen Johst, Cornelia B Krug, PW Leadley, SCF Palmer, Jelena H Pantel, Andreas Schmitz, Patrick A Zollner, and Justin M J Travis. Improving the forecast for biodiversity under climate change. *Science*, 353 (6304):aad8466, 2016.

Egon L van den Broek and Eva M van Rikxoort. Evaluation of color representation for texture analysis. In *Paper presented at 16th Belgium-Dutch Conference on Artificial Intelligence, BNAIC 2004, Groningen, Netherlands.*, pages 35–42, 2004.

Marcel GA Van Der Heijden, Richard D Bardgett, and Nico M Van Straalen. The unseen majority: soil microbes as drivers of plant diversity and productivity in terrestrial ecosystems. *Ecology letters*, 11(3):296–310, 2008.

Tyler J VanderWeele and Mirjam J Knol. A Tutorial on Interaction. *Epidemiologic Methods*, 3(1), 2014.

Jan Velíšek and Karel Cejpek. Pigments of higher fungi: a review. *Czech J Food Sci*, 29 (2):87–102, 2011.

Mark Vellend. Conceptual synthesis in community ecology. *The Quarterly review of biology*, 85(2):183–206, 2010.

Stepan Vodka, Martin Konvicka, and Lukas Cizek. Habitat preferences of oak-feeding xylophagous beetles in a temperate woodland: implications for forest history and management. *Journal of Insect Conservation*, 13(5):553–562, 2009.

Bibliography

Alexander von Humboldt. Ideen zu einer Geographie der Pflanzen nebst einem Naturgemälde der Tropenländer von AI. von Humboldt und A. *Bonpland. Bearbeitet u. herausgegeben von dem erstem. Tübingen u. Paris*, 1807.

Rudi Wagenführ and Christian Scheiber. *Holzatlas.* Fachbuchverlag Leipzig, 2007.

Jianjun Wang, Ji Shen, Yucheng Wu, Chen Tu, Janne Soininen, James C Stegen, Jizheng He, Xingqi Liu, Lu Zhang, and Enlou Zhang. Phylogenetic beta diversity in bacterial assemblages across ecosystems: deterministic versus stochastic processes. *The ISME journal*, 7(7):1310, 2013.

Campbell O Webb, David D Ackerly, Mark A McPeek, and Michael J Donoghue. Phylogenies and Community Ecology. *Annual Review of Ecology and Systematics*, 33(1): 475–505, 2002.

John Webster and Roland Weber. *Introduction to fungi.* Cambridge University Press, 2007.

James T Weedon, William K Cornwell, Johannes HC Cornelissen, Amy E Zanne, Christian Wirth, and David A Coomes. Global meta-analysis of wood decomposition rates: a role for trait variation among tree species? *Ecology Letters*, 12(1):45–56, 2009.

Cassie Marie Welker, Vimal Kumar Balasubramanian, Carloalberto Petti, Krishan Mohan Rai, Seth DeBolt, and Venugopal Mendu. Engineering plant biomass lignin content and composition for biofuels and bioproducts. *Energies*, 8(8):7654–7676, 2015.

Dirk Wesenberg, Frédéric Buchon, and Spiros N Agathos. Degradation of dye-containing textile effluent by the agaric white-rot fungus clitocybula dusenii. *Biotechnology Letters*, 24(12):989–993, 2002.

Ethan P White, SK Morgan Ernest, Andrew J Kerkhoff, and Brian J Enquist. Relationships between body size and abundance in ecology. *Trends in ecology & evolution*, 22 (6):323–330, 2007.

Hadley Wickham. *ggplot2: Elegant Graphics for Data Analysis.* Springer-Verlag New York, 2016.

Hadley Wickham. *httr: Tools for Working with URLs and HTTP*, 2017. R package version 1.3.1.

Hadley Wickham, Jim Hester, and Winston Chang. *devtools: Tools to Make Developing R Packages Easier*, 2018. R package version 1.13.6.

Donald T Wicklow. Fire as an environmental cue initiating ascomycete development in a tallgrass prairie. *Mycologia*, 67(4):852–862, 1975.

Lars-Ove Wikars, Erik Sahlin, and Thomas Ranius. A comparison of three methods to estimate species richness of saproxylic beetles (Coleoptera) in logs and high stumps of Norway spruce. *The Canadian Entomologist*, 137:304–324, 2005.

Craig E Williamson, Richard G Zepp, Robyn M Lucas, Sasha Madronich, Amy T Austin, Carlos L Ballaré, Mary Norval, Barbara Sulzberger, Alkiviadis F Bais, Richard L McKenzie, Sharon A Robinson, Donat P Häder, Nigel D Paul, and Janet F Bornman. Solar ultraviolet radiation in a changing climate. *Nature Climate Change*, 4(6):434–441, 2014.

Paul G Willmer and Dennis M Unwin. Field analyses of insect heat budgets: Reflectance, size and heating rates. *Oecologia*, 50(2):250–255, 1981.

Christina R Wilson, John-Michael Sauer, and Stephen B Hooser. Taxines: a review of the mechanism and toxicity of yew (taxus spp.) alkaloids. *Toxicon*, 39(2):175–185, 2001.

Isaac S Winkler, Charles Mitter, and Sonja J Scheffer. Repeated climate-linked host shifts have promoted diversification in a temperate clade of leaf-mining flies. *Proceedings of the National Academy of Sciences*, pages pnas–0904852106, 2009.

Benjamin E Wolfe, Rodham E Tulloss, and Anne Pringle. The irreversible loss of a decomposition pathway marks the single origin of an ectomycorrhizal symbiosis. *PLoS One*, 7(7):e39597, 2012.

Simon N Wood. Fast stable restricted maximum likelihood and marginal likelihood estimation of semiparametric generalized linear models. *Estimation of Semiparametric Generalized Linear Models*, 73(1):3–36, 2010.

James J Worrall, Susan E Anagnost, and Robert A Zabel. Comparison of wood decay among diverse lignicolous fungi. *Mycologia*, pages 199–219, 1997.

David Hamilton Wright. Species-energy theory: an extension of species-area theory. *Oikos*, pages 496–506, 1983.

Baojun Wu, Jill Gaskell, Benjamin W Held, Cristina Toapanta, Thu Vuong, Steven Ahrendt, Anna Lipzen, Jiwei Zhang, Jonathan S Schilling, Emma Master, Igor V

Bibliography

Gregoriev, Robert A Blanchette, Daniel Cullen, and David S Hibbett. Substrate-specific differential gene expression and rna editing in the brown rot fungus fomitopsis pinicola. *Applied and environmental microbiology*, 84:e00991–18, 2018.

Wenxue Wu, Hsiao-Pei Lu, Akash Sastri, Yi-Chun Yeh, Gwo-Ching Gong, Wen-Chen Chou, and Chih-Hao Hsieh. Contrasting the relative importance of species sorting and dispersal limitation in shaping marine bacterial versus protist communities. *The ISME journal*, 2017.

Rajiv K Yadav, Claudia Bragalini, Laurence Fraissinet-Tachet, Roland Marmeisse, and Patricia Luis. Metatranscriptomics of soil eukaryotic communities. In *Microbial Environmental Genomics (MEG)*, pages 273–287. Springer, 2016.

Haichen Yin, Qihao Shi, Muhammad Shakeel, Jing Kuang, and Jianhong Li. The environmental plasticity of diverse body color caused by extremely long photoperiods and high temperature in Saccharosydne procerus (Homoptera: Delphacidae). *Frontiers in Physiology*, 7, 2016.

Amy E Zanne, David C Tank, William K Cornwell, Jonathan M Eastman, Stephen A Smith, Richard G FitzJohn, Daniel J McGlinn, Brian C O'Meara, Angela T Moles, Peter B Reich, Douglas E Stevens Peter F Westoby Mark Wright Ian J Aarssen Lonnie Bertin Robert I Calaminus Andre Govaerts Rafaël Hemmings Frank Royer, Dana L Soltis, Michelle R. Leishman, Jacek Oleksyn, Pamela S Soltis, Nathan G Swenson, Laura Warman, and Jeremy M Beaulieu. Three keys to the radiation of angiosperms into freezing environments. *Nature*, 506(7486):89–92, 2013.

Dirk Zeuss, Roland Brandl, Martin Brändle, Carsten Rahbek, and Stefan Brunzel. Global warming favours light-coloured insects in europe. *Nature communications*, 5, 2014.

Jizhong Zhou and Daliang Ning. Stochastic community assembly: Does it matter in microbial ecology? *Microbiology and Molecular Biology Reviews*, 81(4):e00002–17, 2017.

Lucie Zinger, Pierre Taberlet, Heidy Schimann, Aurélie Bonin, Frédéric Boyer, Marta De Barba, Philippe Gaucher, Ludovic Gielly, Charline Giguet-Covex, Amaia Iribar, Maxime Réjou-Méchain, Gilles Rayé, Delphine Rioux, Vincent Schilling, Blaise Tymen, Jérôme Viers, Cyril Zouiten, Wilfried Thuiller, Eric Coissac, and Jérôme Chave. Soil community assembly varies across body sizes in a tropical forest. *bioRxiv*, page 154278, 2017.

A Figures

Figure A.1: Phylogeny with SH support values. A zoom-able version with species names and Shimodaira–Hasegawa approximate likelihood ratio test support values (SH-aLRT branch support). Figure see next page.

Nodes: SH-like support values

Million years
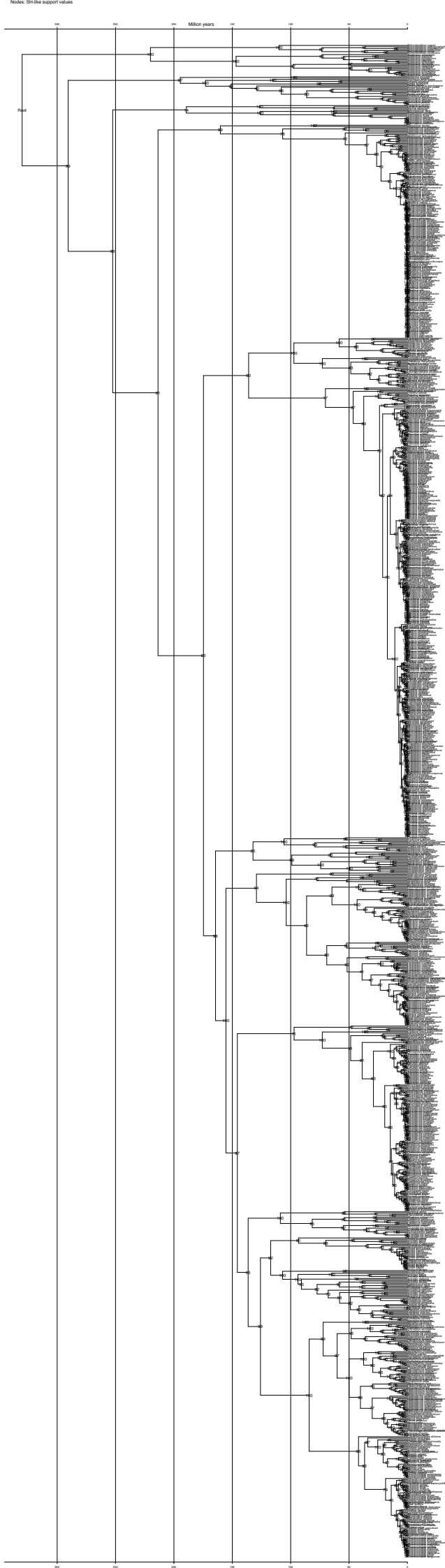
Figure A.2: Maximum-likelihood phylogeny. Branch support is given as Shimodaira–Hasegawa approximate likelihood ratio tests (SH-aLRT). The phylogeny was produced based on a mega-phylogeny approach. Note that branch lengths were rescaled for improved visibility of support values. Lightness values and mean species color values are provided with the tip labels. Figure see next pages.

.

Craterellus tubaeformis
Craterellus cornucopioides
Cantharellus romagnesianus
Cantharellus friesii
Cantharellus subpruinosus
Cantharellus cibarius
Cantharellus ferruginascens
Cantharellus amethysteus
Sistotrema brinkmannii
Sistotrema pistilliferum
Sistotrema oblongisporum
Sistotrema resinicystidium
Sistotrema coroniferum
Sistotrema raduloides
Sistotrema coronilla
Sistotrema athelioides
Sistotrema octosporum
Sistotrema biggsiae
Sistotrema efibulatum
Sistotrema sernanderi
Sistotrema muscicola
Sistotrema alboluteum
Sistotrema confluens
Hydnum umbilicatum
Hydnum ellipsosporum
Hydnum rufescens
Hydnum repandum
Auriscalpium vulgare
Albatrellus confluens
Albatrellus ovinus
Albatrellus citrinus
Lactarius helvus
Lactarius serifluus
Lactarius cremor
Lactarius rostratus
Lactarius camphoratus
Lactarius subumbonatus
Lactarius quietus
Lactarius atlanticus
Lactarius torminosulus
Russula subrubens
Lactarius torminosus
Lactarius acerrimus
Lactarius scrobiculatus
Lactarius leonis
Lactarius ruginosus
Lactarius lignyotus
Lactarius pterosporus
Lactarius subruginosus
Lactarius rufus
Lactarius tabidus
Lactarius subdulcis
Lactarius hepaticus
Lactarius decipiens
Lactarius lacunarum
Lactarius lapponicus
Lactarius omphaliiformis
Lactarius badiosanguineus
Lactarius rubrocinctus
Lactarius sphagneti
Lactarius fulvissimus
Russula camarophylla
Lactarius controversus
Lactarius circellatus
Lactarius musteus
Lactarius porninsis
Lactarius lilacinus
Lactarius lepidotus
Lactarius pallidus
Lactarius semisanguifluus
Lactarius plumbeus
Lactarius zonarioides
Lactarius mairei
Lactarius nanus
Lactarius flavopalustris
Lactarius stephensii
Lactarius illyricus
Lactarius obscuratus
Lactarius aurantiacus
Lactarius cyathuliformis
Lactarius brunneohepaticus
Lactarius necator
Lactarius citriolens
Lactarius tuomikoskii
Lactarius vietus
Russula pallescens
Lactarius piperatus
Lactifluus glaucescens
Lactarius pergamenus
Lactarius spinosulus
Lactarius albocarneus
Lactarius resimus
Lactarius auriolla
Lactarius evosmus
Lactarius dryadophilus
Lactarius aquizonatus
Lactarius pubescens
Lactarius alpinus
Lactarius scoticus
Lactarius hysginoides

212

Lactarius lanceolatus
Lactarius repraesentaneus
Lactarius glyciosmus
Lactarius mammosus
Lactarius uvidus
Lactarius flexuosus
Lactarius blennius
Lactarius fluens
Lactarius azonites
Lactarius romagnesii
Lactarius fuliginosus
Lactarius picinus
Lactarius quieticolor
Lactarius salmonicolor
Lactarius sanguifluus
Lactarius paradoxus
Lactarius deliciosus
Lactarius fennoscandicus
Lactarius chrysorrheus
Lactarius trivialis
Lactarius acris
Lactifluus bertillonii
Lactarius vellereus
Lactifluus volemus
Lactifluus rugatus
Lactarius aspideus
Lactarius pseudouvidus
Lactarius violascens
Lactarius brunneoviolaceus
Lactarius luridus
Russula pallidospora
Russula langei
Russula cyanoxantha
Lactifluus luteolus
Russula mariae
Russula amoenicolor
Russula violeipes
Russula amoena
Russula mustelina
Russula medullata
Russula heterophylla
Russula aeruginea
Russula anatina
Russula parazurea
Russula grisea
Russula virescens
Russula vesca
Russula brunneola
Russula faustiana
Russula atroglauca
Russula ionochlora
Russula variegatula
Russula chloroides
Russula delica
Russula risigallina
Russula fuliginosa
Russula adusta
Russula densifolia
Russula albonigra
Russula nigricans
Russula acrifolia
Russula anthracina
Russula pectinata
Russula illota
Russula subfoetens
Russula fragrantissima
Russula grata
Russula lutensis
Russula amoenolens
Russula sororia
Russula livescens
Russula insignis
Russula pectinatoides
Russula praetervisa
Russula viscida
Russula carpini
Russula cavipes
Russula aquosa
Russula laricina
Russula atropurpurea
Russula azurea
Russula zvarae
Russula minutula
Russula laeta
Russula amethystina
Russula postiana
Russula lilacea
Russula emeticicolor
Russula violacea
Russula cessans
Russula odorata
Russula gracilis
Russula solaris
Russula puellula
Russula violaceoincarnata
Russula graminea
Russula veternosa
Russula rubra
Russula persicina
Russula consobrina

213

Russula puellaris
Russula melitodes
Russula pseudointegra
Russula clariana
Russula integra
Russula helodes
Russula messapica
Russula versicolor
Russula badia
Russula decolorans
Russula maculata
Russula graveolens
Russula sphagnophila
Russula nitida
Russula amoenipes
Russula clavipes
Russula pascua
Russula faginea
Russula xerampelina
Russula favrei
Russula torulosa
Russula carminipes
Russula melzeri
Russula curtipes
Lactarius zonarius
Russula saliceticola
Russula melliolens
Russula caerulea
Russula claroflava
Russula vinosa
Russula dryadicola
Russula nauseosa
Russula sapinea
Russula velenovskyi
Russula aurantiaca
Russula lepidicolor
Russula paludosa
Russula cuprea
Russula brunneoviolacea
Russula pelargonia
Russula fuscorubroides
Russula atrorubens
Russula silvestris
Russula laccata
Russula nana
Russula emetica
Russula decipiens
Russula olivacea
Russula turci
Russula roseipes
Russula luteotacta
Russula betularum
Russula gracillima
Russula queletii
Russula ochroleuca
Russula alnetorum
Russula raoultii
Russula sardonia
Russula sanguinea
Russula fellea
Russula exalbicans
Russula sanguinaria
Russula foetens
Russula farinipes
Russula fragilis
Russula rosea
Russula firmula
Russula gigasperma
Russula aurea
Russula romellii
Russula rubroalba
Russula alutacea
Volvariella volvacea
Volvariella bombycina
Volvariella surrecta
Volvariella strangulata
Volvariella hypopithys
Volvariella pusilla
Volvariella caesiotincta
Volvariella taylorii
Tricholoma sulphurescens
Plicaturopsis crispa
Phyllotopsis nidulans
Hygrophoropsis aurantiaca
Hygrophoropsis rufa
Tapinella atrotomentosa
Tapinella panuoides
Chroogomphus helveticus
Chroogomphus rutilus
Chroogomphus fulmineus
Suillus cavipes
Suillus tridentinus
Suillus grevillei
Suillus bresadolae
Suillus viscidus
Suillus bovinus
Suillus plorans
Suillus granulatus
Suillus lakei
Suillus amabilis

214

Tubaria romagnesiana
Hohenbuehelia fluxilis
Merismodes fasciculata
Megacollybia platyphylla
Gerronema strombodes
Hydropus atramentosus
Hydropus marginellus
Hydropus subalpinus
Arrhenia rustica
Gerronema albidum
Clitocybula lacerata
Marasmiellus candidus
Crinipellis scabella
Marasmius rotula
Marasmius bulliardii
Arrhenia auriscalpium
Marasmius curreyi
Marasmius graminum
Chaetocalathus craterellus
Marasmius oreades
Marasmius torquescens
Marasmius cohaerens
Marasmius wynneae
Macrocystidia cucumis
Rhodocybe truncata
Pholiota flammans
Entoloma rusticoides
Entoloma flocculosum
Entoloma sericeoides
Entoloma phaeocyathus
Cantharellopsis prescotii
Mycena oregonensis
Mycena galopus
Cortinarius mussivus
Lepiota oreadiformis
Galerina discreta
Omphalina rivulicola
Deconica horizontalis
Omphalotus illudens
Omphalotus olearius
Lepista ovispora
Lepista irina
Lepista subconnexa
Lepista densifolia
Ripartites tricholoma
Ripartites metrodii
Ripartites albidoincarnatus
Clitocybe alexandri
Entoloma asprellum
Pseudoclitocybe cyathiformis
Pseudoclitocybe expallens
Pseudoclitocybe obbata
Amanita crocea
Lyophyllum leucophaeatum
Arrhenia epichysium
Flammulaster muricatus
Crepidotus malachius
Crepidotus distortus
Crepidotus crocophyllus
Simocybe haustellaris
Crepidotus applanatus
Crepidotus cesatii
Crepidotus versutus
Crepidotus cinnabarinus
Crepidotus calolepis
Crepidotus mollis
Crepidotus variabilis
Crepidotus subverrucisporus
Crepidotus epibryus
Crepidotus luteolus
Pogonoloma spinulosum
Pogonoloma macrocephalum
Leucopaxillus nauseosodulcis
Limacella illinita
Amanita inopinata
Amanita vittadinii
Amanita gracilior
Amanita strobiliformis
Amanita verna
Amanita virosa
Amanita phalloides
Amanita franchetii
Amanita excelsa
Amanita novinupta
Amanita rubescens
Amanita citrina
Amanita porphyria
Tricholoma roseoacerbum
Amanita pantherina
Amanita gemmata
Amanita muscaria
Amanita regalis
Amanita supravolvata
Amanita fulva
Amanita battarrae
Amanita ceciliae
Amanita nivalis
Amanita vaginata
Amanita friabilis
Amanita beckeri

216

Melanoleuca brevipes
Melanoleuca microcephala
Melanoleuca pseudoluscina
Melanoleuca phaeopodia
Melanoleuca rasilis
Leucocybe connata
Clitocybe truncicola
Clitopilus passeckerianus
Clitocybe vibecina
Clitocybe foetens
Entoloma rhodocylix
Tricholomella constricta
Entoloma strigosissimum
Collybia cirrhata
Collybia tuberosa
Collybia cookei
Clitocybe dryadicola
Clitocybe festiva
Clitocybe odora
Clitocybe phyllophila
Clitocybe agrestis
Hypsizygus ulmarius
Rugosomyces naucoria
Entoloma cuspidiferum
Hypsizygus tessulatus
Tephrocybe anthracophila
Tephrocybe rancida
Lyophyllum semitale
Lyophyllum pseudosinuatum
Lyophyllum paelochroum
Lyophyllum infumatum
Lyophyllum rhopalopodium
Lyophyllum amariusculum
Lyophyllum crassifolium
Lyophyllum deliberatum
Lyophyllum transforme
Lyophyllum aemiliae
Lepista nuda
Clitocybe rivulosa
Clitocybe fragrans
Clitocybe paxillus
Clitocybe brumalis
Clitocybe quercina
Clitocybe ditopa
Clitocybe favrei
Clitocybe robusta
Clitocybe nebularis
Entoloma atrosericeum
Hygrophorus marzuolus
Clitocybe metachroa
Clitocybe amarescens
Entoloma caeruleopolitum
Tephrocybe confusa
Pseudoomphalina kalchbrenneri
Melanoleuca cognata
Gliophorus reginae
Panaeolus cyanescens
Panaeolus olivaceus
Panaeolus acuminatus
Panaeolus rickenii
Panaeolus alcis
Panaeolus papilionaceus
Leucopaxillus alboalutaceus
Leucopaxillus tricolor
Leucopaxillus gentianeus
Leucopaxillus albissimus
Leucopaxillus cerealis
Leucopaxillus paradoxus
Hydropus trichoderma
Tricholoma apium
Tricholoma stans
Tricholoma saponaceum
Tricholoma sudum
Tricholoma aestuans
Chromosera xanthochroa
Tricholoma orirubens
Tricholoma album
Tricholoma lascivum
Tricholoma stiparophyllum
Tricholoma magnivelare
Tricholoma matsutake
Tricholoma caligatum
Tricholoma dulciolens
Clitocybe trulliformis
Tricholoma basirubens
Tricholoma guldeniae
Tricholoma josserandii
Tricholoma joachimii
Tricholoma virgatum
Tricholoma atrosquamosum
Tricholoma sejunctum
Tricholoma olivaceotinctum
Tricholoma viridilutescens
Tricholoma arvernense
Tricholoma terreum
Tricholoma argyraceum
Tricholoma scalpturatum
Tricholoma cingulatum
Tricholoma triste
Tricholoma filamentosum

Entoloma indutoides
Entoloma jubatum
Entoloma fuscotomentosum
Entoloma henricii
Entoloma nitens
Entoloma mougeotii
Entoloma griseocyaneum
Entoloma poliopus
Entoloma incanum
Entoloma serrulatum
Entoloma caesiocinctum
Entoloma querquedula
Entoloma pseudocoelestinum
Entoloma mutabilipes
Entoloma exile
Entoloma atrocoeruleum
Psilocybe subviscida
Psilocybe apelliculosa
Psilocybe inquilina
Psilocybe crobula
Galerina stordalii
Galerina pseudocerina
Galerina clavata
Galerina arctica
Phaeomarasmius erinaceus
Flammulaster carpophilus
Tubaria albostipitata
Tubaria dispersa
Tubaria confragosa
Tubaria conspersa
Tubaria praestans
Tubaria furfuracea
Galerina pumila
Agrocybe pusiola
Agrocybe arvalis
Agrocybe putaminum
Gymnopilus fulgens
Agrocybe pediades
Agrocybe firma
Agrocybe praecox
Phaeolepiota aurea
Cystoderma superbum
Galerina fallax
Gymnopilus picreus
Gymnopilus odini
Gymnopilus decipiens
Gymnopilus junonius
Gymnopilus penetrans
Gymnopilus hybridus
Galerina paludosa
Galerina hypnorum
Galerina sphagnorum
Galerina allospora
Galerina calyptrata
Galerina sphagnicola
Galerina harrisonii
Galerina lubrica
Galerina subcerina
Galerina mniophila
Galerina cephalotricha
Gliophorus psittacinus
Phaeocollybia jennyae
Phaeocollybia festiva
Melanoleuca grammopodia
Melanoleuca curtipes
Melanoleuca humilis
Amanita caesarea
Tricholoma sciodes
Hygrocybe russocoriacea
Tricholoma acerbum
Inocybe arenicola
Inocybe mimica
Inocybe flavella
Inocybe squamata
Inocybe obsoleta
Inocybe perlata
Inocybe rimosa
Inocybe melliolens
Inocybe bulbosissima
Inocybe relicina
Inocybe whitei
Inocybe geophylla
Inocybe phaeodisca
Inocybe cryptocystis
Inocybe posterula
Inocybe maculata
Inocybe cookei
Inocybe quietiodor
Inocybe adaequata
Inocybe erubescens
Inocybe bongardii
Inocybe calamistrata
Inocybe cervicolor
Inocybe ochracea
Inocybe nitidiuscula
Inocybe giacomi
Inocybe flocculosa
Tricholoma pseudonictitans
Inocybe pseudodestricta
Inocybe rufuloides

221

Inocybe exilis
Inocybe tarda
Inocybe paludinella
Inocybe sambucina
Inocybe sapinea
Inocybe castanea
Inocybe godeyi
Inocybe phaeoleuca
Inocybe tjallingiorum
Inocybe ochroalba
Inocybe vulpinella
Inocybe decemgibbosa
Inocybe inodora
Inocybe fibrosoides
Inocybe tabacina
Inocybe pruinosa
Inocybe rivularis
Inocybe taxocystis
Inocybe favrei
Inocybe glabrodisca
Inocybe calida
Inocybe malenconii
Inocybe leucoloma
Inocybe auricomella
Inocybe putilla
Inocybe aurea
Inocybe subcarpta
Inocybe proximella
Inocybe stellatospora
Inocybe acuta
Inocybe pseudoasterospora
Inocybe soluta
Inocybe grammata
Inocybe amethystina
Inocybe subbrunnea
Inocybe catalaunica
Inocybe glabrescens
Inocybe griseovelata
Inocybe sindonia
Inocybe splendens
Inocybe tenebrosa
Inocybe appendiculata
Inocybe grammopodia
Inocybe roseipes
Inocybe assimilata
Inocybe pseudohiulca
Inocybe napipes
Inocybe asterospora
Inocybe praetervisa
Inocybe alnea
Inocybe rennyi
Inocybe salicis
Mycena acicula
Inocybe xanthomelas
Inocybe saliceticola
Inocybe concinnula
Inocybe rufofusca
Inocybe fuscidula
Inocybe hirtella
Inocybe maculipes
Inocybe melanopus
Inocybe subporospora
Inocybe aeruginascens
Inocybe squarrosa
Inocybe serotina
Inocybe leptocystis
Inocybe queletii
Inocybe pseudoreducta
Inocybe cincinnata
Inocybe pusio
Inocybe lacera
Inocybe obscurobadia
Inocybe griseolilacina
Inocybe langei
Inocybe glabripes
Inocybe subnudipes
Inocybe auricoma
Inocybe fuligineoatra
Inocybe calospora
Inocybe tigrina
Inocybe mixtilis
Inocybe hystrix
Leucoagaricus melanotrichus
Inocybe incarnata
Inocybe pyriodora
Inocybe corydalina
Inocybe moelleri
Inocybe haemacta
Inocybe rufoalba
Inocybe brunneotomentosa
Inocybe umbratica
Inocybe fibrosa
Inocybe petiginosa
Inocybe egenula
Inocybe nematoloma
Inocybe leptophylla
Inocybe lanuginosa
Inocybe curvipes
Inocybe impexa
Inocybe dunensis

222

Laccaria lateritia
Laccaria ohiensis
Laccaria laccata
Laccaria tortilis
Laccaria amethystina
Laccaria proxima
Laccaria montana
Laccaria pumila
Laccaria bicolor
Pholiota scamba
Lactocollybia epia
Pholiota decussata
Pholiota carbonaria
Pholiota brunnescens
Pholiota flavida
Pholiota henningsii
Pholiota highlandensis
Pholiota mixta
Pholiota spumosa
Pholiota lenta
Pholiota lubrica
Leratiomyces squamosus
Leratiomyces laetissimus
Leratiomyces ceres
Pholiota subochracea
Hypholoma subericaeum
Hypholoma polytrichi
Hypholoma myosotis
Hypholoma marginatum
Hypholoma dispersum
Hypholoma ericaeum
Hypholoma fasciculare
Hypholoma capnoides
Stropharia hornemannii
Stropharia coronilla
Stropharia rugosoannulata
Stropharia inuncta
Stropharia aeruginosa
Stropharia caerulea
Pluteus salicinus
Pluteus atromarginatus
Pluteus pellitus
Pluteus pseudorobertii
Pluteus petasatus
Pluteus pouzarianus
Pluteus primus
Pluteus alniphilus
Pluteus cervinus
Pluteus brunneoradiatus
Pluteus pallidus
Pluteus luctuosus
Pluteus hispidulus
Pluteus nanus
Naucoria amarescens
Stropharia melanosperma
Kuehneromyces mutabilis
Psilocybe subcoprophila
Phaeogalera stagnina
Deconica xeroderma
Chromosera citrinopallida
Chromosera cyanophylla
Psilocybe silvatica
Psilocybe medullosa
Psilocybe liniformans
Psilocybe fimetaria
Psilocybe cubensis
Psilocybe stuntzii
Galerina salicicola
Psilocybe semilanceata
Flammulaster limulatus
Agrocybe vervacti
Agrocybe dura
Lyophyllum fumosum
Lyophyllum shimeji
Lyophyllum loricatum
Lyophyllum decastes
Parasola auricoma
Parasola megasperma
Parasola kuehneri
Parasola lilatincta
Parasola plicatilis
Parasola hemerobia
Parasola hercules
Parasola leiocephala
Parasola galericuliformis
Psathyrella variata
Lacrymaria lacrymabunda
Lacrymaria glareosa
Coprinopsis marcescibilis
Coprinopsis pannucioides
Coprinopsis cothurnata
Coprinopsis nivea
Coprinopsis pseudonivea
Coprinopsis strossmayeri
Coprinopsis picacea
Coprinopsis stangliana
Psathyrella melanthina
Coprinopsis krieglsteineri
Coprinopsis xenobia
Coprinopsis lagopus

224

Coprinopsis pachyderma
Coprinopsis lagopides
Coprinopsis jonesii
Coprinopsis spelaiophila
Coprinopsis semitalis
Coprinopsis trispora
Coprinopsis narcotica
Coprinopsis sclerotiger
Coprinopsis laanii
Coprinopsis stercorea
Coprinopsis cinerea
Coprinopsis insignis
Coprinopsis spilospora
Coprinopsis sclerotiorum
Coprinopsis urticicola
Coprinopsis episcopalis
Coprinopsis gonophylla
Coprinopsis phaeospora
Coprinopsis pseudofriesii
Coprinopsis friesii
Coprinopsis ochraceolanata
Coprinopsis romagnesiana
Coprinopsis acuminata
Coprinopsis atramentaria
Coprinopsis erythrocephala
Coprinopsis echinospora
Coprinopsis phlyctidospora
Coprinopsis rugosobispora
Coprinopsis martinii
Coprinopsis macrocephala
Coprinopsis candidolanata
Coprinopsis radiata
Coprinopsis tectispora
Coprinopsis scobicola
Coprinopsis ammophilae
Coprinopsis pseudoradiata
Coprinellus verrucispermus
Coprinellus angulatus
Coprinellus sclerocystidiosus
Coprinellus subimpatiens
Coprinellus disseminatus
Coprinellus bisporiger
Coprinellus truncorum
Coprinellus micaceus
Coprinellus xanthothrix
Coprinellus domesticus
Coprinellus radians
Coprinellus heptemerus
Coprinellus curtus
Coprinellus flocculosus
Coprinellus marculentus
Coprinellus subdisseminatus
Coprinellus velatopruinatus
Coprinellus canistri
Coprinellus heterothrix
Coprinellus heterosetulosus
Coprinellus congregatus
Coprinellus bisporus
Coprinellus callinus
Coprinellus amphithallus
Coprinellus plagioporus
Coprinellus impatiens
Coprinellus sassii
Coprinellus subpurpureus
Coprinellus pellucidus
Coprinellus brevisetulosus
Psathyrella badiophylla
Psathyrella lacuum
Psathyrella leucotephra
Psathyrella candolleana
Psathyrella bipellis
Psathyrella cotonea
Psathyrella microrhiza
Psathyrella squamosa
Psathyrella corrugis
Psathyrella amarescens
Psathyrella pseudogracilis
Laccaria fraterna
Psathyrella effibulata
Psathyrella calcarea
Psathyrella orbitarum
Hemimycena tortuosa
Psathyrella ammophila
Psathyrella spadiceogrisea
Psathyrella fatua
Psathyrella phegophila
Psathyrella clivensis
Psathyrella longicauda
Psathyrella mesobromionis
Psathyrella typhae
Pterula subulata
Psathyrella multipedata
Psathyrella tephrophylla
Psathyrella fusca
Psathyrella panaeoloides
Coprinellus ellisii
Coprinellus hiascens
Psathyrella reticulata
Psathyrella pygmaea
Psathyrella lutensis

Psathyrella impexa
Psathyrella maculata
Psathyrella vestita
Psathyrella supernula
Psathyrella prona
Psathyrella stercoraria
Psathyrella olympiana
Psathyrella piluliformis
Psathyrella pertinax
Psathyrella dunensis
Psathyrella senex
Psathyrella obtusata
Psathyrella vernalis
Psathyrella orbicularis
Psathyrella pennata
Psathyrella fulvescens
Psathyrella pseudocasca
Psathyrella fagetophila
Psathyrella murcida
Psathyrella pseudocorrugis
Psathyrella rubiginosa
Psathyrella flexispora
Psathyrella cortinarioides
Psathyrella fibrillosa
Psathyrella artemisiae
Psathyrella sphagnicola
Psathyrella spintrigeroides
Psathyrella rostellata
Psathyrella hirta
Psathyrella gordonii
Psathyrella pervelata
Psathyrella sphaerocystis
Psathyrella tenuicula
Psathyrella umbrina
Psathyrella seymourensis
Psathyrella dicrani
Psathyrella scatophila
Psathyrella kitsiana
Psathyrella sacchariolens
Simocybe reducta
Phaeocollybia christinae
Simocybe centunculus
Simocybe sumptuosa
Inocybe fastigiella
Inocybe arthrocystis
Inocybe fulvipes
Inocybe terrigena
Inocybe umbrinofusca
Inocybe fuscomarginata
Inocybe gymnocarpa
Inocybe leucoblema
Calocybe gambosa
Lyophyllum favrei
Volvariella media
Volvopluteus gloiocephalus
Hygrophorus latitabundus
Melanoleuca albifolia
Pluteus poliocnemis
Pluteus diettrichii
Pluteus umbrosus
Pluteus leoninus
Pluteus roseipes
Pluteus variabilicolor
Pluteus thomsonii
Pluteus insidiosus
Pluteus plautus
Pluteus semibulbosus
Pluteus cinereofuscus
Pluteus aurantiorugosus
Pluteus romellii
Pluteus podospileus
Pluteus ephebeus
Pluteus phlebophorus
Lepiota tomentella
Lepiota pyrochroa
Coprinopsis geesterani
Lepiota subalba
Cystolepiota icterina
Lepiota apatelia
Coprinus comatus
Battarrea phalloides
Montagnea arenaria
Coprinus sterquilinus
Cystolepiota adulterina
Lepiota parvannulata
Macrolepiota procera
Macrolepiota fuliginosa
Macrolepiota permixta
Macrolepiota excoriata
Macrolepiota mastoidea
Macrolepiota prominens
Macrolepiota konradii
Macrolepiota gracilenta
Lepiota castanea
Lepiota cingulum
Lepiota pilodes
Leucoagaricus barssii
Hygrophorus chrysodon
Hygrophorus hedrychii
Cortinarius talus

226

Cortinarius rapaceus
Descolea antarctica
Agrocybe rivulosa
Psilocybe caerulipes
Cortinarius subtortus
Rugosomyces obscurissimus
Rugosomyces carneus
Tephrocybe platypus
Tephrocybe coracina
Hygrophorus camarophyllus
Tricholoma inamoenum
Tricholoma sulphureum
Tricholoma bufonium
Tricholoma portentosum
Tricholoma frondosae
Tricholoma equestre
Lepiota brunneoincarnata
Lepiota helveola
Lepiota boudieri
Lepiota lilacea
Lepiota hymenoderma
Lepiota speciosa
Lepiota cristatoides
Lepiota ochraceofulva
Melanophyllum eyrei
Echinoderma asperum
Lepiota clypeolarioides
Cystolepiota seminuda
Melanophyllum haematospermum
Cystolepiota cystophora
Lepiota elaiophylla
Lepiota fuscovinacea
Cystolepiota pulverulenta
Lepiota magnispora
Lepiota clypeolaria
Lepiota cortinarius
Lepiota grangei
Lepiota cristata
Lepiota psalion
Lepiota pseudolilacea
Lepiota subgracilis
Lepiota forquignonii
Lepiota xanthophylla
Lepiota echinella
Lepiota felina
Lepiota subincarnata
Cortinarius assiduus
Leucoagaricus georginae
Leucoagaricus serenus
Leucoagaricus tener
Leucoagaricus crystallifer
Leucoagaricus sublittoralis
Leucoagaricus rubrotinctus
Leucoagaricus littoralis
Leucoagaricus meleagris
Leucoagaricus americanus
Leucoagaricus sericifer
Leucocoprinus cretaceus
Leucocoprinus brebissonii
Leucocoprinus birnbaumii
Leucoagaricus pilatianus
Leucocoprinus fragilissimus
Leucoagaricus croceovelutinus
Leucoagaricus ionidicolor
Leucocoprinus cepistipes
Leucoagaricus cinerascens
Leucoagaricus nympharum
Leucoagaricus subcretaceus
Leucoagaricus gaillardii
Leucoagaricus leucothites
Chlorophyllum hortense
Chlorophyllum molybdites
Agaricus subrufescens
Chlorophyllum agaricoides
Leucoagaricus medioflavoides
Lepiota pseudofelina
Lepiota griseovirens
Chlorophyllum brunneum
Chlorophyllum olivieri
Agaricus campestris
Agaricus depauperatus
Agaricus langei
Agaricus phaeolepidotus
Agaricus porphyrocephalus
Agaricus moellerianus
Agaricus moelleri
Agaricus bohusii
Agaricus pequinii
Agaricus gennadii
Agaricus hondensis
Agaricus pseudopratensis
Agaricus xanthodermus
Agaricus placomyces
Agaricus iodosmus
Agaricus bisporus
Agaricus subfloccosus
Agaricus devoniensis
Agaricus bitorquis
Agaricus subperonatus
Agaricus fuscofibrillosus

227

Cortinarius bivelus
Cortinarius scandens
Cortinarius diasemospermus
Cortinarius comptulus
Cortinarius scotoides
Cortinarius atropusillus
Cortinarius saturatus
Cortinarius praestigiosus
Cortinarius vernalis
Cortinarius oreobius
Cortinarius rufostriatus
Cortinarius laetissimus
Cortinarius evernius
Cortinarius cagei
Hygrophorus erubescens
Cortinarius fuscoperonatus
Cortinarius ionosmus
Cortinarius disjungendus
Cortinarius brunneofulvus
Cortinarius parvannulatus
Cortinarius laniger
Cortinarius phaeopygmaeus
Cortinarius helvelloides
Cortinarius torvus
Cortinarius umbrinolens
Cortinarius venustus
Cortinarius agathosmus
Cortinarius canabarba
Cortinarius urbicus
Cortinarius colus
Cortinarius anthracinus
Cortinarius bulliardii
Cortinarius cinnabarinus
Cortinarius traganus
Cortinarius suberi
Cortinarius malachius
Cortinarius aprinus
Cortinarius turgidus
Cortinarius triformis
Cortinarius biformis
Cortinarius balaustinus
Cortinarius alboviolaceus
Cortinarius armeniacus
Cortinarius tortuosus
Cortinarius casimiri
Cortinarius saturninus
Cortinarius vernus
Cortinarius helobius
Cortinarius erythrinus
Cortinarius inops
Cortinarius fusisporus
Cortinarius albonigrellus
Cortinarius parevernius
Cortinarius pulchripes
Cortinarius psammocephalus
Cortinarius alnetorum
Cortinarius flexipes
Cortinarius angelesianus
Cortinarius decipiens
Cortinarius paleaceus
Cortinarius cotoneus
Cortinarius venetus
Cortinarius gentilis
Cortinarius crassus
Cortinarius vacciniophilus
Cortinarius patibilis
Cortinarius spadicellus
Cortinarius violaceomaculatus
Cortinarius infractus
Cortinarius olivaceofuscus
Cortinarius uliginosus
Cortinarius polaris
Cortinarius claricolor
Cortinarius superbus
Cortinarius nanceiensis
Cortinarius inamoenus
Cortinarius subbalteatus
Cortinarius turmalis
Cortinarius sebaceus
Cortinarius fulminoides
Cortinarius aquilanus
Cortinarius polymorphus
Cortinarius camptoros
Cortinarius terpsichores
Cortinarius anserinus
Cortinarius eucaeruleus
Cortinarius spilomeus
Phaeomarasmius rimulincola
Cortinarius odorifer
Cortinarius alnobetulae
Cortinarius corrosus
Cortinarius cisticola
Cortinarius citrinolilacinus
Cortinarius napus
Cortinarius claroflavus
Cortinarius xanthophyllus
Cortinarius fulmineus
Cortinarius cliduchus
Cortinarius obsoletus
Cortinarius balteatus

Cortinarius suaveolens
Cortinarius cedretorum
Cortinarius olearioides
Cortinarius odoratus
Cortinarius dalecarlicus
Cortinarius olivascentium
Cortinarius camphoratus
Cortinarius illibatus
Cortinarius delibutus
Cortinarius violaceus
Cortinarius hercynicus
Cortinarius cumatilis
Cortinarius vulpinus
Dendrocollybia racemosa
Cortinarius atrovirens
Cortinarius ionochlorus
Cortinarius hemitrichus
Cortinarius testaceofolius
Cortinarius populinus
Cortinarius renidens
Cortinarius tubulipes
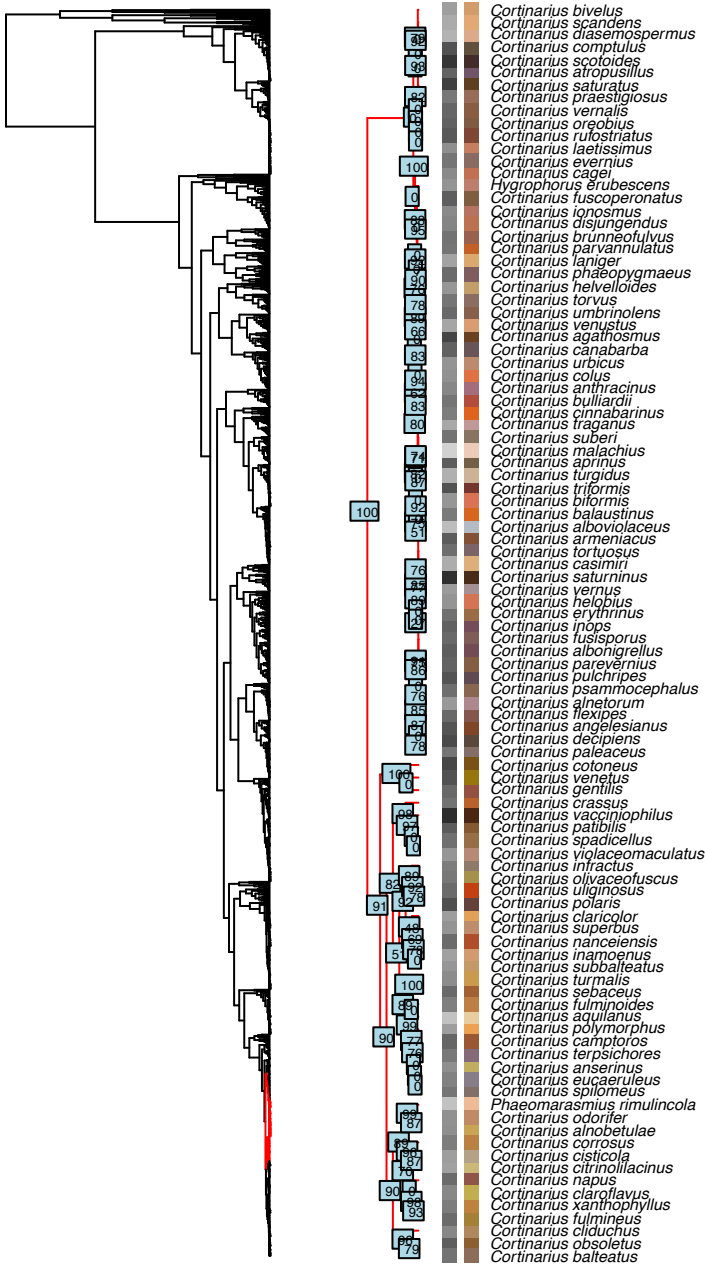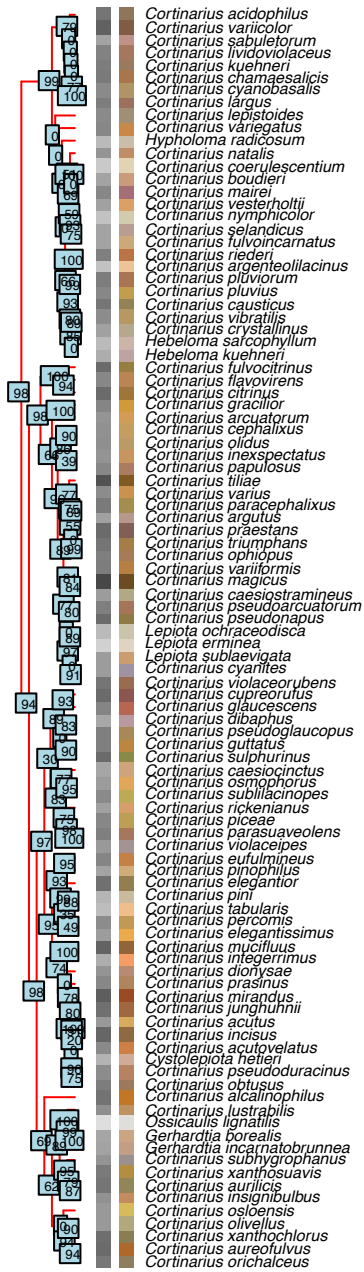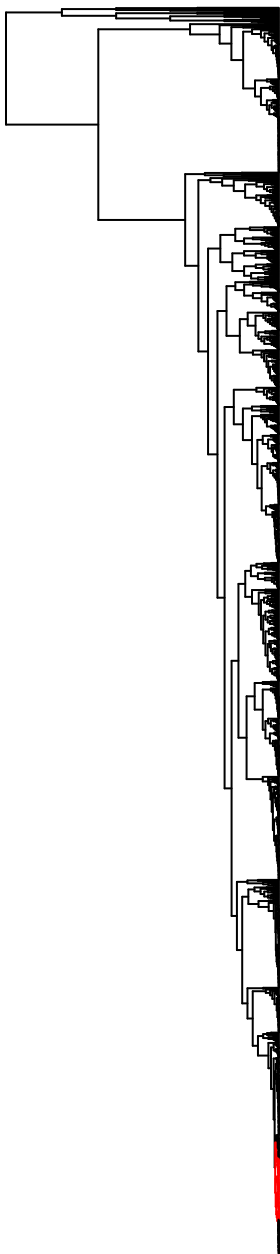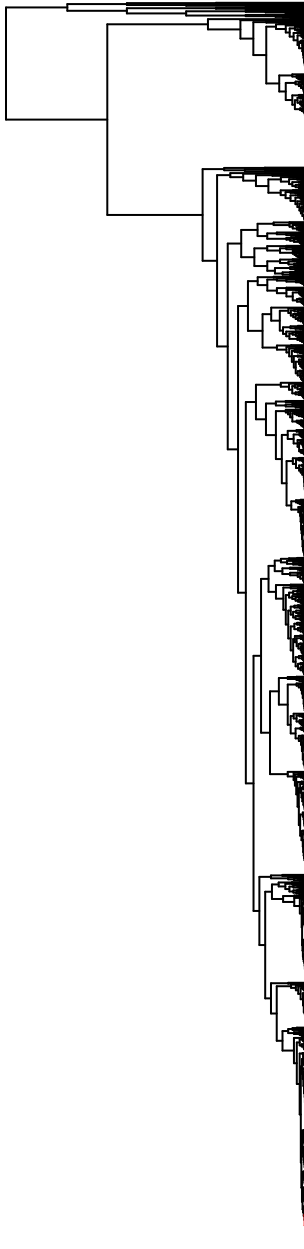*Cystoderma jasonis*
Cystoderma carcharias
Cystoderma subvinaceum
Cystoderma amianthinum
Cortinarius humolens
Cortinarius catharinae
Cortinarius barbarorum
Cortinarius arquatus
Cortinarius luhmannii
Cortinarius caperatus
Cortinarius splendens
Cortinarius meinhardii
Cortinarius caesiocortinatus
Cortinarius caesiocanescens
Cortinarius caerulescens
Cortinarius platypus
Cortinarius lilacinovelatus
Cortinarius sodagnitus
Cortinarius subarquatus
Cortinarius spectabilis
Cortinarius saporatus
Cortinarius volvatus
Cortinarius gentianeus
Cortinarius pseudocyanites
Cortinarius sphagnophilus
Cortinarius montanus
Cortinarius scaurus
Cortinarius bolaris
Cortinarius balteatocumatilis
Cortinarius albidus
Cortinarius saniosus
Cortinarius chrysomallus
Cortinarius splendificus
Cortinarius citrinofulvescens
Cortinarius callisteus
Cortinarius tofaceus

232

B Tables

Table B.1: List of fruiting species of fungi and total number of records (sector count, see 'Fruit body sampling') found in the experiment of Chapter 4

No.	Species	Total number of records
1	*Aleurodiscus amorphus*	185
2	*Amphinema byssoides*	6
3	*Amylostereum chailletii*	849
4	*Antrodia serialis*	10
5	*Armillaria lutea*	2
6	*Ascocoryne cylichnium*	5
7	*Ascocoryne sarcoides*	550
8	*Ascocoryne solitaria*	15
9	*Ascodichaena rugosa*	93
10	*Asterosporium hoffmannii*	7
11	*Athelia arachnoidea*	2
12	*Athelia cystidiolophora*	1
13	*Athelia decipiens*	2
14	*Athelia epiphylla*	32
15	*Athelia neuhoffii*	1
16	*Auricularia auriculajudae*	1
17	*Basidioradulum radula*	1
18	*Bertia latispora*	39
19	*Bertia moriformis*	30
20	*Biscogniauxia nummularia*	33
21	*Bisporella antennata*	1904
22	*Bisporella citrina*	68
23	*Bisporella pallescens*	145
24	*Bjerkandera adusta*	706
25	*Botryobasidium candicans*	7
26	*Botryobasidium laeve*	3

No.	Species	Total number of records
27	*Botryobasidium obtusisporum*	3
28	*Botryobasidium subcoronatum*	17
29	*Botryobasidium vagum*	28
30	*Botryohypochnus isabellinus*	4
31	*Bulgaria inquinans*	11
32	*Byssomerulius corium*	1
33	*Calocera cornea*	358
34	*Calocera furcata*	77
35	*Calocera viscosa*	1
36	*Calycina discreta*	1
37	*Calycina languida*	2
38	*Calycina vulgaris*	1
39	*Capitotricha fagiseda*	2
40	*Ceraceomyces serpens*	4
41	*Ceratobasidium cornigerum*	15
42	*Ceriporia excelsa*	1
43	*Ceriporia purpurea*	1
44	*Ceriporiopsis gilvescens*	1
45	*Ceriporiopsis rivulosa*	2
46	*Cerrena unicolor*	2
47	*Chaetosphaeria myriocarpa*	9
48	*Chondrostereum purpureum*	4
49	*Cistella dentata*	2
50	*Claussenomyces atrovirens*	5
51	*Clitocybe ditopus*	6
52	*Clitopilus hobsonii*	21
53	*Columnocystis abietina*	1
54	*Coniochaeta ligniaria*	131
55	*Coniochaeta malacotricha*	124
56	*Coniochaeta pulveracea*	432
57	*Coniochaeta subcorticalis*	18
58	*Coniochaete velutina*	984
59	*Coniophora arida*	4
60	*Coniophora olivacea*	8
61	*Coprinus micaceus*	8

No.	Species	Total number of records
62	*Creopus gelatinosus*	1
63	*Crepidotus cesatii*	14
64	*Crocicreas cyathoideum*	6
65	*Cryptocoryneum condensatum*	3
66	*Cyathicula cyathoidea*	9
67	*Cylindrobasidium laeve*	2070
68	*Dacrymyces capitatus*	10
69	*Dacrymyces stillatus*	1492
70	*Datronia mollis*	85
71	*Dematioscypha dematiicola*	1
72	*Dentipellis fragilis*	1
73	*Diatrype decorticata*	219
74	*Diatrype disciformis*	942
75	*Diatrype flavovirens*	3
76	*Diatrypella verrucaeformis*	84
77	*Durandiella gallica*	59
78	*Eutypa lata*	1
79	*Eutypa spinosa*	16
80	*Eutypella quaternata*	46
81	*Exarmidium inclusum*	268
82	*Exidia pithya*	250
83	*Exidia plana*	1349
84	*Exidiopsis effusa*	142
85	*Flammulina velutipes*	1
86	*Fomes fomentarius*	55
87	*Fomitopsis pinicola*	955
88	*Ganoderma lipsiense*	18
89	*Gloeocystidiellum porosum*	3
90	*Gloeophyllum sepiarium*	1402
91	*Grandinia aspera*	2
92	*Granulobasidium vellereum*	1
93	*Graphium calicioides*	30
94	*Gymnopilus sapineus*	4
95	*Gymnopus androsaceus*	4
96	*Haglundia perelegans*	3

No.	Species	Total number of records
97	*Hamatocanthoscypha laricionis*	146
98	*Helminthosphaeria stuppea*	7
99	*Heterobasidion annosum*	122
100	*Hohenbuehelia atrocoerulea*	5
101	*Hohenbuehelia fluxilis*	5
102	*Hohenbuehelia pinacearum*	9
103	*Hyalorbilia berberidis*	1
104	*Hyalorbilia inflatula*	7
105	*Hyaloscypha aureliella*	5
106	*Hymenoscyphus caudatus*	1
107	*Hymenoscyphus conscriptus*	1
108	*Hymenoscyphus improvisus*	1
109	*Hymenoscyphus scutula*	2
110	*Hymenoscyphus virgultorum*	95
111	*Hyphoderma argillaceum*	1
112	*Hyphoderma mutatum*	4
113	*Hyphoderma praetermissum*	2
114	*Hyphoderma setigerum*	102
115	*Hyphodiscus hemiamyloideus*	2
116	*Hyphodontia breviseta*	2
117	*Hypholoma capnoides*	50
118	*Hypholoma fasciculare*	66
119	*Hypholoma marginatum*	2
120	*Hypochnicium albostramineum*	2
121	*Hypochnicium bombycinum*	4
122	*Hypochnicium eichleri*	4
123	*Hypochnicium lundellii*	4
124	*Hypochnicium punctulatum*	18
125	*Hypochnicium subrigescens*	2
126	*Hypochnicium wakefieldiae*	2
127	*Hypocrea aureoviridis*	3
128	*Hypocrea rufa*	124
129	*Hypoxylon cohaerens*	1382
130	*Hypoxylon fragiforme*	8702
131	*Hypoxylon rubiginosum*	7

No.	Species	Total number of records
132	*Inonotus hastifer*	1
133	*Inonotus nodulosus*	48
134	*Irpex lacteus*	178
135	*Ischnoderma benzoinum*	2
136	*Laccaria amethystea*	9
137	*Lachnellula abietis*	4
138	*Lachnellula calyciformis*	296
139	*Lachnellula gallica*	174
140	*Lachnellula subtilissima*	9
141	*Lachnum fasciculare*	1
142	*Lachnum virgineum*	1
143	*Lasiosphaeria canescens*	2
144	*Lasiosphaeria hirsuta*	15
145	*Lasiosphaeria ovina*	34
146	*Lasiosphaeria spermoides*	10
147	*Lasiosphaeria strigosa*	48
148	*Laxitextum bicolor*	77
149	*Lenzites betulinus*	234
150	*Leptosporomyces mutabilis*	4
151	*Leptosporomyces roseus*	4
152	*Lopadostoma turgidum*	23
153	*Lopharia spadicea*	15
154	*Lophiotrema boreale*	11
155	*Lophium mytilinum*	542
156	*Melanomma pulvispyrius*	946
157	*Melanomma sanguinarium*	5
158	*Melanospora parasitica*	1
159	*Melanotus phillipsii*	1
160	*Merismodes anomalus*	160
161	*Mollisia aquosa*	26
162	*Mollisia conifericola*	1
163	*Mollisia fusca*	5
164	*Mollisia ligni*	3
165	*Mollisia lividofusca*	1
166	*Mollisia olivaceocinerea*	80

No.	Species	Total number of records
167	*Mycena abramsii*	1
168	*Mycena amicta*	1
169	*Mycena galopus*	2
170	*Nectria cinnabarina*	42
171	*Nectria coccinea*	1189
172	*Nectria cosmariospora*	2
173	*Nectria episphaeria*	50
174	*Nectria fuckeliana*	351
175	*Nectria magnusiana*	17
176	*Nectria peziza*	5
177	*Nematogonum ferrugineum*	20
178	*Neobulgaria pura*	168
179	*Neodasyscypha cerina*	475
180	*Oligoporus ptychogaster*	1
181	*Olla scropulosa*	1
182	*Ombrophila janthina*	1
183	*Ombrophila violacea*	1
184	*Orbilia coccinella*	1
185	*Orbilia delicatula*	8
186	*Oudemansiella mucida*	10
187	*Panellus mitis*	96
188	*Panellus stypticus*	5
189	*Panellus violaceofulvus*	132
190	*Patinella sanguineoatra*	6
191	*Pellidiscus pallidus*	6
192	*Peniophora aurantiaca*	1
193	*Peniophora cinerea*	604
194	*Peniophora incarnata*	89
195	*Peniophora piceae*	31
196	*Peniophora pithya*	22
197	*Peniophora violaceolivida*	1
198	*Pezicula acericola*	16
199	*Pezicula cinnamomea*	14
200	*Phaeohelotium carneum*	1
201	*Phaeohelotium trabinellum*	1

No.	Species	Total number of records
202	*Phanerochaete filamentosa*	1
203	*Phanerochaete galactites*	2
204	*Phanerochaete laevis*	3
205	*Phanerochaete raduloides*	1
206	*Phanerochaete sordida*	92
207	*Phanerochaete tuberculata*	2
208	*Phanerochaete velutina*	9
209	*Phellinus hartigii*	4
210	*Phlebia acerina*	1
211	*Phlebia radiata*	121
212	*Phlebia rufa*	31
213	*Phlebia tremellosa*	15
214	*Phlebiella vaga*	116
215	*Phlebiopsis gigantea*	58
216	*Pholiota cerifera*	2
217	*Pholiota lenta*	2
218	*Pholiota tuberculosa*	2
219	*Physisporinus sanguinolentus*	27
220	*Pleurotus cornucopiae*	1
221	*Pleurotus ostreatus*	35
222	*Pleurotus pulmonarius*	13
223	*Plicaturopsis crispa*	28
224	*Pluteus semibulbosus*	2
225	*Polydesmia pruinosa*	4
226	*Polyporus brumalis*	97
227	*Polyporus ciliatus*	6
228	*Psilocybe crobula*	1
229	*Pycnoporus cinnabarinus*	436
230	*Radulomyces confluens*	5
231	*Resinicium bicolor*	20
232	*Resupinatus applicatus*	7
233	*Rigidoporus vitreus*	4
234	*Rosellinia aquila*	40
235	*Rosellinia thelena*	229
236	*Schizophyllum commune*	2803

No.	Species	Total number of records
237	*Schizopora paradoxa*	37
238	*Scutellinia cejpii*	13
239	*Scutellinia scutellata*	11
240	*Scutellinia subhirtella*	8
241	*Scutellinia umbrorum*	8
242	*Sebacina epigaea*	1
243	*Sebacina grisea*	137
244	*Sebacina incrustans*	1
245	*Serpula himantioides*	3
246	*Simocybe centunculus*	1
247	*Sistotrema brinkmannii*	274
248	*Sistotrema confluens*	1
249	*Sistotrema coroniferum*	1
250	*Sistotrema diademiferum*	2
251	*Sistotrema efibulatum*	1
252	*Sistotrema oblongisporum*	3
253	*Sistotrema octosporum*	10
254	*Sistotremastrum niveocremeum*	2
255	*Sistotremastrum suecicum*	7
256	*Skeletocutis nivea*	1
257	*Solenia candida*	1
258	*Spongiporus caesius*	6
259	*Spongiporus stipticus*	6
260	*Steccherinum ochraceum*	5
261	*Stereum hirsutum*	1222
262	*Stereum rameale*	3
263	*Stereum rugosum*	65
264	*Stereum sanguinolentum*	2918
265	*Thelephora terrestris*	253
266	*Tomentellopsis zygodesmoides*	3
267	*Trametes gibbosa*	31
268	*Trametes hirsuta*	1934
269	*Trametes versicolor*	411
270	*Trechispora farinacea*	2
271	*Tremella encephala*	5

No.	Species	Total number of records
272	*Tremella foliacea*	24
273	*Trichaptum abietinum*	137
274	*Trichophaea pseudogregaria*	1
275	*Tromeropsis microtheca*	92
276	*Tubeufia cerea*	3
277	*Tulasnella albida*	1
278	*Tulasnella eichleriana*	2
279	*Tulasnella violacea*	1
280	*Tulasnella violea*	3
281	*Tylospora asterophora*	2
282	*Tylospora fibrillosa*	1
283	*Tympanis hypopodia*	22
284	*Tympanis truncatula*	1
285	*Typhula erythropus*	13
286	*Typhula setipes*	18
287	*Unguicularia cirrhata*	2
288	*Valsaria insitiva*	146
289	*Velutarina rufoolivacea*	1
290	*Xylaria hypoxylon*	52
291	*Zignoella ovoidea*	6

C Curriculum Vitae

The CV can be found on the next page. For a current and updated version of the CV see `https://franzkrah.github.io/files/cv_english.pdf`.

Franz-Sebastian Krah

Curriculum Vitæ

Education

2015–2019   **PhD Biology**, *Technical University of Munich (TUM)*, *summa cum laude*.
Thesis: *Pattern and Processes of Fungal Community Ecology*
Supervision: Prof. Dr. Hanno Schäfer & Dr. Claus Bässler;
Funding: PhD scholarship by the "Rudolf und Helene Glaser-Stiftung" (50.000 EUR, TO83/26495/2015/kg) and "Zempelin Stiftung" (7.000 EUR, T214/32357/2018/sm)

2013–2015   **Masters of Science - Biology**, *Technical University of Munich (TUM)*, *passed with high distinction*.
Thesis: Pattern of host associations and dynamics of substrate switching in wood decay fungi using phylogenetic comparative methods and a mega-phylogeny of the Basidiomycota;
Supervision: Prof. Dr. David Hibbett & Prof. Dr. Hanno Schäfer

2010–2013   **Bachelor of Science - Forest Science and Resource Management**, *Technical University of Munich (TUM)*, passed with merit.
Thesis: Forest fungal α- and β-diversity: environmental factors and functional role of saprotrophic and ectomycorrhizal fungi in an unmanaged mature *Picea abies* stand
Supervision: Dr. Claus Bässler

2008–2010   **Magister - Philosophy**, *Ludwigs-Maximilians-Universität (LMU)*, Munich, *Majors:* Analytical philosophy and Philosophy of language.
Midterm exam passed with high distinction

Experience

June – Oct., 2013   **Freelancer**, *Bavarian Forest National Park*, Grafenau.
Project BIOHOLZ, Fungal species identification based on macro- and micromorphology.

Nov., 2010 – March, 2013   **Student Assistant**, *Technical University of Munich (TUM)*, Chair for Ecophysiology of Plants.
e.g., teaching plant identification, various field work

March, 2015   **Teaching assistant**, *Technical University of Munich (TUM)*, RG Biodiversity of Plants.
Introduction to bryophyte ecology and evolution.

📱 *(+49) 1705221189* • ✉ *franz.krah@tum.de*
🐦 *#Franz_Krah*   ⭘ *FranzKrah*

Awards

Sept. 2016	1st prize in poster session, 23rd Symposium on 'Biodiversity and Evolutionary Biology' of the German Botanical Society in Munich

Computer skills

Basic	Linux, SQL
Intermediate	LaTeX, GitHub, **Rcpp**
Advanced	**R** programming, Inkscape, AffinityDesigner, Microsoft Office, Geneious, MAFFT, RAxML, BEAST, data mining, statistics and phylogenetic comparative methods (PCM) in **R**
Software	⯃FranzKrah, e.g., rUSDA, rMyCoPortal, rSymbiota, rGUIDANCE

Conferences - Seminars - Presentations

March. 2019	Invited **Talk** at the Ecological and Socio-Economic. Challenges and Opportunities of Climate Change in Rural Southern Europe. Workshop 14th – 16th Feb 2019, link
Dec. 2018	Invited **Talk** at the Julius-Maximilians Universität Würzburg. Invited by Peter. H. Biedermann (Department of Animal Ecology and Tropical Biology)
Sept. 2018	**Talk** at the 48th Annual Meeting of the Ecological Society of Germany, Austria and Switzerland. Gesellschaft für Ökologie
Nov. 2017	**Talk** at the Bayerische Akademie für Naturschutz und Landschaftspflege, Hochschule Weihenstephan-Triesdorf.
Oct. 2017	**Talk** at the PhD-colloquium in Ecology. Technical University of Munich
July 2017	Invited **talk** at the Yale University about color in fungal fruit bodies (Invited by Michael Donoghue). New Haven, (Connecticut), USA.
June 2017	**Talk** at the Evolution meetings conference. Portland (Oregon), USA.
Sept. 2016	**Poster** at the 23rd Symposium on 'Biodiversity and Evolutionary Biology' of the German Botanical Society. Munich.
Sept. 2016	**Talk** at the Conference of the Deutsche Gesellschaft für Mykologie (DGfM) in Bernried
May 2016	EMBO Practical **Course** on Computational Molecular Evolution on Crete and poster presentation
Jan. 2016	**Seminar**: Improving your Intercultural Skill Set. Frauenchiemsee. Germany
Dec. 2015	**Seminar**: Towards Sustainable Development in Harmony With Nature in "Crocker Range Biosphere Reserve (CRBR)". Kota Kinabalu, Sabah

Research Visits

Nov. – Dec., 2015	Institute for Tropical Biology and Conservation (ITBC), University Malaysia Sabah. Dr. Jaya Seelan Sathiya Seelan
Feb. – May, 2015	Clark University, Massachusetts (USA). Prof. Dr. David Hibbett

March, 2014   Rooiklip Research Station, Namibia, Dr. Thomas Wagner

Languages

- German - Mothertongue
- French - Basic communication skills
- English - fluent
- Bengali - Basic communication skills

Peer-review for

- Fungal Ecology
- Biological Conservations
- Web ecology

Supervisions

S. Lenz	Research project (6 weeks)
E. Koc	Research project (6 weeks)
B. Ludl	Research project and B.Sc. thesis (6 months)
T. Endriß	M.Sc. thesis (6 months)
L. Schmid	Research project (6 months)
A. Zarvoc	PhD student in Bavarian Forest National Park
B. Olou	PhD student from Benin, Africa (DAAD scholarship, 2017 - 2019)

Interests

- Squash, Hiking
- Traveling
- Movies
- Tabla

Publications

1. Maria-Barbara Winter, Claus Bässler, Markus Bernhardt-Römermann, **Franz-S. Krah**, Hanno Schäfer, Sebastian Seibold, Jörg Müller. On the structural and species diversity effects of bark beetle disturbance in forests during initial and advanced early-seral stages at different scales. *European Journal of Forest Research* 2017, 136:357-373

2. **Franz-S. Krah**, Sebastian Seibold, Roland Brandl, Petr Baldrian, Jörg Müller, Claus Bässler (2018). Independent effects of host and environment on the diversity of wood-inhabiting fungi. *Journal of Ecology* 2018, 106:1428-1442

3. **Franz-S. Krah**, Hanno Schäffer, Christoph Heibl, Claus Bässler, John Soghigian, David Hibbett. Evolutionary dynamics of host specialization in wood-decay fungi. *BMC Evolutionary Biology* 2018, 18:119-132

4. Sebastian Seibold, Jörg Müller, Petr Baldrian, Marc W. Cadotte, M. Štursová, Peter H. Biedermann, **Franz-S. Krah**, C. Bässler. Fungi associated with beetles dispersing from dead wood – Let's take the beetle bus! *Fungal Ecology* 2018, 39:100-108

5. Boris A. Olou, Nourou S. Yorou, Manuel Striegel, Claus Bässler, **Franz-S. Krah**. Effects of macroclimate and resource on the diversity of tropical wood-inhabiting fungi. *Forest Ecology and Management* 2019, 436:79-87

☐ *(+49) 1705221189* • ✉ *franz.krah@tum.de*
🐦 *#Franz_Krah* ⚲ *FranzKrah*

6 **Franz-S. Krah**, Andrew N. Miller and Scott T. Bates. rMyCoPortal - an R package to interface with the Mycology Collections Portal. *Biodiversity Data Journal* 2019, 7:e31511

7 Leonie Schmid, Claus Bässler, Hanno Schaefer, **Franz-S. Krah**. A test of camera surveys to study fungus-animal interactions. *Mycoscience* 2019, accepted; `https://doi.org/10.1016/j.myc.2019.04.002`

8 **Franz-S. Krah** and Christoph Heibl. rGUIDANCE – alignment confidence score computation in R. *Journal of Open Source Software* 2019, 4(36):1350

 (+49) 1705221189   •   *franz.krah@tum.de*
 #Franz_Krah   *FranzKrah*